Development of Polymeric Micelles for Site Specific Delivery of Nonsteroidal Anti-Inflammatory Drugs: Effect on the Cardiovascular Risk in an Experimental Model of Arthritis

by

Hanan Mustafa Al Lawati

A thesis submitted in partial fulfillment of the requirements for the degree of

Doctor of Philosophy

in

Pharmaceutical Sciences

Faculty of Pharmacy and Pharmaceutical Sciences
University of Alberta

Abstract

Non-steroidal anti-inflammatory drugs (NSAIDs), which inhibit cyclooxygenase (COX) enzymes, are among the most widely used medications worldwide with proven efficacy in controlling inflammation and pain associated various disease conditions. The chronic systemic use of most NSAIDs, however, is known to be associated with an increased risk of cardiovascular (CV) events, including myocardial infarction and stroke. Cardiovascular complications associated with the use of NSAIDs are believed to be partly linked to the extent of their exposure to the cardiac tissue among other factors.

Research in the field of nanomedicine has shown a remarkable progress in the design of targeted drug delivery systems which can improve drug disposition towards the diseased sites. A systematic search of the scientific literature revealed that reports on the use of such advanced systems for the delivery of NSAIDs that show evidence of improved cardiac safety are lacking. Therefore, in this research work we considered designing nano-formulations for the delivery of diclofenac as a model NSAID for its known serious CV toxicity. The aim was to improve diclofenac pharmacokinetics and biodistribution whereby reducing its accumulation and toxicity in the cardiac tissue. We hypothesize that reduced diclofenac cardiac exposure will lower its CV side effects.

Towards this goal, different polymeric micellar formulations based on a shell of poly(ethylene oxide) (PEO) and various hydrophobic polyesters as the hydrophobic core were tried for the encapsulation of diclofenac or its ethyl ester prodrug. The micellar formulations were characterized for size, size distribution, morphology, and *in vitro* as well as *ex vivo* drug release.

The results pointed to the superiority of polymeric micelles with a core of poly(ε-caprolactone) (PCL) or poly(α-benzyl carboxylate -ε-caprolactone) (PBCL) encapsulating diclofenac ethyl ester as the optimal formulations.

In the next step, the biodistribution of the optimal polymeric micellar formulations of diclofenac was investigated *in vivo* in healthy rats following intravenous (*iv*) and/or intraperitoneal (*ip*) administration and compared to that of the free diclofenac. The intravenous administration of the polymeric micellar formulation resulted in prolonged diclofenac systemic circulation and reduced its accumulation in the heart and kidneys compared to the free drug. The polymeric micellar formulations of diclofenac administered through *ip* route proved to be equally bioavailable as the *iv* administration.

In the following step, multiple dose administration of polymeric micellar formulation of diclofenac in an experimental model of arthritis in rats was employed to assess the anti-inflammatory activity and the safety of the micellar formulation over free drug. To assess the cardiac safety of polymeric micellar formulation versus free drug, the levels of cardioprotective versus cardiotoxic metabolites of arachidonic acid (ArA) was measured in plasma, heart and kidneys following drug administration to these rats with adjuvant arthritis. The results showed that the micellar formulation provided similarly effective therapy for the management of inflammation when compared to the free drug. On the other hand, administration of diclofenac as polymeric micellar formulation reduced the ratio of cardiotoxic over cardioprotective metabolites of ArA in the heart and plasma when compared to the free drug administration. These results provide the first evidence for a potential role in the tissue disposition of diclofenac on its cardiac-safety. It also points to the potential of developed formulations for effective and safe delivery of NSAIDs.

Preface

The following papers are published or considered for publication in refereed journals and are part of the work presented in this thesis:

Section 1.5 of chapter 1 is considered for publication as Al-Lawati H., Binkhathlan Z., Lavasanifar A., Nanomedicine for the effective and safe delivery of non-steroidal anti-inflammatory drugs: a review of preclinical research. H. Al Lawati is the lead author and was responsible for identifying and screening relevant reports, analysing the reports, data collection, and composition of the manuscript. Dr. Z. Binkhathlan reviewed the included reports and helped with the article revision. Dr. A. Lavasanifar was the supervisory author and was involved in formulation of concepts, analysis and composition of manuscript.

Chapter 2 has been published as Al-Lawati H., Vakili M. R., Jamali F., Lavasanifar A., Polymeric micelles for the delivery of diclofenac and its ethyl ester derivative, Pharmaceutical Nanotechnology 2016; 4(2): 109 – 119. H. Al Lawati is the lead author and was responsible for data collection and analysis as well as for manuscript composition. Dr. M. R. Vakili helped with study design. Dr. F. Jamali and Dr. A. Lavasanifar were the supervisory authors and were involved in formulation of concept, analysis and composition of manuscript.

Chapter 3 has been published as Al-Lawati H., Vakili M. R., Lavasanifar A., Ahmed S., Jamali F., Delivery and biodistribution of traceable polymeric micellar diclofenac in the rat, Journal of Pharmaceutical Sciences (in press, appeared online). H. Al Lawati is the lead author and was responsible for data collection and analysis as well as the manuscript composition. Dr. M. R. Vakili helped with study design. S. Ahmed helped with some data acquisition. Dr. A. Lavasanifar and

Dr. F. Jamali were the supervisory authors and were involved in formulation of concept, analysis and composition of manuscript.

Chapter 4 is to be submitted for publication as Al-Lawati H., Vakili M. R., Lavasanifar A., Ahmed S., Jamali F., Pharmacokinetics and pharmacodynamics of traceable polymeric micellar diclofenac in experimental arthritis. H. Al Lawati is the lead author and was responsible for data collection and analysis as well as the manuscript composition. Dr. M. R. Vakili helped with study design. S. Ahmed helped with some data acquisition. Dr. A. Lavasanifar and Dr. F. Jamali were the supervisory authors and were involved in formulation of concept, analysis and composition of manuscript.

The supplementary chapter is part of a manuscript to be submitted for publication as Binkhathlan Z., Ali R., Qamar W., Al-Lawati H., and Lavasanifar A. Pharmacokinetic and tissue distribution study of orally administered cyclosporine A-loaded poly(ethylene oxide)-block-poly(ε-caprolactone) micelles versus Sandimmune® in rats. H. Al Lawati was completely responsible for the *in vitro* and *in vivo* experiments presented in this thesis in the supplementary chapter. She wrote the methods and results sections related to these experiments in the manuscript and helped with the article revision. Dr. Z. Binkhathlan, Dr. R. Ali, and Dr. W. Qamar were responsible for the other data collection and analysis as well as the manuscript composition. Dr. A. Lavasanifar was the supervisory author and was involved in formulation of concept, analysis and composition of manuscript.

In addition, the following refereed journal papers, report research work that was carried out by H. Al Lawati in parallel to the work presented in this thesis and is indirectly related to the thesis:

- Al Lawati H. and Jamali F. Onset of action and efficacy of ibuprofen liquigel as compared to solid tablets: a systematic review and meta-analysis. J Pharm Pharm Sci 2016; 19 (3): 301-311.
- Al-Lawati H. Aliabadi H. M., Makhmalzadeh B. S., Lavasanifar, A., Nanomedicine for immunosuppressive therapy: achievements in pre-clinical and clinical research. Expert Opin Drug Deliv. 2018 Apr; 15(4):397-418.

Dedication

To my beloved parents Mustafa and Batool

for their endless love and support

Acknowledgments

I would like to express my sincere gratitude and appreciation to my supervisor Dr. Fakhreddin Jamali. His encouragement, ideas, continuous help and guidance, interesting courses, and many valuable discussions made this dissertation and my degree possible. I have been fortunate to have had him as my advisor during my studies at the University of Alberta.

I would like to also extend my appreciation to my co-supervisor Dr. Afsaneh Lavasanifar for introducing me to the world of nanomedicine and for the many valuable ideas, discussions, suggestions, and for her continuous support and encouragement which made this work possible. I enjoyed working with both Dr. Fakhreddin Jamali and Dr. Afsaneh Lavasanifar on this project.

I would like to thank Dr. Raimer Löbenberg and the other members of my thesis committee, Dr. Michael Doschak and Dr. Hasan Uludag, for their valuable comments and suggestions which better shaped this work.

Special thanks go to the members of the Dr. Jamali and Dr. Lavasanifar labs, in particular Dr. Mohamed R. Vakili, Dr. Waheed Asghar, Igor Paiva, Nasim Ghasemi, Dr. Forough Sanaee and Surur Ahmed, for their encouragement and help from time to time. I wish them and all my fellow graduate students all the best. A special thanks go to the faculty and staff of the Faculty of Pharmacy and Pharmaceutical Sciences.

Above all, I would like to thank my parents Mustafa and Batool, my husband Mohamed, and my wonderful kids Abdullah, Sara and Ali. Their constant support and encouragement and their prayers made all this possible.

Table of Contents

List of Tables

List of Figures

Chapter 1: Introduction*

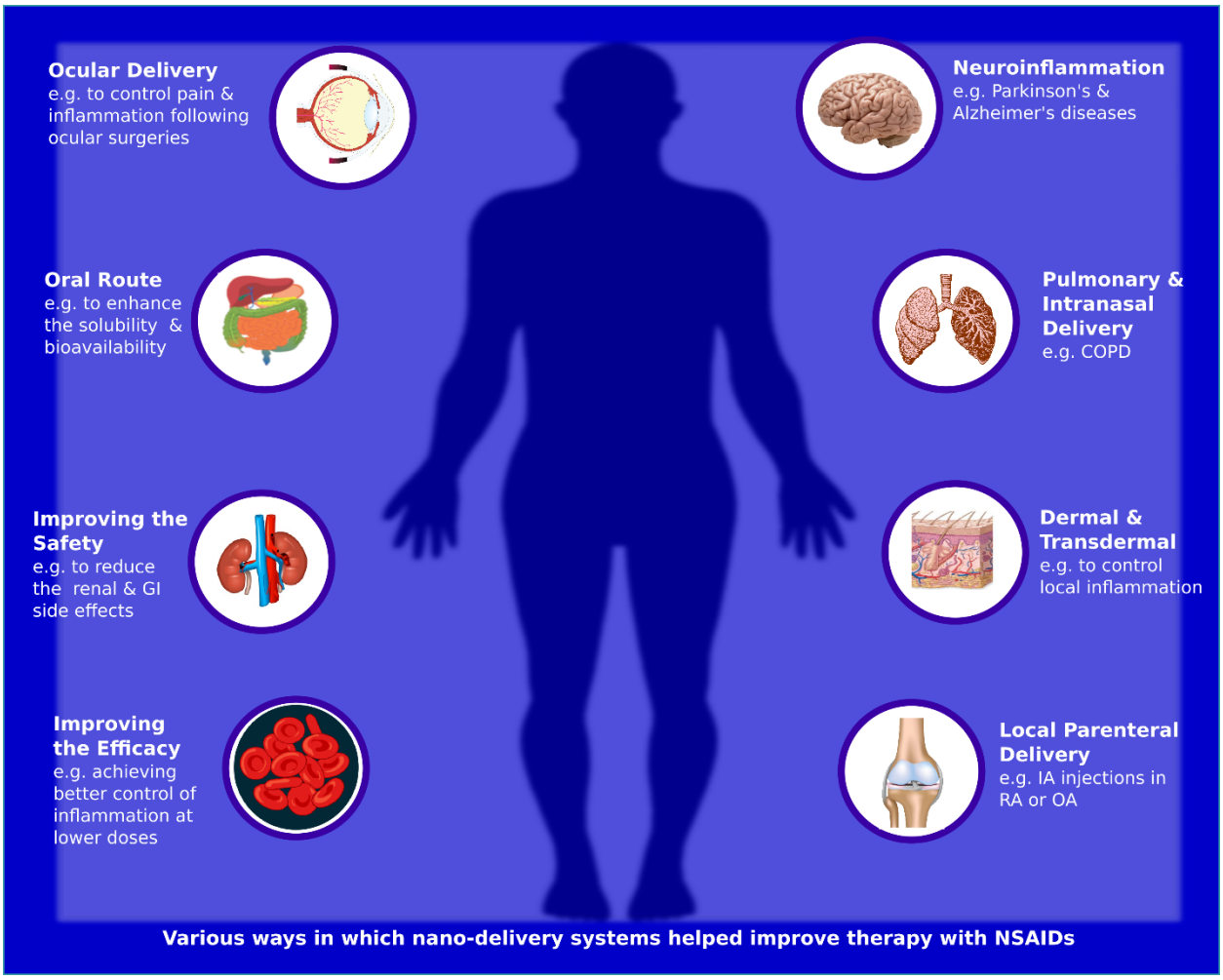

Various ways in which nano-delivery systems helped improve therapy with NSAIDs

---

* A version of section 1.5 of this chapter is submitted for publication:

Al-Lawati H, Binkhathlan Z, Lavasanifar, A. Nanomedicine for the effective and safe delivery of non-steroidal anti-inflammatory drugs: a review of preclinical research.

1.1. Non-steroidal anti-inflammatory drugs (NSAIDs)

Non-steroidal anti-inflammatory drugs (NSAIDs) are a chemically diverse group of agents (Table 1-1) which are among the most widely used medications worldwide with demonstrated efficacy in controlling inflammation and pain that associate various conditions including rheumatoid arthritis, osteoarthritis, ankylosing spondylitis, gout, dysmenorrhea, dental pain, or headache [1]. Aspirin is also used in low doses as an anti-platelet agent.

1.1.1. The arachidonic acid cascades

Arachidonic acid (ArA) is a polyunsaturated fatty acid of the omega-6 class, that is released from its esterified form mostly by the actions of the lipid-cleaving enzyme, phospholipase A2. The importance of ArA and its metabolites in the regulation of inflammatory processes came into light with the discovery that NSAIDs exert their anti-inflammatory effect by selectively inhibiting the biosynthesis of prostaglandin (PG), a metabolite of ArA [2]. Research has now established that ArA is a precursor of numerous biologically active metabolise, referred to as eicosanoids, which regulate inflammation and various other homeostatic biological functions. There are three main pathways for the ArA metabolism, namely (i) the cyclooxygenase (COX) pathway which produces PGH_2 that is further converted by down-stream isomerases to various bioactive prostanoids including thromboxane (e.g. TXA_2), prostaglandins (e.g. PGE_2) and prostacyclin (PGI_2), (ii) the lipoxygenase (LOX) pathway which leads to the formation of leukotrienes (e.g. LTC_4, LTD_4, LTE_4) and lipoxins (e.g. LXA_4, LXB_4), and (iii) cytochrome P450 metabolism which catalyzes the biotransformation of ArA to hydroxyeicosatetraenoic acids (HETEs) (20-HETE) and epoxyeicosatrienoic acids (EETs) (5,6-, 8,9-, 11,12-, 14,15-EET) [3].

Table 1-1. Nonsteroidal anti-inflammatory drugs classified by chemical structure

Group	Example(s)
Salicylates	Acetyl salicylic acid (Aspirin), salsalate, diflunisal, benorilate, meseclazone, Salol
Propionic acid derivatives	Ibuprofen, dexibuprofen, naproxen, ketoprofen, flurbiprofen, fenoprofen, oxaprozin, dexketoprofen, loxoprofen
Heteroaryl acetic acid	Tolmetin, diclofenac, ketorolac, aceclofenac
Alkanones	Nabumetone
Indoleacetic, Indeneacetic acids	Indomethacin, sulindac, etodolac
Oxicams	Piroxicam, meloxicam, tenoxicam, droxicam, lornoxicam
Diaryheterocycles (COXIBs)	Rofecoxib, celecoxib, valdecoxib, parecoxib, etoricoxib, lumiracoxib, fluorocoxib
Fenamates	Mefenamic acid, meclofenamic acid, niflumic acid, flufenamic acid, tolfenamic acid

1.1.2. Mechanisms of action of NSAIDs

NSAIDs exert their anti-inflammatory, antipyretic, and analgesic effects mainly by inhibiting the biosynthesis of prostaglandins and prostacyclin, which are potent mediators of inflammation derived from ArA, by blocking the activities of the COX-1 and COX-2 enzymes at various degrees. Nevertheless, other activities which are secondary to the COX inhibition on other mediators have been reported for these agents including inhibition of neutrophil activation, leukotriene production, and T and B cell proliferation. Moreover, prostaglandin-independent properties have also been suggested to account for some of their effect [4].

Among the two isoforms, COX-1 is constitutively expressed in most tissue and has a role in gastric cytoprotection and hemostasis, vascular hemostasis, and platelet aggregation. COX-2, on the other hand, is present in various tissues (e.g. brain, kidneys) at low levels, but its expression is increased locally during states of inflammation. Earlier studies have suggested that the analgesic and anti-inflammatory effects of NSAIDs could be mediated mainly through inhibition of the inducible COX-2 isoenzyme while the gastrointestinal adverse events associated with these drugs and the toxicity appeared to correlate closely with the inhibition of COX-1. Therefore, attempts were directed towards producing NSAID agents which selectively inhibit COX-2, and thus do not affect the activities of the COX-1 isoform. These newer agents are commonly referred to as selective COX-2 inhibitors. Table 1-2 lists some widely used NSAIDs based on COX selectivity, as measured by their potency (micromolar IC80 values) to inhibit the two COX isoforms.

1.1.3. Side effects of NSAIDs

The use of NSAIDs is associated with a range of side effects many of which are related to their main mode of action, i.e. the inhibition of prostaglandin synthesis. These adverse effects which appear to be dose-dependent and increase with co-morbidities include gastrointestinal (GI), renal, and cardiovascular effects. The most important GI adverse-effects include dyspepsia, peptic ulcer disease, and bleeding, however less frequent but more serious events which affect the lower GI tract and have the potential to lead to harmful conditions such as the diaphragm disease have also been reported [1].

Theoretically, there is an advantage to the use of COX-2 selective NSAIDs over non-selective NSAIDs in terms of reduction in the GI adverse effects. This was suggested clinically in a number

Table 1-2. NSAIDs classification based on COX selectivity

< 5-folds COX-2 selectivity	5-50 folds COX-2 selectivity	> 50-folds COX-2 selectivity
Fenoprofen, ibuprofen, tolmetin, naproxen, aspirin, indomethacin, ketoprofen, flurbiprofen, Ketorolac	Etodolac, sulindac, diclofenac, celecoxib, meloxicam	Lumiracoxib, etoricoxib, rofecoxib, valdecoxib

in vitro selectivity for the COX enzymes based on IC_{80} (data obtained from [5]).

of RCTs which directly compared agents from the two classes including the VIGOR, the SUCCESS, and the TARGET studies [6]. However, results from other RCTs (including MEDAL, and CLASS) as well as data from some current observational studies have questioned these conclusions and proposed a comparable GI safety profile for both groups [7].

1.1.4. Cytochrome P450 metabolites and the cardiovascular risk of NSAIDs

At the turn of the century, serious concerns were raised about the safety of the then newly introduced COX-2 selective NSAID agents, including celecoxib, rofecoxib and valdecoxib, with reports of increased occurrence of serious cardiovascular (CV) events and deaths from these agents. This subsequently led to the withdrawal of rofecoxib and valdecoxib from the market and alarmed on the CV risks associated with the chronic use of most NSAIDs. The CV risk was thought to be related to the extent of COX selectivity of the different NSAIDs, i.e. NSAIDs which inhibit COX-2 more than COX-1 were suggested to have a higher cardiovascular risk compared to the other agents. However, a review of existing and newly emerged evidence on the composite CV side effects of NSAIDs suggested ruling out the notion of COX-2 inhibition as a reason behind the CV risk of NSAIDs [1].

The use of NSAIDs has been found to alter the balance between cytochrome P450 (CYP) metabolites of ArA which are known to affect the CV system. In 2010, Liu *et al* demonstrated that rofecoxib given for a 3-month period resulted in over 120-fold higher blood level of 20-HETE, which correlated with a shorter tail bleeding time in a murine model [8]. Their data suggested 20-HETE as a marker of rofecoxib exposure and, possibly, the adverse CV events associated with this NSAID. 20-HETE is a cardio-toxic eicosanoid with several mechanisms involved in its cardiotoxicity [9, 10]. For example, 20-HETE was found to increase NADPH oxidase-derived ROS production and to stimulate L-type Ca^{2+} channel currents in cardiac myocytes [11]. In a different study, Zhang *et al* found that a combined therapy with rofecoxib and HET0016, a potent 20-HETE inhibitor, was effective in reducing colon tumor growth, and reduced rofecoxib-induced cerebrovascular damage and stroke outcomes in MC38 tumor-bearing mice [12]. EETs on the other hand are cardio-protective eicosanoids that play a major role in maintaining vascular homeostasis and have been found to decrease inflammation and platelet aggregation [13]. In the heart, EETs enhance coronary blood flow and myocyte contraction. Recent finding have linked the alteration of the levels of CYP metabolites of arachidonic acid including 20-HETE, EETs (5-6,8-9,11 -12,14-15) and DHETs (5-6,8-9,11-12,14-15) to the CV risk of NSAIDs [14]. In particular, the ratio of 20-HETE/EETs has been found to serve as a biomarker for the CV risk.

1.1.5. Diclofenac: a model NSAID

Diclofenac is an NSAID of the phenyl acetic acid derivative class, that is widely used in the management of chronic inflammatory and degenerative disorders such rheumatoid arthritis, osteoarthritis, and ankylosing spondylitis. This agent, which is on the list of essential drugs of many countries, is usually formulated as a sodium or potassium salt and is available in various

forms for oral, rectal, intramuscular, intravenous or topical administration [15]. The anti-inflammatory potency of diclofenac was established in several animal models of inflammation as well as in several clinical trials. In one of the early studies a daily diclofenac dose of 100 mg was shown to produce superior relief from pain and stiffness and to improve joint mobility in a larger number of osteoarthritis patients when compared to naproxen at 500 mg dose [16, 17]. Another study also found diclofenac to be superior to indomethacin, a derivative of indoleacetic acid, in patients with rheumatoid arthritis [18]. A systematic review and meta analysis of clinical trials found that diclofenac at a dose of 150 mg/day is at least as effective as the other NSAIDs in improving physical function, but is likely to be more effective in alleviating pain than several other NSAIDs including celecoxib (200 mg/day), naproxen (1000 mg/day), and ibuprofen (2400 mg/day) and comparable to etoricoxib (60 mg/day) [19]. In terms safety, diclofenac was found to be well tolerated and to be safer than aspirin, comparable to ibuprofen and naproxen, and to cause fewer side effects than aspirin, ibuprofen, and piroxicam in terms of effects on the GI, renal, hepatic, and hemostatic systems [20].

The main mechanism underlying the analgesic action of diclofenac in RA is similar to other NSAIDs: inhibition of the COX isozymes in blood and synovial tissues thereby inhibiting the biosynthesis of proinflammatory prostaglandins. However, unlike many of the traditional NSAIDs (e.g. ibuprofen, naproxen, indomethacin), diclofenac has been found to be several-folds more selective for COX-2 than it is for COX-1 (Table 1-2) [5, 21]. In fact, diclofenac has shown similar COX1/COX2 biochemical selectivity as the selective COX-2 inhibitor, celecoxib [21]. The CV risk associated with the use of diclofenac has been consistently ranked high. For example, a systematic review of observational studies carried out in 2011 and included 30 case control studies

(with 184,946 CV events) and 21 cohort studies (over 2.7 million exposed individuals) found that the overall CV risk observed with diclofenac (relative risk (RR), 1.40; 95% CI, 1.27,1.55) was high and comparable to that observed with rofecoxib (RR, 1.45; 95% CI, 1.33, 1.59) [22]. This was higher than the risk observed with other NSAIDs such as ibuprofen (RR, 1.18; 95% CI, 1.11, 1.25), and naproxen (RR, 1.09; 95% CI, 1.02, 1.16). Even low dose diclofenac (100 mg/day or lower) which can be available without prescription was associated with increased CV risk (RR, 1.22; 95% CI, 1.12, 1.33). This high-risk profile makes diclofenac a good model drug representing the CV risk of various NSAIDs.

Diclofenac is a Biopharmaceutics Classification System (BCS) class II drug, i.e. it is highly permeable, but its solubility in aqueous media is low and not enough for the complete dose to be dissolved in the GI tract. Dissolution is, therefore, the rate limiting step for its absorption. Pharmacokinetic analysis of diclofenac has revealed that the drug is absorbed rapidly and completely when administered orally, intramuscularly or rectally with the potassium salt showing more rapid absorption than the sodium salt when given orally leading to a more uniform absorption [23, 24]. Diclofenac binds extensively to plasma proteins and eliminates mainly through hepatic metabolism (hydroxylation followed by glucuronidation), and very little fraction of the drug is eliminated unchanged [25]. Substantial concentrations of diclofenac are maintained in inflamed tissues, such as the synovium and synovial fluid of inflamed joints in inflammatory arthritis, which are the main sites of action of NSAIDs. Several mechanisms have been suggested to explain this accumulation including [26]: (i) ion trapping, in which the acidic microenvironment caused by inflammation can lead to the diffusion of the unionized drug molecules into the cell interior where they are ionized due to the higher intracellular pH and are trapped, (ii) escape of drug molecules

(protein-bound or unbound) to the inflamed tissues due to inflammation-induced localized hemodynamic changes, and (iii) increase in albumin concentration in the synovial fluid due to increases in vascular permeability and consequently increase in drug concentrations which shows high affinity to albumin.

1.2. Inflammation

Inflammation is a defensive response of the body in the vasculature as a reaction to injury, harmful stimuli or infection [27]. This response is beneficial when it lasts for a short-term leading to repairing of affected tissue structure and function. However, inflammation can become uncontrolled and contribute to the pathogenesis of other serious conditions [28]. Inflammation is usually classified based on its duration and on pathological features as being acute, which lasts from minutes to several days, or chronic, when its lasts for longer periods (months or years). Acute inflammation includes conditions such as acute rhinitis and sepsis, and is characterized by redness, heat, swelling and pain which are attributed to extravasation of plasma and infiltration of leukocytes into the site of injury [29]. This inflammatory response most often resolves and restores tissue to homeostasis. However, persistent presence of infections, hypersensitivity, or noxious agents can lead to chronic inflammation, dominated by infiltration of the tissue by lymphocytes, dendritic cells, and macrophages. Chronic inflammation is a major cause of human inflammatory pathologies, including obesity, diabetes, arthritis, asthma, cancers, cardiovascular diseases and Alzheimer's disease [28, 30]. Arthritis, defined as inflammation of the joints, includes many different conditions including rheumatoid arthritis, osteoarthritis, fibromyalgia and systemic lupus erythematosus among others.

1.2.1. Mechanisms of inflammatory response

The inflammatory response involves the interaction of a network of effector and target cells including for the most part, cells of the reticuloendothelial system (RES) which include circulating and tissue macrophages, monocytes, natural killer cells, neutrophils, lymphocytes, mast cells, endothelial cells, and fibroblasts [31]. These cells and their products including cytokines as well as other mediators (Table 1-3) such as growth factors and eicosanoids cause the most damage from inflammation.

Cytokines are small protein mediators (usually less than 40 kDa) secreted by different cells and modulate the immune response. They are usually classified as being pro-inflammatory (e.g. interleukin-1 (IL-1), tumor necrosis factor-α (TNF-α), γ-interferon (IFN-γ), IL-6 and granulocyte-macrophage colony stimulating factor (GM-CSF)) or anti-inflammatory (e.g. IL-4, IL-10, IL-13, IFN-α and transforming growth factor-β (TGF- β)), even though some cytokines can act as both depending on their concentration and site of action [32]. During an inflammatory response, IL-1 and TNF-α, released from damaged and nearby cells, have a crucial role in initiating and amplifying the inflammatory response leading to a cascade of mediators [33]. These pro-inflammatory mediators act to mobilize and activate leukocytes and enhance the proliferation of B and T cells and the cytotoxicity of natural killer cells, whereas IL-6 causes an increase in the synthesis and secretion of immunoglobulins by B cells. IL-6 is also a major inducer of acute phase proteins including C-reactive protein (CRP), fibrinogen, and mannose-binding lectin which have a role in sustaining inflammation and activating the complement system. IFN-γ is a potent chemoattractant that promotes recruitment of neutrophils and T cells and upregulates major

Table 1-3. Responses from various inflammatory mediators ***(adapted from [37])***

Vasodilation	Increased vascular permeability	Chemotaxis and leukocyte activation
Prostaglandins (PGI2, PGE1, PGE2, PGD2) Nitric oxide (NO)	Histamine Complement components (C3a, C5a) Bradykinin Leukotrienes (LTC4, LTD4, LTE4), Platelet-activating factor Substance P	C5a LTB4 Lipoxins (LXA4, LXB4)
Tissue damage	**Fever**	**Pain**
Neutrophil Macrophage Oxygen radicals NO	Interleukin-1 (IL-1) IL-6 Tumor necrosis factor (TNF) LTB4 LXA4 and LXB4	PGE2 and PGI 2 Bradykinin

histocompatibility complex (MHC)-I expression on target cells leading to enhanced T-cell-mediated cytotoxicity [34].

Leukotrienes (LT), are a class of mediators of inflammation generated by mast cells, basophils, eosinophils, neutrophils, and monocytes. These compounds together with prostaglandins, thromboxanes and lipoxins, are the major oxygenated products, known as eicosanoids, of arachidonic acid. Leukotriene LTB4 is a very potent chemoattractant for various inflammatory cells including neutrophils, monocytes and macrophages and induces adhesion of these cells to the vascular endothelium [35, 36]. It also stimulates the production of a range of proinflammatory cytokines and mediators and consequently has a major role prolonging tissue inflammation. Cysteinyl LTs (i.e. LTC4 and its metabolites LTD4 and LTE4) increase vascular permeability and are potent bronchoconstrictors that have been found to play a role in triggering acute asthma attacks and in chronic asthma [38].

Prostaglandins (PG) are another group of eicosanoids that mediate the inflammatory responses. These products of arachidonic acid, derived in the cyclooxygenases (COX) enzyme (i.e. COX-1 and COX-2) pathway and include PGD_2, PGE_1, PGE_2, $PGF_{2\alpha}$, PGI_2, and thromboxane (TX) A_2, are released out of the cells and exert autocrine and/or paracrine functions. In acute inflammation, prostaglandins induce vasodilatation, and as a result allow other inflammatory mediators to act on dilated venules causing increase vascular permeability [39]. Some prostaglandins including $PGF_{2\alpha}$ and TXA_2 cause smooth muscle contraction and vasoconstriction. In chronic inflammation, prostaglandins are found to enhance the pro-inflammatory effect of cytokines in gene expression at the transcription level in mesenchymal, epithelial, and immune cells.

1.2.2. Diseases associated with inflammation

Research has provided evidence to support that inflammation is an important component of and a pathophysiologic premise for many common diseases which include arthritis, cancer, cardiovascular diseases and many others [28, 30].

1.2.2.1. Cardiovascular disease

In addition to some well-established risk factors for CV disease, a great deal of evidence has found inflammation to be associated with enhanced CV risk [40]. The exact mechanism of this association is not fully understood but is suggested to be through the initiation and progression of atherosclerosis which is implicated in most cardiovascular disease events. In fact, evidence suggests that every step in atherogenesis involves cytokines and other cells and bioactive molecules which are peculiar to inflammation [41]. Therefore, monitoring pro-inflammatory factors such as oxidized low-density lipoproteins (LDL), cytokines including IL-1 and TNF-α,

adhesion molecules, arachidonic acid metabolites, as well as proteins synthesized by the liver such as CRP can aid in understanding the inflammatory process and the CV risk it brings about [42].

The role that inflammatory processes play in the etiology of cardiac disease gained attention when researchers started to look at the potential for pro-inflammatory cytokines to directly affect cardiac receptors and ion channels. A randomized controlled trial (RCT) found that a 3 months treatment of patients with heart failure with etanercept, a recombinant TNF factor receptor fusion protein, resulted in a significant dose-dependent improvement in left ventricular structure and function and showed signs of improvements in patient functional status [43]. In a more recent RCT, the Canakinumab Anti-inflammatory Thrombosis Outcomes Study (CANTOS), it was found that an anti-inflammatory strategy with targeting IL-1β, which resulted in a decrease in CRP with no decrease in LDL-C, reduced CV events in patients with existing atherosclerotic CV disease [44]. This gave clinical evidence that reducing inflammation without affecting lipid levels can reduce the risk of CV disease.

1.2.2.2. Inflammation and cancer

Chronic inflammation considerably contributes to the development of cancer, and there is epidemiological evidence that supports the theory that there is an extrinsic inflammatory pathway that stimulates the progression and in certain cases initiates cancer [30]. The prolonged exposure to inflammatory mediators including the metabolites of arachidonic acid, chemokines, cytokines, and free radicals leads to elevated cellular proliferation and mutagenesis, and the activation of oncogenes, which have the potential to cause cancer. On the other hand, cancer can also cause inflammation by promoting the over expression of the COX-2 enzyme and pro-inflammatory

mediators, which at later stages of tumor growth become controlled by the tumors themselves [45]. The over expression of COX-2 due to solid malignancies has been reported in many studies for colon, prostate, breast, pancreas, and other types of cancer, which suggests a role for COX-2 inhibitors in the treatment plan for cancer patients [46].

1.2.2.3. Neural inflammation, Alzheimer's disease

Alzheimer's disease (AD) is the most common type of dementia, accounting for 60% to 80% of all dementia cases and characterized by loss of intellectual and social skills with memory impairment and an unstoppable progression of cognitive decline [47]. The hallmark of the disease is the accumulation of amyloid-beta (Aβ) peptides in the brain. There is growing evidence which suggests that inflammation may have a contributory role in AD and emerging data points to finding inflammatory processes and oxidative stress prior to appearance of classical signs of disease pathology [48]. The neurodegeneration in AD is associated with activation of microglial cells, brain-tissue macrophages, and increased levels of inflammatory mediators including nitric oxide (NO), reactive oxygen species (ROS), cytokines (TNF-α, IL-1β, IL-6. TGF- β, IL-12, IL-18) and eicosanoids (PGE_2) [49, 50].

Furthermore, the long-term use of non-steroidal anti-inflammatory drugs, which inhibit COX-mediated biosynthesis of prostaglandins and downstream effectors, have been associated with reduced incidence of AD in epidemiologic studies [51]. These observations suggest a role for the management of inflammation in the prevention and delaying the progression of AD. Moreover, they provide a basis to support the need for a better understanding of the inflammatory process in

AD in order to identify potential targets (such as activated microglia) for developing more effective anti-inflammatory treatment of AD.

1.2.2.4. Rheumatoid arthritis

Rheumatoid arthritis (RA) is a chronic autoimmune disease of undetermined aetiology causing inflammation in the synovial membrane of one or multiple joints, and resulting in pain, stiffness, and swelling of the joints [52, 53]. RA patients may experience some periods without symptoms, however, RA is a progressive illness that has the potential to cause joint destruction, functional disability, and even premature death when the condition is unchecked [54]. However, with early and proper control of the disease and with the use of aggressive treatment strategies and therapeutics, patient outcome has been substantially improved in the last two decades rendering RA in many cases a remitting illness [55].

The exact cause of RA is not known; however, many different risk factors have been found to influence the onset of inflammation and the outcome of the condition. Some of these factors are listed in Table 1-4.

1.2.2.4.1. Epidemiology

Rheumatoid arthritis is one of the leading causes of disability in Canada with over 4.6 million Canadian adults (aged 15 years and older) reported having arthritis. In 2010, 272,299 Canadians

Table 1-4. Rheumatoid arthritis risk factors

Risk factor	Description
Old age	While rheumatoid arthritis can develop at any age, it is most likely to develop between the ages of 20 and 50 years. An onset after the age of 60 years, had been found to cause a more rapid decline in functional ability [58].
Female gender	Women are 2.5 to 3 times more likely to develop rheumatoid arthritis compared to men and the peak age of onset in women is about 10 years earlier than that of men [59]. This suggest a hormonal link in the development of rheumatoid arthritis.
Genetic Factors	A person is more likely to develop rheumatoid arthritis if there are other family members with this condition or with some other autoimmune disorder. Certain genes are known to be associated with rheumatoid arthritis; however, it is still not clear which of these genes are responsible for susceptibility to rheumatoid arthritis and which are for its severity. As an example, it is suggested that while a normal person has a likelihood of 0.8% to develop rheumatoid arthritis, the likelihood of a member of two identical twins to have rheumatoid arthritis increases to 15% if the other member has the condition [60].
Weight	Excess weight has been found to be associated with the development of rheumatoid arthritis. Results of a study suggest that women with a higher body mass index (>30 Kg/m^2) might be more likely to develop rheumatoid arthritis [61]. In addition, excess weight may worsen arthritis symptoms by straining joints and causing the breakdown of joint tissues.
Smoking	Research has linked smoking to rheumatoid arthritis [61].
Infection	In a substantial proportion of the cases, it is found that rheumatoid arthritis starts after an infection episode. While no single organism has been suggested to cause rheumatoid arthritis, the Epstein-barr virus has been linked to rheumatoid arthritis for over 10 years and so are mycobacteria [59, 62].

were living with RA, which is a prevalence of 0.9% of the adult population [56, 57]. The annual incidence rates for RA are expected to increase, and by 2040 the number of new cases of RA are expected to rise to an estimated 23,732 cases from around 19,000 new cases in 2015 [57]. Moreover, the prevalence of RA is expected to continue to be higher among women than men (average women: men ratio = 2.33:1) over the next 30 years. RA can occur at any age, but the age of onset is usually 25-50 years and the condition peaks in the fourth decade of life. In Canada, the majority (46%) of the new RA cases are among the elderly aged over 60 years old.

1.2.2.4.2. Pathophysiology and clinial manifestations

The fundamental pathogenesis of RA is the formation of the pannus because of sustained inflammation and hypertrophy of the synovium (Figure 1-1). The Pannus is a sheet of invasive cellular tissue that is continuous with the synovial lining and causes erosion of bone and cartilage at the margin of joints [58]. This process is mediated by the production of various inflammatory cytokines such as TNF-α, IL-1, and IL-6 which are produced by mast cells, macrophages, fibroblasts, and the antigen activated T lymphocytes accumulated within the joint [63]. At the cellular level, these mediators stimulate synoviocytes to produce cartilage-degrading enzymes resulting in destruction of bone and cartilage. One group of these enzymes is the metalloproteinases, which are secreted from synoviocytes and chondroblasts in response to cytokines [62].

The hallmark of RA is an additive symmetric swelling of peripheral joints particularly small joints of the hands and wrists. The onset of the condition is variable, but for most of the cases is a slow

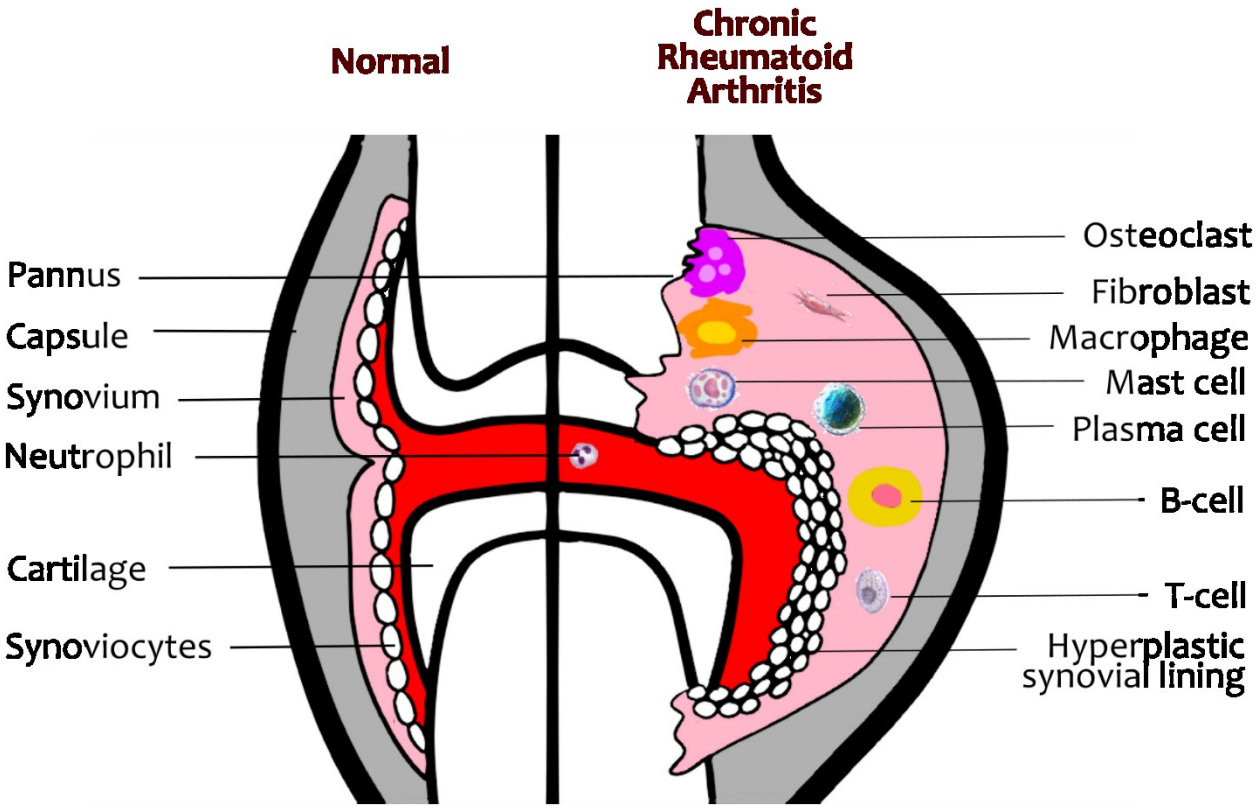

Figure 1-1. A normal joint and a joint affected by rheumatoid arthritis ***(Adapted with modifications from [65])***

onset which progresses with steady deterioration of functional ability and little overall systemic upset [62, 63]. In the long run the patients suffer severe disability. Less common is an acute onset in which the disease progresses more rapidly with widespread joint involvement and systemic complications. This type of onset affects less than 15% of the RA patients [64]. Symptoms vary in terms of intensity, localization, and duration. Pain is the most common symptom which usually moves from joint to joint, increases with immobility, and is not relieved by rest. RA patients also suffer from morning stiffness which usually lasts for over 30 minutes and can remain throughout the day. Swelling of the joints with an apparent redness and warmth is another symptom which is caused by fluid accumulation, proliferation of soft tissues or enlargement of bone. In addition tothese articular symptoms, there are several systemic symptoms such as weight loss, malaise, lethargy, and fatigue which are commonly experienced by RA patients. Table 1-5 lists many of these extra-articular manifestations of RA.

1.2.2.4.3. Treatment for rheumatoid arthritis

The ongoing progresses in the knowledge of the pathogenetic mechanisms of RA and the availability of innovative approaches have led to a significant change in the treatment approach used for the management of the condition. Historically, the treatment for RA was introduced in a pyramidal manner where first line agents such as analgesics and non-steroidal anti-inflammatory drugs (NSAIDs) were used to relieve symptoms [66, 67]. After several months or even years, a second line agent among the disease-modifying anti-rheumatic drugs (DMARDs) such as methotrexate or sulfasalazine was introduced. In case of DMARD failure, another drug in this category would have been tried until all the second-line agents have been used. Finally, third line agents such as corticosteroids were used [66].

Table 1-5. Extra-articular manifestations of rheumatoid arthritis ***(Adapted with modifications from [72])***

Affected tissue or organ	Extra-articular manifestations
General symptoms	Weight loss, fever, prolonged early morning stiffness, fatigue, generalised muscle weakness, low mood and depression
Inflammatory-process associated feature	Normochromic-normocytic anaemia, secondary Sjögren's syndrome, sarcopenia Osteoporosis
Skin	Rheumatoid nodules, cutaneous vasculitis
Eyes	Keratoconjunctivitis sicca, scleritis, episcleritis, peripheral ulcerative keratitis, vasculitis involving retinal vessels
Pulmonary system	Pulmonary nodules, pleural effusion, interstitial lung disease
Cardiovascular system	Pericarditis, myocarditis, cardiac amyloidosis, coronary vasculitis, arrhythmia valve diseases, congestive heart failure, ischaemic heart disease
Nervous system	Cognitive dysfunction, cervical myelopathy, central nervous system vasculitis, rheumatoid nodules located within the central nervous system or meningitis, stroke, mononeuritis multiplex, sensory peripheral neuropathy
Kidneys	Glomerulonephritis, interstitial, secondary amyloidos
Haematological system	Felty's syndrome

However, it is currently known that RA is an aggressive disease which causes major destruction to the joints within two years of onset [68]. There is also increasing evidence that treatment in the early stages of RA with DMARDs can significantly increase the potential for positive patient outcome and prevention of irreversible damage [67]. Moreover, there is an increased awareness of the toxicity of NSAIDs and the fact that clinical studies as well as data from patient registries have shown no much increase in serious complications from some DMARDs compared to high dose NSAIDs, and long-term use of corticosteroids [69-71]. This support the current widely accepted

therapeutic approach which relies on a more aggressive treatment with DMARDs for early RA and investigates all the available treatment options.

Disease-modifying anti-rheumatic drugs (or frequently referred to as DMARDs) are a class of medications which have the potential to reduce or prevent joint damage and preserve joint integrity and function. Although both NSAIDs, discussed in the following section, and DMARD agents improve symptoms of active RA, only DMARD agents have been shown to alter the disease course and improve radiographic outcomes [73]. The most commonly used DMARD agents include methotrexate, leflunomide, sulfasalazine, and hydroxychloroquine. These agents have different chemical structures and different mechanisms of actions; however, most of them inhibit the immune responses of monocytes and of T and B lymphocytes [74].

DMARD agents in general are relatively slow acting, with a delay of one to six months before any results are seen. While the effectiveness of DMARDs cannot be predicted for the individual patient, it is found that some patients fail to respond adequately to DMARD therapy and many others fail to maintain a response [75]. Each DMARD has specific toxicity or side effects that require careful monitoring. The choice of DMARD is therefore usually based on a balance between efficacy and adverse effects. Current guidelines recommend the RA treatment to start as early as possible with DMARDs to control the symptoms and to delay the progression of the condition. According to the Canadian Rheumatology Association (CRA) recommendations for the pharmacological management of RA, patients with persistent synovitis should be started on a DMARD as soon as possible and those with active RA should be monitored for disease activity as frequently as every 1 to 3 months [73].

In recent years, advances in biomedical science have been successful in explaining the role of cytokines and other mediators of chronic inflammation in the onset and progression of RA and in bringing our understanding of this role to the level were new therapeutic interventions were generated. In fact, a major breakthrough in the treatment of RA was the development of biological agents which mainly counteract the effects of cytokines such as TNF-α and IL-1 in the rheumatoid synovium [76]. Unlike traditional RA treatments, these biological agents are the first RA therapies that have a well-defined mechanism of action, each inhibiting a single cytokine [77]. The current biological agents licensed for RA in Canada include: TNF- α inhibitors (etanercept, infliximab, adalimumab, golimumab, and certolizumab pegol), T cell costimulatory inhibitor (abatacept), B lymphocyte-depleting agents (rituximab), IL-6 antagonist (tocilizumab, sarilumab), IL-1 antagonist (anakinra), and IL-12 /23 antagonist (ustekinumab) [73]. These biological agents have been shown to rapidly reduce disease activity and improve the outcomes of the condition in patients with active RA, when used alone, or in combination with methotrexate [77].

Systemic corticosteroids have long been used in the management of RA because of their anti-inflammatory and immunoregulatory activity. The major mechanisms involved in their anti-inflammatory effects include down-regulation of the production of inflammatory cytokines (TNF factors, IL-1, etc.) and inhibition of COX II activity. These agents provide rapid relief from inflammatory symptoms in RA and suppress disease activity as detected radiographically [78].

The major role of corticosteroids in recent year has been as bridge therapy where oral steroids at lower doses are used along with DMARDs in the first 2-3 months of the treatment. Once the DMARD commences its action, the corticosteroid is tapered off and stopped [79]. Corticosteroids

may also have a role as a rescue therapy in patients with aggressive disease which cannot be controlled adequately with a combination of DMARDs.

1.2.3. Effect of inflammation on pharmacokinetics/pharmacodynamics

Inflammation and inflammatory conditions have been reported to alter the pharmacokinetics of numerous drugs leading to higher drug plasma concentrations and causing a variability in response to these agents as well as increasing the risk of side effects [1, 80]. For example, levels of the beta blocker agent propranolol have been found to be higher than normal in patients with inflammatory diseases [81], as well as in rats with inflammation [82, 83]. Similarly, RA was found to cause an increase in the plasma concentration of the calcium channel blocker verapamil, an effect that was thought to be due to altered protein binding and/or decreased hepatic clearance [84].

One of the mechanisms believed to be responsible for the altered drug disposition during inflammation is the downregulation in the expression of drug-metabolizing enzymes and transporters, which can lead to higher drug plasma concentrations. *In vitro* and *in vivo* investigations have shown decreased levels of drug transporting proteins including members of the multi-drug resistance (MDR), multi-drug resistance-associated protein (MRP), and organic anion transporter (OATP) families during inflammatory periods which is proposed to be due to the involvement of various pro-inflammatory cytokines including IL-1β, IL-6, and TNF-α [85]. Furthermore, these cytokines are also implicated in the observed downregulation of the expression and activities of most CYP enzymes, involved in the hepatic metabolism of drugs, during inflammatory periods or during exposure to infections, thus leading to a decrease in the capacity of the liver and other organs to metabolize the drugs [86].

Inflammation and inflammatory conditions have also been found to alter the pharmacodynamics of drugs, which appears to depend on the severity of the inflammatory response. For instance, in our lab it was found that despite increased plasma drug concentrations, the use of verapamil in RA patients was associated with reduced efficacy as measured by prolongation of PR interval and atrioventricular node block [84]. However, patients on remission from active disease, due to infliximab or other anti-rheumatic therapy, showed relatively normal verapamil pharmacokinetics and pharmacodynamics [87].

In the heart, inflammation has been found to alter some pharmacological responses by downregulating target receptors leading to reduced pharmacodynamic effect despite increased plasma drug concentration. These include (i) proteins involved in the action of the calcium channels, which could explain the reduced effect reported for verapamil in RA patients [84], (ii) proteins involved in the actions of the potassium channels, which could explain the reduced response to sotalol, a β-adrenergic receptor and potassium channel antagonist, observed in an animal model of inflammation [88], (iii) and β-adrenergic receptors which could explain the reduced effect of propranolol, a β-adrenergic receptor antagonist, in an animal model of inflammation [89]. These effects are associated with over expression of pro-inflammatory cytokines and other mediators of inflammation and substantially add to the variability in response that is attributed to inflammation.

1.3. Nano-delivery systems: an overview[1]

Since early 20th century, Paul Ehrlich, the director of the Royal Institute for Experimental Therapy at Frankfort-on-Main, coined the phrase "Magische Kugel" or magic bullet to explain his ideal drug that can specifically and exclusively target the diseased tissue without affecting the healthy organs of the body [90]. His vision has been inspirational. Numerous research efforts since then have focused on creating drug delivery systems that can come close to the specificity required to create the "magic" he envisioned. In practice, while most research contributions were not completely successful in developing the magic bullet, they provided delivery systems capable of tackling problems associated with the administration of many drugs by one or a combination of following means:

(a) *Enhancing bioavailable drug concentration:* One of the challenges with traditional dosage forms is the high proportion of the drug that is "lost" enroute to the systemic circulation. Different factors that contribute to this loss include poor drug solubility, incomplete drug permeability, or both. Nano-delivery systems have been used as solubilizing agents or tools to enhance drug permeability through different routes of administration.

(b) *Protecting the drug from early elimination:* Early enzymatic degradation or elimination of the drug through kidneys could be an obstacle in obtaining the required drug concentration for

[1] Part of this section has been published:

Al-Lawati H, Aliabadi H.M, Makhmalzadeh B.S, Lavasanifar A. Nanomedicine for immuno-suppressive therapy: achievements in pre-clinical and clinical research. Expert Opinion on Drug Delivery 2018: 15 (4), 397-418

therapeutic effect. Peptides [91], and short interfering RNAs (siRNAs) are examples of molecules that need to be protected in biological fluids to exert an effect. For these drugs, the necessity for a substantial increase in the required doses of medication due to drug loss in body possesses direct risks. The emergence of potentially toxic metabolite(s) of the active ingredient can pose additional risks [92, 93]. Such risks can be mitigated by the use of nano-drug formulations.

(c) *Limiting the distribution of the drug to undesired healthy organs and tissues:* Uncontrolled distribution of the drug to non-target organs and tissues is a main reason for unwanted side-effects [94]. This has been the major focus by nanotechnology research during the past few decades; to achieve novel drug formulations that can reduce non-specific distribution of drugs to healthy organs and reduce their side effects by doing so. Several successful examples of nano-formulations of different anti-cancer drugs and antifungals achieving reduced drug toxicity are currently in use in clinic.

(d) *Increasing drug distribution in the diseased organs and cells:* Enhanced distribution of a drug to the site of the drug's action can potentiate its therapeutic activity and fulfil an important part of Ehrlich's vision. Restricting the therapeutic effect to the affected cells or organs has been one of the main missions of targeted delivery systems. In this context, passive targeting of anti-cancer agents to the tumor tissue based on enhanced permeation and retention (EPR) effect through the use of nano particulate delivery systems has attracted the most attention, to date [95]. Delivery of different cargos to phagocytic cells, e.g., dendritic cells, by taking advantage of the natural capacity of these cells for uptake of nanoparticles (NPs) has also been applied successfully.

1.3.1. Design of polymeric micelles for drug delivery applications

Polymeric micelles are advanced nano-drug delivery systems which are created from amphiphilic block copolymers that spontaneously self-assemble in aqueous media [96]. They typically consist of a hydrophobic core which acts as a microenvironment for the encapsulation of active agents (e.g., water insoluble drugs) and a hydrophilic shell that interacts with the biological environment and can act as a physical barrier to protein binding and opsonization during systemic administration.

The superiority of polymeric micelles as delivery systems stems from the fact that they can be tailor-made for the desired application. In general, polymeric micelles possess spherical morphology when the soluble segment predominates; however based on the size of the core/shell segments, other morphologies can be fabricated, such as rods, lamellas, or vesicles (polymersomes) [97]. Polyethylene oxide (PEO) is the most widely used non-ionic hydrophilic segment in micelles due to its ability to sterically stabilize the nanocarriers reducing their tendency to aggregate during application or storage [98]. Nevertheless, micelles based on other hydrophilic segments such as poloxamer, poly(N-vinyl pyrrolidone) and poly(N-isopropyl acrylamide) have also been studied. For the hydrophobic segment of micelle-forming amphiphilic block copolymers, a more diverse variety of blocks have been studied including biodegradable poly(esters) (e.g. poly(ε-caprolactone), poly(D,L-lactic acid), poly(glycolic acid), poly(lactic-co-glycolic acid)) as well as poly(amines), and poly(L-amino acids) [99]. Moreover, alterations in the chemical structures of these core-forming blocks have been considered and have enabled fabrication of micelles with better characteristics including improved drug encapsulation, enhanced thermodynamic and kinetic stability, and controlled rate of drug release [100]. Chemical

modifications of the core and/or shell forming blocks have also enabled the design of "smart delivery systems" which target specific organs or tissue by attaching specific ligands on the surfaces or by making them stimuli-responsive.

One of the main advantages of polymeric micelles is their ability to solubilize hydrophobic molecules within their core which can provide the encapsulated drug with chemical and physical stability and can improve its water solubility. Micelles possess key characteristics that make them stand out among other nanocarriers. These include their high loading capacity, low polydispersity, and their small size usually in the range (10 - 100 nm), which is small enough to allow for diffusion and passive targeting and accumulation into inflamed tissues through their leaky vasculature, but is also large enough to escape renal excretion or extravasation at healthy tissues [101]. Moreover, when poly(ethylene oxide) (PEO) is used as the hydrophilic shell, micelles avoid the rapid uptake by the RES, and hence can circulate in the blood for longer time. This makes them suitable vehicles for the development of injectable depots and gives the carrier better chance for drug targeting at inflamed sites [102].

There are three major approaches that have been investigated for the encapsulation of drugs in the core of polymeric micelle: (1) chemical conjugation, (2) physical entrapment, and (3) poly-ionic complexation.

1.3.1.1. Chemical conjugation

In this encapsulation approach, a polymer-drug conjugate is created by forming a hydrolysable bond between the functional groups of the backbone of the hydrophobic core of the amphiphilic block copolymer and the drug. For example, the conjugation on PEO-*block*-poly(esters) can be

carried out through the formation of a covalent bond between the terminal hydroxyl group of the core-forming block and the functional group on the drug molecule [100]. The polymer-drug conjugate is able to self-assemble to form core-shell structured micelles. Drug release from such micelles requires drug cleavage from the copolymer backbone by hydrolysis, and thus these micelles can provide a delayed and specific release of drug at the site of action and prevent its premature release in the systemic circulation. Moreover, the use of stimuli responsive linker to form the drug-polymer conjugate can be employed to control drug release when excessive stability, that may render the micelles inactive at the site of action, is anticipated [99].

1.3.1.2. Physical entrapment

Physical entrapment of the drug within the micellar core is a more attractive option since it is not limited to drugs with reactive functional groups on their structures and does not lead to modifications of the drug molecule such as forming polymer prodrugs which may affect its PK. In this approach, drug is entrapped in the core segment of the micelle which acts as a micellar nanocontainer when hydrophobic interactions (which occur since most drugs contain hydrophobic moieties in their chemical structures) or hydrogen bonds are formed between the drug and the core forming segments of the micelles. Several factors have been reported to influence the performance (e.g. degree of drug encapsulation, rate and extent of drug release, etc.) of micelles based on this approach, and in Table 1-6 we list some of those which affect the rate of drug release.

1.3.1.3. Poly-ion complexation

Poly-ion complexation is a micellization design that is suitable for charged therapeutics such as charged drugs, peptides or DNA. In this approach, oppositely charged ionic copolymers (two or

Table 1-6. Factors that affect the rate of drug release from polymeric micelles

Factor	Description
Compatibility between the drug and the core-forming block	The degree of compatibility between the drug and the core-forming block (e.g. as measured by the Flory-Huggins interaction parameter) has been reported to influence the release kinetics of the drug from the micelles. Increased compatibility between the core forming block with the drug considerably decreased the rate of drug release [99, 103].
Physical state of the micelle core	Diffusion of incorporated drug molecules from micelles with glassy cores (high viscosity) is slower in comparison to those from micelles with more amorphous cores [100, 104].
Physical state of the drug	The drug molecules, if it is in the dissolved state in the core forming block polymer, it can decrease the glass transition temperature of the polymer, making the drug release faster. On the other hand, crystallized drug molecules can act as reinforcing filler and enhance the glass transition temperature resulting in a decrease in the drug release rate [100, 103, 104].
location of the incorporated molecules within polymer micelle	The location of the encapsulated drug in the micelle (whether it is mainly in the core or possibly also at the interface between the core and the corona) determines its rate of release. Hydrophobic drugs tend to solubilize in the micelle core, while less hydrophobic molecules may reside at the core/shell interface or even in the shell segment. The release of the latter molecules is generally more rapid and accounts for the" burst release" observed [99, 104].
The length of the core forming block	The release rate of a drug encapsulated in the core of polymeric micelles inversely correlates with the length of the core forming block. The length of the core, however, does not influence the burst release or the release rate [99, 103, 104].
Molecular volume	The molecular volume of a drug (i.e. the volume occupied by one mole of the drug) encapsulated in the core of micelles affects its release rate. In general, it is found that the larger the size of the drug molecule is, the slower the release rate obtained. [99, 103, 104].
Temperature of the environment	A change in temperature can affect the structure of the micelle core-forming block and therefore, can affect the drug release [103]. In a study, a drop in temperature from 43° to 37° resulted in a 36% increase in the release of methotrexate loaded in micelles based on biotin-poly(ethylene glycol)-*block*-poly(N-isopropylacrylamide-co-N-hydroxy methyl- acrylamide) in 96 h due to a temperature-induced structural change in the micelles [105].
Stability of the micelles	Factors which affect the stability of the polymeric micelles such as cross-linking can affect drug release rate [100, 104].
Method of drug incorporation	The method used for the drug incorporation in polymeric micelles can affect the release rate by influencing the extent of drug loading, localization of drug, or the physical state of the drug [100].

more) attached to hydrophilic segments (e.g. PEO) and drug molecules spontaneously assemble in aqueous media due to electrostatic interactions to form poly-ion complexes which isolate form the aqueous exterior to form the core segment that is surrounded by the hydrophilic shell [99].

1.3.2. Methods of physical drug encapsulation

Different methods can be used for the physical entrapment of the drug into polymeric micelles, including: direct dissolution, dialysis, solvent evaporation, and col-solvent evaporation techniques among many others. Some of these methods are described below (Figure 1-2).

1.3.2.1. Direct dissolution

This method can be used when the copolymer is marginally soluble in water (e.g. Pluronics). First the micelles are prepared by adding the copolymer to water or an aqueous buffer such as phosphate-buffered saline (PBS) under heating and stirring to induce micellization. The drug is loaded either by simultaneously adding it with the copolymer, or by adding it to preformed micelles. In the latter approach, the drug can be dissolved in a vial in a solvent such as acetone, which is allowed to evaporate [104]. The micellar solution can then be added to the vial to incorporate the drug in the micelles. Alternatively, the drug can be added to the micellar formulation as an oil/water emulation with the organic solvent being allowed to evaporate. Direct dissolution, however, is not feasible for many of the copolymers researched [100].

1.3.2.2. The dialysis methods

In the dialysis method, the copolymer and drug are first dissolved in a common water miscible solvent (e.g. ethanol, N-N-dimethylformamide). This is followed by the dialysis of the mixture

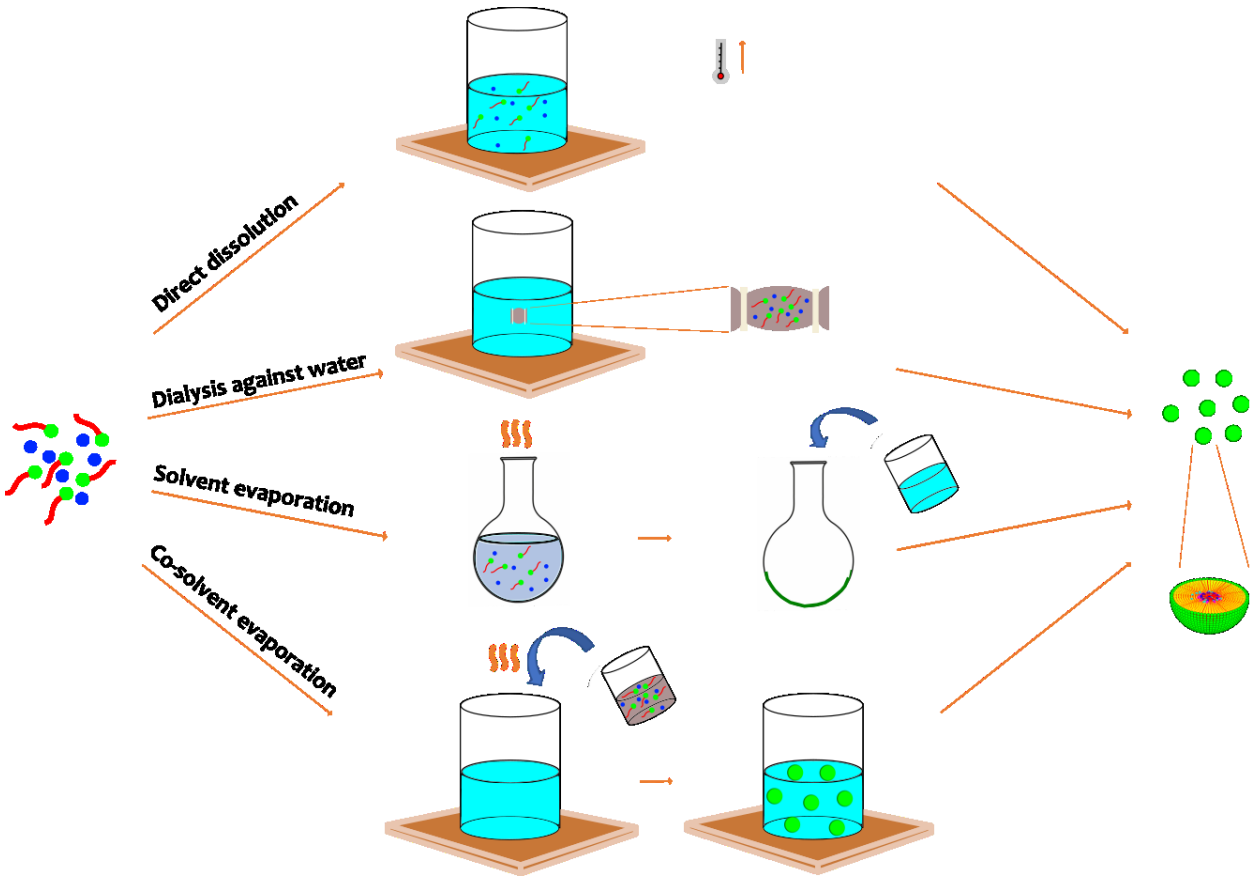

Figure 1-2. Methods of polymeric micelle preparation and physical drug encapsulation

against water, where the gradual replacement of organic solvent with water triggers micellization [106]. The dialysis method is a widely used method in research and is very versatile as it applies to a range of copolymers with low solubility and allows the use of a range of organic solvents including high-boiling solvents such as dimethyl sulfoxide (DMSO). However, the dialysis method may be more suitable for laboratory setting and less feasible for large scale production [100]. Moreover, the lengthy dialysis procedure may cause the release of drug already encapsulated.

1.3.2.3. The solvent evaporation method

In the solvent evaporation method (also referred to as dry-down method), the drug and copolymer are dissolved in a common volatile organic solvent (ethanol, chloroform, acetonitrile, or dimethylformamide (DMF) in a round-bottom flask. The organic solvent is evaporated leading to the formation of a thin film of polymer and drug. The thin film is subsequently dehydrated with water and under shaking leading to the formation of micelles. This final process, however, may only be possible for copolymers with high hydrophilic-lipophilic balance (HLB) [100].

1.3.2.4. The co-solvent evaporation method

In the co-solvent evaporation method, both the copolymer and drug are dissolved in a common volatile organic solvent (e.g. acetone, Tetrahydrofuran (THF)) to form the organic phase. The organic phase is mixed with the aqueous phase which is a non-solvent for the core-forming block under stirring, triggering micellization and encapsulation of the drug as the organic phase evaporates. Several factors are known to influence the properties of the resulting micelles, including the type of solvent used, the ratio of the aqueous phase to the organic phase, and the

order of adding the two phases (i.e. organic phase added to the aqueous phase or vice versa). These factors can be controlled to optimize the micellar formulation [107].

1.4. Nanomedicine for the effective and safe delivery of non-steroidal anti-inflammatory drugs: a review of preclinical research

Nanotechnology based drug delivery systems have been researched tremendously, as means to improve the therapeutic index of different drugs. Most often this has been achieved through an increase in the levels of drugs causing toxic side effects rather than a decrease in drug's effective doses by the nano-delivery systems. The mechanism by which nano-technology devices increase drug product safety, is either by replacing the toxic solubilizing agents by safe nano-delivery systems that can rapidly make the incorporated drug available to the systemic circulation; and/or by redirecting the drug from normal tissues towards the diseased site. Depending on the drug and its intended route of administration, nano-delivery systems have also been used to enhance the absorption of drugs through different biological membranes, and/or provide means for sustained drug delivery via local or systemic administration. Such properties were behind the successful translation of several nano-formulations such as Doxil, Abraxane, DepoCyt, Genxol, AmBisome, etc., from preclinical research to clinical use [108].

Non-steroidal anti-inflammatory drugs (NSAIDs) are an old class of drugs in extensive clinical use for arthritis and other inflammatory conditions. The clinical performance of NSAIDS, as anti-inflammatory, antipyretic and analgesic drugs can potentially benefit from nano-drug delivery by reducing drugs; toxicity profile, increasing drug's dissolution thus reducing drug's onset of action, and/or increasing their permeability through biological membranes [109]. The high cost and

difficulty in the generation of nano-technology products in large scale, have limited the progress of nano-pharmaceuticals for this class of drugs to clinic, however. Numerous nanodelivery systems have been investigated for different NSAIDs for various related disease conditions. Herein, we will provide an overview on the development of nano-delivery systems for NSAIDs with a focus on the effect of nanodelivery on the pharmacokinetics and pharmacodynamics of the delivered drugs in preclinical setting.

1.4.1. Merits of the nanodelivery of non-steroidal anti-inflammatory drugs (NSAIDs)

Non-steroidal anti-inflammatory drugs (NSAIDs) are a chemically diverse group of agents (Table 1-1) which are among the most widely used medications worldwide with demonstrated activity in controlling inflammation and pain that associate various conditions including rheumatoid arthritis, osteoarthritis, ankylosing spondylitis, gout, dysmenorrhea, dental pain, headache [109]. These agents exert their anti-inflammatory, antipyretic, and analgesic effects by inhibiting the biosynthesis of prostaglandins and prostanoids derived from arachidonic acid by blocking the activities of the cyclooxygenase enzymes (COX), COX-1 and COX-2, at various degrees.

There are several ways, by which nanodelivery systems can enhance the clinical performance of NSAIDs. Most NSAIDs are weak acid and are classified as Biopharmaceutics Classification System (BCS) class II drugs because of their low aqueous solubility at acidic pH, even though they show relatively high bioavailability following oral administration [110]. However, the onset of absorption of these agents greatly depends on the dissolution of drug from the dosage form, which can substantially delay the onset of analgesic effect [111]. Nanodelivery systems, by enhancing the solubility of NSAIDs, can provide a rapid rise in plasma drug concentrations and

hence, can accelerate the onset of analgesia which may be desired in the management of acute episode of pain such as dental pain or pain following surgeries [112]. Moreover, by prolonging the systemic circulation of these agents and sustaining their release, nanodelivery system can enhance the efficacy and safety of these agents for chronic use such as in rheumatoid arthritis or osteoarthritis.

A major deterrent to the chronic use of most NSAIDs is the range of adverse effects that associate these agents including gastrointestinal (GI) as well as renal side effects in addition to an increase in the cardiovascular (CV) risks to patients. Interestingly, the mechanism that is responsible for the anti-inflammatory effect of NSAIDs is also suggested to be responsible, at least in part, for many of these side effects. The risk of GI and CV complications is believed to be linked to the relative selectivity of the different agents to inhibit the two COX isomers even though evidence to support this assertion are lacking [109, 113].

Extensive evidence suggests that the GI side effects of most acidic NSAID arise, in part, from their contact with the mucosal epithelium [114]. This topical interaction can induce gastroduodenal mucosal injury which can lead to local and systemic toxic effects and can impair the defensive properties of the mucosa. Encapsulation of NSAIDs in nano-delivery systems can reduce their contact with the mucus layer following oral administration, thus reducing their topical irritating effects on the epithelium resulting in a substantial reduction in the GI side effects [115].

In terms of reducing the systemic toxicity, the superiority of nano-particulate delivery systems stems from their ability to favorably alter the pharmacokinetics and biodistribution of the encapsulated NSAIDs keeping them away from sites of drug toxicity, such as kidneys and heart.

To that effect, nanodelivery systems possessing the appropriate composition and particle size have been found to preferentially accumulate in tissues with inflammatory pathologies, such as rheumatoid arthritis, through the enhanced permeability and retention effect (EPR) [116]. This passive targeting mechanism and other active targeting strategies such as the targeting of activated macrophage expressing folate receptors and abundantly present in the inflamed synovial membrane by folate linked nanodelivery systems have been explored to improve the therapeutic index of NSAIDs [117].

Nanodelivery systems can improve the safety of NSAIDs by providing viable means for their localized administration limiting their systemic exposure. NSAIDs have long been administered orally or parenterally even when local anti-inflammatory effect is desired. The currently available topical formulations of NSAIDs are favored over oral NSAIDs mainly because they present fewer side effects. However, there are no convincing evidence that show these topical formulations to be as effective as oral ones [118]. Nano delivery systems particularly with the addition of penetration enhancing components and techniques may improve the dermal delivery of NSAIDs to deeper layers of the skin and with minimum systemic exposure [119]. Alternatively, the formulations can provide enhanced transdermal delivery of the NSAID agents where drugs reach the systemic circulation while prolonging the release of the loaded drug [120]. Such formulations can reduce the GI side effects of NSAIDs and/or reduce the frequency of NSAID use.

Nanodelivery systems can also be designed to enhance the localized delivery of NSAIDs through parenteral administration, such as intraarticular or subcutaneous injections to inflamed joints. Such formulations are usually designed to prolong the residence of the encapsulated NSAID at the

inflamed site and regulate its release, providing a sustained therapeutic activity in order to reduce the need for frequent injections [121].

Ocular administration of NSAIDs has also been widely considered, as a less toxic alternative to ocular corticosteroids, for the relief of eye inflammation and pain associated with ocular surgeries such as cataract and refractive procedures. Several formulations of NSAIDs with relatively favorable solubility profiles have been approved for these indications and others are being explored [122]. However, these formulations face several challenges including limited drug delivery to the anterior and posterior segment of the eye due to wash out by tears; and/or corneal barrier function that hinders drug penetration [123]. Nanodelivery systems having the appropriate size and surface composition can substantially improve the corneal permeation of NSAIDs and sustain their release. As a result, the ocular bioavailability of NSAIDs can be improved without use of any pH adjusting excipients that can cause eye irritation [124]. Nanodelivery systems can potentially encapsulate a much wider range of NSAIDs than currently used in the eye, and thus expand the therapeutic choices and scope of clinical use for ocular NSAIDs.

It has always been thought that NSAIDs can be used for off-label therapeutic indications. In fact, there are reports which support disease-modifying properties of NSAIDs in spondyloarthritis [125] and Alzheimer's disease [126]. However, the safety profile of these agents has limited the range of doses that can be considered for such indications. For example, while observational studies have found an association between NSAID use and decreased risk of developing Alzheimer's disease, clinical trials failed to find such an association. This has been attributed, at least partly, to the low NSAID doses used [127]. By improving the safety profile and biodistribution of the

encapsulated NSAIDs, nanodelivery systems can permit the use of higher doses of the encapsulated drugs opening the door for research for their off-label use in other disease conditions.

1.4.2. The review of pre-clinical *in vivo* research on the nano-delivery of NSAIDs

We identified published reports on the nanodelivery of NSAIDs through a systematic search of PubMed from inception until December 2018. Key words used in the search included (i) the different nanodelivery systems, e.g. nanoparticle, liposome, micelle, etc., (ii) the various conditions, e.g. osteoarthritis, rheumatoid arthritis, pain, inflammation, etc., (iii) and the various NSAIDs listed in Table 1-1. We examined the retrieved reports and include in this review those which presented preclinical research on nanocarriers of NSAIDs, where we consider nanocarriers to be colloidal systems in the size range of 1-500 nm. A summary of the studies and their main elements stratified by route of administration is given in Tables 1-(7-11). The studies are classified in the following section, based on the key intended benefit of nanotechnology products for NSAID delivery in different indications, where the benefits are as assessed and reported by the authors.

1.4.2.1. Nanodelivery for enhancing the solubility and bioavailability of NSAIDs

NSAIDs, in general, show poor water solubility and therefore present variable bioavailability when administered orally. Encapsulation of these agents in nanodelivery systems present an attractive option to improve their oral bioavailability and also to permit their use in parenteral and liquid dosage forms. Celecoxib, a diaryl substituted pyrazole and a selective inhibitor of COX-2, is a practically water insoluble NSAID (solubility ~ 3 μg/mL). It shows considerable inter- and intra-subject variability in its pharmacokinetics in patients. In a study by Mennini *et al*, several nano-formulations were developed encapsulating celecoxib in polymeric micelles based on ammonium

Table 1-7. Preclinical studies on the parenteral nano-delivery of NSAIDs

NSAID/ Carrier	Indication, route	Main Composition	physicochemical properties*	Key results	Ref
Aceclofenac					
SLN	OA, *iv*	Tristearin, HSPC, chondroitin sulfate	Size: 154.2 nm; PDI: 0.4; ZP: 19.8 mV; EE: 65.4%	↑ uptake in knee joints & prolonged control of OA	[128]
Aspirin					
CD	Cervical cancer, *ip*	Hydrazine monohydrate	Size: 2-5.5 nm	↑ anti-inflammatory, ↓ side effects	[129]
Celecoxib					
SLN	Arthritis, *ia*	C888, Poloxamer 407, sucrose	Size: 257 nm; EE: 98.75%	↑ retention in inflamed joints, ↓ systemic levels	[130]
Diclofenac					
NP	INF, *iv*	Ionosilica (ammonium substructure)	Size: 150 nm; ZP: 31.3	↓ lipopolysaccharides-induced inflammation	[131]
PM	INF, *iv*	DFEE, PEO-poly(ester)s	Size: 27.9-50.3 nm; PDI: 0.21-0.49; EE: 41-82%	SR, improved characteristics	[132]
LIPO	INF, *iv*	HSPC, Chol, DCP, DLA, DLQ	Size: 135-186 nm; ZP: ~ ⁻34 - ⁻47 mV; EE: ~29-35%	↑ therapeutic availability at inflamed sites, ↑ AUC	[133]
LIPO	INF, im	PC, Chol, α-tocopherol	Size: ~39.5 nm; PDI: ~0.29;	Protection against local tissue damage	[134]
NP	*Im*	PLA, Epikuron 170, benzyl benzoate/ Miglyol 810	Size: 171-252 nm	↓ muscular damage caused by	[135]
LIPO	OA, *ia*	Phospholipon 90G, DPPE, collagen, hyaluronan	EE: 79, 87%	Prolonged control of inflammation in OA	[136]
LGS	RA, *ia*	DMPC, Chol, DCP	EE: 10.8%	↑ anti-inflammatory efficacy	[137]
Etoricoxib					
NP	RA, *iv*	Bovine serum albumin, folic acid	Size: 215.8 nm; ZP: ⁺7.8 mV; EE 72%	targeting potential to activated macrophages	[138]
Flurbiprofen					
PN	Acute injury, *iv*	Span 20 & 80, cholesterol, sorbitol	Size: 153-283 nm; E[91]E:60-94%	SR & ↑ AUC, $t_{½}$, & MRT	[139]
LIPO	Arthritis, *iv*, *ip*	PC, DSPC, PE-PEG	Size: 168-192; ZP: ⁻24.3 mV; EE: 52-68%;	↑ AUC, $t_{1/2}$, MRT, ↓ Cl, targeting arthritic joints	[140]
DEN	Pain, INF, *iv*	Polyamidoamine	-	Anti-inflammation, ↑ $t_{1/2}$, MRT	[141]
Ibuprofen					
NS	INF & Pain, *sc*	Polysorbate-20 derivatized by glycine	Size: 122.1 nm; PDI: 0.4; ZP: ⁻40.2 mV	pH sensitive, ↑ antinociceptive & anti-inflammatory effect	[142]
NP	Pain, & INF, *iv*	PEG, type A gelatin	Size: ~200 nm; ZP: ⁻23.1 mV; EE: ~70%	SR, ↑ AUC & Vd, ↓ Cl	[143]
LNC	Pain, *iv*	Labrafac CC, Solutol HS15, Lipoid S75-3	Size: 47-56.5 nm; PDI: 0.054-0.094; ZP: 0.46-0.97 mV; EE: 94.2-97.7%	↑ AUC, $t_{1/2}$ & MRT, anti-inflammatory effect	[144]
Indomethacin					
NE	INF, *iv*	DSPC, PEG-DSPE, Chol, olive oil	Size: 180-220 nm; PDI: 0.05-0.18; ZP: ⁻30 Mv	↑ anti-inflammatory effect & ↓ side effects	[145]

PM	RA & OA, *sc*	β-cyclodextrin-modified PCL-PEG-PCL	Size: <40 , >100 nm EE: 39.12-63.89%	Sustained anti-inflammatory effect	[146]
NC	AD, *ip*	PCL, CCT, sorbitan monostearate	Size: 236 nm; PDI: 0.17; ZP: $^{-}$6.9 mV; EE: ~100%	Negatively modulated neu-roinflammation triggered by Aβ	[147]
NC	INF(acute, chronic),*ip*	PCL, CCT, sorbitan monostearate	Size: 240 nm; PDI:<0.19; ZP: $^{-}$6.9 mV; EE: ~100%	↑ long term anti-inflammation, ↑ safety	[148]
NP, NE	OPTH INF, *ip*	Chitosan & TPP / lecithin, Medium chain triglyceride;	NP size: 280 nm, ZP:$^{+}$17 mV; EE: 85%; NE size: 240-690 nm	SR to external and internal ocular tissues.	[149]
PM	RA, *sc*	PNIPAAm with ethyl 4-aminobenzoate as side group	LC: 12-20.6%	↑ circulation, sustained efficacy ↓ GI side effects	[150]
MS	Arthritis, *iv*	Soybean oil, PC, Chol, DSPE-PEG	Size: 150 nm; EE: 95%	↑ AUC, $t_{1/2}$, MRT, ↓ Cl, ↑ uptake in inflamed joints	[151]
DEN	Arthritis, *iv*	Polyamidoamine	-	↑ AUC, $t_{1/2}$, MRT, ↓ Cl, ↑ uptake in inflamed joints,	[152]
LIPO	RA, *ip*	PC, Chol, stearlyamine	Size: 50, 100 nm	SR ↑ anti-inflammatory effect	[153]
SANS	OA, *ia*	PLGA, Poloxamer 407, Tetronic 90R4, glucosamine	Size: 173.9 nm; PDI: 0.24; ZP: $^{-}$0.66	↓ knee diameter, TNF-α levels in osteoarthritis model	[154]
PM	RA, *ia*	PNIPAAm, ethyl glycinate	Size: ~65-360 nm	pH dependent release, ↑ circulation, ↓ GI side effects	[155]
Ketoprofen					
NP	Pain , it	Iron-oxide	Size 6.8 nm (unloaded)	magnetic field-dependent analgesia, ↓ COX expression	[156]
Lornoxicam					
PM	RA, *ip*	Tetronic® 701, Synperonic® PE/P84	Sze: 169.5 nm; PDI: 0.243	↓ elevated inflammatory serum biomarkers	[157]
Meloxicam					
NSus	INF, *iv*	Bovine serum albumin	Size: 78.67 nm; PDI: 0.133; ZP: −11.87 mV	↑$t_{½}$, MRT, & AUC, ↑drug in inflamed tissue	[158]
Piroxicam					
NP	Arthritis, *ia*	Eudragit RL, PLGA, PVA	Size: 221.8 nm; PDI: 0.02; ZP: $^{+}$11.5 mV; LC: 4.06%	↑ retention in the joint & ↓ systemic exposure	[159]

Abbreviations:

nanodelivery systems: CD: Carbon dots; CS: Cubosomes; DEN: Dendrimer; ES: Ethosomes; INS: intranasal spray; LDH: nanocarrier layered double hydroxide; LGS: Lipogelosomes; LIPO: Liposomes; LNC: Lipid nanocapsules; ME: Micro-emulsion; MMEI: Mucoadhesive microemulsion; MP: Microparticle; MS: Microspheres; NC: Nanocapsule; ND: Nanodispersion; NE: Nano-emulsion; NLC: Nanostructured lipid carrier; NP: Nanoparticle; NS: Nano-system; Nsus: Nano-suspension; NV: Nanovesicular system; PM: Polymeric micelles; PN: Proniosomes; SANS: self-assembling nano-system; SEDDS: Self emulsifying drug delivery system; SLN: Solid lipid nanoparticles; SNLC: Supramolecular nano-engineered lipidic carriers

Composition: C888: Compritol® ATO 888; CCT: capric/caprylic triglycerides; Chol: Cholesterol; CMC: Carboxymethyl cellulose; DCP: dicetyl phosphate; C-RH 40: Cremophor RH 40; DFEE: diclofenac ethyl ester; DLA: ascorbyl palmitate; DLQ: co-enzyme Q10; DMPC: Dimyristoylphosphatidylcholine; DSPC: distearoyl phosphatidyl choline; DSPE: Distearoyl-sn-glycero-3-phosphocholine; HPβCD: hydroxypropyl-β-cyclodextrin; HPC: hydroxypropyl cellulose SSL; HSPC: Hydrogenated soya phosphatidylcholine; IPM: isopropyl myristate; PC: Phosphatidylcholine; PCL: Poly(ε-caprolactone); PE: Phosphatidylethanolamine; PEO: Polyethylene oxide; PEG: polyethylene glycol; PL: Phospholipion 90G; PLA: Poly lactic acid; PLGA: Polylactic glycolic acid; PNIPAAm: poly(N-isopropylacrylamide); PVA: Polyvinyl alcohol; PVP: Polyvinylpyrrolidone; SA: Stearic acid; TPP: sodium tripolyphosphate; TPP: sodium tripolyphosphate; Tw80: Tween 80; VP: vinyl pyrrolidone

Conditions: AAU: acute anterior uveitis; AD: Alzheimer's disease; IBD: Inflammatory bowel disease; INF: Inflammation; OA: Osteoarthritis; OPTH: Ophthalmic; PD: Parkinson's disease; RA: Rheumatoid arthritis

Routes of Delivery: buc: buccal; *ia*: Intraarticular; *im*: Intramuscular; *ip*: Intraperitoneal; *it*: intrathecal; *iv*: Intravenous; *sc*: Subcutaneous

Properties and other: ↑: increased; ↓: decreased; AUC: Area under the curve; COX: Cyclooxygenase; GI: Gastrointestinal; EE: Entrapment efficiency; MRT: Mean residence time; PDI: Polydispersity index; SR: Sustained release; $t_{½}$: half-life; ZP: Zeta potential

Table 1-8. Preclinical studies on dermal and transdermal nano-delivery of NSAIDs

NSAID/ Carrier	Indication	Main Composition	physicochemical properties*	Key results	Ref
Aceclofenac					
NP	Gout	PLGA, PVA (NP given with uricase)	Size: 288.5 nm; PDI: 0.23; ZP: ⁻30.5; EE: 85.4%	removed urate crystals, ↓ gout inflammation	[160]
NLC gel	INF	Stearic acid, Pluronic F68, Phospholipon 90G, oleic acid	Size: 233-286 nm; ZP: ⁻9.2 - ⁻13.1 mV; EE: 67-82%	Faster and prolonged anti-inflammatory activity	[161]
Aspirin					
NE	INF	Polysorbate 80, soybean oil	Size: 90 nm	↓ ear lobe thickness, ↓ auricular levels of IL-1α & TNFα	[162]
PM	INF	PEG-600 with pendant functional groups	Size: 20-50 nm; LC: 20%	↑ anti-inflammatory effect	[163]
NE	wound healing	Stratifin, CMC, medium chain triglyceride;	Size: 113-205 nm; ZP: ⁻8.1-⁺4.5	SR, ↓ scar elevation & inflammation	[164]
Celecoxib					
SLN	RA	Capmul MCM C10 Tw80, Transcutol	Size: 240 nm, PDI < 0.3; EE:~ 86%	↑ skin permeation, ↓ arthritis index	[165]
LIPO gel	OA	PC, Chol, Pluronic F127	Size: 600-1000 nm; EE: 90-97%	↑ skin permeation, ↑ anti-inflammatory effect	[166]
NE	INF	Lecithin, OA, chitosan, Pluronic F68	Size: 238,285 nm; ZP: ⁺42.2,⁻ 33.9 mV; EE: ~99%	↑ skin accumulation, ↓ skin permeation	[167]
NLC gel	INF	Glyceryl dilaurate, Capmul MCM, C-RH 40, Transcutol	Size: 169 nm; PDI: 0.624; EE: 35%	faster onset, elicited prolonged activity (24 h)	[168]
ME	UVB- INF	IPM, C8/C10 mono-/di-glycerides, Carbopol 934	Size: 104-316 nm	Anti-inflammatory effect, ↑ skin permeation	[169]
Diclofenac					
ES	INF	Chol, soy phosphatidylcholine	Size: 144 nm; ZP: ⁻23 mV; EE: 71%	↑ skin permeation & ↑ anti-inflammatory effect	[170]
Diflunisal					
SNLC gel	RA	Phospholipion 90G, C888, oleic acid, Carbopol 934	Size: ~188 nm; PDI: 0.25; ZP: -12.28, EE: 87%	↑ inhibition of ear & paw oedema	[171]
SLN	Arthritis	C888, Tw80, Butanol	Size: 124 nm; PDI: 0.29; ZP:-13.6, EE: 76.8%	↑ skin permeation & retention, ↓ oedema, ↓ leukocytes	[172]
DEN	Chronic arthritis	Polyamidoamine	-	↑ skin permeation, bioavail-ability & antinociceptive effect	[173]
Etoricoxib					
CS	RA	Poloxamer 407, monoolein	Size: 136-288 nm; ZP: ⁻18.4-⁻36.10 mV;	↑ bioavailability, half-life, MRT (vs. oral capsules)	[174]
ME	Arthritis, INF	1-butyl-3-Methylimidazolium hexafluorophosphate, Tw80	Size: 32.44 nm; PDI: 0.21; ZP: 0.221 mV;	↓ inflammation w/o anatomical or pathological changes	[175]
Fenoprofen					
NV	Arthritis	Span 60, Tween 60	Size: 536 nm; ZP: ⁻29.8 mV; EE: 49.1%	↓ inflammation & oedema	[176]
Flurbiprofen					
NS	INF	PLGA/PLGA-PEG, HPβCD	Size: 96-234 nm; PDI: 0.048-0.12; ZP:⁻32-⁻10 mV	SR, reservoir & anti-inflammatory effect	[119]

SLN	RA, OA	Stearic acid, Chol, lecithin, butanol	Size: 640-990 nm; ZP: -49- -20; EE: 71.5-92.7%	↑ & sustained anti-inflammatory effect	[177]
Ibuprofen					
NE	Arthritis	Almond oil, Tw80, Span 80, ethanol	Size: 21-24 nm; LC: 2.5%	Improved analgesic and anti-inflammatory effect	[178]
NP gel	RA	Carbopol 934, HPβCD, methylcellulose	Size: 208 nm	↓ inflammation, ↓ side effects, ↑ permeability	[179]
NLC	OA	Witepsol E85, Miglyol 812, Lutrol F68	Size: 106 nm; LC: 9.85%; EE: 98.51%; ZP -18.4 mV	↑ skin permeation	[180]
ME	Chronic INF	Nonionic surfactants & poloxamer 407	Size: 15-17 nm	↑ anti-hyperalgesic effects in prophylactic treatment	[181]
LIPO	RA	PC, Chol, Carbopol® 934	Size: 159 nm; PDI: 0.33; ZP: -70 mV; EE: 49%	↑ skin permeation, ↑ AUC & C_{max}	[182]
ES gel	INF, fever	Buspirone HCL, Carbopol	Size: 200 nm; ZP: 7.16 mV	↑ circulation, ↑ bioavailability	[120]
Indomethacin					
NP	INF	HPC, zirconia beads, hydrophilic ointment	Size: 72 nm	↑ skin permeation, ↓ inflammation	[183]
NP gel	RA	HPβCD, methylcellulose, Carbopol 934	Size: 173 nm	↑ anti-inflammation & localization in the skin	[184]
Ketoprofen					
NP	INF	HPC, zirconia beads, hydrophilic ointment	Size: 68 nm	↑ skin permeation, ↓ inflammation	[183]
NP gel	RA	Methylcellulose, Carbopol 934	Size: 83 nm	↑ skin penetration, ↑ Ka & AUC in skin	[185]
ME gel	INF	Clove oil, Propylene glycol, Tween 20, gelling agent	Size: 396 nm; ZP: -12 mV	SR, ↑ skin permeation	[186]
DEN	Chronic arthritis	Polyamidoamine	-	↑ skin permeation, bioavailability	[173]
Lornoxicam					
SLN, NLC, NE	INF	C888, Lanette O, oleic acid	Size: 141-295 nm	↑ drug skin penetration	[187]
NE	INF	Pluronic® F68, Tween® 80, oleic acid	Size: 139 nm; PDI: 0.233; ZP: -36 mV	↑ skin permeation, ↑ anti-inflammatory effect	[188]
Meloxicam					
ES	INF	Phospholipon® 90G, Carbopol® 934	Size: 142.3 nm; PDI: 0.26; EE: 78.25%	↑ skin permeation, ↑ anti-inflammatory effect	[189]
NS	INF	Span 60, Chol	Size: 187.3 nm;	↑ skin permeation, ↑ anti-inflammatory effect	[190]
Naproxen					
ME	Pain & INF	IPM, Span 80, Labrafil M, Labrasol, Cremophor	Size: 1.4-2.8 nm; PDI: 0.37-0.48	↑ skin permeation	[191]
PM	INF	PEG-600 (& pendant groups)	Size: 20-50 nm; LC: 7%	↑ anti-inflammatory effect	[163]
Piroxicam					
NP	INF	HPC, zirconia beads, hydrophilic ointment	Size: 75 nm	↑ skin permeation, ↓ inflammation	[183]
SLN	RA, OA, trauma	Glycerol monostearate, Tw80, lecithin, Oleic Acid	Size: ~102 nm; PDI: 0.262; ZP: +30.2 mV; EE: 87.5%	↑ skin penetration, ↑ anti-inflammatory effect	[192]
LIPO	INF	Soya PC, Chol, stearylamine	Size: 278 nm; EE: 12.73%	↑ topical anti-inflammation	[193]

Tenoxicam					
SLN Gel	RA	Precirol, poloxamer 188, lecithin	Size: 58.1 nm; EE: 69.6%	↑ anti-inflammation, ↑ skin AUC (vs. *in vitro* results)	[194]
ME	Arthritis	Captex 300, oleic acid, Tw80	Size: 106,122 nm; ZP: ≈0 mV	↑ skin permeation, ↑ anti-inflammatory effect	[195]
Valdecoxib					
NLC gel	INF	Glyceryl dilaurate, Caproyl 90, C-RH 40, Transcutol	Size: 157 nm; PDI: 0.582; EE: 51%	faster onset, elicited prolonged activity (24 h)	[196]

Abbreviations: (See foot note in Table 1-7)

Table 1-9. Preclinical studies on the ocular nano-delivery of NSAIDs

NSAID/ Carrier	Indication	Main Composition	physicochemical properties*	Key results	Ref
Aceclofenac					
NP	OPTH INF	Eudragit RS 100	Size: 238.9 nm; ZP: 40.3 mV; EE: 94.53	↑ inhibition of PMN migration, lid closure scores	[197]
NP	OPTH INF	Eudragit RL 100	Size: ~135 nm; PDI: 0.186; ZP: $^{+}$30.5 mV; EE: 95.73%	↑ corneal permeation, ↑ anti-inflammatory activity	[198]
Celecoxib					
SLN	OPTH INF	Glycerol monostearate, PVA	Size: 198.77 nm; ZP: $^{-}$16.2 mV; EE: 92.5%	Anti-inflammatory effect, ↑ retention on ocular surfaces	[199]
Diclofenac					
NP	OPTH INF	N-Trimethyl chitosan, TPP	Size: 155 nm; PDI: 0.2; ZP: 8.3 mV; EE:93.3%	↑ ocular bioavailability & ↓ dosing frequency	[200]
Dexibuprofen					
NS	OPTH INF	PEG, PLGA	Size: 136, 173.7 nm; PDI: 0.084 -0.097; ZP: $^{-}$15.9- $^{-}$14.1	Anti-inflammatory, ↑ corneal permeation & retention	[201]
Flurbiprofen					
NP	Cataract surgery	PLGA-PEG-POD (Peptide for ocular delivery), Lutrol F68	Size: 170-220 nm; PDI: 0.06-0.09; ZP: $^{-}$30-30 mV	SR, ↑ anti-inflammatory effect	[202]
NP	OPTH INF	PLGA, poloxamer 188	Size: 232.8,277.6 nm; ZP: 25, $^{-}$27.5 mV; EE: 95,94%	↑ anti-inflammatory effect	[203]
NE	OPTH INF	Flurbiprofen axetil, Caster oil, Tw80, Carbopol 974	Size: ~152-238 nm; PDI: 0.20-0.26; EE: 98.1-99.2%	↑ exposure in aqueous humor, anti-inflammatory	[204]
LIPO Gel	OPTH INF	PC, dipalmitoyl phosphatidylglycerol, Chol	Size: 113.8 nm; PDI: 0.2; ZP: $^{-}$23.8 mV, EE: 2.91%	↑bioavailability & MRT in aqueous humor & retina	[205]
Ibuprofen					
NP	OPTH INF	Eudragit RS100	Size: ~100 nm; ZP: +40/+60 Mv	↑ exposure in aqueous humor, anti-inflammation	[206]
Indomethacin					
NP	OPTH INF	HPβCD, methylcellulose;	Size: 76 nm	↑ ocular bioavailability, ↑ corneal wound healing	[207]
Ketoprofen					
ND	OPTH INF	Eudragit RL 100, PVA	Size: 252.8 nm; PDI: 0.51; ZP: 16.8 mV; EE: 91.6%	↑ Ocular bioavailability & residence time	[208]

PM	OPTH INF	NIPAAM, VP, acrylic acid, Bis-acrylamide	Size: 35 nm	↑ bioavailability, prolong anti-inflammatory effect	[209]
Piroxicam					
NP	AAU	Eudragit RS100, PVA	Size: 230-250; ZP: ~35 mV	↓ inflammation locally	[210]

Abbreviations: (See foot note in Table 1-7)

Table 1-10. Preclinical studies on pulmonary and intranasal nano-delivery of NSAIDs

NSAID/ Carrier	Indication	Main Composition	physicochemical properties*	Key results	Ref
Ibuprofen					
MMEI	PD	Polycarbophil, Labrafil M 1944 CS, Tw80, Trans	Size: 46.73 nm; PDI 0.201,	↑ DA in the brain, improved motor function	[211]
NP	COPD & CF	PEG, PLGA	Size: 344 nm; PDI: 0.12;	Targeting of neutrophilic airway inflammation	[212]
MMEI	PD	Capmul MCM, Smix, Polycarbophil	Size: 66 nm; PDI: 0.18; ZP: $^{-}$21.4;	↑ DA in brain, ↑ TH neurons cour in substantia nigra	[213]
Meloxicam					
Nano INS	Pain	PVA, sodium hyaluronate	Size: 135 nm	↑ residence time, better diffusion, ↑AUC	[214]

Abbreviations: (See foot note in Table 1-7)

Table 1-11. Preclinical studies on the oral or buccal nano-delivery of NSAIDs

NSAID/ Carrier	Indication*	Main Composition	physicochemical properties*	Key results	Ref
Aspirin					
NE	INF	Pluronic F68 /L90, Transcutol, Cremophor	Size: 216,400 nm; ZP:-13.6 mV, EE: 76.8%	↑ anti-inflammatory & analgesic effects	[215]
Celecoxib					
SEDDS	Oral NF, buc	Labrafil M 2515, Tw80, PEG 400	Size: 116.9 & 124 nm; PDI: 0.499 & 0.591	↑ drug permeation, ↑ edema inhibition	[216]
NP	INF	PLGA	Size: 79.13 nm; PDI: 0.17; ZP: 21.37 mV; EE: 86.3%	↑ exposure, no change in electrolyte parameters	[217]
PM	Pain, INF	Quaternary-ammonium-palmitoyl-glycol-chitosan	Size: 185.8 nm; PDI: 0.145; ZP: $^{+}$42.9 mV	Faster and more prolonged pain relief	[112]
MP	Arthritis	Capmul MCM, Aerosil 380	EE: 70-91%	↑ anti-inflammatory effect, ↑ oral bioavailability	[218]
Dexibuprofen					
NS	AD	PEG, PLGA	Size: 195.4 nm	↓ memory impairment & brain inflammation	[219]
Diclofenac					

NP	INF	PLGA	Size: 221.03 nm; ZP: 20.86; EE: 76.48%	↓ renal necrosis	[220]
LIPO	Pain	Pro-lipo^{TM} duo	Size: 260.2 nm; PDI: 0.27; EE: 87.4%	↑ antinociceptive efficacy dose dependently	[221]
Ibuprofen					
LNC	Pain	Labrafac CC, Solutol HS15, Lipoıd S75-3	Size: 47-57 nm; PDI: 0.05-0.09; ZP: 0.46-0.97 mV; EE: 94.2-97.7%	↑ AUC, $t_{1/2}$ & MRT, anti-inflammatory effect	[144]
Indomethacin					
Solid NP	RA	HPβCD, methylcellulose;	Size: 76 nm	↑ bioavailability & reduce GI side effects	[222]
Redox NP	Chronic INF	MeO-PEG-b-poly(chloromethylstyrene)	Size: 39.6,46.3 nm; PDI: 0.147,0.39; EE: 100%	↑bioavailability, ↓ side effects in small intestine	[223]
PM	RA	PNIPAAm, ethyl glycinate;	Size: ~65-360 nm	pH dependent release, ↑ circulation, ↓ GI side effects	[155]
DEN	RA	Folate-PEG-PAMAM	EE: ~55%	↑ AUC, $t_{1/2}$, MRT, ↓ GI effects, ↑ uptake in inflamed joints	[117]
LIPO	INF	PC monophasic vesicles	Size: ~500 nm	↓ or eliminated gastric and intestinal ulceration	[115]
Mefenamic acid					
LDH	Pain, INF	Magnesium, aluminum	Size: 132 nm; ZP: $^{+}$36.3 mV	Hemolysis, ↓ leucocytes, neutrophils, inflammation,	[224]
Meloxicam					
SNEG	Arthritis	Labrafil M 1944 CS, SA, Tw80, C-RH 40, PEG400	Size: 173.8 nm; PDI: 0.37; ZP: ≈0 mV	Rapid onset of anti-inflammation	[225]
NC	Pain, INF	Carbopol 940, Span 60	Size: 283 nm; ZP: $^{-}$14.5 mV	↑ prolonged anti-inflammatory effect	[226]
Mesalazine					
NP	Colitis	Silica	Size: 136 nm;	↓ inflammation, ↓ toxicity	[227]
NP	IBD	PCL	Size: 221,330 nm; PDI: 0.12,0.21, ZP: $^{-}$1.2,$^{-}$2.5 mV	↓ dose, ↓ clinical activity score & myeloperoxidase activity	[228]

* Oral delivery unless indicated otherwise
Abbreviations: (See foot note in Table 1-7)

palmitoyl glycol chitosan [112]. The optimal formulation showed about 57-fold increase in celecoxib aqueous solubility, while an *in vivo* study showed a faster (30 min vs. 120 min) and more intense analgesia in writhing test in mice compared to an aqueous suspension made from the marketed capsule celecoxib formulation (Celebrex®).

To address the limited bioavailability and rapid elimination of ibuprofen, from the systemic circulation, a PEGylated gelatin-based nanoparticle formulation of ibuprofen sodium for *iv* dosing was investigated [143]. Toxicity studies and histological analysis of tissues confirmed the safety of the formulation. PK analysis in healthy rats demonstrated a sustained release of ibuprofen from the nanoparticles lasting for about 4 days with complete clearance from the body in 5 days, and a 4.5-fold increase in the area under the plasma concentration curve (AUC) compared to free ibuprofen suggesting improved bioavailability from the formulation. This formulation has the potential to reduce the frequency of ibuprofen administration in future clinical application, especially when *iv* dosing is warranted.

1.4.2.2. Nanodelivery for improving the activity of NSAIDs

In general, all NSAIDs show good activity in the management of pain and inflammation at the recommended doses. However, it is still desirable to improve the activity of these agents in order to achieve the anticipated therapeutic outcomes at lower and less frequent doses, so that their dose dependant toxic side effects can be controlled better. Several nanodelivery systems have been designed to achieve this aim. For example, a cremophore EL based nanoemulsion formulation of aspirin, the most widely used NSAID agent in the world, resulted in a substantial inhibitory effect on carrageenan-induced paw edema model of inflammation in rats at 4 h post oral dose of 60

mg/kg, about double of the inhibitory effect achieved with an aspirin suspension at the same dose [215]. Moreover, the same formulation led to higher inhibition of abdominal writhing, (~ 91% vs 81%) compared to the aspirin suspension in an acetic acid-induced writhing model of pain. The authors attribute the improvements to properties of the nanoemulsion, in general, including that it is kinetically stable and often lead to increased drug solubility, rapid dissolution velocity, and result in high bioavailability after oral administration, probably due to their escaping first-pass effect.

Nagai *et al* prepared an oral formulation encapsulating indomethacin, a derivative of indoleacetic acid, in solid nanoparticles, composed of methylcellulose and 2-hydroxypropyl-β-cyclodextrin and prepared using bead milling. They investigated these nanoparticles administered at two indomethacin doses, a low dose of 0.4 mg/kg and a higher therapeutic dose of 2 mg/kg, in comparison to the high dose of 2 mg/kg of a conventional indomethacin formulation, also prepared with methylcellulose and 2-hydroxypropyl -β-cyclodextrin [222]. The nanoparticles, at the low and high doses treatments, resulted in indomethacin absolute bioavailability that are comparable and 5.3-fold higher when compared to the conventional formulation in adjuvant arthritic (AA) rats. This translated for the low dose formulation to a comparable activity in controlling paw edema resulting from AA for up to 42 days, to that achieved with the higher dose of the conventional formulation of indomethacin. Equally as important, the nanoparticles showed a significant reduction in GI lesions.

In another study, diclofenac, a phenylacetic acid derivative, was encapsulated in liposomes based on propanediol and lecithin for oral administration and its antinociceptive activity was studied in different nociceptive experimental models [221]. The liposomes resulted in a potent

antinociceptive activity on acetic acid-induced abdominal constriction in mice which appear to be dose-dependent, reaching an antinociceptive effect at 78.97% compared to 55.89% for the free diclofenac, both at the dose of 20 mg/kg. Moreover, the liposomes showed a potent pain inhibition effect in the formalin test in rats, resulting in 78.8% pain inhibition compared to 60.71% for free diclofenac. The authors suggest a stronger peripheral mediated antinociceptive effect for the liposomal formulation compared to the free drug, which they attribute to improvements in the diclofenac solubility and a more effective delivery to the intended sites of action.

Verma *et al* investigated the delivery of flurbiprofen, a propionic acid derivative NSAID, as a single intravenous dose which can provide sustained relief from acute pain and inflammation over several days [139]. They formed preniosomes, dehydrated formulations, based on a sorbitol, cholesterol and an optimized ratio of the non-ionic surfactants Span 80 and Span 20, that spontaneously form niosomes upon aqueous hydration. A PK study revealed that the preniosomes provided higher concentrations post 8 h and remained in the systemic circulation for 3 days resulting in an AUC that is 2.6-fold higher compared to a reference flurbiprofen solution at the same dose, which cleared from the body in 24 h. The pharmacodynamics study, on the other hand, showed that the preniosomes provided a superior anti-inflammatory effect as evidenced by a higher inhibition of paw edema, in a carrageenan-induced edema model in rats, for an extended period of 2-24 h with a maximum inhibition of 88.6% at 0.16 h compared to a reference flurbiprofen solution which showed a maximum inhibition of 64% at the same time.

In another report, a micellar formulation based on commercially available polymers Tetronic 701 and Synperonic PE/P84 encapsulating lornoxicam, an NSAID from the oxicam group, was developed as a potential therapeutic option for RA [157]. In the carrageenan-induced hind-paw

acute edema model in rats, the micellar formulation at an intraperitoneal (*ip*) dose of 1.3 mg/kg showed higher inhibitory effect on paw edema at 3 and 4 h post induction of edema compared to a free lornoxicam at the same dose. However, it is not clear from the report if the difference is statistically significant. Moreover, the micellar formulation at a dose of 0.325 mg/kg was found to produce comparable results to diclofenac 3 mg/kg in the same model. However, the report failed to include a justification on the dose of diclofenac used in the comparison. The micellar formulation, at the lower dose of 0.325 mg/kg/day, was also found to reduce edema for a prolonged period (28 days) in a Freund's complete adjuvant (FCA)-induced chronic arthritis model in rats, in contrary to the free drug which failed to achieve significant anti-inflammatory effects.

A different nanoformulation, developed with the same aim of improving the efficacy of an NSAID agent for the treatment of chronic inflammatory disease such as RA, is a polymeric nanocapsule formulation that encapsulated indomethacin [148]. The formulation was tested *in vivo* in several experimental models of inflammation. In the carrageenan-induced edema acute model of inflammation in rats, the nanocapsules were found to be as effective as the free indomethacin. On the other hand, the nanocapsules established superior efficacy in comparison to free indomethacin in two other longer-term models, resulting in a 1.6-fold and a 2.5-fold increase in efficacy in the sub-chronic edema model and the arthritis model, respectively, both of which are induced by CFA. The nanoformulation also showed reduction in GI damage, measured by reported indices of GI damage to be less than that after free indomethacin (by around 58%, 72%, and 69% for duodenum, jejunum and ileum respectively).

1.4.2.3. Nanodelivery for improving the safety of NSAIDs

The most frequent side effect of NSAIDs are in the GI tract which can limit their long-term use. To reduce these side effects, Soehngen *et al* developed liposomal formulations of indomethacin constructed with egg phosphatidylcholine for oral dosing [115]. The administration of indomethacin encapsulated in liposomes provided over 75% protection against ulceration in a 4 h acute model of ulceration in rats for a range of indomethacin doses (2-10 mg/kg) in comparison with free indomethacin dissolved in polyethylene glycol (PEG)-400. Moreover, in a 2-week chronic ulceration model in rats, over 99% protection against intestinal ulceration was observed by the liposomes in comparison with free indomethacin suspended in 1% methylcellulose in saline. This protection was achieved while maintaining comparable indomethacin blood concentration and efficacy. The authors attributed this improvement in GI safety to protection against local effects of indomethacin but did not rule out protection against systemic effects.

In a different study, Harirforoosh *et al* attempted to study the GI and renal safety of diclofenac encapsulated in poly(lactic-co-glycolic) (PLGA) nanoparticles given orally to rats at a diclofenac dose of 10 mg/kg in comparison to free diclofenac [220]. Histological assessment at 24 h post-dose revealed that, while free diclofenac resulted in higher renal necrosis compared to vehicle, the nanoparticle did not significantly affect renal necrosis. All other parameters studied which included urinary and blood electrolytes as well as duodenal and gastric prostaglandin E_2 (PGE_2) and myeloperoxidase levels did not differ between the free and encapsulated diclofenac, which could be due to the short exposure time to the NSAID. The renal protection observed with encapsulated diclofenac encapsulation was not observed when the investigators encapsulated celecoxib instead [217]. Instead, encapsulation of celecoxib in PLGA nanoparticles appear to

have provided a GI protection by stabilizing the reduction in PGE_2 observed with the free celecoxib solution.

Nanodelivery system can also improve the safety of parenterally administered NSAIDs by reducing the toxicity at the injection site. Guterres *et al* investigated diclofenac loaded in PLA nanocapsules with different oily cores for intramuscular (*im*) administration in rats by measuring plasma creatine phosphokinase (CPK) activity, which indicates muscle damage at the injection site [135]. Nanoformulations prepared with Miglyol 810 core (caprylic/capric triglyceride) (containing 0.8 mg of diclofenac) showed significantly lower CPK activity compared to the diclofenac solution. Meanwhile, when a core of benzyl benzoate was used in the preparation of nano-formulations, no reduction in CPK activity was observed compared to diclofenac solution. Histopathological assessment 3 days after the injection confirmed a reduction in local inflammation following administration of the former nano-formulations of diclofenac.

Using the same approach, the safety of a liposomal formulation of diclofenac based on phosphatidylcholine, cholesterol, and α-tocopherol, was established. Liposomal diclofenac (0.2 mg diclofenac) given *im* to rats resulted in no change in CPK activity compared to the control untreated groups, to the contrary of free diclofenac. Histopathological assessment of muscles around the injection site performed at 3- and 7-days post-injection showed intense damages in rats that received free diclofenac, but not in those that received liposomal diclofenac.

1.4.2.4. Alternative routes of delivery

NSAIDs are most commonly dosed orally especially in chronic use, but other routes such as parenteral, topical and per-rectal are also applied and shown to provide comparable management

of pain and inflammation [229]. The low safety profile of systemically administered NSAIDs and the demand to improve the local delivery of these agents have led to development of several nanodelivery formulations which consider alternative routes including dermal/transdermal, ocular, and pulmonary delivery as well as local parenteral delivery for drug administration.

1.4.2.4.1. Dermal and transdermal delivery

The dermal and transdermal (TD) nanodelivery of NSAIDs have received much attention due to the range of conditions that can benefit from delivery through these routes which include chronic conditions such as RA and OA. Besides, NSAID delivery by non-systemic means have attracted attention owing to a potential to reduce NSAID induced toxicity. In one study, Kaur *et al* incorporated diflunisal, a salicylic acid derivative, into Phospholipion 90G to form a drug-phospholipid complex which was then incorporated in a nanostructured lipid carrier (NLC) based on Compritol and oleic acid as the solid and liquid lipids [171]. The NLC was incorporated in Cabopol 934 to make it suitable for topical/TD delivery. In the mice ear edema model of acute inflammation, the NLC formulation (1 g containing 400 µg diflunisal applied locally) led to a 2.5-fold increase in percent inhibition of mice ear edema compared to a conventional diflunisal o/w cream, prepared by the researchers, given at the same dose. Moreover, in the CFA induced arthritis chronic model in rats, a twice daily application of the NLC formulation for 10 weeks led to a 7-fold increase in percent inhibition of paw edema and a 27% reduction in the level of the pro-inflammatory cytokine TNF-α in serum and in synovial fluid compared to the conventional cream (both applied topically on paws and joints of arthritic rats).

Cubosomal nanoparticles, nanostructured liquid crystalline particles, loaded with the selective COX-2 inhibitor etodolac were developed based on poloxamer 407 and monoolein and were clinically studied [174]. A single dose cross-over PK study in six human volunteers revealed that the TD delivery of the nanoparticles resulted in a sustained absorption, a 3.8-fold prolongation of half-life, and a 2.7-fold increase in AUC over 48 h resulting in a relative bioavailability of 266.11% compared to commercially available oral capsules. However, the difference in the side effects due to the treatments, if any, were not reported.

Nanodelivery systems can result in faster onset of and/or prolonged action through the TD route. For example, an ibuprofen (2.5% w/v) nanoemulsion formulation, based on almond oil as the oil phase was developed and compared to two formulations, a corresponding microemulsion also based on almond oil and a commercially available 5% ibuprofen gel (Raha Pharmaceutical Industries, Tehran, Iran). both of which had double the ibuprofen content (i.e. 5% w/v) [178]. The nanoemulsion resulted in a faster onset of anti-inflammatory effect in a carrageenan-induced rat paw oedema model, showing a decrease in inflammation in the first-hour while the microemulsion and the commercial product had an onset at 2 and 3 h post-dose, respectively.

Using a different approach, Cheng *et al* investigated the encapsulation of two different NSAIDs, diflunisal and ketoprofen, a propionic acid derivative, in polyamidoamine (PAMAM) dendrimers to facilitate their TD delivery [173]. PK analysis of the formulations following TD administration in rats revealed a higher plasma concentration for both drugs from the dendrimer complexes compared to free drug suspensions for the 12 h study duration. In effect, a 2.5- and 2.7-fold increase in AUC from the dendrimers compared to the free suspension for diflunisal and ketoprofen was observed, respectively. Furthermore, in an acetic acid-induced writhing model in

mice, TD administration of the ketoprofen loaded dendrimers (0.1 mL of 2 mg/mL) resulted in rapid and prolonged anti-nociceptive activity lasting from 0.5-6 h post-dose. Whereas a ketoprofen suspension resulted in a significant activity during 4-6 h following TD administration. Meanwhile, an oral dose of ketoprofen (at a dose of 10 mg/kg) provided significant activity during 0.5-2 h post-dose. Similar results were reported for the diflunisal formulation.

1.4.2.4.2. Ocular delivery

NSAIDs have an important role in the control of pain and ocular inflammation in various conditions or following ocular surgery. In this case local delivery to the eye is preferred but maintaining a therapeutic concentration of the agents for an appropriate duration has proven to be a challenge. Nano-formulations can improve the ocular bioavailability of NSAIDs and increase their residence time at the desired sites.

An example is the study by Pachis *et al* who investigated the benefits that an intravitreal injection of a hydrogel consisting of flurbiprofen entrapped in liposomes would bring to the bioavailability of flurbiprofen in the retina [205]. An in vivo study in pigmented rabbits revealed that this formulation increased the flurbiprofen bioavailability by 1.9-folds and the mean residence time (MRT) by 1.4-folds in the vitreous, aqueous humor and retina while making its clearance half when compared to a flurbiprofen solution at the same dose.

A nanoparticle formulation of ibuprofen sodium based on Eudragit RS100, a polymethacrylate-based copolymer, was found to produce rapid reduction in conjunctival inflammation and iris hyperemia induced by sodium arachidonate in rabbits [206]. The nanoformulation, administered pre-emptively 30 min prior to induction of ocular inflammation, showed a significant reduction

in inflammation that started at 30 min post inflammation-induction and was maintained up to 6 h A comparable dose of an aqueous solution of ibuprofen lysinate showed a significant but smaller reduction only at 2 h. This could be attributed to an increase in drug concentration in the aqueous humor due to the nanoformulation, which at 2 h was about double of that of the drug solution. Another group investigated, Eudragit RL100 nanoparticles encapsulating aceclofenac, a phenylacetic acid derivative NSAID, for ocular instillation [198]. Both Eudragit RL and SL have quaternary ammonium groups that gives these copolymers positive charge. This can improve their interaction with anionic components of mucin and the cornea. The aceclofenac loaded nanoparticles showed a stronger anti-inflammatory effect as measured by higher inhibition of polymorphonuclear leukocytes migration and by lid closure scores, which dropped by 50% or more at 1-4 h post dose, in comparison to an aqueous aceclofenac solution in an arachidonic acid induced inflammation model in rabbits.

N-trimethyl chitosan nanoparticles encapsulating diclofenac sodium [200] showed a 2.4-fold increase in time to reach maximum diclofenac concentration (T_{max}) and a 2.5-fold increase in AUC in the aqueous humor of rabbits' eyes compared to a commercial diclofenac eye drop possibly due to the mucoadhesive property of the nanocarrier. The nanoparticles prolonged diclofenac residence time with therapeutic concentration being detected up to 12 hours, while diclofenac from the commercial eye drops fell below detection at that time.

1.4.2.4.3. Pulmonary and intranasal administration

The nanodelivery through the intranasal or pulmonary route has been investigated for several classes of therapeutic agents including NSAIDs because of the role these delivery systems play for

the local control of inflammation. An example is ibuprofen encapsulated in PEGylated PLGA nanoparticles conjugated with an anti-neutrophil antibody (NIMP-R14) for targeting neutrophils in chronic obstructive pulmonary disease (COPD) [212]. Intranasal (INS) administration of the nanoparticles was investigated in two experimental models of COPD in mice, *pseudomonas aeruginosa* lipopolysaccharide (LPS) induced and cigarette smoke induced inflammatory lung diseases. The nanoparticles were found to be effective in both models showing a significant decrease in the induced NFkB nuclear localization and expression as well as a decrease in the number of infiltrating neutrophils. However, the study did not compare the *in vivo* activity of this ibuprofen nanoformulation to other formulations of ibuprofen (or other indicated agents), to unloaded nanoparticles, or to free antibody.

Using a different approach, a nanoformulation was developed for the INS administration of meloxicam. First, meloxicam particle size was reduced to the nanoscale using wet milling technology which were then incorporated into a liquid formulation with the use of sodium hyaluronate [214]. PK analysis revealed that the nanoformulation resulted in higher meloxicam plasma concentration during the first hour post-dose, which was 3-fold higher at 5- and 60-min post-dose than two equivalent formulations containing either raw or micro-sized meloxicam particles. The nanoformulation resulted in meloxicam AUC that was 3.6- and 2.3-folds higher than the equivalent dose of raw or micro-sized meloxicam particles, respectively. The authors attribute the enhanced bioavailability from the nanoformulation to improvements in the dissolution of meloxicam due to the small particle size and also to the mucoadhesive properties of sodium hyaluronate. These results show that INS nanodelivery systems encapsulating NSAIDs not only

can improve the local delivery of these agents to the lungs, but also provide an alternative route to oral dosing for their systemic delivery.

1.4.2.4.4. Parenteral administration

Local parenteral delivery involves injecting the NSAIDs close to the site of action, such as the intraarticular (*ia*) injections at inflamed joints. These routes are favored when local anti-inflammatory effect is needed and are useful to avoid the side effects associated with full systemic delivery. With this in mind, Zhang *et al* developed a polymeric micellar formulation encapsulating indomethacin based on polyphosphazene with poly(N-isopropyl acrylamide) and ethyl glycinate as side groups [155]. A PK study in rats revealed that the subcutaneous (*sc*) administration of the formulation resulted the AUC of indomethacin by half while increasing the MRT of drug by 1.6-fold compared to administration of free indomethacin solution by the same route. Anti-inflammatory effect assessment, carried out in carrageenan induced inflammation model rats, showed a significantly lower paw edema for nano-formulation compared to the control formulations starting at 2 h post-dose. The oral suspension (5 mg/kg, *po*) and the free indomethacin solution (1.5 mg/kg, *sc*) showed significant effects at 4 h and 6 h post dose, respectively. Interestingly, a lower dose of the micellar formulation (0.5 mg/kg, *sc*) produced comparable or even superior activity to that achieved with the free drug given orally or as a parenteral solution. The local delivery of the nano-formulation was explored in In the AA model of inflammation. All doses of the formulation (0.5, 1.5, 4.5 mg/kg) given as *ia* injections showed superior activity in controlling paw edema to that achieved with the free indomethacin solution (1.5 mg/kg, *ia*) and comparable to the oral suspension (5 mg/kg, *po*) at 10- and 15-days post-AA induction. However, while the oral dosing resulted in significant gastric ulceration (as measured by number hemorrhage

points, number of ulcerations, and average trauma degree), the *ia* administration of the micelles all doses considered, showed a substantial reduction in ulceration.

A different group encapsulated celecoxib in solid lipid nanoparticles with the aim of increasing its retention in the inflamed joints following *ia* administration [130]. A PK and biodistribution study of *ia* administration in arthritic rabbits (CFA-induced) showed that the celecoxib loaded nanoparticles caused a significantly lower blood concentration compared to free celecoxib, which appeared to have experienced a rapid clearance from the inflamed articular joint into the systemic circulation. In a pharmacodynamic study in rats with CFA-induced arthritis, a 15-fold increase in the articular celecoxib concentrations was observed at 24 h post-dose for the nanoparticles compared to free celecoxib. The authors attribute this increase in articular celecoxib concentration from the nanoparticles to phagocytosis by the macrophages of the inflamed joints.

In another study, diclofenac sodium was encapsulated in lipogelosomes, liposomes with a polar core that is in semi-solid state of gel [137]. A biodistribution study in rabbits showed that *ia* administration of the nanoformulation resulted in > 4-fold increase in diclofenac concentration in the inflamed joints at 24 h post-dose compared to a free diclofenac solution. Moreover, a single dose of the nanoformulation showed an improved efficacy (over 2-fold increase) in reducing swelling of inflamed knees in rabbits (CFA-induced) compared to a commercial diclofenac product (VE-CP®, 13 mg/ml of diclofenac sodium), applied topically, containing 10-fold higher diclofenac content.

1.4.2.5. Nanoformulations for the targeted delivery NSAIDs by active mechanisms

In addition to passive targeted delivery to inflamed tissues, active targeting strategies have also been investigated in preclinical studies for the delivery of NSAIDs. One strategy is the targeting of the folate receptor, isoform FR-β, that is overexpressed in activated macrophages associated with chronic inflammatory diseases such as RA. Folate-linked imaging agents have been reported to highly accumulate in arthritic joints. In one report, folate coupled PEG conjugates of the anionic PAMAM dendrimer encapsulating indomethacin were investigated for inflammatory tissue targeted delivery [117]. PK analysis following *ip* administration in AA rats revealed an increase to about 1.5-fold in AUC, 2.8-fold in $t_{½}$, and 1.8-fold in MRT for one of the folate-PEG conjugates (which contained 7 folate-PEG arms) compared to free indomethacin, and an increase to about 1.24-fold in AUC and similar $t_{½}$ and MRT compared the indomethacin PAMAM dendrimers lacking the folate conjugate. Moreover, a tissue distribution study showed that the folate-PEG conjugate resulted in 8.5-folds and 11-folds reduced uptake in the stomach in comparison to an indomethacin PAMAM dendrimers lacking the folate conjugate and free indomethacin, respectively. Less, but significant, reductions in indomethacin accumulation were also seen in the heart and kidneys, the other major sites of NSAID related toxicities.

Another folate conjugated system investigated is a bovine serum albumin nanoparticle formulation encapsulating etoricoxib for *iv* administration [138]. The folate conjugated nanoparticles significantly sustained etoricoxib release and prolonged its circulation showing an AUC that is 4.6- and 1.7- folds higher and an MRT that is 7- and 2.4-folds higher than free etoricoxib and non-targeting nanoparticles, respectively, in mice. Tissue accumulation at 24 h post-dose showed a 2.9-fold increase in etoricoxib concentration in inflamed joints compared to non-targeting

nanoparticles, while the free etoricoxib fell below detection limit at the same time. The authors report that superior anti-inflammatory effect was observed for the folate-conjugated nanoparticles in controlling inflammation in a carrageenan induced edema model when compared to both the free etoricoxib and the non-targeting nanoparticles. However, statistical data on the comparison were not found in the report.

The delivery of NSAIDs have also been investigated in pH sensitive nanodelivery systems which are designed to make use of the decrease in pH in various pathological conditions such as RA to promote release of the drug at the target tissues. In a study by Rinaldi *et al*, ibuprofen was encapsulated in two niosomal formulations based on polysorbate-20 or its pH-sensitive derivative polysorbate-20 derivatized by glycine [142]. The two formulations were tested for nociceptive activity *in vivo* using the formalin test in mice, and the pH sensitive niosomes were found to significantly reduce licking activity at two phases of measurement, while the plain niosomes or the free ibuprofen did not show any effect. Moreover, the anti-inflammatory effect of the pH sensitive niosomes was observed in Zymosan-induced paw edema in mice where significant reduction in paw edema was observed at 1 h and maintained up to 24 h post-inflammation induction. The non-sensitive niosomes or the free ibuprofen, on the other hand, failed to show any significant effect compared to mice given the vehicle.

1.4.2.6. Expanding the role of NSAIDs

Inflammation plays a major role in the pathogenesis of many disease states and NSAIDs may have an expanded role in the management of such conditions, especially if combined with advanced delivery techniques. For instance, NSAIDs are believed to have a role in controlling

neuroinflammation that associates various neurological diseases such as Alzheimer's disease (AD) and Parkinson's disease (PD) [230]. Properly designed nanocarrier systems can improve the permeation of NSAIDs across the blood-brain-barrier for use in such conditions. Sánchez-López *et al* developed PEG-PLGA based nanospheres for the encapsulation of dexibuprofen, a propionic acid derivative NSAID, to increase its delivery to the brain in AD [219]. A biodistribution in mice showed that at 24 h post- oral dose, the nanospheres were found in the brain as well as the liver, which appears to be the elimination route of the nanospheres. A behavior test performed in a mice model of familial AD (Morris water maze) using a chronic dexibuprofen treatment for 3 months (*po* dose of 50 mg/kg/day; nanospheres given on alternate days) revealed that the nanospheres were more effective in spatial memory improvements compared with free dexibuprofen. Moreover, the nanospheres significantly lowered the level of β-amyloid (Aβ) plagues, a marker of AD, in transgenic mice compared to the free dexibuprofen and untreated groups. In terms of side effects, the nanospheres did not result in a significant change in gastric damage compared to the control group, while free dexibuprofen increased stomach lesions compared to both the control and the nanosphere groups.

PD is another neurological condition that has the potential to benefit from nanodelivery of NSAIDs. Mandal *et al* developed a mucoadhesive microemulsion encapsulating ibuprofen for INS delivery, and explored its neuroprotective effect for inflammation mediated by dopaminergic neuro-damage in 1-methyl-4-phenyl-1,2,3,6-tetrahydropyridine (MPTP) model of PD in mice [213]. The microemulsion (ibuprofen 2.86 mg/kg) resulted in improvements of up to 2-folds in the motor coordination activity (in a rota-rod test) compared to the untreated group, while free ibuprofen at the same dose did not result in significant changes. Moreover, the microemulsion

showed protective effect on gross neurological activity assessed through an open-field test, showing over 2-fold increase in total spontaneous activity compared to the untreated group, while free ibuprofen did not result in significant change. Furthermore, the nanospheres reduced dopamine depletion and increased tyrosine hydroxylase neurons count in the substantial nigra in comparison to the untreated group.

1.5. Thesis hypothesis and objectives

The aim of this research work is to prepare nano-formulations of an NSAID with potent CV side effects and use them as tools to limit the distribution of the NSAID into the heart and kidneys. We hypothesize that '*reduced cardiac exposure of NSAIDs, will lower their CV side effects*.' As a model NSAID, we consider using diclofenac which has a cardiotoxicity profile that is ranked high. Diclofenac is among the world's most widely prescribed NSAIDs commonly used to relieve the symptoms associated with chronic inflammatory conditions such as RA and osteoarthritis. In spite of its good anti-inflammatory activity, diclofenac suffers from a short biological half-life and an elevated risk of CV risk.

The research work can be divided, broadly, into the following topics each covering an objective and specifying a project:

1. Development of polymeric micellar formulations for controlled delivery of diclofenac.
2. Assessing the pharmacokinetics biodistribution of traceable polymeric micellar diclofenac in healthy rats following parenteral administration.
3. Assessing the pharmacokinetics and pharmacodynamics of traceable polymeric micellar diclofenac in adjuvant arthritic rat model following parenteral administration.

Moreover, some preliminary studies on the biodistribution of traceable polymeric micelles following oral administration in healthy rats is presented in Supplement 1.

References

1. Harirforoosh, S., W. Asghar, and F. Jamali, *Adverse effects of nonsteroidal antiinflammatory drugs: an update of gastrointestinal, cardiovascular and renal complications.* Journal of Pharmacy & Pharmaceutical Sciences, 2014. **16**(5): p. 821-847.
2. Vane, J.R., *Inhibition of prostaglandin synthesis as a mechanism of action for aspirin-like drugs.* Nat New Biol, 1971. **231**(25): p. 232-5.
3. Hanna, V.S. and E.A.A. Hafez, *Synopsis of arachidonic acid metabolism: A review.* J Adv Res, 2018. **11**: p. 23-32.
4. Furst, D.E., *Are there differences among nonsteroidal antiinflammatory drugs? Comparing acetylated salicylates, nonacetylated salicylates, and nonacetylated nonsteroidal antiinflammatory drugs.* Arthritis Rheum, 1994. **37**(1): p. 1-9.
5. Warner, T.D., et al., *Nonsteroid drug selectivities for cyclo-oxygenase-1 rather than cyclo-oxygenase-2 are associated with human gastrointestinal toxicity: a full in vitro analysis.* Proc Natl Acad Sci U S A, 1999. **96**(13): p. 7563-8.
6. Ong, C.K., et al., *An evidence-based update on nonsteroidal anti-inflammatory drugs.* Clin Med Res, 2007. **5**(1): p. 19-34.
7. Straube, S., *Anti-inflammatory and antipyretic analgesics and drugs used in gout*, in *Side Effects of Drugs Annual*. 2011, Elsevier. p. 241-255.
8. Liu, J.Y., et al., *Metabolic profiling of murine plasma reveals an unexpected biomarker in rofecoxib-mediated cardiovascular events.* Proc Natl Acad Sci U S A, 2010. **107**(39): p. 17017-22.
9. Williams, J.M., et al., *20-hydroxyeicosatetraeonic acid: a new target for the treatment of hypertension.* J Cardiovasc Pharmacol, 2010. **56**(4): p. 336-44.
10. Roman, R.J., *P-450 metabolites of arachidonic acid in the control of cardiovascular function.* Physiol Rev, 2002. **82**(1): p. 131-85.
11. Zeng, Q., et al., *20-HETE increases NADPH oxidase-derived ROS production and stimulates the L-type Ca2+ channel via a PKC-dependent mechanism in cardiomyocytes.* Am J Physiol Heart Circ Physiol, 2010. **299**(4): p. H1109-17.
12. Zhang, Y., et al., *Combined therapy with COX-2 inhibitor and 20-HETE inhibitor reduces colon tumor growth and the adverse effects of ischemic stroke associated with COX-2 inhibition.* Am J Physiol Regul Integr Comp Physiol, 2014. **307**(6): p. R693-703.
13. Imig, J.D., *Epoxides and soluble epoxide hydrolase in cardiovascular physiology.* Physiol Rev, 2012. **92**(1): p. 101-30.
14. Aghazadeh-Habashi, A., W. Asghar, and F. Jamali, *Drug-Disease Interaction: Effect of Inflammation and Nonsteroidal Anti-inflammatory Drugs on Cytochrome P450 Metabolites of Arachidonic Acid.* J Pharm Sci, 2017.

15. McGettigan, P. and D. Henry, *Use of non-steroidal anti-inflammatory drugs that elevate cardiovascular risk: an examination of sales and essential medicines lists in low-, middle-, and high-income countries.* PLoS Med, 2013. **10**(2): p. e1001388.
16. Brogden, R.N., et al., *Diclofenac sodium: a review of its pharmacological properties and therapeutic use in rheumatic diseases and pain of varying origin.* Drugs, 1980. **20**(1): p. 24-48.
17. Siraux, P., *Diclofenac (Voltaren) for the treatment of osteo-arthrosis: a double-blind comparison with naproxen.* J Int Med Res, 1977. **5**(3): p. 169-74.
18. Durrigl, T., et al., *Diclofenac sodium (Voltaren): results of a multi-centre comparative trial in adult-onset rheumatoid arthritis.* J Int Med Res, 1975. **3**(3): p. 139-44.
19. van Walsem, A., et al., *Relative benefit-risk comparing diclofenac to other traditional non-steroidal anti-inflammatory drugs and cyclooxygenase-2 inhibitors in patients with osteoarthritis or rheumatoid arthritis: a network meta-analysis.* Arthritis Res Ther, 2015. **17**: p. 66.
20. Catalano, M.A., *Worldwide safety experience with diclofenac.* Am J Med, 1986. **80**(4B): p. 81-7.
21. Capone, M.L., et al., *Pharmacodynamic of cyclooxygenase inhibitors in humans.* Prostaglandins Other Lipid Mediat, 2007. **82**(1-4): p. 85-94.
22. McGettigan, P. and D. Henry, *Cardiovascular risk with non-steroidal anti-inflammatory drugs: systematic review of population-based controlled observational studies.* PLoS Med, 2011. **8**(9): p. e1001098.
23. John, V.A., *The pharmacokinetics and metabolism of diclofenac sodium (Voltarol) in animals and man.* Rheumatol Rehabil, 1979. **Suppl 2**: p. 22-37.
24. Chuasuwan, B., et al., *Biowaiver monographs for immediate release solid oral dosage forms: diclofenac sodium and diclofenac potassium.* J Pharm Sci, 2009. **98**(4): p. 1206-19.
25. Degen, P.H., et al., *Pharmacokinetics of diclofenac and five metabolites after single doses in healthy volunteers and after repeated doses in patients.* Xenobiotica, 1988. **18**(12): p. 1449-55.
26. Calatayud, S. and J.V. Esplugues, *Chemistry, Pharmacodynamics, and Pharmacokinetics of NSAIDs*, in *NSAIDs and Aspirin*. 2016, Springer. p. 3-16.
27. *Rubin's pathology: clinicopathologic foundations of medicine.*, ed. R. Rubin, D.S. Strayer, and E. Rubi. 2008, New York: Lippincott Williams & Wilkins.
28. Nathan, C. and A. Din, *Nonresolving Inflammation.* Cell, 2010. **140**: p. 871–882.
29. Harada, A., et al., *Essential involvement of interleukin-8 (IL-8) in acute inflammation.* J Leukoc Biol, 1994. **56**(5): p. 559-64.
30. Coussens, L.M. and Z. Werb, *Inflammation and cancer.* Nature, 2002. **420**(6917): p. 860-867.
31. Decker, K., *Basic mechanisms of the inflammatory response*, in *Molecular aspects of inflammation*. 1991, Springer. p. 1-23.
32. Cavaillon, J.M., *Pro- versus anti-inflammatory cytokines: myth or reality.* Cell Mol Biol (Noisy-le-grand), 2001. **47**(4): p. 695-702.

33. Lentsch, A.B. and P.A. Ward, *Regulation of inflammatory vascular damage.* J Pathol, 2000. **190**(3): p. 343-8.
34. Bhat, P., et al., *Interferon-gamma derived from cytotoxic lymphocytes directly enhances their motility and cytotoxicity.* Cell Death Dis, 2017. **8**(6): p. e2836.
35. Sharma, J.N. and L.A. Mohammed, *The role of leukotrienes in the pathophysiology of inflammatory disorders: is there a case for revisiting leukotrienes as therapeutic targets?* Inflammopharmacology, 2006. **14**(1-2): p. 10-6.
36. De Caterina, R. and A. Zampolli, *From asthma to atherosclerosis--5-lipoxygenase, leukotrienes, and inflammation.* N Engl J Med, 2004. **350**(1): p. 4-7.
37. Golan, D.E. and A.H. Tashjian, *Principles of pharmacology : the pathophysiologic basis of drug therapy*. Third edition. ed. 2012, Philadelphia: Wolters Kluwer Health/Lippincott Williams & Wilkins. xxi, 954 pages.
38. Berger, A., *What are leukotrienes and how do they work in asthma?* BMJ, 1999. **319**(7202): p. 90.
39. Narumiya, S., T. Yokomizo, and J. Aoki, *Lipid Mediators in Inflammation.* Inflammation: From Molecular and Cellular Mechanisms to the Clinic, 2018: p. 651-694.
40. Woods, A., et al., *Genetics of inflammation and risk of coronary artery.* European Heart Journal, 2000. **21**: p. 1574-1583.
41. Wilerson, J.T. and P.M. Ridker, *Willerson, James T., and Paul M. Ridker. "Inflammation as a cardiovascular risk factor.* Circulation 2004. **109**(21): p. II2-10.
42. Biasucci, L.M., et al., *Elevated levels of C-reactive protein at discharge in patients with unstable angina predict recurrent instability.* Circulation, 1999. **99**: p. 855-860.
43. Bozkurt, B., et al., *Results of targeted anti-tumor necrosis factor therapy with etanercept (ENBREL) in patients with advanced heart failure.* Circulation, 2001. **103**(8): p. 1044-7.
44. Ridker, P.M., et al., *Antiinflammatory Therapy with Canakinumab for Atherosclerotic Disease.* N Engl J Med, 2017. **377**(12): p. 1119-1131.
45. Shacter, E. and S.A. Weitzman, *Chronic inflammation and cancer.* Oncology, 2002. **16**(2): p. 217-232.
46. Rakoff-Nahoum, *Why cancer and inflammation.* Yale Journal of Biology and Medicine, 2006. **79**: p. 123-130.
47. Barnes, D.E. and K. Yaffe, *The projected effect of risk factor reduction on Alzheimer's disease prevalence.* Lancet Neurol, 2011. **10**(9): p. 819-28.
48. Dorey, E., et al., *Apolipoprotein E, amyloid-beta, and neuroinflammation in Alzheimer's disease.* Neurosci Bull, 2014. **30**(2): p. 317-30.
49. Akiyama, H., et al., *Cell mediators of inflammation in the Alzheimer disease brain.* Alzheimer Dis Assoc Disord, 2000. **14 Suppl 1**: p. S47-53.
50. Swardfager, W., et al., *A meta-analysis of cytokines in Alzheimer's disease.* Biol Psychiatry, 2010. **68**(10): p. 930-41.
51. Deardorff, W.J. and G.T. Grossberg, *Targeting neuroinflammation in Alzheimer's disease: evidence for NSAIDs and novel therapeutics.* Expert Rev Neurother, 2017. **17**(1): p. 17-32.
52. Akilesh, S., et al., *The MHC class I-like Fc receptor promotes humorally mediated autoimmune disease.* J Clin Invest, 2004. **113**(9): p. 1328-33.

53. Emery, P., *Rheumatoid arthritis: an overview*, in *Pocket Reference to Early Rheumatoid Arthritis*. 2011, Springer. p. 1-6.
54. Scott, D.L., et al., *Long-term outcome of treating rheumatoid arthritis: results after 20 years.* Lancet, 1987. **1**(8542): p. 1108-11.
55. Brown, P.M. and J.D. Isaacs, *Rheumatoid arthritis: from palliation to remission in two decades.* Clin Med (Lond), 2014. **14 Suppl 6**: p. s50-5.
56. Widdifield, J., et al., *The epidemiology of rheumatoid arthritis in Ontario, Canada.* Arthritis Rheumatol, 2014. **66**(4): p. 786-93.
57. Bombardier, C., G. Hawker, and D. Mosher, *The impact of arthritis in Canada: today and over the next 30 years*. 2016: Arthritis Alliance of Canada.
58. van der Heijde, D.M., et al., *Older versus younger onset rheumatoid arthritis: results at onset and after 2 years of a prospective followup study of early rheumatoid arthritis.* J Rheumatol, 1991. **18**(9): p. 1285-9.
59. Symmons, D.P., *Epidemiology of rheumatoid arthritis: determinants of onset, persistence and outcome.* Best Pract Res Clin Rheumatol, 2002. **16**(5): p. 707-22.
60. Silman, A.J., et al., *Twin concordance rates for rheumatoid arthritis: results from a nationwide study.* Br J Rheumatol, 1993. **32**(10): p. 903-7.
61. Voigt, L.F., et al., *Smoking, obesity, alcohol consumption, and the risk of rheumatoid arthritis.* Epidemiology, 1994. **5**(5): p. 525-32.
62. Walker, R. and C. Whittlesea, *Clinical pharmacy and therapeutics*. 5th ed. 2012, Edinburgh: Churchill Livingston/Elsevier. xii, 983 p.
63. Arnett, F.C., et al., *The American Rheumatism Association 1987 revised criteria for the classification of rheumatoid arthritis.* Arthritis Rheum, 1988. **31**(3): p. 315-24.
64. Firestein, G.S., *Rheumatoid arthritis. Etiology and pathogenesis of rheumatoid arthritis.* Kelley's textbook of rheumatology, 2005: p. 996-1042.
65. Smolen, J.S., D. Aletaha, and I.B. McInnes, *Rheumatoid arthritis.* Lancet, 2016. **388**(10055): p. 2023-2038.
66. Wood, J., *MUSCULOSKELETAL DISORDERS.(4). RHEUMATOID ARTHRITIS: MANAGEMENT WITH DMARDS.* Pharmaceutical journal, 1999. **263**(7056): p. 162-167.
67. Burmester, G.R. and J.E. Pope, *Novel treatment strategies in rheumatoid arthritis.* Lancet, 2017. **389**(10086): p. 2338-2348.
68. Astorri, E., et al., *Towards a stratified targeted approach with biologic treatments in rheumatoid arthritis: role of synovial pathobiology.* Curr Pharm Des, 2015. **21**(17): p. 2216-24.
69. van Jaarsveld, C.H., et al., *Toxicity of anti-rheumatic drugs in a randomized clinical trial of early rheumatoid arthritis.* Rheumatology (Oxford), 2000. **39**(12): p. 1374-82.
70. Malysheva, O.A., et al., *Low-dose prednisolone in rheumatoid arthritis: adverse effects of various disease modifying antirheumatic drugs.* J Rheumatol, 2008. **35**(6): p. 979-85.
71. Fries, J.F., et al., *The relative toxicity of disease-modifying antirheumatic drugs.* Arthritis Rheum, 1993. **36**(3): p. 297-306.
72. Vela, P., *Extra-articular manifestations of rheumatoid arthritis, now.*

73. Bykerk, V.P., et al., *Canadian Rheumatology Association recommendations for pharmacological management of rheumatoid arthritis with traditional and biologic disease-modifying antirheumatic drugs.* J Rheumatol, 2012. **39**(8): p. 1559-82.
74. Danning, C.L. and D.T. Boumpas, *Commonly used disease-modifying antirheumatic drugs in the treatment of inflammatory arthritis: an update on mechanisms of action.* Clin Exp Rheumatol, 1998. **16**(5): p. 595-604.
75. Curtis, J.R. and J.A. Singh, *Use of biologics in rheumatoid arthritis: current and emerging paradigms of care.* Clin Ther, 2011. **33**(6): p. 679-707.
76. Smith, J.B. and M.K. Haynes, *Rheumatoid arthritis--a molecular understanding.* Ann Intern Med, 2002. **136**(12): p. 908-22.
77. Mariette, X., *Emerging biological therapies in rheumatoid arthritis.* Joint Bone Spine, 2004. **71**(6): p. 470-4.
78. Moreland, L.W. and J.R. O'Dell, *Glucocorticoids and rheumatoid arthritis: back to the future?* Arthritis Rheum, 2002. **46**(10): p. 2553-63.
79. Quinn, M.A., P.G. Conaghan, and P. Emery, *The therapeutic approach of early intervention for rheumatoid arthritis: what is the evidence?* Rheumatology (Oxford), 2001. **40**(11): p. 1211-20.
80. Schmith, V.D. and J.F. Foss, *Effects of inflammation on pharmacokinetics/pharmacodynamics: increasing recognition of its contribution to variability in response.* Clin Pharmacol Ther, 2008. **83**(6): p. 809-11.
81. Schneider, R.E., et al., *Effect of inflammatory disease on plasma concentrations of three beta-adrenoceptor blocking agents.* Int J Clin Pharmacol Ther Toxicol, 1981. **19**(4): p. 158-62.
82. Piquette-Miller, M. and F. Jamali, *Influence of severity of inflammation on the disposition kinetics of propranolol enantiomers in ketoprofen-treated and untreated adjuvant arthritis.* Drug Metab Dispos, 1995. **23**(2): p. 240-5.
83. Piquette-Miller, M. and F. Jamali, *Selective effect of adjuvant arthritis on the disposition of propranolol enantiomers in rats detected using a stereospecific HPLC assay.* Pharm Res, 1993. **10**(2): p. 294-9.
84. Mayo, P.R., et al., *Decreased dromotropic response to verapamil despite pronounced increased drug concentration in rheumatoid arthritis.* Br J Clin Pharmacol, 2000. **50**(6): p. 605-13.
85. Petrovic, V., S. Teng, and M. Piquette-Miller, *Regulation of drug transporters during infection and inflammation.* Mol Interv, 2007. **7**(2): p. 99-111.
86. Aitken, A.E., T.A. Richardson, and E.T. Morgan, *Regulation of drug-metabolizing enzymes and transporters in inflammation.* Annu Rev Pharmacol Toxicol, 2006. **46**: p. 123-49.
87. Ling, S., et al., *Influence of controlled rheumatoid arthritis on the action and disposition of verapamil: focus on infliximab.* J Clin Pharmacol, 2009. **49**(3): p. 301-11.
88. Kulmatycki, K.M., et al., *Drug-disease interactions: reduced beta-adrenergic and potassium channel antagonist activities of sotalol in the presence of acute and chronic inflammatory conditions in the rat.* Br J Pharmacol, 2001. **133**(2): p. 286-94.

89. Guirguis, M.S. and F. Jamali, *Disease-drug interaction: Reduced response to propranolol despite increased concentration in the rat with inflammation.* J Pharm Sci, 2003. **92**(5): p. 1077-84.
90. Strebhardt, K. and A. Ullrich, *Paul Ehrlich's magic bullet concept: 100 years of progress.* Nat Rev Cancer, 2008. **8**(6): p. 473-80.
91. Choonara, B.F., et al., *A review of advanced oral drug delivery technologies facilitating the protection and absorption of protein and peptide molecules.* Biotechnol Adv, 2014. **32**(7): p. 1269-1282.
92. Corsini, A. and M. Bortolini, *Drug-induced liver injury: the role of drug metabolism and transport.* J Clin Pharmacol, 2013. **53**(5): p. 463-74.
93. Aliabadi, H.M., et al., *Disposition of drugs in block copolymer micelle delivery systems: from discovery to recovery.* Clin Pharmacokinet, 2008. **47**(10): p. 619-34.
94. Krishna, R. and L.D. Mayer, *Modulation of P-glycoprotein (PGP) mediated multidrug resistance (MDR) using chemosensitizers: recent advances in the design of selective MDR modulators.* Curr Med Chem Anticancer Agents, 2001. **1**(2): p. 163-74.
95. Maeda, H., H. Nakamura, and J. Fang, *The EPR effect for macromolecular drug delivery to solid tumors: Improvement of tumor uptake, lowering of systemic toxicity, and distinct tumor imaging in vivo.* Adv Drug Deliv Rev, 2013. **65**(1): p. 71-9.
96. Bronich, T.K., et al., *Polymer micelle with cross-linked ionic core.* Journal of the American Chemical Society, 2005. **127**(23): p. Bronich, Tatiana K., Paul A. Keifer, Luda S. Shlyakhtenko, and Alexander V. Kabanov. "Polymer micelle8236-8237.
97. Alexander-Bryant, A.A., W.S.V. Berg-Foels, and X. Wen, *Bioengineering strategies for designing targeted cancer therapies*, in *Advances in cancer research*. 2013, Elsevier. p. 1-59.
98. Knop, K., et al., *Poly(ethylene glycol) in drug delivery: pros and cons as well as potential alternatives.* Angew Chem Int Ed Engl, 2010. **49**(36): p. 6288-308.
99. Batrakova, E.V., et al., *Polymer micelles as drug carriers*, in *Nanoparticulates as drug carriers*. 2006, World Scientific. p. 57-93.
100. Aliabadi, H.M. and A. Lavasanifar, *Polymeric micelles for drug delivery.* Expert Opin Drug Deliv, 2006. **3**(1): p. 139-62.
101. Husseini, G.A. and W.G. Pitt, *Micelles and nanoparticles for ultrasonic drug and gene delivery.* Advanced drug delivery reviews, 2008. **60**(10): p. 1137-1152.
102. Rangel-Yagui, C.O., A. Pessoa Jr, and L.C. Tavares, *Micellar solubilization of drugs.* J. Pharm. Pharm. Sci, 2005. **8**(2): p. 147-163.
103. Solmaz, A., *Amphiphilic block copolymer micelles for drug delivery vehicles.* University of Groningen, Faculty of Mathematics and Natural Sciences, 2010.
104. Allen, C., D. Maysinger, and A. Eisenberg, *Nano-engineering block copolymer aggregates for drug delivery.* Colloids and Surfaces B: Biointerfaces, 1999. **16**(1-4): p. 3-27.
105. Cheng, C., et al., *Biotinylated thermoresponsive micelle self-assembled from double-hydrophilic block copolymer for drug delivery and tumor target.* Biomaterials, 2008. **29**(4): p. 497-505.
106. Jones, M. and J. Leroux, *Polymeric micelles - a new generation of colloidal drug carriers.* Eur J Pharm Biopharm, 1999. **48**(2): p. 101-11.

107. Aliabadi, H.M., et al., *Encapsulation of hydrophobic drugs in polymeric micelles through co-solvent evaporation: the effect of solvent composition on micellar properties and drug loading.* Int J Pharm, 2007. **329**(1-2): p. 158-65.
108. Weissig, V., T.K. Pettinger, and N. Murdock, *Nanopharmaceuticals (part 1): products on the market.* Int J Nanomedicine, 2014. **9**: p. 4357-73.
109. Harirforoosh, S., W. Asghar, and F. Jamali, *Adverse effects of nonsteroidal antiinflammatory drugs: an update of gastrointestinal, cardiovascular and renal complications.* J Pharm Pharm Sci, 2013. **16**(5): p. 821-47.
110. Waterbeemd, H.v.d. and B. Testa, *Drug bioavailability : estimation of solubility, permeability, absorption and bioavailability*. Second, completely revised edition. ed. Methods and principles in medicinal chemistry. 2009, Weinheim: Wiley-VCH. xxv, 624 pages.
111. Al Lawati, H.A. and F. Jamali, *Onset of Action and Efficacy of Ibuprofen Liquigel as Compared to Solid Tablets: A Systematic Review and Meta-Analysis.* J Pharm Pharm Sci, 2016. **19**(3): p. 301-311.
112. Mennini, N., et al., *Development of a chitosan-derivative micellar formulation to improve celecoxib solubility and bioavailability.* Drug Dev Ind Pharm, 2014. **40**(11): p. 1494-502.
113. Warner, T.D. and J.A. Mitchell, *COX-2 selectivity alone does not define the cardiovascular risks associated with non-steroidal anti-inflammatory drugs.* Lancet, 2008. **371**(9608): p. 270-3.
114. Wolfe, M.M., D.R. Lichtenstein, and G. Singh, *Gastrointestinal toxicity of nonsteroidal antiinflammatory drugs.* N Engl J Med, 1999. **340**(24): p. 1888-99.
115. Soehngen, E.C., et al., *Encapsulation of indomethacin in liposomes provides protection against both gastric and intestinal ulceration when orally administered to rats.* Arthritis Rheum, 1988. **31**(3): p. 414-22.
116. Arias, J.L., *Nanoparticle therapy in arthritis.* Nanomedicine in health and disease. CRC press: Enfield, USA, 2011: p. 293.
117. Chandrasekar, D., et al., *Folate coupled poly(ethyleneglycol) conjugates of anionic poly(amidoamine) dendrimer for inflammatory tissue specific drug delivery.* J Biomed Mater Res A, 2007. **82**(1): p. 92-103.
118. Derry, S., et al., *Topical NSAIDs for chronic musculoskeletal pain in adults.* Cochrane Database Syst Rev, 2016. **4**: p. CD007400.
119. Vega, E., et al., *Flurbiprofen PLGA-PEG nanospheres: role of hydroxy-beta-cyclodextrin on ex vivo human skin permeation and in vivo topical anti-inflammatory efficacy.* Colloids Surf B Biointerfaces, 2013. **110**: p. 339-46.
120. Shumilov, M., et al., *Ibuprofen transdermal ethosomal gel: characterization and efficiency in animal models.* J Biomed Nanotechnol, 2010. **6**(5): p. 569-76.
121. Zhang, Z. and G. Huang, *Intra-articular lornoxicam loaded PLGA microspheres: enhanced therapeutic efficiency and decreased systemic toxicity in the treatment of osteoarthritis.* Drug Deliv, 2012. **19**(5): p. 255-63.
122. Kim, S.J., A.J. Flach, and L.M. Jampol, *Nonsteroidal anti-inflammatory drugs in ophthalmology.* Surv Ophthalmol, 2010. **55**(2): p. 108-33.

123. Hoffman, R.S., et al., *Cataract surgery and nonsteroidal antiinflammatory drugs.* J Cataract Refract Surg, 2016. **42**(9): p. 1368-1379.
124. Ahuja, M., et al., *Topical ocular delivery of NSAIDs.* AAPS J, 2008. **10**(2): p. 229-41.
125. Poddubnyy, D., et al., *Effect of non-steroidal anti-inflammatory drugs on radiographic spinal progression in patients with axial spondyloarthritis: results from the German Spondyloarthritis Inception Cohort.* Ann Rheum Dis, 2012. **71**(10): p. 1616-22.
126. Weggen, S., et al., *A subset of NSAIDs lower amyloidogenic Abeta42 independently of cyclooxygenase activity.* Nature, 2001. **414**(6860): p. 212-6.
127. Cote, S., et al., *Nonsteroidal anti-inflammatory drug use and the risk of cognitive impairment and Alzheimer's disease.* Alzheimers Dement, 2012. **8**(3): p. 219-26.
128. Bishnoi, M., et al., *Aceclofenac-loaded chondroitin sulfate conjugated SLNs for effective management of osteoarthritis.* J Drug Target, 2014. **22**(9): p. 805-12.
129. Xu, X., et al., *Aspirin-Based Carbon Dots, a Good Biocompatibility of Material Applied for Bioimaging and Anti-Inflammation.* ACS Appl Mater Interfaces, 2016. **8**(48): p. 32706-32716.
130. Thakkar, H., R. Kumar Sharma, and R.S. Murthy, *Enhanced retention of celecoxib-loaded solid lipid nanoparticles after intra-articular administration.* Drugs R D, 2007. **8**(5): p. 275-85.
131. Bouchal, R., et al., *Biocompatible Periodic Mesoporous Ionosilica Nanoparticles with Ammonium Walls: Application to Drug Delivery.* ACS Appl Mater Interfaces, 2017. **9**(37): p. 32018-32025.
132. Al Lawati, H., et al., *Polymeric micelles for the delivery of diclofenac and its ethyl ester derivative.* Pharmaceutical Nanotechnology, 2016. **4**(2): p. 109-119.
133. Jukanti, R., et al., *Drug targeting to inflammation: studies on antioxidant surface loaded diclofenac liposomes.* Int J Pharm, 2011. **414**(1-2): p. 179-85.
134. Lima, E.M. and A.G. Oliveira, *Tissue tolerance of diclofenac sodium encapsulated in liposomes after intramuscular administration.* Drug Dev Ind Pharm, 2002. **28**(6): p. 673-80.
135. Guterres, S.S., et al., *Poly(rac-lactide) nanocapsules containing diclofenac: protection against muscular damage in rats.* J Biomater Sci Polym Ed, 2000. **11**(12): p. 1347-55.
136. Elron-Gross, I., Y. Glucksam, and R. Margalit, *Liposomal dexamethasone-diclofenac combinations for local osteoarthritis treatment.* Int J Pharm, 2009. **376**(1-2): p. 84-91.
137. Turker, S., et al., *Enhanced efficacy of diclofenac sodium-loaded lipogelosome formulation in intra-articular treatment of rheumatoid arthritis.* J Drug Target, 2008. **16**(1): p. 51-7.
138. Bilthariya, U., et al., *Folate-conjugated albumin nanoparticles for rheumatoid arthritis-targeted delivery of etoricoxib.* Drug Dev Ind Pharm, 2015. **41**(1): p. 95-104.
139. Verma, P., et al., *Single Intravenous Dose of Novel Flurbiprofen-Loaded Proniosome Formulations Provides Prolonged Systemic Exposure and Anti-inflammatory Effect.* Mol Pharm, 2016. **13**(11): p. 3688-3699.
140. Begum, M., K. Abbulu, and M. Sudhakar, *Flurbiprofen-loaded stealth liposomes: studies on the development, characterization, pharmacokinetics, and biodistribution.* J Young Pharm, 2012. **4**(4): p. 209-19.

141. Asthana, A., et al., *Poly(amidoamine) (PAMAM) dendritic nanostructures for controlled site-specific delivery of acidic anti-inflammatory active ingredient.* AAPS PharmSciTech, 2005. **6**(3): p. E536-42.
142. Rinaldi, F., et al., *pH-sensitive niosomes: Effects on cytotoxicity and on inflammation and pain in murine models.* J Enzyme Inhib Med Chem, 2017. **32**(1): p. 538-546.
143. Narayanan, D., et al., *Poly-(ethylene glycol) modified gelatin nanoparticles for sustained delivery of the anti-inflammatory drug Ibuprofen-Sodium: an in vitro and in vivo analysis.* Nanomedicine, 2013. **9**(6): p. 818-28.
144. Lamprecht, A., et al., *Lipid nanocarriers as drug delivery system for ibuprofen in pain treatment.* Int J Pharm, 2004. **278**(2): p. 407-14.
145. Kwasigroch, B., et al., *Oil-in-water nanoemulsions are suitable for carrying hydrophobic compounds: Indomethacin as a model of anti-inflammatory drug.* Int J Pharm, 2016. **515**(1-2): p. 749-756.
146. Wei, X., et al., *Thermosensitive beta-cyclodextrin modified poly(epsilon-caprolactone)-poly(ethylene glycol)-poly(epsilon-caprolactone) micelles prolong the anti-inflammatory effect of indomethacin following local injection.* Acta Biomater, 2013. **9**(6): p. 6953-63.
147. Bernardi, A., et al., *Indomethacin-oaded lipid-core nanocapsules reduce the damage triggered by Abeta1-42 in Alzheimer's disease models.* Int J Nanomedicine, 2012. **7**: p. 4927-42.
148. Bernardi, A., et al., *Effects of indomethacin-loaded nanocapsules in experimental models of inflammation in rats.* Br J Pharmacol, 2009. **158**(4): p. 1104-11.
149. Badawi, A.A., et al., *Chitosan based nanocarriers for indomethacin ocular delivery.* Arch Pharm Res, 2008. **31**(8): p. 1040-9.
150. Zhang, J.X., et al., *Local delivery of indomethacin to arthritis-bearing rats through polymeric micelles based on amphiphilic polyphosphazenes.* Pharm Res, 2007. **24**(10): p. 1944-53.
151. Palakurthi, S., S.P. Vyas, and P.V. Diwan, *Biodisposition of PEG-coated lipid microspheres of indomethacin in arthritic rats.* Int J Pharm, 2005. **290**(1-2): p. 55-62.
152. Chauhan, A.S., et al., *Solubility enhancement of indomethacin with poly(amidoamine) dendrimers and targeting to inflammatory regions of arthritic rats.* J Drug Target, 2004. **12**(9-10): p. 575-83.
153. Srinath, P., S.P. Vyas, and P.V. Diwan, *Preparation and pharmacodynamic evaluation of liposomes of indomethacin.* Drug Dev Ind Pharm, 2000. **26**(3): p. 313-21.
154. Kamel, R., A.H. Salama, and A.A. Mahmoud, *Development and optimization of self-assembling nanosystem for intra-articular delivery of indomethacin.* Int J Pharm, 2016.
155. Zhang, J.X., et al., *Physicochemical characterization, in vitro, and in vivo evaluation of indomethacin-loaded nanocarriers self-assembled by amphiphilic polyphosphazene.* J Biomed Mater Res A, 2008. **86**(4): p. 914-25.
156. Wu, P.C., et al., *Magnetic field distribution modulation of intrathecal delivered ketorolac iron-oxide nanoparticle conjugates produce excellent analgesia for chronic inflammatory pain.* J Nanobiotechnology, 2018. **16**(1): p. 49.
157. Helmy, H.S., et al., *Therapeutic effects of lornoxicam-loaded nanomicellar formula in experimental models of rheumatoid arthritis.* Int J Nanomedicine, 2017. **12**: p. 7015-7023.

158. Li, Q., et al., *A novel albumin wrapped nanosuspension of meloxicam to improve inflammation-targeting effects.* Int J Nanomedicine, 2018. **13**: p. 4711-4725.
159. Kim, S.R., et al., *Increased localized delivery of piroxicam by cationic nanoparticles after intra-articular injection.* Drug Des Devel Ther, 2016. **10**: p. 3779-3787.
160. Tiwari, S., et al., *Urate crystal degradation for treatment of gout: a nanoparticulate combination therapy approach.* Drug Deliv Transl Res, 2015. **5**(3): p. 219-30.
161. Patel, D., et al., *Nanostructured Lipid Carriers (NLC)-Based Gel for the Topical Delivery of Aceclofenac: Preparation, Characterization, and In Vivo Evaluation.* Sci Pharm, 2012. **80**(3): p. 749-64.
162. Subramanian, B., et al., *Enhancement of anti-inflammatory property of aspirin in mice by a nano-emulsion preparation.* Int Immunopharmacol, 2008. **8**(11): p. 1533-9.
163. Kumar, R., et al., *Supramolecular assemblies based on copolymers of PEG600 and functionalized aromatic diesters for drug delivery applications.* J Am Chem Soc, 2004. **126**(34): p. 10640-4.
164. Rahmani-Neishaboor, E., et al., *Topical application of a film-forming emulgel dressing that controls the release of stratifin and acetylsalicylic acid and improves/prevents hypertrophic scarring.* Wound Repair Regen, 2013. **21**(1): p. 55-65.
165. Nirbhavane, P., et al., *Preclinical Explorative Assessment of Celecoxib-Based Biocompatible Lipidic Nanocarriers for the Management of CFA-Induced Rheumatoid Arthritis in Wistar Rats.* AAPS PharmSciTech, 2018. **19**(7): p. 3187-3198.
166. Fetih, G., D. Fathalla, and M. El-Badry, *Liposomal gels for site-specific, sustained delivery of celecoxib: in vitro and in vivo evaluation.* Drug Dev Res, 2014. **75**(4): p. 257-66.
167. Tamilvanan, S. and R. Baskar, *Effect of non-phospholipid-based cationic and phospholipid-based anionic nanosized emulsions on skin retention and anti-inflammatory activity of celecoxib.* Pharm Dev Technol, 2013. **18**(4): p. 761-71.
168. Joshi, M. and V. Patravale, *Nanostructured lipid carrier (NLC) based gel of celecoxib.* Int J Pharm, 2008. **346**(1-2): p. 124-32.
169. Subramanian, N., S.K. Ghosal, and S.P. Moulik, *Enhanced in vitro percutaneous absorption and in vivo anti-inflammatory effect of a selective cyclooxygenase inhibitor using microemulsion.* Drug Dev Ind Pharm, 2005. **31**(4-5): p. 405-16.
170. Jain, S., et al., *Quality by design approach for formulation, evaluation and statistical optimization of diclofenac-loaded ethosomes via transdermal route.* Pharm Dev Technol, 2015. **20**(4): p. 473-89.
171. Kaur, A., et al., *Supramolecular nano-engineered lipidic carriers based on diflunisal-phospholipid complex for transdermal delivery: QbD based optimization, characterization and preclinical investigations for management of rheumatoid arthritis.* Int J Pharm, 2017. **533**(1): p. 206-224.
172. Kaur, A., S. Goindi, and O.P. Katare, *Formulation, characterisation and in vivo evaluation of lipid-based nanocarrier for topical delivery of diflunisal.* J Microencapsul, 2016: p. 1-12.
173. Cheng, Y., et al., *Transdermal delivery of nonsteroidal anti-inflammatory drugs mediated by polyamidoamine (PAMAM) dendrimers.* J Pharm Sci, 2007. **96**(3): p. 595-602.

174. Salah, S., A.A. Mahmoud, and A.O. Kamel, *Etodolac transdermal cubosomes for the treatment of rheumatoid arthritis: ex vivo permeation and in vivo pharmacokinetic studies.* Drug Deliv, 2017. **24**(1): p. 846-856.
175. Goindi, S., R. Kaur, and R. Kaur, *An ionic liquid-in-water microemulsion as a potential carrier for topical delivery of poorly water soluble drug: Development, ex-vivo and in-vivo evaluation.* Int J Pharm, 2015. **495**(2): p. 913-23.
176. Farghaly, D.A., et al., *Topical Delivery of Fenoprofen Calcium via Elastic Nano-vesicular Spanlastics: Optimization Using Experimental Design and In Vivo Evaluation.* AAPS PharmSciTech, 2017. **18**(8): p. 2898-2909.
177. Jain, S.K., et al., *Solid lipid nanoparticles bearing flurbiprofen for transdermal delivery.* Drug Deliv, 2005. **12**(4): p. 207-15.
178. Azizi, M., et al., *Efficacy of nano- and microemulsion-based topical gels in delivery of ibuprofen: an in vivo study.* J Microencapsul, 2017. **34**(2): p. 195-202.
179. Nagai, N., T. Tanino, and Y. Ito, *Pharmacokinetic Studies of Gel System Containing Ibuprofen Solid Nanoparticles.* J Oleo Sci, 2016. **65**(12): p. 1045-1053.
180. Suto, B., et al., *Development of ibuprofen-loaded nanostructured lipid carrier-based gels: characterization and investigation of in vitro and in vivo penetration through the skin.* Int J Nanomedicine, 2016. **11**: p. 1201-12.
181. Djekic, L., et al., *Design of Block Copolymer Costabilized Nonionic Microemulsions and Their In Vitro and In Vivo Assessment as Carriers for Sustained Regional Delivery of Ibuprofen via Topical Administration.* J Pharm Sci, 2015. **104**(8): p. 2501-12.
182. Gaur, P.K., et al., *Development of ibuprofen nanoliposome for transdermal delivery: Physical characterization, in vitro/in vivo studies, and anti-inflammatory activity.* Artif Cells Nanomed Biotechnol, 2016. **44**(1): p. 370-5.
183. Yokota, J. and S. Kyotani, *Influence of nanoparticle size on the skin penetration, skin retention and anti-inflammatory activity of non-steroidal anti-inflammatory drugs.* J Chin Med Assoc, 2018. **81**(6): p. 511-519.
184. Nagai, N., C. Yoshioka, and Y. Ito, *Topical therapies for rheumatoid arthritis by gel ointments containing indomethacin nanoparticles in adjuvant-induced arthritis rat.* J Oleo Sci, 2015. **64**(3): p. 337-46.
185. Nagai, N., et al., *Pharmacokinetics and Antiinflammatory Effect of a Novel Gel System Containing Ketoprofen Solid Nanoparticles.* Biol Pharm Bull, 2015. **38**(12): p. 1918-24.
186. Nikumbh, K.V., S.G. Sevankar, and M.P. Patil, *Formulation development, in vitro and in vivo evaluation of microemulsion-based gel loaded with ketoprofen.* Drug Deliv, 2015. **22**(4): p. 509-15.
187. Gonullu, U., et al., *Formulation and characterization of solid lipid nanoparticles, nanostructured lipid carriers and nanoemulsion of lornoxicam for transdermal delivery.* Acta Pharm, 2015. **65**(1): p. 1-13.
188. Dasgupta, S., et al., *In vitro & in vivo studies on lornoxicam loaded nanoemulsion gels for topical application.* Curr Drug Deliv, 2014. **11**(1): p. 132-8.
189. Ahad, A., et al., *Enhanced anti-inflammatory activity of carbopol loaded meloxicam nanoethosomes gel.* Int J Biol Macromol, 2014. **67**: p. 99-104.

190. El-Menshawe, S.F. and A.K. Hussein, *Formulation and evaluation of meloxicam niosomes as vesicular carriers for enhanced skin delivery.* Pharm Dev Technol, 2013. **18**(4): p. 779-86.
191. Ustundag Okur, N., A. Yavasoglu, and H.Y. Karasulu, *Preparation and evaluation of microemulsion formulations of naproxen for dermal delivery.* Chem Pharm Bull (Tokyo), 2014. **62**(2): p. 135-43.
192. Peng, L.H., et al., *Sustained release of piroxicam from solid lipid nanoparticle as an effective anti-inflammatory therapeutics in vivo.* Drug Dev Ind Pharm, 2016: p. 1-12.
193. Canto, G.S., S.L. Dalmora, and A.G. Oliveira, *Piroxicam encapsulated in liposomes: characterization and in vivo evaluation of topical anti-inflammatory effect.* Drug Dev Ind Pharm, 1999. **25**(12): p. 1235-9.
194. Elkomy, M.H., et al., *Development of a nanogel formulation for transdermal delivery of tenoxicam: a pharmacokinetic-pharmacodynamic modeling approach for quantitative prediction of skin absorption.* Drug Dev Ind Pharm, 2017. **43**(4): p. 531-544.
195. Goindi, S., M. Narula, and A. Kalra, *Microemulsion-Based Topical Hydrogels of Tenoxicam for Treatment of Arthritis.* AAPS PharmSciTech, 2016. **17**(3): p. 597-606.
196. Joshi, M. and V. Patravale, *Formulation and evaluation of Nanostructured Lipid Carrier (NLC)-based gel of Valdecoxib.* Drug Dev Ind Pharm, 2006. **32**(8): p. 911-8.
197. Katara, R., S. Sachdeva, and D.K. Majumdar, *Design, characterization, and evaluation of aceclofenac-loaded Eudragit RS 100 nanoparticulate system for ocular delivery.* Pharm Dev Technol, 2018: p. 1-12.
198. Katara, R. and D.K. Majumdar, *Eudragit RL 100-based nanoparticulate system of aceclofenac for ocular delivery.* Colloids Surf B Biointerfaces, 2013. **103**: p. 455-62.
199. Sharma, A.K., et al., *Fabrication and evaluation of lipid nanoparticulates for ocular delivery of a COX-2 inhibitor.* Drug Deliv, 2016. **23**(9): p. 3364-3373.
200. Asasutjarit, R., et al., *Development and Evaluation of Diclofenac Sodium Loaded-N-Trimethyl Chitosan Nanoparticles for Ophthalmic Use.* AAPS PharmSciTech, 2015. **16**(5): p. 1013-24.
201. Sanchez-Lopez, E., et al., *PEGylated PLGA nanospheres optimized by design of experiments for ocular administration of dexibuprofen-in vitro, ex vivo and in vivo characterization.* Colloids Surf B Biointerfaces, 2016. **145**: p. 241-50.
202. Vasconcelos, A., et al., *Conjugation of cell-penetrating peptides with poly(lactic-co-glycolic acid)-polyethylene glycol nanoparticles improves ocular drug delivery.* Int J Nanomedicine, 2015. **10**: p. 609-31.
203. Vega, E., et al., *Flurbiprofen loaded biodegradable nanoparticles for ophtalmic administration.* J Pharm Sci, 2006. **95**(11): p. 2393-405.
204. Shen, J., et al., *Novel NSAIDs ophthalmic formulation: flurbiprofen axetil emulsion with low irritancy and improved anti-inflammation effect.* Int J Pharm, 2011. **412**(1-2): p. 115-22.
205. Pachis, K., et al., *Sustained release of intravitreal flurbiprofen from a novel drug-in-liposome-in-hydrogel formulation.* Eur J Pharm Sci, 2017. **109**: p. 324-333.
206. Bucolo, C., et al., *Enhanced ocular anti-inflammatory activity of ibuprofen carried by an Eudragit RS100 nanoparticle suspension.* Ophthalmic Res, 2002. **34**(5): p. 319-23.

207. Nagai, N., et al., *A nanoparticle formulation reduces the corneal toxicity of indomethacin eye drops and enhances its corneal permeability.* Toxicology, 2014. **319**: p. 53-62.
208. Morsi, N., et al., *Ketoroloac tromethamine loaded nanodispersion incorporated into thermosensitive in situ gel for prolonged ocular delivery.* Int J Pharm, 2016. **506**(1-2): p. 57-67.
209. Gupta, A.K., et al., *Ketorolac entrapped in polymeric micelles: preparation, characterisation and ocular anti-inflammatory studies.* Int J Pharm, 2000. **209**(1-2): p. 1-14.
210. Adibkia, K., et al., *Piroxicam nanoparticles for ocular delivery: physicochemical characterization and implementation in endotoxin-induced uveitis.* J Drug Target, 2007. **15**(6): p. 407-16.
211. Mandal, S., et al., *Preclinical Study of Ibuprofen Loaded Transnasal Mucoadhesive Microemulsion for Neuroprotective Effect in MPTP Mice Model.* Iran J Pharm Res, 2018. **17**(1): p. 23-38.
212. Vij, N., et al., *Neutrophil targeted nano-drug delivery system for chronic obstructive lung diseases.* Nanomedicine, 2016. **12**(8): p. 2415-2427.
213. Mandal, S., et al., *Design and evaluation of mucoadhesive microemulsion for neuroprotective effect of ibuprofen following intranasal route in the MPTP mice model.* Drug Dev Ind Pharm, 2016. **42**(8): p. 1340-50.
214. Bartos, C., et al., *Study of sodium hyaluronate-based intranasal formulations containing micro- or nanosized meloxicam particles.* Int J Pharm, 2015. **491**(1-2): p. 198-207.
215. Tang, S.Y., et al., *Anti-inflammatory and analgesic activity of novel oral aspirin-loaded nanoemulsion and nano multiple emulsion formulations generated using ultrasound cavitation.* Int J Pharm, 2012. **430**(1-2): p. 299-306.
216. Salem, H.F., et al., *Formulation development of self-nanoemulsifying drug delivery system of celecoxib for the management of oral cavity inflammation.* J Liposome Res, 2018: p. 1-11.
217. Harirforoosh, S., et al., *Assessment of celecoxib poly(lactic-co-glycolic) acid nanoformulation on drug pharmacodynamics and pharmacokinetics in rats.* Eur Rev Med Pharmacol Sci, 2016. **20**(22): p. 4818-4829.
218. Nguyen, T.H., et al., *Silica-lipid hybrid (SLH) formulations enhance the oral bioavailability and efficacy of celecoxib: An in vivo evaluation.* J Control Release, 2013. **167**(1): p. 85-91.
219. Sanchez-Lopez, E., et al., *New potential strategies for Alzheimer's disease prevention: pegylated biodegradable dexibuprofen nanospheres administration to APPswe/PS1dE9.* Nanomedicine, 2017. **13**(3): p. 1171-1182.
220. Harirforoosh, S., et al., *Examination of the pharmacodynamics and pharmacokinetics of a diclofenac poly(lactic-co-glycolic) acid nanoparticle formulation in the rat.* Eur Rev Med Pharmacol Sci, 2016. **20**(23): p. 5021-5031.
221. Goh, J.Z., et al., *Evaluation of antinociceptive activity of nanoliposome-encapsulated and free-form diclofenac in rats and mice.* Int J Nanomedicine, 2015. **10**: p. 297-303.
222. Nagai, N. and Y. Ito, *Effect of solid nanoparticle of indomethacin on therapy for rheumatoid arthritis in adjuvant-induced arthritis rat.* Biol Pharm Bull, 2014. **37**(7): p. 1109-18.

223. Yoshitomi, T., et al., *Indomethacin-loaded redox nanoparticles improve oral bioavailability of indomethacin and suppress its small intestinal inflammation.* Ther Deliv, 2014. **5**(1): p. 29-38.
224. Cunha, V.R., et al., *Delivery system for mefenamic acid based on the nanocarrier layered double hydroxide: Physicochemical characterization and evaluation of anti-inflammatory and antinociceptive potential.* Mater Sci Eng C Mater Biol Appl, 2016. **58**: p. 629-38.
225. Parekh, V.J., et al., *Self nanoemulsifying granules (SNEGs) of meloxicam: preparation, characterization, molecular modeling and evaluation of in vivo anti-inflammatory activity.* Drug Dev Ind Pharm, 2017. **43**(4): p. 600-610.
226. Villalba, B.T., et al., *Meloxicam-loaded nanocapsules have antinociceptive and antiedematogenic effects in acute models of nociception.* Life Sci, 2014. **115**(1-2): p. 36-43.
227. Moulari, B., et al., *The targeting of surface modified silica nanoparticles to inflamed tissue in experimental colitis.* Biomaterials, 2008. **29**(34): p. 4554-60.
228. Pertuit, D., et al., *5-amino salicylic acid bound nanoparticles for the therapy of inflammatory bowel disease.* J Control Release, 2007. **123**(3): p. 211-8.
229. Tramer, M.R., et al., *Comparing analgesic efficacy of non-steroidal anti-inflammatory drugs given by different routes in acute and chronic pain: a qualitative systematic review.* Acta Anaesthesiol Scand, 1998. **42**(1): p. 71-9.
230. Moore, A.H., et al., *Non-Steroidal Anti-Inflammatory Drugs in Alzheimer's Disease and Parkinson's Disease: Reconsidering the Role of Neuroinflammation.* Pharmaceuticals (Basel), 2010. **3**(6): p. 1812-1841.

Chapter 2: Polymeric micelles for the delivery of diclofenac and its ethyl ester derivative*

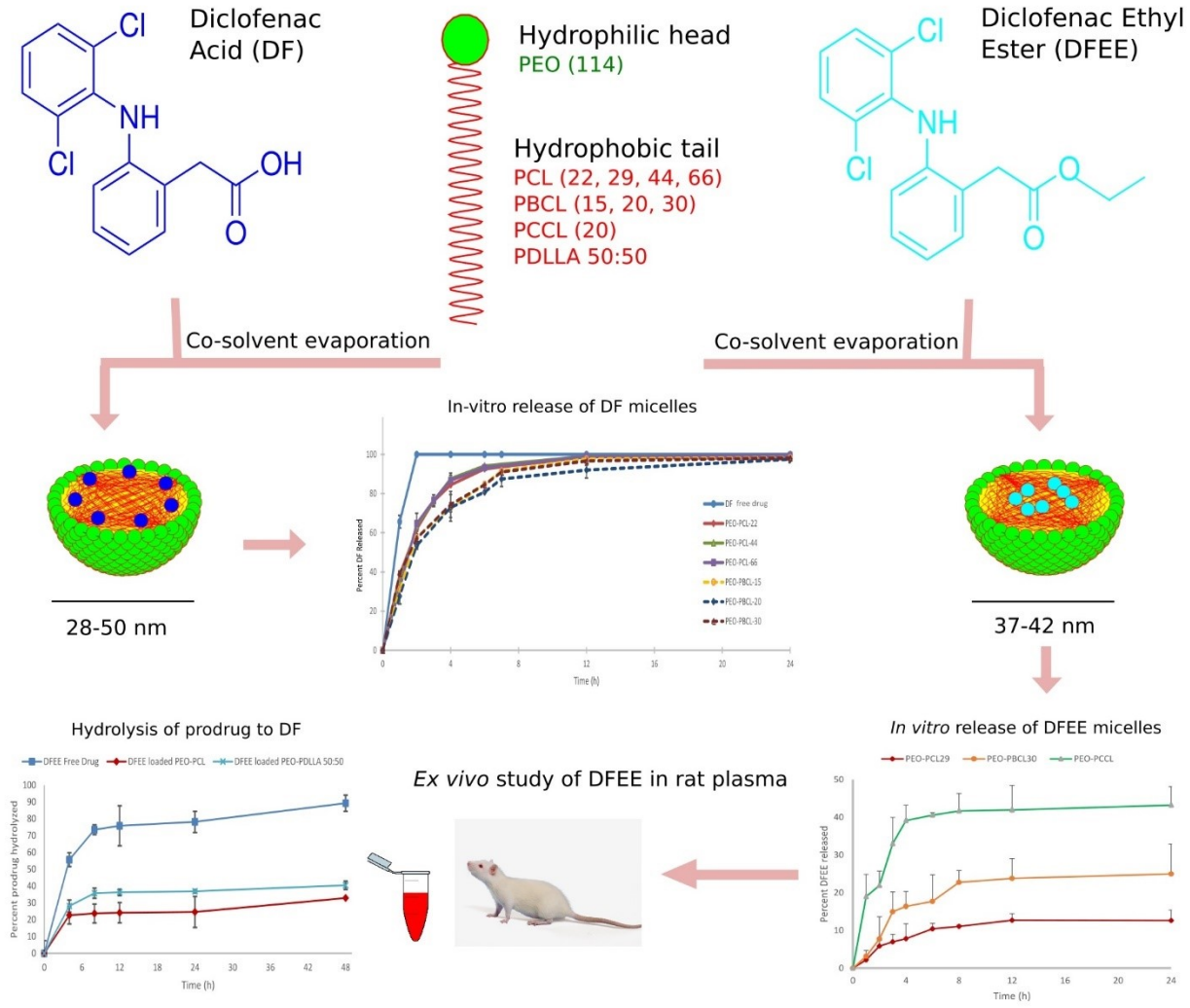

*A version of this chapter has been published:

Al-Lawati, H., R Vakili, M., Jamali, F., & Lavasanifar, A. (2016). Polymeric Micelles for the Delivery of Diclofenac and Its Ethyl Ester Derivative. *Pharmaceutical Nanotechnology*, 4(2), 109-119

Abstract

Purpose: This study aimed to develop a polymeric micellar formulation of diclofenac, an NSAID with known cardiovascular (CV) toxicity. **Methods:** Diclofenac (DF) and diclofenac ethyl ester (DFEE) were encapsulated in polymeric micelles prepared from several block copolymers based on methoxy poly(ethylene oxide)-poly(ester)s (PEO-poly(ester)s. Prepared micelles were characterized for their particle size, polydispersity, encapsulation efficiency, drug loading content, and *in-vitro* drug release. The kinetics of enzymatic hydrolysis for DFEE micelles versus free DFEE was then examined at 37±0.5°C in rat plasma. **Results:** The DF and DFEE loaded polymeric micelles exhibited particle size in the range of 27.9-50.3 nm. The slowest release for DF micelles was achieved with micelles of PEO-block-poly(α-carboxyl-ε-caprolactone) with a side chain of N,N-dimethyl dipropylenetriamine which showed 71±3.2% drug release in 4 h followed by a sustained drug release reaching 100% within 24 h. The DFEE micelles showed slower release in comparison to DF, and the optimal results were achieved with PEO-poly(ε-caprolactone) micelles with percent release of 7.8±4.0% of DFEE in 4 h and 12.6±2.7% in 24 h. Incubation with plasma of polymeric micellar DFEE for 48 h revealed slow appearance of DF as compared to that with the free DFEE and a good correlation with *in vitro* DFEE release data. **Conclusions:** The results show a great potential for DFEE polymeric micelles in controlled delivery of diclofenac.

Keywords

Polymeric micelles, diclofenac, inflammation, delivery

2.1. Introduction

Inflammatory conditions such as various forms of arthritis cause cardiovascular (CV) complications, hence, significantly add to the morbidity and mortality of the disease [1]. In fact, inflammation is considered as an independent risk factor for CV disease [2]. The underlying mechanisms behind CV side effects of inflammation are unknown, but the involvement of pro-inflammatory cytokines and chemicals generated in response to inflammation has been implicated [3].

Non-steroidal anti-inflammatory drugs (NSAIDs), which inhibit cyclooxygenase (COX) enzymes are often considered the first line therapy for inflammatory conditions including various forms of arthritis. However, the chronic use of most of these agents is also known to be associated with an increase in CV risk [4]. The reason for the cardiotoxicity of various NSAIDs is unknown.

It is reasonable to suggest, however, that the CV effect of NSAIDs may be due to their intrinsic potency and/or to the extent of their presence in target organs. We have reported that, in experimental animals, the electrolyte retention associated with NSAIDs is related to their extent of presence in the kidney [5]. Therefore, NSAIDs with high concentrations in the kidney (e.g., rofecoxib) but not those with minimal presence in the organ (e.g., meloxicam) cause electrolyte retention that, in turn, can interfere with both renal and CV functions. In addition, we have generated some preliminary data suggesting that the cardiotoxicity of NSAIDs may also be influenced by the extent of their presence in the cardiac tissue. While we cannot rule out the influence of a given drug's intrinsic potency, a deeper understanding of this observation is imperative.

With this in mind, we aimed to prepare nano-formulations of an NSAID with potent CV side effects, to limit its distribution into the heart and kidneys. Diclofenac is among the world's most widely prescribed NSAIDs commonly used to relieve the symptoms associated with chronic inflammatory conditions such as RA and osteoarthritis. In spite of its good anti-inflammatory activity, diclofenac suffers from a short biological half-life and an elevated risk of CV risk [4-7]. We hypothesize that a reduced cardiac exposure of diclofenac to these organs by nano-formulations of diclofenac will lower its CV side effects.

Extensive research in the field of nano-medicine has focused on the design of drug delivery systems that can carry active drug molecules specifically to the diseased sites, while avoiding distribution in healthy tissues, thus potentiating drug activity and reducing drug associated toxicities [8]. Among different nano-delivery systems, polymeric micelles are promising systems for the delivery of poorly water-soluble drugs. Polymeric micelles are created from amphiphilic macromolecules that spontaneously self-assemble to nano-sized colloidal particles when exposed to aqueous solutions [6]. In an aqueous environment, they typically consist of a hydrophobic core where hydrophobic drug molecules can be solubilized, and a hydrophilic shell that can act as a physical barrier to protein binding and opsonization. Micelles possess key characteristics that make them stand out among other nano-carriers. These include their high loading capacity for hydrophobic molecules, and their small size usually in the range of 10 to 80 nm. At this size range, they are small enough to allow for passive accumulation into inflamed tissues through big openings of the vasculature, but large enough to escape renal excretion and/or extravasation at healthy tissues [9,10].

For an effective change on the *in vivo* biodistribution of the incorporated drug by its nano-delivery system, the nano-carrier should be able to stay stable and hold onto its cargo while in the blood circulation. In an effort to develop such delivery system, we have evaluated the potential of several micelle-forming di-block co-polymers composed of methoxy poly(ethylene oxide) (PEO) as the shell forming block and poly(ε-caprolactone) (PCL) or PCL with different repeating side groups on the PCL block for the delivery of diclofenac as well as its hydrophobic ethyl ester derivative. Optimal formulations which showed sufficient level of drug encapsulation and slow drug release extending over 24 h were then examined for their stability and drug release in plasma making comparisons with free (un-encapsulated) drugs. Our results showed the superiority of the more hydrophobic diclofenac ethyl ester for formulation in polymeric micelles particularly in terms of drug release profile.

2.2. Materials and methods

2.2.1. Materials

Diclofenac acid was purchased from TCI, Portland, Oregon. Diclofenac ethyl ester was purchased from TRC, Toronto, Canada. All other chemicals and reagents used were of analytical grade.

2.2.2. Preparation and characterization of block copolymers

Di-block copolymers of PEO-PCL and PEO-b-poly(α-benzyl carboxylate-ε-caprolactone) (PEO - PBCL) with different degrees of polymerization in the PCL (22, 29, 44, 66) and PBCL (15, 20, 30) as well as PEO-b-poly(α-carboxyl-ε-caprolactone) (PEO-PCCL) were synthesized as per [11]. PEO-b-poly(D, L- lactide) with a 50–50 racemic mixture of L-lactide and D-lactide (PEO-PDLLA

50-50) was synthesize as per [12]. The PEO-PCCL with a partial substitution of N,N-dimethyldipropylenetriamine on the PCCL block (PEO-P(CL-g-DP)) was prepared as per [13].

Synthesized block copolymers were characterized for their number average molecular weight (M_n) using ^{1}H NMR spectroscopy as reported before [11-13]. The di-block copolymers were characterized for their weight average molecular weight (M_w) and molecular weight distribution (M_w/M_n) by gel permeation chromatography (GPC), which was carried out at 25°C using an HP instrument equipped with Waters Styragel HT4 column (Waters Inc., Milford, MA, USA). The elution pattern was detected at 35°C by refractive index (PD2000, Precision Detectors, Inc.) and light scattering (Model 410, Waters Inc.) detectors. THF was used as an eluent at a flow rate of 0.8 mL/min. The column was calibrated with PEO standards covering a range of molecular weights.

2.2.3. Preparation of the diclofenac (DF) and diclofenac ethyl ester (DFEE) loaded polymeric micelles

Diclofenac (DF) and diclofenac ethyl ester (DFEE) were encapsulated in polymeric micelles of different block copolymers using the co-solvent evaporation method. All block copolymers had a shell forming block of methoxy PEO (average M_n of 5000 Da). The core-forming block consisted of either one of the following structures: PCL of different degrees of polymerization (22, 29, 44, 66), PBCL of different degrees of polymerization (15, 20, 30), PCCL, PDLLA 50-50, or P(CL-g-DP). In a typical encapsulation process, 0.5 mg of the drug (DF or DFEE) and 10 mg of the polymer were co-dissolved in 525 µL of acetone to give a drug-to-polymer ratio of 1:20 w/w. The resulting solution was added drop-wise to 3150 µL of double distilled water under moderate stirring to give

a ratio of 1:6 v/v for the organic-to-aqueous phases. The mixture was stirred for 24 h at room temperature, to allow for the evaporation of the organic solvent. To optimize the loading process, the type of organic solvent used as well as the drug and polymer concentrations were changed in some experiments.

The encapsulation was also achieved using the direct dialysis method for some of the formulations. Briefly, the drug and the polymer with amounts as described above were dissolved in 1 mL of tetrahydrofuran (THF) each and then mixed together. The mixture was stirred at room temperature and then dialyzed against water using cellulose dialysis membrane (Spectrapor, MWCO: 3.5 kD) with 2L of ultrapure water for 24 h. The solution was sonicated and then centrifuged to eliminate unloaded drug.

2.2.4. Particle size distribution

The particle size distribution (Zeta average diameter and the polydispersity index (PDI)), of the prepared micellar formulations was estimated by dynamic light scattering (DLS) using a Malvern Zetasizer 3000 (Malvern Instruments, UK) at 25˚C.

2.2.5. High performance liquid chromatography

The high-performance liquid chromatography (HPLC) unit consisted of a Shimadzu Prominence HPLC system (Mandel Scientific, Guelph, ON, Canada) with an SPDA-6A variable UV spectrophotometer set at 280 nm. Chromatographic separations were performed on a C18 column (100 × 4.6 mm, pore size: 3 μm). The mobile phase consisted of acetonitrile-water-acetic acid (70:30:0.2, v/v/v), the flow rate was 1 mL/min and the injection volume was 50 μL. Mefenamic

acid was used as an internal standard (IS). DF, IS, and DFEE were detected at the retention times of 2.9, 3.9, and 7.4 min, respectively.

2.2.6. Drug encapsulation efficiency and loading content

Drug encapsulation efficiency and loading content were determined by analyzing samples of the micellar formulations as follows. A 100 µL aliquot of each formulation was dissolved in 900 µL of acetonitrile to disrupt the self-assembled structure of the micelles, and an additional 100 µL of 0.3 mg/mL solution of the IS was added. After vortex mixing, the samples were analyzed by HPLC (as described above) and the concentrations were obtained from standard calibration curves based on the concentration range of 0.12 – 500 µg/mL. The drug entrapment efficiency (EE) and the drug loading content (DLC) weight/weight were calculated using the following equations

$$Entrapment\ Efficiency\ (EE, \%) = \frac{Weight\ of\ loaded\ drug}{Weight\ of\ drug\ initially\ added} \times 100,$$

$$Drug\ Loading\ Content\ (DLC\ w/w, \%) = \frac{Weight\ of\ loaded\ drug}{Weight\ of\ block\ copolymer} \times 100.$$

2.2.7. *In vitro* release profile

The kinetics of the *in-vitro* release of the various DF and DFEE loaded micelles were studied using the dialysis bag method as previously reported [14]. Briefly, a dialysis bag (Spectrapor, MWCO: 3.5 kD) containing 2 mL of the drug-loaded micelle solution was incubated in phosphate buffer saline (PBS; pH 7.4) at 37° C under mild agitation in a Julabo SW 22 water bath (Seelbach, Germany). Sampling with water replacement was carried out from the dialysis bag at

predetermined time intervals, and the incubation solution was replaced by fresh PBS. The samples (100 µL) were diluted with 900 µL of acetonitrile and 100 µL of the IS solution (0.3 mg/mL), and were analyzed by HPLC. A control experiment to determine the release behaviour of the free DF in 2 mL of acetonitrile-water (1:3 v/v) was also carried out as described above.

2.2.8. Hydrolysis of diclofenac ethyl ester loaded micelles incubated with rat plasma

Rat plasma was obtained from Sprague-Dawley rats as follows. Blood was withdrawn from anesthetized rats via cardiac puncture and placed in Eppendorf tubes that were pre-treated with heparin to avoid blood coagulation. The supernatant plasma was collected after centrifugation at 3000×g.

The hydrolysis of two DFEE loaded micellar formulations in rat plasma was examined using a previously reported method [15], with some modifications. Briefly, 100 µL of the micelle solution, equivalent to 38.5 µg of DFEE, was added to 3.6 mL of preheated plasma. The solution was incubated in water bath at 37±0.5° C under mild agitation, and at predetermined time intervals, 100 µL samples were withdrawn. The samples were spiked with IS and acidified with 1 M phosphoric acid. The matrix was extracted twice with 3 mL diethyl ether and the organic phase, collected after centrifugation, was aspirated and dried under nitrogen. The dried residue was re-dissolved in 100 µL of mobile phase and analyzed by HPLC. The concentrations were obtained from standard curves in the range of 0.08-40 µg/mL. A control experiment to determine the *ex-vivo* release of the DFEE free drug in rat plasma was also carried out as described above.

Table 2-1. Characteristics of block copolymers under study

Amphiphilic block copolymer	M_n[1](g/mol)	M_w[2] (g/mol)	M_n[2] (g/mol)	M_w/M_n[2]
PEO-PCL-22	7,500	15,535	13,280	1.17
PEO-PCL-29	8,306	14,831	8,561	1.73
PEO-PCL-44	10,000	17,004	10,044	1.70
PEO-PCL-66	12,500	14,277	7,798	1.83
PEO-PBCL-15	8,720	11,914	8,692	1.37
PEO-PBCL-20	9,960	15,245	9,607	1.59
PEO-PBCL-30	12,440	20,294	12,484	1.63
PEO-PCCL	8,792	27,185	9,346	2.91
PEO-PDLLA 50:50	8,908	10,236	9,349	1.09
PEO-P(CL-g-DP)	6,000	6,632	6,489	1.02

[1]Based on ^{1}H NMR
[2]Based on gel permeation chromatography (GPC)
Weight-average molecular weight (M_w), number-average molecular weight (M_n)

Table 2-2. The effects of the encapsulation method on the properties of DF loaded micelles based on PEO-PCL$_{29}$

Encapsulation method	Diameter (nm) ± SD	PDI ± SD	EE (%) ± SD	DLC w/w (%) ± SD	Drug release at 4 h (%) ± SD
Co-Solvent evaporation	39.9 ± 0.49	0.300 ± 0.021	72 ± 7.7	3.6 ± 0.4	87 ± 3.1
Direct dialysis	80.3 ± 0.64	0.421 ± 0.004	42 ± 8.5	2.1 ± 0.4	90 ± 3.9

Polydispersity index (PDI), entrapment efficiency (EE), drug loading content (DLC)

Table 2-3. The effect of organic solvent in a co-solvent evaporation process on the properties of DF loaded PEO-PCL$_{29}$ micelles

Organic solvent	Diameter (nm) ± SD	PDI ± SD	EE (%) ± SD	DLC w/w (%) ± SD	Drug release at 4 h (%) ± SD
Acetone	44.5 ± 0.60	0.170 ± 0.002	76 ± 2.6	1.9 ± 0.07	84 ± 0.8
THF	53.9 ± 1.20	0.289 ± 0.008	78 ± 10.6	2.0 ± 0.2	85 ± 4.5

Polydispersity index (PDI), entrapment efficiency (EE), drug loading content (DLC)

2.2.9. Statistical analysis

The data on particle size distribution (Zeta average diameters and PDI), the entrapment efficiency, and the *in-vitro* release are expressed as mean ± standard deviation (SD). The statistical significance was calculated using the unpaired Student's t-test to compare the means of two groups or the one-way analysis of variance (ANOVA) to compare the means of more than two groups, and a value of $p<0.05$ was considered to be statistically significant. The difference in the *in-vitro* release profiles among the various formulations were assessed statistically by calculating the similarity factor, f_2 given by

$$f_2 = 50 \times \log\left(\left[1 + \frac{1}{n}\sum_{i=1}^{n}(R_i - T_i)^2\right]^{-0.5} \times 100\right),$$

where R_i and T_i represent the percent released at time t_i from the two formulations, labeled as reference (R) and tested (T) [16]. Two release profiles were considered to be equivalent when their f_2 value was within the range of 50-100.

2.3. Results and discussion

DF and its prodrug DFEE were considered for loading as sources for the active drug into polymeric micelles. Several biodegradable amphiphilic block copolymers with various hydrophobic block structures were selected in order to find the micelle system which possesses the optimum encapsulation efficiency and *in vitro* drug release properties. The shell forming block of methoxy PEO (average M_n of 5000 Da) was chosen to provide stealth properties for the carrier so it can

Table 2-4. Characteristic properties of DF loaded micelles based on various block copolymers

Block copolymer	Diameter (nm) ± SD	PDI ± SD	EE (%) ± SD	DLC w/w (%) ± SD	Drug release at 4 h (%) ± SD
PEO-PCL_{22}[a]	28.9 ± 0.12	0.208 ± 0.006	82 ± 8.6	4.1 ± 0.4	84 ± 0.7
PEO-PCL_{44}	27.9 ± 0.22	0.243 ± 0.001	79 ± 16	4.0 ± 0.8	88 ± 3.0
PEO-PCL_{66}	37.8 ± 0.44	0.213 ± 0.002	64 ± 8.4	3.2 ± 0.4	87 ± 2.6
PEO-$PBCL_{15}$	39.1 ± 0.20	0.395 ± 0.043	50 ± 7.1	2.5 ± 0.4	73 ± 6.8
PEO-$PBCL_{20}$	47.4 ± 0.08	0.422 ± 0.004	54 ± 5.8	2.7 ± 0.3	73 ± 2.3
PEO-$PBCL_{30}$	47.8 ± 0.31	0.490 ± 0.060	61 ± 2.2	3.1 ± 0.1	75 ± 6.6
PEO-P(CL-g-DP)	50.3 ± 0.57	0.242 ± 0.002	41 ± 4.7	2.1 ± 0.2	71 ± 3.2

[a] The number refers to the degree of polymerization of the hydrophobic block
Polydispersity index (PDI), entrapment efficiency (EE), drug loading content (DLC)

circulate longer in blood and not be eliminated early by mono-nuclear phagocytes (MPs). The relevant characteristics of the block copolymers are summarized in Table 2-1.

2.3.1. Optimization of the DF encapsulation in polymeric micelles

2.3.1.1. The effect of encapsulation process

DF was loaded in the PEO-PCL block copolymers with PCL degree of polymerization of 29, following two commonly used encapsulation methods, i.e., the co-solvent evaporation and the direct dialysis. The co-solvent evaporation method provided a micellar system with better characteristics including a drug EE of 72 ± 7.7% which was significantly better than that achieved with the direct dialysis method (an EE of 42 ± 8.5%) ($p<0.05$, unpaired Student's t-test) (Table 2-2). Moreover, the co-solvent evaporation method provided micelles with smaller average diameters (40 versus 80 nm).

The difference in the *in vitro* release profile of micelles prepared by the two methods, however, was not significant and the similarity factor between the mean profiles was $f_2 = 81.6$ (>50) indicating equivalent release profiles. Both micellar formulations released the drug relatively rapidly with about 99% released in 24 h. The lower EE achieved with the dialysis method is in accordance to what is reported in the literature and could be attributed to the release of the encapsulated drug during the lengthy dialysis step [17]. Based on these results, we used the co-solvent evaporation method for further experiments.

Table 2-5. Similarity factor (f_2) between the in-vitro release profiles of DF micellar formulations

	DF Free Drug	**PEO-PCL$_{22}$**	**PEO-PCL$_{44}$**	**PEO-PCL$_{66}$**	**PEO-P(CL-g-DP)**	**PEO-PBCL$_{15}$**	**PEO-PBCL$_{20}$**	**PEO-PBCL$_{30}$**
DF Free Drug		**33.9**	**33.9**	**33.5**	**22.4**	**30.9**	**28.7**	**32.4**
PEO-PCL$_{22}$	**33.9**		80.4	73.9	**41.2**	59.2	51.9	62.5
PEO-PCL$_{44}$	**33.9**	80.4		89.2	**40.9**	56.4	50.3	56.9
PEO-PCL$_{66}$	**33.5**	73.9	89.2		**41.3**	57.4	51.3	56.5
PEO-P(CL-g-DP)	**22.4**	**41.2**	**40.9**	**41.3**		52.6	57.9	**47.6**
PEO-PBCL$_{15}$	**30.9**	59.2	56.4	57.4	52.6		71.4	72.3
PEO-PBCL$_{20}$	**28.7**	51.9	50.3	51.3	57.9	71.4		62.2
PEO-PBCL$_{30}$	**32.4**	62.5	56.9	56.5	**47.6**	72.3	62.2	

f_2 <50 (presented in bold font) indicate non-equivalent profiles

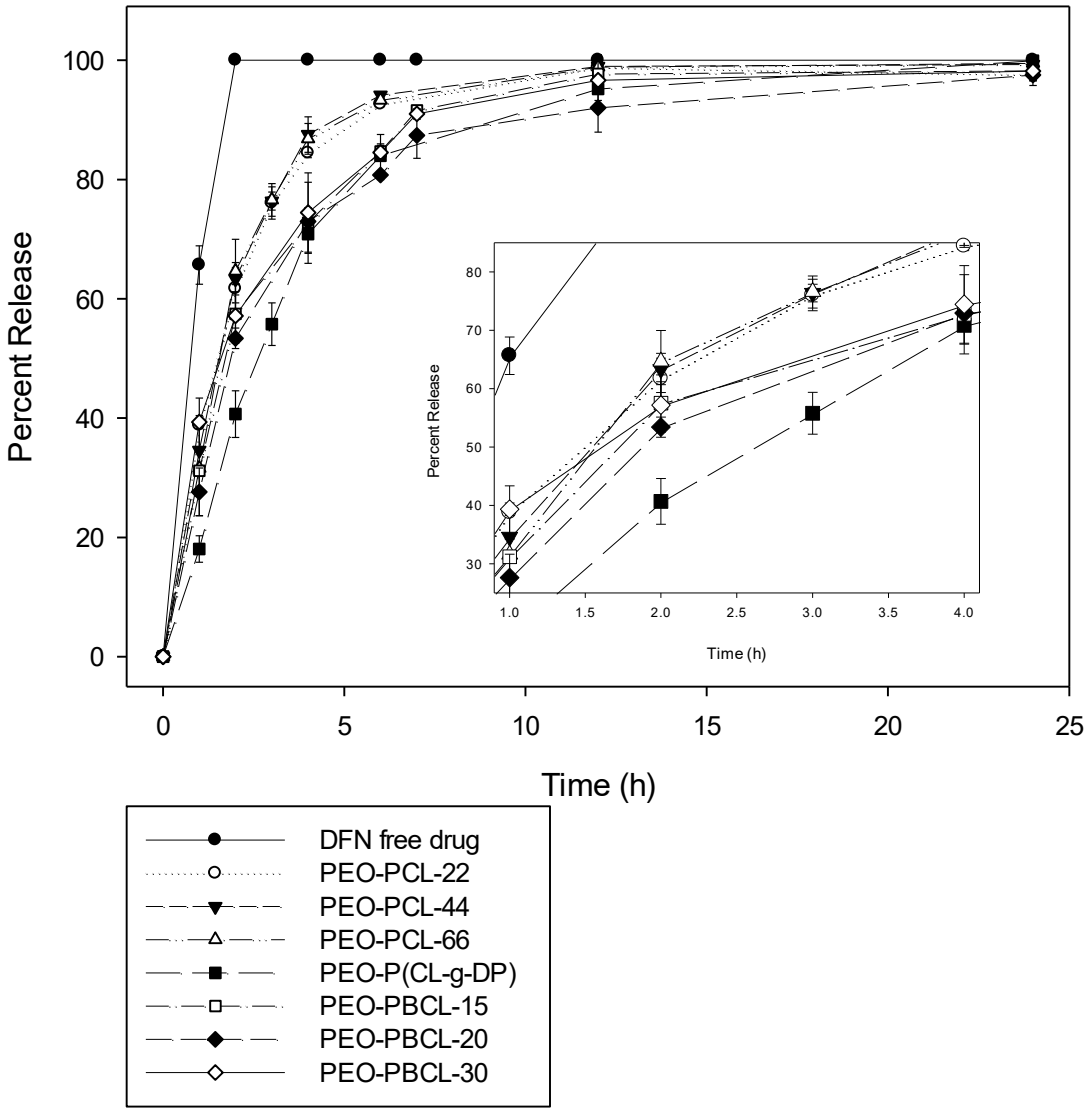

Figure 2-1. A 0-24 hour in-vitro release profile of free DF and DF loaded polymeric micelles

2.3.1.2. The Effect of Organic Solvent in the Co-Solvent Evaporation Process

The effect of applied organic solvent in the co-solvent evaporation procedure on the characteristics of DF loaded PEO-PCL micelles was investigated (Table 2-3). Application of THF in place of acetone led to the production of micelles which had a significantly larger particle diameter (54 versus 45 nm*)* and a more polydispersed system (PDI of 0.289 compared to 0.170). Similar observations were made previously in our lab in the loading of cyclosporine using these two solvents [17]**.** Therefore, acetone was used as the organic phase of the co-solvent evaporation procedure in further micellar encapsulations.

2.3.1.3. The Effect of Core-Forming Block Structure

DF was loaded in different block copolymers which varied from each other by the structure of the core-forming block (Table 2-4). PEO-PCL micelles showed high drug entrapment efficiency, a relatively small PDI, and small particle sizes. The micellar system with the smallest degree of polymerization of 22 in this class had the highest drug entrapment with a mean EE of 82 ± 8.6%. The entrapment efficiency showed a decreasing trend with an increase in the degree of polymerization reaching 64 ± 8.4% for the system based on PEO-PCL_{66}. The difference was, however, statistically not significant (p>0.05, One-way ANOVA).

The results showed DF loaded micelles of PEO-PBCL to have particles with larger diameters (39-47 nm on average) than those obtained with PEO-PCL and a slightly larger (moderate) polydispersity. Moreover, the EE of DF was reduced in PEO-PBCL micelles in comparison to

PEO-PCL ones. In this class, the EE achieved with PEO-PBCL$_{30}$ was significantly higher than that with PEO-PBCL$_{15}$.

The PEO-P(CL-g-DP) block copolymer micelles had an average particle size of 50.3 ± 0.57 nm and an EE of 41 ± 4.7%, which was lower than PEO-PCL and PEO-PBCL micelles.

2.3.2. In vitro release of DF loaded polymeric micelles

The in-vitro release profiles obtained for the examined DF micellar formulations showed a slower release than that of the free DF. As reported in Table 2-5, the f2 factor for all formulations was lower than 50 when compared to free drug. All micellar formulations showed a similar bi-phasic release of DF which included an initial burst release in the first 4 h, followed by a more sustained release with almost 99% of the drug being released in 24 h (Figure 2-1). The initial burst may be attributed to the fraction of DF which is close to the surface of the micelles. The rapid release of DF from polymeric micelles suggests the loaded drug is either not incorporated in the micellar core or there is a weak interaction between the micellar core and DF. A previous study has shown a similar two stage release behavior for DF loaded PEO-PCL, however, with ~ 30% of the DF micelles remaining encapsulated after 24 h [18].

The release profiles of PEO-PCL based micelles with all three degrees of polymerization in the PCL block, i.e. x=22, 44, and 66, were comparable. The PEO-PBCL based micelles had a slightly slower release at early time points compared to those based on PEO-PCL ones, but based on the f_2 factor the difference between the overall release profiles of the micellar formulations were not significant (Table 2-5).

Table 2-6. Characteristic properties of DFEE loaded polymeric micelles

Block copolymer	Diameter (nm) ± SD	PDI ± SD	EE (%) ± SD	DLC w/w (%) ± SD	Drug release at 4 h (%) ± SD
PEO-PCL_{29}	37.0 ± 0.43	0.239 ± 0.002	64 ± 0.7	3.2 ± 0.04	7.8 ± 4.0
PEO-$PBCL_{30}$	38.9 ± 0.38	0.177 ± 0.008	44 ± 14.0	2.2 ± 0.7	16 ± 3.9
PEO-PCCL	150 ± 1.59	0.130 ± 0.003	1.8 ± 0.3	0.1 ± 0.02	39 ± 4.1
PEO-PDLLA 50-50	41.8 ± 0.16	0.164 ± 0.009	18 ± 0.1	0.9 ± 0.01	25 ± 2.2

Polydispersity index (PDI), entrapment efficiency (EE), drug loading content (DLC)

Table 2-7. Similarity factor (f_2) between the in-vitro release profiles of DFEE micellar formulations

	PEO-PCL_{29}	**PEO-$PBCL_{30}$**	**PEO-PCCL**	**PEO-PDLLA 50:50**
PEO-PCL_{29}		52.8	**28.4**	**33.7**
PEO-$PBCL_{30}$	52.8		**36.2**	**44.0**
PEO-PCCL	**28.4**	**36.2**		55.1
PEO-PDLLA 50:50	**33.7**	**44.0**	55.1	

f_2 <50 (presented in bold font) indicate non-equivalent profiles

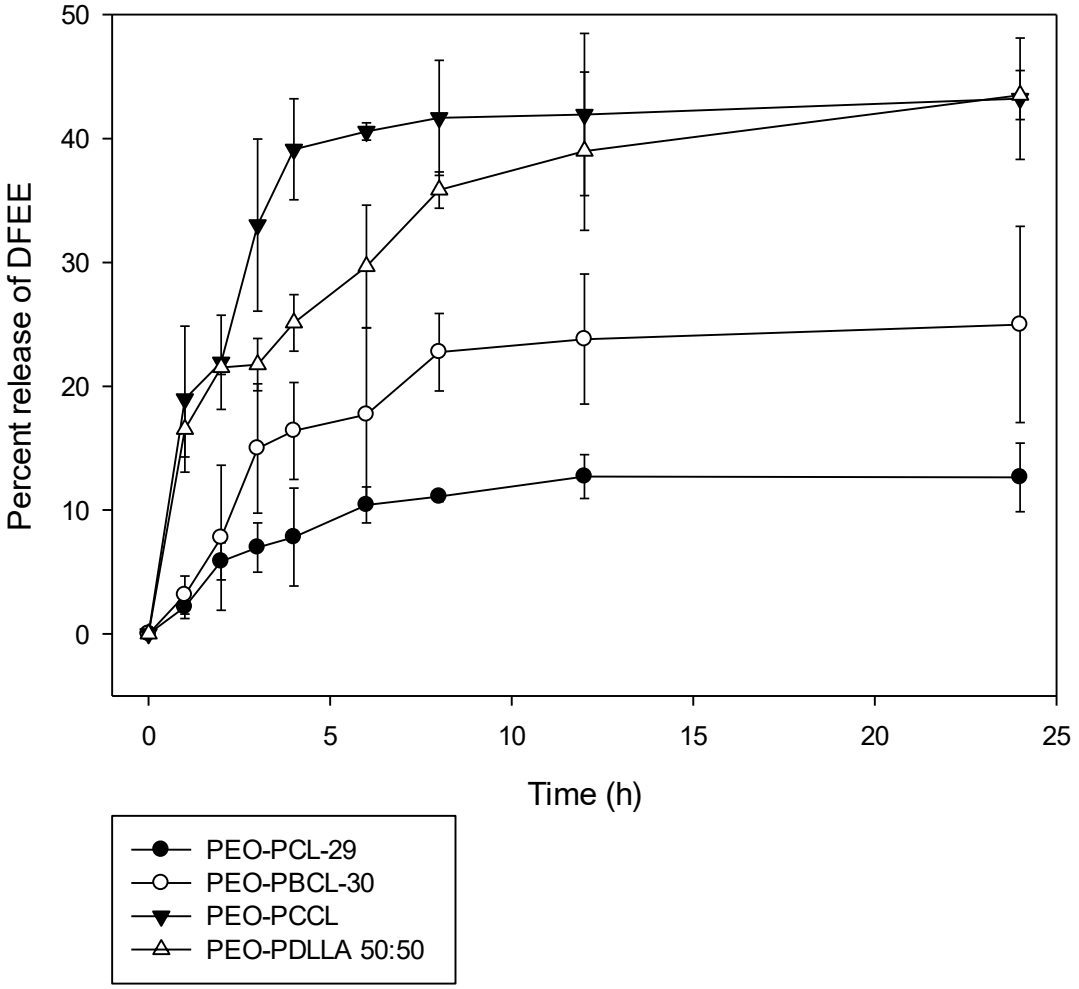

Figure 2-2. A 0-24 hour in-vitro release profile of DFEE loaded polymeric micelles

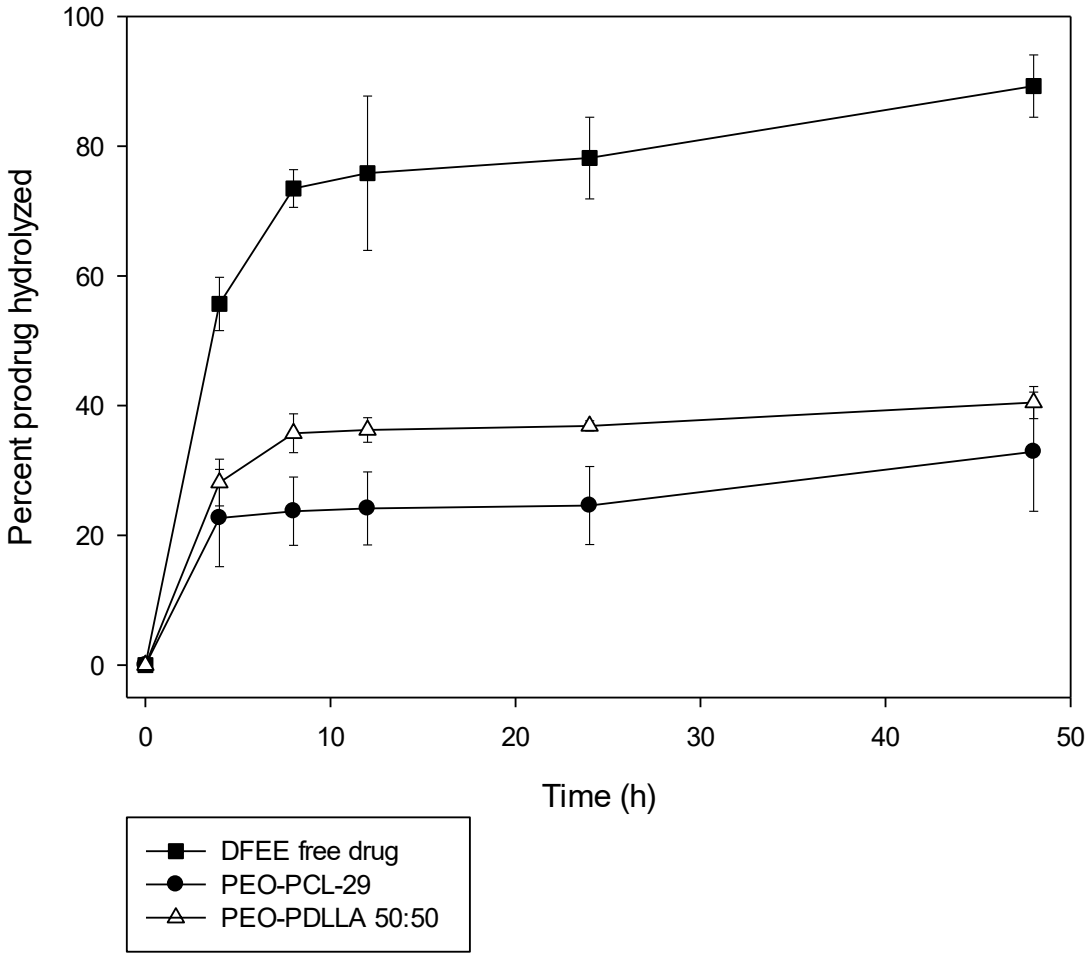

Figure 2-3. Hydrolysis of DFEE prodrug to the parent DF upon incubation within rat plasma

The PEO-P(CL-g-DP) based micelles showed the slowest release profile for DF with 71 ± 3.2% drug released in the first 4 h followed by a sustained release with near complete release at 24 h. This could be attributed to the interaction of DP with DF through hydrogen bond formation.

Alternatively, the slower release from PEO-PBCL and then PEO-P(CL-DP) may be a result of lower loaded drug levels in these two micellar formulations. This is suggested by the strong positive correlation between the percent drug loading content (DLC w/w) and the 4 h percent *in-vitro* drug release for all of the DF loaded micelle formulations presented in Table 2-4 (Pearson's correlation coefficient r=0.847). This release profile was slower than that of all three PEO-PCL formulations and that of PEO-$PBCL_{30}$ based on the f_2 factor. Overall, based on the obtained data none of the DF polymeric micellar formulations were ideal.

2.3.3. Characterization of DFEE loaded polymeric micelles

Recently, it has been reported that NSAIDs do not require the presence of carboxylic acid to exert their anti-inflammatory effect [19]. We investigated the loading of a more hydrophobic derivative of DF where COOH was esterified, i.e., DFEE in polymeric micelles. This prodrug of diclofenac is expected to enzymatically hydrolyse to the parent drug in the systemic circulation.

DFEE was loaded in various block copolymer micelles as reported in Table 2-6 using the same procedure described for the loading of DF, which is based on a co-solvent evaporation procedure using acetone as the organic solvent. In a similar manner to what was observed with DF loaded micelles, PEO-PCL and PEO-PBCL continued to provide high entrapment of DFEE with an EE of 64 ± 0.7 and 44 ± 14 % with the PEO-PCL_{29} and PEO-$PBCL_{30}$, respectively, PEO-PCCL

provided the least entrapment of DFEE with an EE of 1.8 ± 0.3%, while the PEO-PDLLA 50-50 provided a moderate EE of 18 ± 0.1%. In the absence of block copolymers, DFEE precipitated in water, however.

All micelles had small particles (average diameters below 42 nm), with the exception of PEO-PCCL which appeared to form aggregates. Moreover, they all had a relatively small PDI, suggesting a narrow polydispersity.

2.3.4. In vitro release of DFEE from polymeric micelles

Polymeric micellar DFEE showed a sustained release behavior and less initial burst, particularly in PEO-PCL and PEO-PBCL (Figure 2-2), implying encapsulation of the more hydrophobic DEFF in the core of these micelles. Moreover, the micelles based on PEO-PCL_{29} and PEO-$PBCL_{30}$ showed a rather slow *in-vitro* release amounting to approximately 12% and 24% of the loaded drug, respectively, in a 24 hour cycle, while those based on PEO-PDLLA 50-50 or PEO-PCCL showed a release of over 43% of the encapsulated drug in the same period. The similarity factor f_2 values obtained (Table 2-7) reveal that the PEO-PCL_{29} and the PEO-$PBCL_{30}$ *in-vitro* release profiles are comparable to one another, but slower than that of PEO-PDLLA 50-50 or of PEO-PCCL. The optimal DFEE micellar formulation was found to be the one based on PEO-PCL_{29}, because of the high entrapment of the drug and the slower *in-vitro* release profile which included an initial release of 7.8 ± 4.0% in the first four hours, and a sustained release totaling 12.6 ± 2.7% of the drug in 24 h under current experimental conditions.

We could not confirm the presence of a sink condition in the DFEE release experiment due to the very low water solubility of the DFEE in PBS that was below the HPLC detection limits. For this reason and also to better mimic the *in vivo* conditions, further studies were conducted to investigate the transformation of free and loaded DFEE to DF in rat plasma.

2.3.5. Hydrolysis of DFEE loaded polymeric micelles incubated within rat plasma

The enzymatic hydrolysis in rat plasma after 48 h of incubation of PEO-PCL_{29} and PEO-PDLLA 50:50 based polymeric micellar DFEE, revealed the appearance of ~ 30% and ~40% of the parent compound (DF) in the plasma, respectively (Figure 2-3). The initial rapid appearance of free DF following incubation of DFEE loaded micelles in rat plasma within 4 h may reflect the release and hydrolysis of DFEE loaded in the micellar core/shell interface. The bulk of DFEE which is encapsulated in the core was hydrolyzed slowly. The PEO-PCL based formulations showed a slower hydrolysis of DFEE into DF compared to those based on PEO-PDLLA 50:50, with the difference between the two mean profiles being significant at each time interval above 4 h (p<0.05, unpaired Student's t-test). This observation is in line with the *in-vitro* release data observed for the two formulations. On the contrary, around 90% of the free DFEE was converted to the parent DF upon incubation in plasma within 48 h. The results imply the stability of both polymeric micelles particularly the PEO-PCL micellar formulations of DFEE in plasma.

2.4. Conclusions

We have developed polymeric micellar formulations for DF and its more hydrophobic derivative, DFEE. In general, the more hydrophobic DFEE micellar formulations illustrated more favorable

properties and *in vitro* release characteristics compared to DF formulations. Stability of DFEE formulations in PEO-PCL or PEO-PDLLA 50:50 micelles was also confirmed in rat plasma implying a potential for these formulations in changing the normal pharmacokinetics and biodistribution of loaded DFEE and its active metabolite DF.

References

1. Peters MJL, Symmons DPM and McCarey D. EULAR evidence-based recommendations for cardiovascular risk management in patients with rheumatoid arthritis and other forms of inflammatory arthritis. *Ann Rheum Dis* 2010*;* 69: 325-321.
2. Woods A, Brull DJ, Humphries SE and Montgomery HE. Genetics of inflammation and risk of coronary artery. *European Heart Journal* 2000; 21: 1574-1583.
3. Wilerson JT and Ridker PM. Inflammation as a cardiovascular risk factor. *Circulation* 2004; 109(21): II2-10.
4. Harirforoosh S, Asghar W and Jamali, F. Adverse effects of nonsteroidal antiinflammatory drugs: an update of gastrointestinal, cardiovascular and renal complications. *Journal of Pharmacy & Pharmaceutical Sciences* 2014; 16(5): 821-847.
5. Harirforoosh S, Jamali F. Renal adverse effects of nonsteroidal anti-inflammatory drugs. *Expert opinion on drug safety*. 2009; 8(6):669-81.
6. Bronich TK, Keifer PA, Shlyakhtenko LS and Kabanov AV. Polymer micelle with cross-linked ionic core. *Journal of the American Chemical Society* 2005; 127(23):8236-8237.
7. Khazaeinia T, Jamali F. Effect of drug release rate on therapeutic outcomes: formulation dependence of gastrointestinal toxicity of diclofenac in the rat. Inflammopharmacology. 2004 Feb 1;12(1):69-80.
8. Arias JL. Nanoparticle Therapy in Arthritis. In: *Nanomedicine in Health and Disease.* 2011. CRC press, Enfield, USA. p. 293.
9. Husseini GA and Pitt WG. Micelles and nanoparticles for ultrasonic drug and gene delivery. *Advanced drug delivery reviews* 2008; 60(10): 1137-1152.
10. Rangel-Yagui CO, Pessoa Jr A and Tavares LC. Micellar solubilization of drugs. *J. Pharm. Pharm. Sci* 2005; 8(2) 147-163.
11. Mahmud A, Xiong X-B and Lavasanifar A. Novel Self-Associating Poly (ethylene oxide)-b lock-poly (ε-caprolactone) Block Copolymers with Functional Side Groups on the Polyester Block for Drug Delivery. *Macromolecules* 2006; 39 (26): 9419-9428.
12. Abyaneh HS, Vakili MR and Lavasanifar A. The Effect of Polymerization Method in Stereo-active Block Copolymers on the Stability of Polymeric Micelles and their Drug Release Profile. *Pharmaceutical research* 2014; 31(6) 1485-1500.

13. Xiong X-B, Uludağ H and Lavasanifar A. Biodegradable amphiphilic poly (ethylene oxide)-block-polyesters with grafted polyamines as supramolecular nanocarriers for efficient siRNA delivery. *Biomaterials 2009*; 30(2):242-253.
14. Shahin M and Lavasanifar A. Novel self-associating poly (ethylene oxide)-b-poly (ε-caprolactone) based drug conjugates and nano-containers for paclitaxel delivery. *International journal of pharmaceutics* 2010; 389(1): 213-222.
15. Tammara VK, Narurkar MM, Crider AM and Khan MA. Morpholinoalkyl ester prodrugs of diclofenac: synthesis, in vitro and in vivo evaluation. *Journal of pharmaceutical sciences* 1994; 83(5):644-648, 1994.
16. Moore JW and Flanner H. Mathematical comparison of dissolution profiles. *Pharmaceutical technology 1996*; 20: 64-74.
17. Aliabadi HM, Elhasi S, Mahmud A, Gulamhusein R, Mahdipoor P and Lavasanifar A. Encapsulation of hydrophobic drugs in polymeric micelles through co-solvent evaporation: the effect of solvent composition on micellar properties and drug loading. *International journal of pharmaceutics* 2007; 329(1): 158-165.
18. Li X, Zhang Z, Li J, Sun S, Weng Y and Chen H. Diclofenac/biodegradable polymer micelles for ocular applications. *Nanoscale* 2012; 4(15):4667-4673.
19. Ullah N, Huang Z, Sanaee F, Rodriguez-Dimitrescu A, Aldawsari F, Jamali F and Velázquez-Martínez CA. NSAIDs do not require the presence of a carboxylic acid to exert their anti-inflammatory effect–why do we keep using it? *Journal of Enzyme Inhibition and Medicinal Chemistry* 2015: 1-11.

Chapter 3: Delivery and biodistribution of traceable polymeric micellar diclofenac in healthy rats*

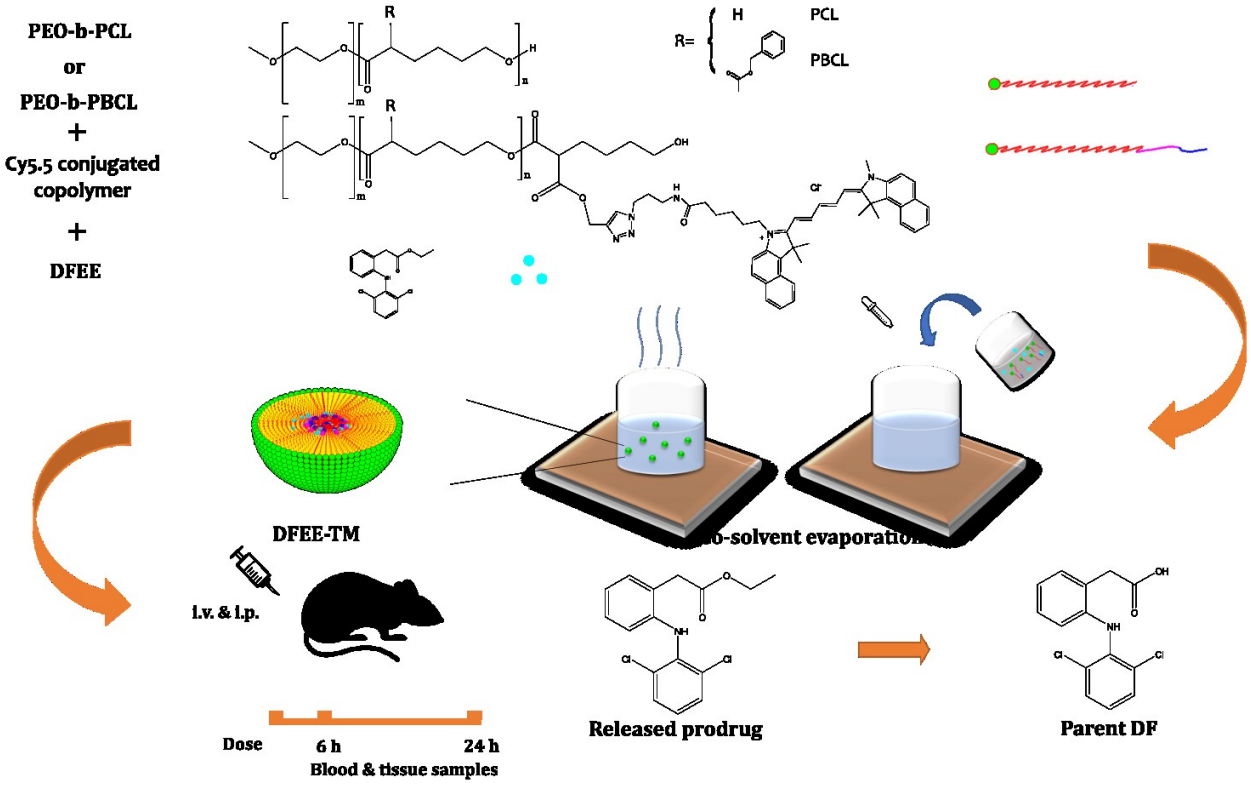

*A version of this chapter is accepted for publication with revisions:

Al-Lawati, H., Vakili, M.R., Lavasanifar, A., Ahmed, S., Jamali F. Delivery and biodistribution of traceable polymeric micellar diclofenac in the rat. Journal of Pharmaceutical Sciences. (in press, appeared online).

Abstract

Purpose: The nonsteroidal anti-inflammatory drugs elevate cardiovascular risk, perhaps, due to their accumulation in the heart and kidneys. We designed nanodelivery systems for cardiotoxic diclofenac to reduce its presence in these organs. **Methods:** Diclofenac ethyl ester (DFEE) was encapsulated in traceable micelles based on poly(ethylene oxide)-*b*-poly(ε-caprolactone) (DFEE-PCL-TM) or poly(ethylene oxide)-*b*-poly(α-benzyl carboxylate-ε-caprolactone)(DFEE-PBCL-TM). Diclofenac pharmacokinetics and tissue distribution were studied following intravenous (*iv*) and intraperitoneal (*ip*) administration of the nano-formulations and compared with those after *iv* doses of free diclofenac (n=3-6/group). **Results:** The average diameters for DFEE-PBCL-TM and DFEE-PCL-TM were 37.2±0.06 and 45.1±0.06 nm, respectively. Drug concentration dropped below the assay sensitivity after free drug administration in 6 h, but, persisted for 24 h following DFEE-PBCL-TM (2.3±1.4 μg/mL) and DFEE-PCL-TM (1.9±0.6 μg/mL) *iv* administration. The diclofenac heart:blood and kidney:blood ratios were 5-12-fold lower with the nano-formulations than free diclofenac. Near-infrared fluorescence measurements in tissues suggested exposure patterns to nano-carriers parallel with those achieved for delivered diclofenac by nano-formulations. Administration of DFEE-PCL-TM by *iv* or *ip* injection, resulted in comparable pharmacokinetics and 6 h post-dose near-infrared fluorescence in the heart, kidneys, liver and spleen. When compared to each other, DEFF-PBCL-TM showed significantly lower diclofenac levels in the heart compared to DFEE-PCL-TM (0.3±0.03 vs. 0.5±0.1 μg/g). **Conclusions:** Developed nano-formulations of diclofenac prolonged diclofenac circulation and reduced its presence in heart and kidney; strongly suggesting a cardiac-safe delivery vehicle for diclofenac.

Key words.

Biodistribution, cardiovascular risk, diclofenac, NSAIDs, pharmacokinetics, polymeric micelles

3.1. Introduction

Nonsteroidal anti-inflammatory drugs (NSAIDs) are among the most widely used medications worldwide with proven efficacy in controlling inflammation and pain associated with various conditions such as chronic arthritis [1]. It is well established that the therapeutic effect of these agents is due to their inhibitory effect on the activity of the cyclooxygenase (COX) enzymes, COX-1 and COX-2, whereby they alter the metabolism of membrane phospholipid arachidonic acid (ArA), leading to the inhibition of the synthesis of prostaglandin (PGE), prostacyclin (PGI) and thromboxane (TxA) among other effects [2, 3]. This mechanism is also suggested to be responsible in part for many side effects of these drugs including elevated gastrointestinal, renal, and cardiovascular (CV) risks [3].

Since the effects of several of the cellular and molecular mechanisms proposed for NSAID-induced cardiotoxicity, e.g., the imbalance in the cytochrome P450 mediated metabolites of ArA, are suggested to be local or tissue-dependent [4, 5], we decided to examine if the presence of NSAIDs in the heart or other tissue, relevant to the cardiovascular system, influences the outcome. Indeed, several reports have shown that the pharmacokinetics of NSAIDs contribute to their efficacy/toxicity profiles considerably [6, 7]. For instance, it is suggested that the magnitude of the renal side effects of NSAIDs is linked to the extent of their exposure in the kidneys [8, 9]. Similarly, studies of other cardiotoxic agents such as the chemotherapeutic agent doxorubicin provide evidence that the extent of retention in the heart can have a profound effect on their

myocardial toxicity [10, 11]. In an experimental arthritis model, cardiotoxic : cardioprotective ratio of both renin-angiotensin system and cytochrome P450 mediated metabolites of ArA are altered toward cardiotoxicity [4]. In the meantime, we have observed that NSAIDs normalize the altered cardiotoxic : cardioprotective ratio of the components of the renin-angiotensin system in the heart, but not the imbalance in the cardiac cytochrome P450 mediated metabolism profile of ArA [12].

We, therefore, hypothesized that altered delivery of NSAIDs can minimize exposure of target organs to the drug. Diclofenac is a popular and effective NSAID agent but is also known to be one of the most cardiotoxic NSAIDs in the market [13], making it suitable model drug for our investigation. Our aim was to prepare a nano-formulation that can limit diclofenac distribution to the heart. Among different nanoparticulate drug delivery systems, polymeric micelles stand out because of their average diameter (10-100 nm) which is sufficiently large to escape extravasation in healthy heart [14] and a poly(ethylene oxide) (PEO) outer shell, which prevents their early removal from blood by the mononuclear phagocytic cells even with repeated administration [15].

We have considered the encapsulation of diclofenac in many published polymeric micelles based on PEO as a shell and different polyesters as hydrophobic core. However, the micellar formulations showed rapid release rates of the active drug molecules at physiological pH. Therefore, we developed polymeric micellar formulations of the more hydrophobic derivative of diclofenac, i.e., diclofenac ethyl ester (DFEE), as a source for the active drug [16]. *In vitro* analysis showed the DFEE micellar formulations using PEO-*block*-poly(ε-caprolactone) (PEO-*b*-PCL) and PEO-*b*-poly(α-benzyl carboxylate-ε-caprolactone) (PEO-*b*-PBCL) to possess favourable characteristics including good encapsulation of DFEE and relatively slow *in vitro* as well as *ex*

vivo release of diclofenac in PBS or plasma, respectively. Such nanocarriers are expected to retain the encapsulated drug while in blood circulation and induce desired pharmacokinetics and biodistribution changes for diclofenac *in vivo*, so that the drug follows the fate of carrier in biological system leading to reduced drug exposure and distribution to normal tissues including heart and kidneys. The validity of this hypothesis was tested in the current manuscript, where the biodistribution of fluorescently-tagged PEO-*b*-PCL and PEO-*b*-PBCL micellar formulations of DFEE as well as the effect of this formulation strategy on the pharmacokinetics and tissue levels of released diclofenac in healthy Sprague Dawley rats was investigated.

3.2. Material and methods

3.2.1. Materials

Diclofenac acid (TCI, Portland, OR), diclofenac sodium (Alfa Aesar, Tewksbury, MA), diclofenac ethyl ester (DFEE) (Toronto Research Chemicals, Toronto, ON), methoxy-polyethylene oxide (PEO) (5000 g/mol) (Sigma–Aldrich, St. Louis, MO), ε-caprolactone (Lancaster Synthesis, UK), α-benzyl carboxylate-ε-caprolactone and α-Propargyl carboxylate-ε-caprolactone (PCC) (Alberta Research Chemicals, Edmonton, AB), stannous octoate (MP Biomedicals, Santa Ana, CA), cyanine (Cy) 5.5 azide (Lumiprobe, Hallandale Beach, FL). All other chemicals and reagents were of analytical grade and were used without any further purification.

3.2.2. Preparation of the diclofenac ethyl ester loaded traceable micelles

As previously reported, di-block copolymers of PEO-*b*-PCL and PEO-*b*-PBCL were synthesized by ring-opening polymerization of ε-caprolactone or α-benzyl carboxylate-ε-caprolactone, respectively, using methoxy PEO (5000 g/mol) as initiator and stannous octoate as catalyst [17]. Subsequently, a fraction of each resulting di-block copolymer, was end-capped with α-propargyl carboxylate-ε-caprolactone (PCC) using stannous octoate as catalyst in a reflux reaction as per a reported procedure [18]. The near infrared fluorophore Cy5.5-azide was then conjugated to the terminal alkyne of PCC using a Cu(I)-catalyzed terminal alkyne-azide click Chemistry reaction.

DFEE was encapsulated in traceable micelles (DFEE-TM) based on PEO-*b*-PCL (DFEE-PCL-TM) or PEO-*b*-PBCL (DFEE-PBCL-TM) using the co-solvent evaporation method reported before [16]. In a typical encapsulation process, 3.0 mg of DFEE and 60 mg of the polymer (e.g. 59.4 mg of the unlabeled PEO-*b*-PCL and 0.6 mg of the dye labeled PEO-*b*-PCL-PCC-Cy5.5 azide) were co-dissolved in 300 µL of acetone to give a drug-to-polymer ratio of 1:20 w/w. The fraction of the dye labeled copolymer used determined the dye content in the formulation. The resulting solution was added drop-wise to 1800 µL of double distilled water under moderate stirring to give a ratio of 1:6 v/v for the organic-to-aqueous phases. The mixture was stirred for 24 h at room temperature to allow for the evaporation of the organic solvent. Next, vacuum was applied to ensure the complete removal of the organic solvent and then the micellar solution was centrifuged at 11,600 × g for 5 min to remove unencapsulated drug and the collected supernatant was filtered through a 0.22 µm filter and then stored at 4°C until used. Micellar formulations used

in the *in vivo* study were made isotonic prior to administration by adding 200 μL of 30% (w/v) dextrose in water per mL of formulation.

In addition to the DFEE-TM, DFEE loaded polymeric micelle (DFEE-PM) which use only the unlabeled di-block copolymers, PEO-*b*-PCL (DFEE-PCL-PM) or PEO-*b*-PBCL (DFEE-PBCL-PM) were also prepared for size distribution, morphology, and *in vitro* release comparisons and so were DFEE-loaded polymeric micelles using PEO-*b*-PCL-PCC in the formulation instead of the labeled copolymer PEO-*b*-PCL-PCC-Cy5.5 azide copolymer or PEO-*b*-PBCL-PCC instead of PEO-*b*-PBCL-PCC-Cy5.5 azide.

3.2.3. Characterization of the DFEE loaded traceable micelles

The prepared DFEE-TM as well as the DFEE-PM were characterized for morphology by transmission electron microscopy (TEM) (Philips/FEI Morgagni, Hillsboro, OR) using phosphotungstic acid (PTA) as a negative stain [19]. The samples were prepared by adding droplets of the micellar formulations, having polymer concentrations of 1-2 mg/mL, to copper-TEM grids, allowing them to air dry, and negative-staining with PTA. The prepared micelles were also characterized for particle size distribution (Zeta average diameter and the polydispersity index (PDI)) by dynamic light scattering (DLS) using a Malvern Zetasizer 3000 (Malvern Instruments, Worcestershire, UK) at 25 ˚C. However, as the Cy5.5 azide excitation and emission spectra could interfere with the DLS measurements [18], only the formulations based on PEO-*b*-PCL-PCC and PEO-*b*-PBCL-PCC as well as the two DFEE-PM formulations (i.e. DFEE-PCL-PM and DFEE-PBCL-PM) were analyzed. The zeta potential was also determined using the same instrument.

Drug encapsulation efficiency and loading content were determined through analyzing samples of the prepared micellar formulations by high performance liquid chromatography (HPLC) [16]. An aliquot of each DFEE-TM formulation (100 µL) was dissolved in 800 µL of acetonitrile to disrupt the self-assembled structure of the micelles. To these samples, 100 µL of 0.3 mg/mL solution of Mefenamic acid, used as internal standard (IS), was added. The concentrations in the samples were obtained from standard calibration curves plotted at a concentration range of 0.12 – 500 µg/mL of DEEF. The HPLC unit consisted of a Shimatzu HPLC system (Mandel Scientific, Guelph, ON) with an SPD-6A variable UV spectrophotometer set at 280 nm. Chromatographic separations were performed on a C18 column (100 × 4.6 mm ID, pore size: 3 µm) (Phenomenex, Torrance CA). The mobile phase consisted of acetonitrile-water-acetic acid (70:30:0.2, v/v/v), the flow rate was 1 mL/min and the injection volume was 50 µL.

The kinetics of the *in vitro* release of the DFEE loaded traceable micelles were studied using the dialysis bag method as previously reported [20]. Briefly, a dialysis bag (Spectra/por molecular porous membrane tubing, MWCO 3.5 kD) containing 2 mL of the micellar solution was incubated in phosphate buffer saline (PBS, pH 7.4) at 37°C under mild agitation in a Julabo SW 22 water bath (Seelbach, Germany). At predetermined time intervals, sampling with water replacement was carried out from the dialysis bag, and the incubation solution was replaced by fresh PBS. The samples (100 µL) were analyzed by HPLC as described above.

3.2.4. Animal studies

All animal studies were carried out in accordance with the guidelines of the Canadian Council on Animal Care and based on protocols approved by the Health Sciences Animal Care and Use

Committee, University of Alberta. Healthy male Sprague-Dawley rats (230-250 g) were obtained from the Health Sciences Laboratory Animal Services, University of Alberta, and were housed in a temperature-controlled room with a 12 h light/dark cycle and were given free access to water and food.

3.2.4.1. Pharmacokinetics and biodistribution of diclofenac

Single dose pharmacokinetics (PK), and biodistribution at 6 and 24 h post-dose of diclofenac from the DFEE-TM were investigated in healthy rats and compared to that following administration of diclofenac - as diclofenac sodium in saline, all at a dose equivalent to diclofenac 10 mg/kg. Under inhaled isoflurane (2%) anesthesia, rats were cannulated in the right jugular vein and were let to recover. Rats were divided into four groups, three of which received either free diclofenac or one of DFEE-PCL-TM or DFEE-PBCL-TM (with a dye content of 0.15 mg/kg body weight) via a bolus intravenous (*iv*) injection through a jugular vein cannula (6-9 rats/group). The fourth group (3 rats) received an intraperitoneal (*ip*) dose of DFEE-PCL-TM. Three rats from each group were euthanized 6 h after drug administration to study the biodistribution of drug and NIR labeled formulations. The remaining 3-6 rats in the *iv*-dosed groups were euthanized at 24 h for the same purpose. Following *iv* injection, the cannula was washed with normal saline. Blood samples (200 μL) were collected from the jugular vein at 0.03, 0.08, 0.25, 0.5, 1, 2, 4, 6, 8, and 12 h post-dose and at the end of the study through cardiac puncture following deep terminal anaesthesia. Sampling for rats which received an *ip* dose was limited to 6 h post-dose. Heart, kidney, liver, and spleen were removed from euthanized rats, washed in ice-cold saline, blotted with paper towel to remove excess fluid, and frozen along with blood samples and stored at −80 °C until analyzed.

The samples were assayed for diclofenac concentrations following a reported procedure with modifications [16, 21]. An aliquot of organ tissue (0.5 g) was added to 2 mL of double distilled water, and the mixture was homogenized using Omni TH (Thomas Scientific, NJ, USA) at 15,000 rpm for 1 min on ice at 0 °C. Blood samples or tissue homogenates (200 µL) were spiked with IS (mefenamic acid) and acidified with 1 M phosphoric acid. The matrix was extracted twice with 3 mL diethyl ether and the organic phase, collected after centrifugation, was aspirated, and dried under nitrogen. The dried residue was re-dissolved in 100 µL of mobile phase and analyzed using HPLC as described in section 3.2.3. The concentrations were calculated from standard curves for blood and individual tissues. A non-compartmental model was used to determine the pharmacokinetic parameters of diclofenac and the analysis was performed using PKSolver. Diclofenac tissue : blood ratios were calculated at each time point (whenever possible) for each rat as the ratio of the diclofenac concentration in the tissue (heart, kidney, liver, or spleen) to the diclofenac blood concentration.

3.2.4.2. Near infrared imaging studies

Images of the dissected tissues including heart, lung, liver, spleen, and kidney from above study were taken using the Kodak imaging station 4000M (Eastman Kodak, New Haven, CT). The fluorescence intensities in the organs were measured using the image processing software ImageJ (v 1.51-h, National Institutes of Health, USA). The total corrected intensities for the organs in the images were obtained by correcting the integrated densities for the background readings. This was followed by correcting for the intensities of the organs in control untreated rats as follows:

Corrected total fluorescence (CTF) intensity = integrated density – (area of selected organ × mean organ fluorescence reading in control rats).

3.2.5. Statistical analysis

Data are expressed as mean ± standard deviation (SD). The statistical significance was calculated using the two-tailed unpaired Student's t-test to compare means of two groups or the one-way analysis of variance (ANOVA) with post-hoc analyses using Fisher's least square difference to compare the means of more than two groups. A $p<0.05$ was considered to be statistically significant. Similarity factors (f_2) were used to assess the difference in the *in vitro* release profiles among the formulations [22]. Two release profiles were considered to be equivalent when their f_2 value was within the range of 50-100.

3.3. Results

3.3.1. Preparation and characterization of the micelles

Methoxy PEO, in the presence of stannous octoate, initiated the ring opening polymerization of either ε-caprolactone or α-benzyl carboxylate-ε-caprolactone and resulted in the formation of di-block copolymers of PEO-*b*-PCL (5000:3500 g/mol) or PEO-*b*-PBCL (5000:7500 g/mol) with similar degrees of polymerization of 30 as confirmed by ^{1}H NMR. The conjugation of PCC to the core blocks end was confirmed by ^{1}H NMR (Figure 3-1). This was followed by the conjugation of the Cy5.5 azide resulting in a molar conjugation efficiency of 50-60% for the different formulations.

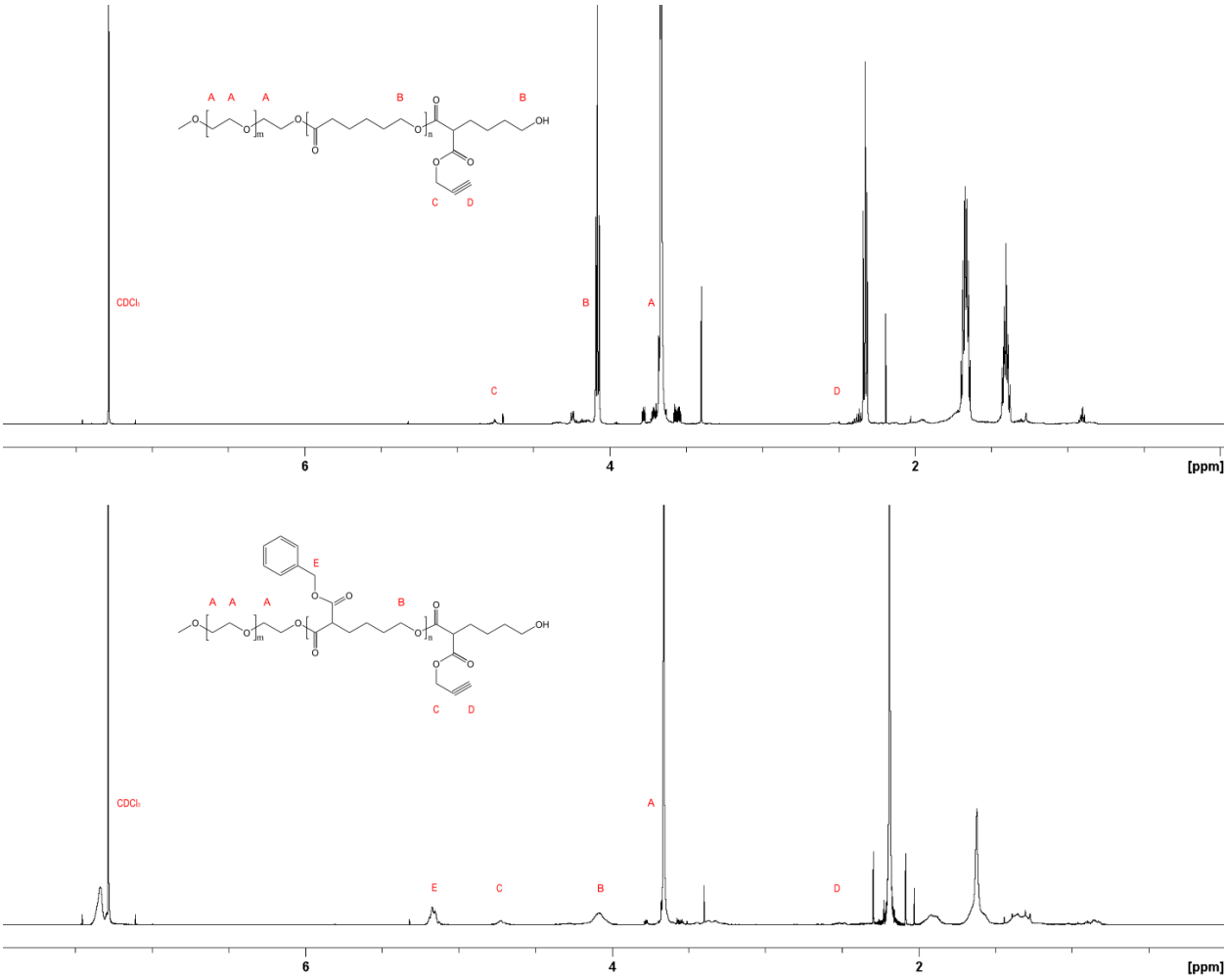

Figure 3-1. ^{1}H NMR spectra of PEO-b-PCL-PCC (top) and PEO-b-PBCL-PCC (bottom).

DFEE was efficiently encapsulated in traceable micelles based on PEO-*b*-PCL (DFEE-PCL-TM) and PEO-*b*-PBCL (DFEE-PBCL-TM), where in each instance a small proportion (~0.8% w/w) of the cy5.5 attached copolymer was used to control the dye content (Figure 3-2). DFEE-PCL-TM showed an entrapment efficiency of 84.7 ± 3.9% and a drug loading content of 4.2 ± 0.2% while the DFEE-PBCL-TM had an entrapment efficiency of 80.0 ± 5.5% and a drug loading content of 4.0 ± 0.3%.

TEM images presented in Figure 3-3 show that the DFEE-TM (both DFEE-PCL-TM and DEFF-PBCL-TM) possess regular spherical morphologies, similar to the unlabeled DFEE-PM, and are uniformly dispersed. The *in vitro* release profiles given in Figure 3-4 show that these labeled micelles sustain the release of DFEE in a manner comparable to that observed for the DFEE-PM [16]. The similarity factor f_2 between the DFEE-PCL-TM and DFEE-PCL-PM is 72.4±3.0 indicating comparable profiles (f_2>50, p<0.05, one sample t test) and that between DFEE-PBCL-TM and DFEE-PBCL-PM is 54.04±1.67 (f_2>50, p<0.05, one sample t test) which also indicates comparable profiles. Among the two traceable micelles, DFEE-PCL-TM appears to show a slightly slower *in vitro* release of DFEE compared to DFEE-PBCL-TM (f_2 of 49.36 ± 0.73 that is not significantly lower than 50; p>0.05, one sample t test). Here we remark that the parent diclofenac was not detected in all of the *in vitro* release experiments.

DLS revealed that modifying a fraction of the copolymer used for the micellar formulation by attaching PCC did not alter the characteristics of the DFEE encapsulated micelles formed, with the PEO-*b*-PCL-PCC and the PEO-*b*-PBCL-PCC based micelles showing an average size of 45.06±0.06 nm and 37.19±0.06 nm in diameter (Figure 3-3) and a PDI of 0.174 ± 0.008 and

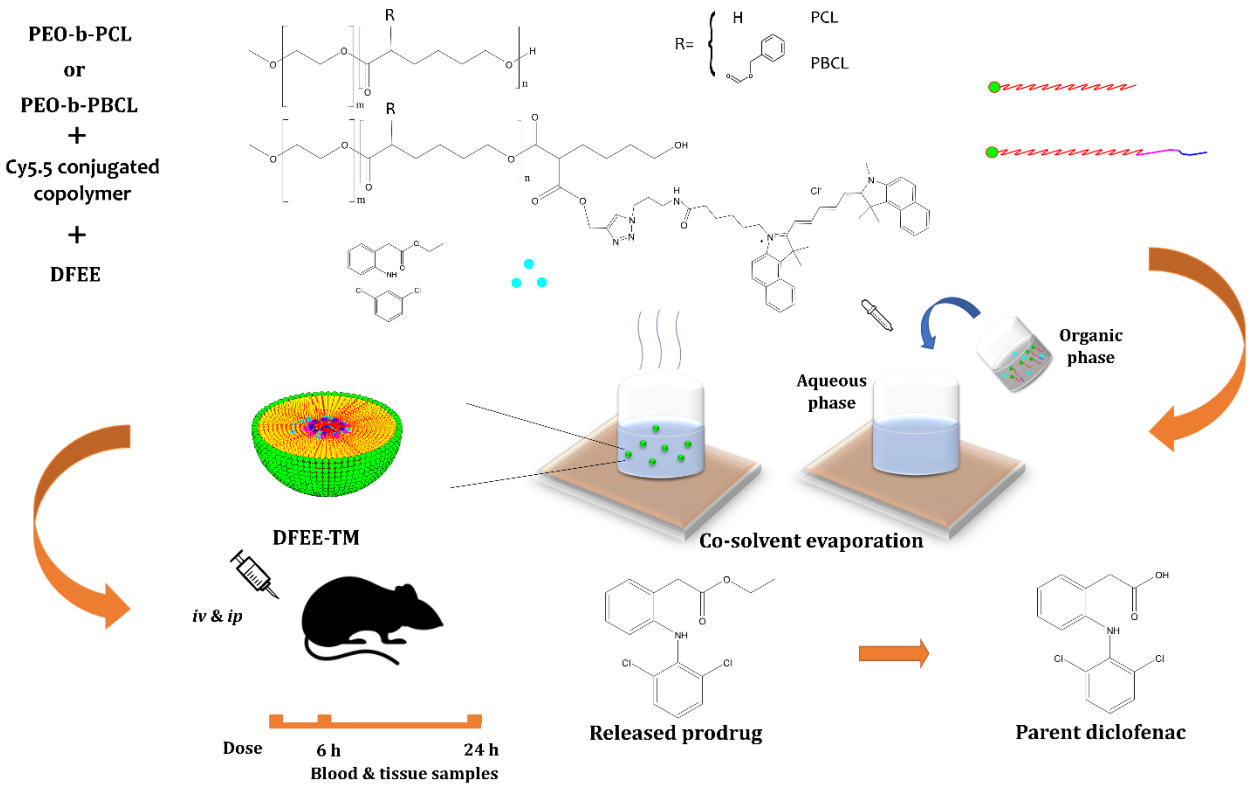

Figure 3-2. The encapsulation procedure used and the enzymatic and hydrolytic conversion of the released DFEE to the parent diclofenac.

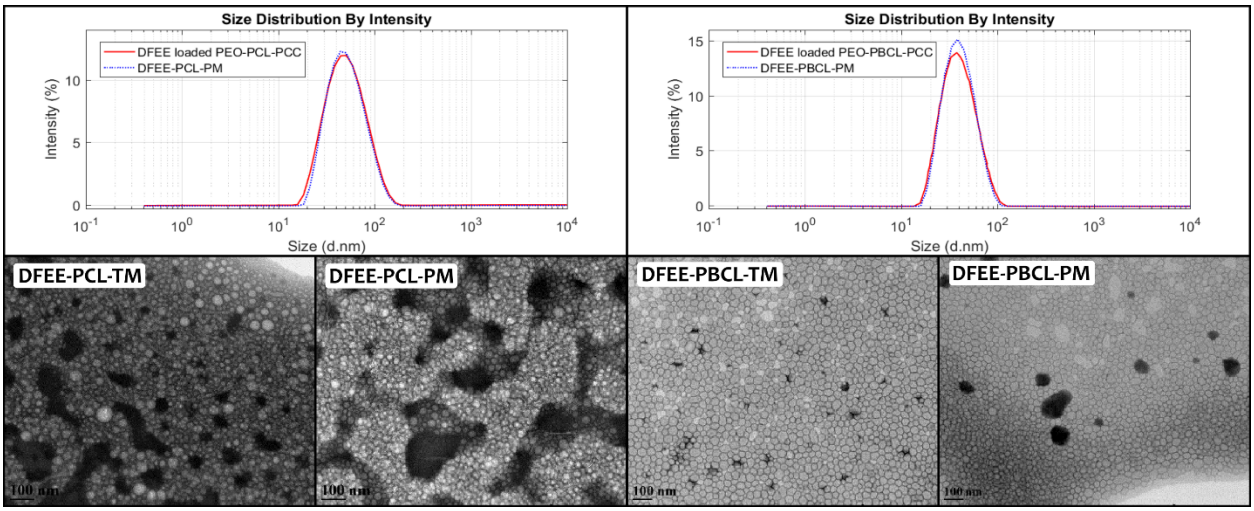

Figure 3-3. Characterization of the size distribution and morphology of the micellar formulations: (Top) DLS size distribution by intensity of the DFEE loaded micelle based on the PCC modified copolymers (PEO-PCL-PCC and PEO-PBCL-PCC) plotted against the unmodified DFEE-PM, and (bottom) TEM image of the Cy5.5 labeled micelles DFEE-TM and the unlabeled DFEE-PM.

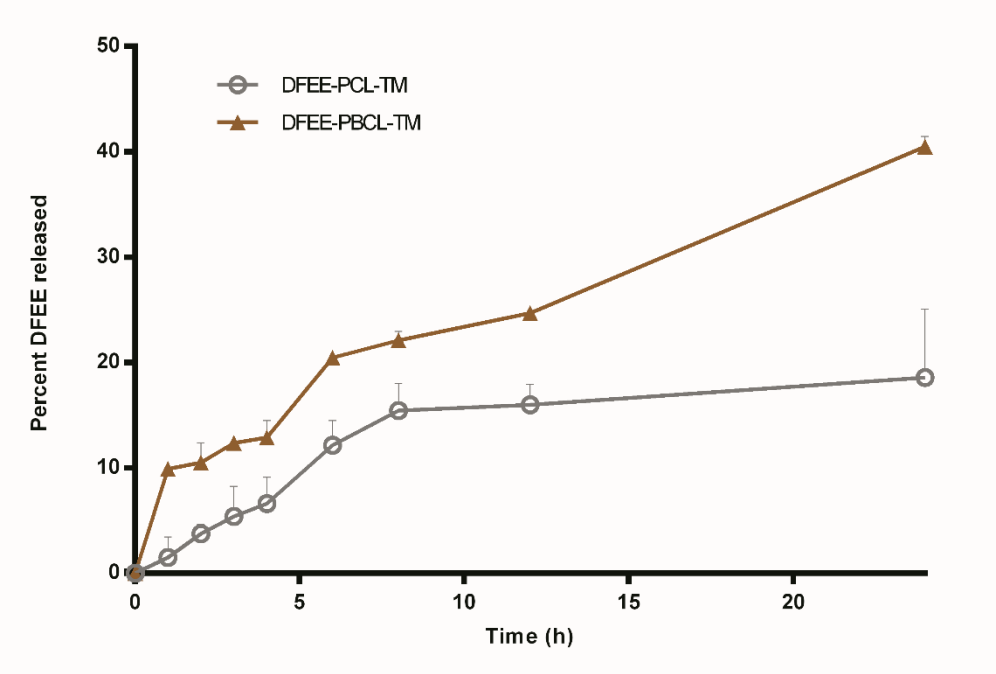

Figure 3-4. A 24-hour in vitro release of DFEE from the DFEE-TM formulations. Data are presented as mean ± SD. The profiles are significantly different at all time points ($p<0.05$, unpaired Student's t-test). The similarity factor, f_2 is 49.36±0.74 (f_2 not significantly lower than 50, $p>0.05$, one sample t-test).

Table 3-1. Characteristic properties of the polymeric micelles encapsulating DFEE.

Polymeric Micelle	Z. Average diameter (nm)	PDI	EE (%)	DLC w/w (%)
DFEE-PCL-TM	-	-	84.7 ± 3.9	4.2 ± 0.2
DFEE loaded PEO-PCL-PCC	45.06 ± 0.10	0.174 ± 0.008	86.3 ± 4.3	4.3 ± 0.2
DFEE-PCL-PM	43.02 ± 0.42*	0.220 ± 0.009	86.7 ± 1.4	4.4 ± 0.1
DFEE-PBCL-TM	-	-	80.0 ± 5.5	4.0 ± 0.3
DFEE loaded PEO-PBCL-PCC	37.19 ± 0.06***	0.131 ± 0.002	86.0 ± 0.9	4.3 ± 0.04
DFEE-PBCL-PM	38.8 ± 0.27&	0.167 ± 0.008	76.62 ± 1.7	3.8 ± 0.09

Data are given as mean ± SD. Asterisks and ampersands indicate significant difference compared to DFEE loaded PEO-PCL-PCC (* $p<0.05$, *** $p<0.0001$) and DFEE loaded PEO-PBCL-PCC (& $p<0.05$), respectively. PDI: polydispersity index; EE: Entrapment efficiency, DLC: Drug loading content.

0.131 ± 0.002, respectively. These characteristic properties are comparable to those obtained for the DFEE-PM based on unmodified di-block copolymers only (Table 3-1).

3.3.2. Concentration-time profiles of diclofenac in blood

HPLC analysis of blood and tissue sample from rats that received either of the DFEE-TM formulations revealed the parent diclofenac as the single detectable analyte. DFEE was not detected in any of these samples.

The 0-24 h concentration–time profile of diclofenac from the two DFEE-TM formulations and that of the free diclofenac in whole blood following an *iv* dose (equivalent to diclofenac 10 mg/kg) in healthy rats is given in Figure 3-5. The free diclofenac profile showed a rapid decline from its maximum value of 65 ± 5.3 μg/mL at 2 min such that diclofenac reached levels past 6 h post-dose that were below analytical sensitivity limit of 75 ng/mL. The micellar formulations, on the other hand, presented different profiles characterized by a sustained decline of the drug concentration when compared to free diclofenac. The DFEE-PCL-TM profile showed a less steep decline from its maximum value of 18.2 ± 6.4 μg/mL and presented diclofenac concentrations at 8, 12, and 24 h that were well above analytical quantification levels. The DFEE-PBCL-TM showed a similar decline from its maximum of 17.95± 6.4 μg/mL and presented with diclofenac concentrations that are not significantly different from those of DFEE-PCL- TM. The 24 h diclofenac pharmacokinetic parameters are summarized in Table 3-2 for free diclofenac while for the micellar formulation, it was not possible to confirm that the elimination phase was reached and thus it was not possible to determine most of the parameters. Both micellar formulations showed comparable area under the concentration-time curves from time zero to 24 h ($AUC_{0\text{-}24\ h}$) of 65.63 and 65.46 μg·h/mL for the

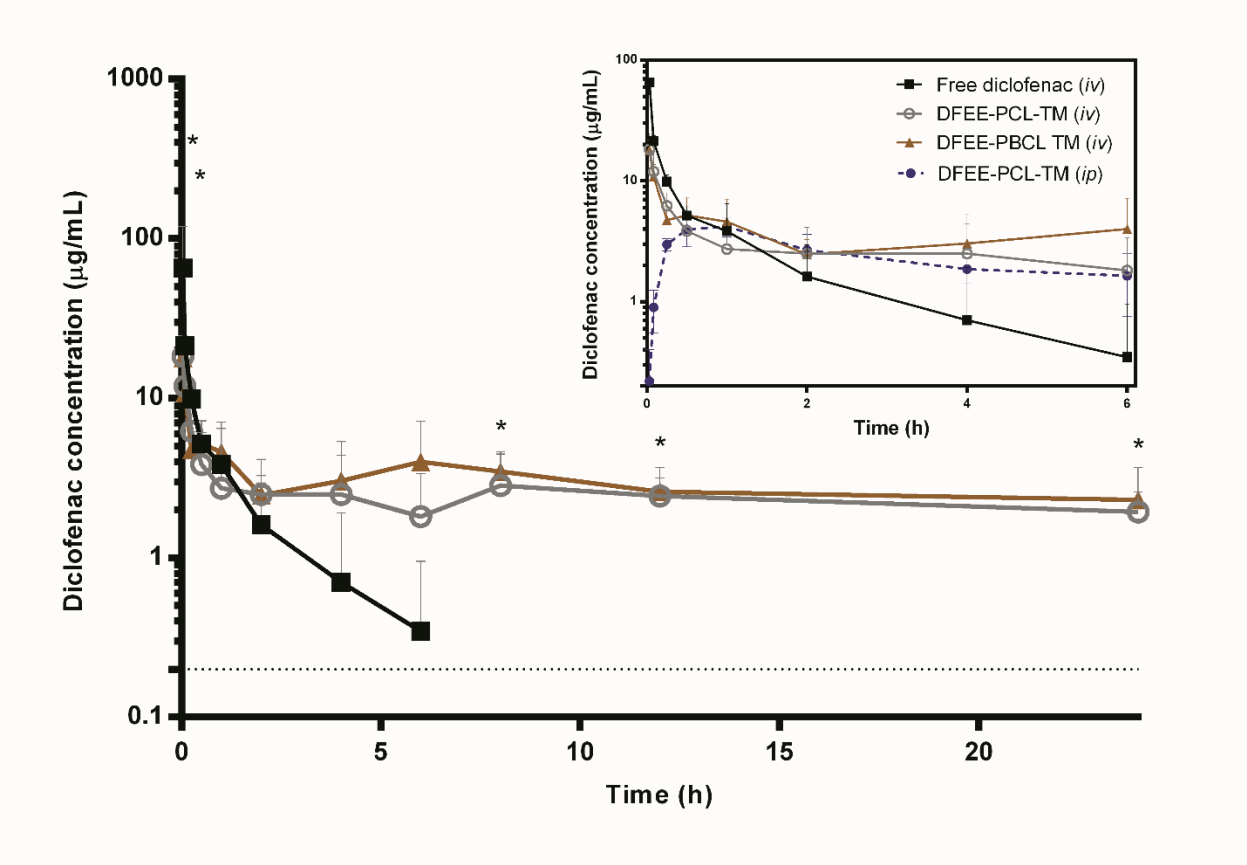

Figure 3-5. The blood concentration-time profile of diclofenac following a single *iv* dose (equivalent to diclofenac 10 mg/kg) of the DFEE-PCL-TM, the DFEE-PBCL-TM, or free diclofenac (n=3-6). The inset plot shows an enhanced view up to 6 h and additionally contains a 0-6 h profile following a single equivalent *ip* dose of the DFEE-PCL-TM (n = 3). Data are presented as mean ± SD. An asterisk indicates a significant difference for each of the micellar formulations in comparison to the free diclofenac at the time interval ($p < 0.05$, unpaired Student's t-test). No significant difference was observed between the two micellar formulations at all time points.

Table 3-2. Pharmacokinetic parameters of diclofenac in rats following a single *iv* dose (equivalent to diclofenac 10 mg/kg) of DFEE-PCL-TM (n=6), DFEE-PBCL-TM (n=3), or the free diclofenac (n=3).

Parameter	Free DF	DFEE-PCL-TM	DFEE-PBCL-TM
λ_z (h^{-1})	0.73 ± 0.16	ND	ND
$t_{½}$ (h)	0.98 ± 0.22	ND	ND
AUC_{0-t} (μg · h /mL)[1]	19.10 ± 9.28	65.63 ± 14.5	65.46 ± 5.89
MRT (h)	1.09 ± 0.47	ND	ND
$V_{\lambda z}$ (L/kg)	0.91 ± 0.34	ND	ND
Cl (L/kg/h)	0.64 ± 0.40	ND	ND

[1] 0-6 h for free diclofenac and 0-24 h for DFEE-PCL-TM and DFEE-PBCL-TM.

Data are presented as mean ± SD.

λ_z: terminal rate constant, MRT: mean residence time, ND: not determined due to potential error in identification of the terminal elimination phase, $t_{½}$: terminal half-life, AUC: area under the concentration-time curve, $V_{\lambda z}$: volume of distribution, Cl: systemic clearance.

The inset plot in Figure 3-5 presents a focused view of the 0-6 h concentration-time curves for diclofenac in whole blood. This graph includes data following a single *ip* dose of DFEE-PCL-TM (equivalent to diclofenac 10 mg/kg), in healthy rats. The curve related to *ip* injection of the micellar formulation, showed a rapid absorption phase with a maximum diclofenac concentration (C_{max}) of 4.36±0.87 μg/mL which was attained at T_{max} of 0.83±0.29 h. This is followed by a distribution, subsequently by an elimination phase that was in line with those observed with *iv* dosing of the micellar formulation.

3.3.3. Biodistribution of diclofenac in the tissues of healthy rats

The diclofenac exposure in the heart, kidneys, liver, and spleen 6 h following a single *iv* dose of either one of the two DFEE-TM or the free diclofenac in healthy rats (Figure 3-6 (A)) showed a significantly lower concentration of diclofenac in the heart by the micellar formulations (1.24±0.41 μg/g for DFEE-PCL-TM, and 1.43±0.42 μg/g for DFEE-PBCL-TM vs 2.22±0.36 μg/g for free diclofenac) but a higher concentration in the spleen (4.58±0.34 μg/g for DFEE-PCL-TM, 4.36±0.38 μg/g for DFEE-PBCL-TM vs 3.13±0.13 μg/g for free diclofenac). The three formulations had comparable diclofenac retention in the kidneys and liver. Similarly, both micellar formulations comparably and significantly reduced diclofenac partition (Table 3-3) in the heart (heart:blood ratios of 0.68 ± 0.22, 0.36 ± 0.11, and 4.35 ± 0.70 for DFEE-PCL-TM, DFEE-PBCL-

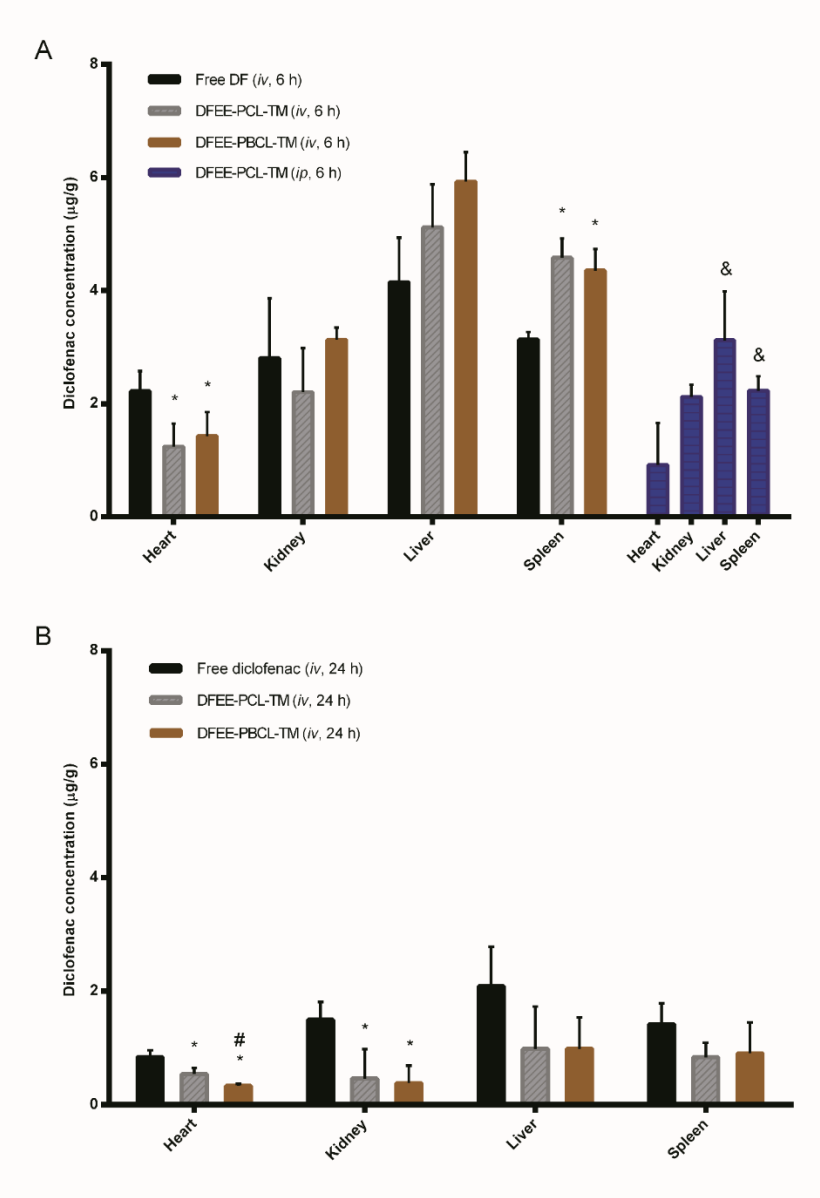

Figure 3-6. The tissue distribution of diclofenac: (A) at 6 h following a single *iv* dose (equivalent to diclofenac 10 mg/kg) of the DFEE-PCL-TM, the DFEE-PBCL-TM, or the free diclofenac (n = 3/group) and following an *ip* dose of DFEE-PCL-TM (n = 3) and (B) at 24 h following a single *iv* dose of the DFEE-PCL-TM (n = 6), the DFEE-PBCL-TM (n = 3), or the free diclofenac (n = 3). Data are presented as mean ± SD. An asterisk and a hash sign indicate significant difference from the free diclofenac or the DFEE-PCL-TM group, respectively, based on one-way ANOVA among the three *iv* dosed groups. An ampersand sign indicates significant difference from *iv* dosed DFEE-PCL-TM group (unpaired Student's t-test).

Table 3-3. Diclofenac tissue : blood concentration ratios in the various organs at 6 h following a single *iv* dose (equivalent to diclofenac 10 mg/kg) of DFEE-PCL-TM, DFEE-PBCL-TM, or the free diclofenac (n=3/group)

Formulation	Heart : Blood	Kidney : Blood	Liver : Blood	Spleen : Blood
Free DF	4.35 ± 0.70	5.50 ± 2.07	8.13 ± 1.54	6.14 ± 0.26
DFEE-PCL-TM	0.68 ± 0.22*	1.22 ± 0.43*	2.83 ± 0.42*	2.53 ± 0.19*
DFEE-PBCL-TM	0.36 ± 0.11*	0.78 ± 0.055*	1.49 ± 0.13*	1.09 ± 0.095*&

Data are given as mean ± SD. An asterisk and an ampersand indicate significant difference compared to Free DF and DFEE-PCL-TM, respectively, based on one-way ANOVA ($p<0.05$).

TM, and free diclofenac, respectively) ($p<0.05$, one-way ANOVA) and the other tissues (kidney:blood, 1.22 ± 0.43, 0.78 ± 0.055, and 5.50 ± 2.07, liver : blood, 2.83 ± 0.42, 1.49 ± 0.13, and 8.13 ± 1.54, spleen : blood: 2.53 ± 0.19, 1.09 ± 0.095, and 6.14 ± 0.26, for DFEE-PCL-TM, DFEE-PBCL-TM, and free diclofenac, respectively). No significant difference in the tissue : blood ratios was observed between the two micellar formulations in the heart, kidneys, or the liver, but the spleen : blood ratio of 1.09 ± 0.095 for DFEE-PBCL-TM was significantly lower compared to 2.53 ± 0.19 for DFEE-PCL-TM.

The diclofenac tissue exposure at 6 h following an *ip* dosing of the DFEE-PCL-TM is also presented in Figure 3-6 (A). DFEE-PCL-TM at a dose equivalent to diclofenac 10 mg/kg when given *ip* resulted in a significantly lower diclofenac concentrations in the liver (3.12 ± 0.86 μg/g vs 5.12 ± 0.76 μg/g) and spleen (2.23 ± 0.01 μg/g vs 4.58 ± 0.34 μg/g) compared to its *iv* administration ($p<0.05$, Student's t-test). The difference in the heart and kidney drug levels following *iv* versus *ip* administration did not reach statistical significance.

The diclofenac tissue exposure at 24 h post single *iv* dose administration of the two micellar formulations, DFEE-TM, or the free diclofenac in healthy rats is given in Figure 3-6 (B). Both micellar formulations presented a significantly lower diclofenac tissue retention in the heart (0.54 ± 0.11 μg/g for DFEE-PCL-TM, 0.34 ± 0.03 μg/g for DFEE-PBCL-TM vs 0.84 ± 0.11 μg/g for free diclofenac) and the kidneys (0.46 ± 0.52 μg/g for DFEE-PCL-TM, 0.38±0.31 μg/g for DFEE-PBCL-TM vs 1.5± 0.31 μg/g for free diclofenac) compared to the free diclofenac ($p<0.05$, one-way ANOVA). When compared to each other, while both micellar formulations showed equivalent

diclofenac concentrations at 6 h post dose in all organs studied, at 24 h post dose DFEE-PBCL-TM showed a trend for lower concentration in the kidneys and heart but only the diclofenac concentration in the heart was significantly different in this comparison ($p<0.05$, one-way ANOVA).

3.3.4. Near infrared imaging studies of the traceable micelles

Near-infrared images of the organs of healthy rats that received DFEE-TM formulations either as (i) an *iv* dose and collected at 6 h post-dose, (ii) an *ip* dose (only DFEE-PCL-TM) and collected at 6 h post-dose, or (iii) an *iv* dose and collected at 24 h post-dose were captured and representative images are given in Figure 3-7. The *ip* administration of DFEE-PCL-TM resulted in comparable corrected total fluorescence (CTF) intensities, a measure of labeled copolymer exposure, to those obtained with its *iv* administration in each of the heart, kidneys, liver, lungs and spleen at 6 h post-dose ($p>0.05$, Student's t-test). Among the two micellar formulations given *iv*, DFEE-PBCL-TM showed comparable CTF intensities to those achieved with DFEE-PCL-TM at 6 h post-dose ($p>0.05$, Student's t-test). At 24 h post-dose, however, DFEE-PBCL-TM resulted in higher CTF intensities in the kidneys, liver, and lungs compared to DFEE-PCL-TM ($p<0.05$, Student's t-test), but not in the heart or spleen.

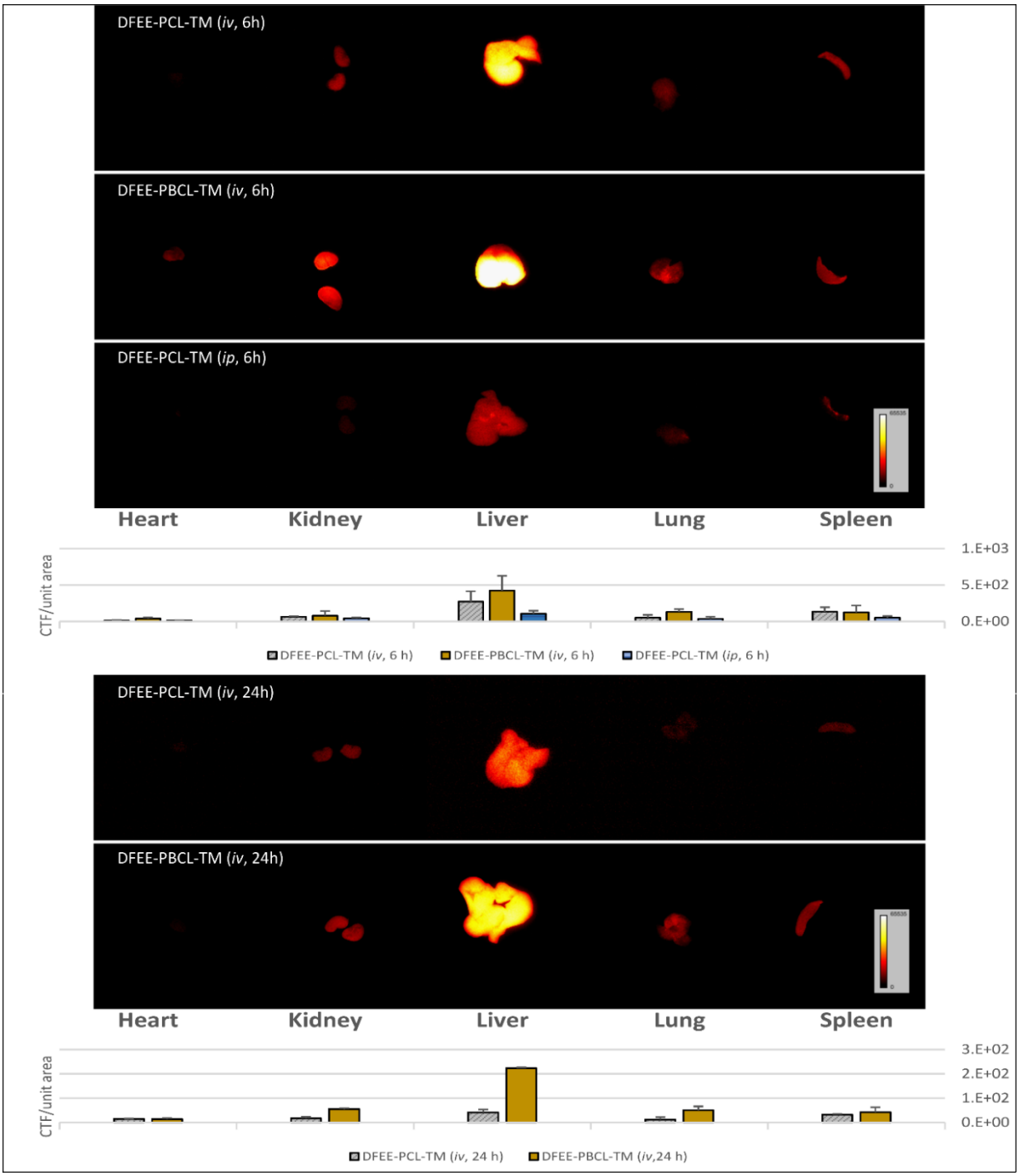

Figure 3-7. Figure 3-8. *Ex vivo* Near-infrared optical images of the major organs of representative rats given a single dose of DFEE-PCL-TM or DFEE-PBCL-TM as *iv* or *ip* (as indicated) and bar graphs of the corrected fluorescence intensities in the organs (mean ± SD) (n=3/group) at (A) 6 h or (B) 24 h post-dose.

3.4. Discussion

Our previous studies pointed to polymeric micelles based on PEO-*b*-PCL and PEO-*b*-PBCL, as potential formulations of DFEE capable of inducing a change in the *in vivo* PK of diclofenac. A principal rationale for developing the DFEE loaded micellar formulations was to modify the distribution of diclofenac throughout the body so that its safety can be improved. Therefore, we studied the PK and biodistribution of the micellar formulations in comparison to free diclofenac in healthy Sprague Dawley rats to investigate the potential of the developed formulations for this purpose.

To investigate the fate of the nano-carrier, in this study the NIR dye was attached to the hydrophobic core rather than the shell of nanocarriers, in order to avoid the potential influence of the dye on the circulation kinetics and stealth characteristics of the unlabeled polymeric micelles [14]. Similar to what was previously observed for unlabeled PEO-*b*-PCL and PEO-*b*-PBCL micelles [16], DFEE was encapsulated with high efficiency (Table 3-1) in traceable polymeric micelles (DEFF-TM) based on either of the two di-blocks copolymers (Figure 3-2).

In order to examine whether the inclusion of the dye-attached copolymer through the PCC linker (Figure 3-1) has affected the properties of the prepared micelles, both the DFEE-TM (i.e. DFEE-PCL-TM and DFEE-PBCL-TM) and unlabeled DFEE encapsulating polymeric micelles (DFEE-PM) were characterized for their morphology, and the *in vitro* release profile. Moreover, as the excitation and emission spectra of the Cy5.5 probe may interfere with the helium-neon laser (λ=633 nm) in the Zetasizer instrument, the size distribution of micelles based on the PCC modified di-blocks (PEO-*b*-PCL-PCC and PEO-*b*-PBCL-PCC) were analyzed by DLS as an

alternative to the labeled copolymer and was compared to that of the unlabeled micelles. In general, no difference was observed between DFEE-PM and their PCC modified counterparts in terms of micellar size distribution or between DFEE-PM and the NIR labeled DFEE-TM in terms of morphology (Figure 3-3, Table 3-1). The favorable *in vitro* release profile observed previously for the unlabeled micelles was also not affected, and the traceable micelles presented with a slow release of DFEE that is desired and motivated us to consider these formulations for *in vivo* analysis (Figure 3-4). When compared to each other, the two DFEE-TMs presented slightly different *in vitro* release profiles as measured by the similarity factor f_2 which fell slightly below 50, but not significantly. This is not much different from what was observed for unlabeled micelles based on PEO-*b*-PCL and PEO-*b*-PBCL where an f_2 value of just above 50 was observed [16].

Extensive *in vitro* characterization of the physicochemical properties of the di-block PEO-*b*-PCL and PEO-*b*-PBCL including molecular weight and polydispersion, and those of micelles based on these copolymers including thermodynamic and kinetic stability, physical stability against degradation and dissociation, cell uptake, biocompatibility, and immunogenicity have been investigated earlier in other reports [16, 18, 20, 23, 24].

The 0-24 h diclofenac blood concentration-time profile following a single *iv* dose of free diclofenac (Figure 3-5) reveals a rapid initial decline in the diclofenac blood concentration within the first hour followed by a slower-yet still fast- decline with a $t_{½}$ of 0.98 ± 0.22 h. Subsequently, drug concentration reached below the analytical sensitivity of our assay past 6 h post-dose. This behaviour was also reported in earlier studies and was suggested to indicate an extensive distribution of the free drug into the extravascular tissues but could also be due to fast elimination [16]. Both micellar formulations, on the other hand, presented PK profiles with long and sustained

systemic presence of diclofenac which reflect the *in vitro* release characteristics of DFEE from the formulations. However, in contrary to the *in vitro* release study where only DFEE was detected in the release media from both micellar formulations, the *in vivo* analysis showed the release of only the parent drug diclofenac.

Our HPLC assay was capable of detecting DFEE. However, in none of the blood or tissue samples following the administration of the polymeric micelles to rats did we detect DFEE. This is suggestive of complete hydrolysis of the released ester to the parent diclofenac. We have previously studied the enzymatic conversion of DFEE loaded in polymeric micelles, in comparison to free DFEE, *ex vivo* when incubated in fresh rat plasma [16]. Similar complete conversion of the released drug from the micelles to the parent diclofenac was seen, which is in accordance to the current results.

Two processes are involved in the release of diclofenac from the micelles in the biological samples, namely (i) the release of the encapsulated drug from the micelles whether it is the encapsulated DFEE or the parent drug if hydrolytic activation of the prodrug has occurred, and (ii) the enzyme-mediated hydrolysis of DFEE to parent diclofenac. The data points to a rapid conversion of the ethyl ester derivative to the parent diclofenac with its release. These two processes combined rendered the PK profile of the two DFEE-TM be more comparable to each other when compared to *in vitro* release which lacked the enzymes-mediated second process.

From the 0-24 h diclofenac concentration-time profiles following administration of the micellar formulations presented in Figure 3-5, it appears that the terminal phases could reflect the release rates of the encapsulated drug from the micelles more than the elimination phase of the drug. Free

diclofenac on the other hand, showed a multicompartmental profile with well defined distribution and elimination phases. Overall, the micelles showed an increase in the diclofenac exposure as measured by AUC. Here we remark, that the terminal phase half-life and the volume of distribution obtained for free diclofenac are likely to be underestimated, due to the sensitivity limit of the diclofenac assaying technique we used which could not detect low diclofenac concentrations beyond 6 h post-dose. Using analytical techniques with limited sensitivity needed to detect small quantities of drugs, have been found to underestimate drug half-lives [25], and hence lead to miscalculation in other PK parameters such as the volumes of distribution. For instance, it was reported for procainamide that using data up-to 12 h post-dose for analysis, which is the range of commonly used analytical techniques, resulted in a $t_{½}$ of 3.5 h while using data up-to 24 h, provided by a more sensitive analytical method, resulted in a $t_{½}$ of 8.52 h [25].

Several reports have shown polymeric micelles to prolong systemic circulation of the encapsulated drug [26-28], and factors related to the composition of the copolymer-based carrier are believed to contribute to this effect [29]. Our results show that the use of a nonionizable prodrug which is more hydrophobic than diclofenac and has a better *in vitro* compatibility with the core of polymeric micelles to be beneficial and has likely contributed to the observed improved PK profile of diclofenac by micellar formulations of DFEE [16]. The systemic conversion of a nano-delivered ethyl ester derivative of another NSAID was reported in a study by Cattani et al in which an Indomethacin ethyl ester loaded nanoparticle system was administered to rats, and only the parent indomethacin was exclusively detected in blood samples. However, contrary to our results, in that study a rapid clearance of the nanoparticles presumably by the reticuloendothelial system was

observed, which could be explained by the relatively larger size of the particles (~267 nm) and the lack of a stealth hydrophilic shell in that formulation [30].

We also investigated the tissue distribution from the two formulations at 6 and 24 h post-dose (Figure 3-6). The diclofenac concentrations in two major organs of the cardiovascular system, i.e. the heart and kidneys, from the two DFEE-TM formulations at 24 h post the single *iv* dose, presented in Figure 3-6, were significantly lower than those due to the free diclofenac. Diclofenac is a weak acid with a pKa value of 4.15, a reported $t_{½}$ of 1-2 h, and extensive protein binding. NSAIDs with such characteristics have been found to distribute in the whole body, but preferentially accumulate in the excretory tissues as well as the synovial fluid where their concentrations remain constant for prolonged periods of time [31]. The tissue distribution of free diclofenac reflected quantifiable diclofenac concentrations being found at 24 h post-dose in the four detected organs, even though diclofenac blood concentration reached levels below assay detection limit. Diclofenac from both traceable micelle formulations showed a different pattern of tissue exposure compared to the free diclofenac which appears to reflect the distribution profiles of the nano-carriers, shown in Figure 3-7, more than that of the drug itself. The reduced concentrations of diclofenac in the heart and the kidneys by the two micellar formulations is a promising result which shows a strong potential for these in the safe delivery of diclofenac and possibly other NSAIDs. This is especially important considering the reports that associate the extent of the toxicity of NSAIDs and other agents with their degree of accumulation in the relevant organs [10, 32]. Both DFEE-TM formulations showed a comparable reduction of diclofenac concentrations in the kidneys, but the DFEE-PBCL-TM showed a more pronounced reduction of drug concentrations in the heart.

The tissue-to-blood concentration ratios obtained with the two DFEE-TM formulations at 6 h post-dose for the different organs are low compared to that for the free diclofenac (Table 3-3). These ratios reflect higher diclofenac localization by the micellar formulations in the blood compartment, which acts as a depot for the encapsulated drug, and lower ability of diclofenac to accumulate in the organs studied. This has favorable safety implications for the delivery of diclofenac and warrants further investigation of the micellar formulations in inflamed preclinical models. Similar observations were reported with other PEO-*b*-PCL based micellar formulations [33].

A comparison between the two micellar formulations shows that, at 6 h time point, both DFEE-TMs resulted in similarly lower diclofenac concentrations in the heart, comparable concentrations in the kidneys and the liver, and similarly higher concentrations in the spleen in comparison to free diclofenac. NIR optical images reflecting nanocarrier exposure of different organs (Figure 3-7 A), also showed a comparable distribution profile for both nano-carriers at 6 h post-dose with no significant difference detected between the two formulations in the different organs when given as *iv* doses.

At 24 h post-dose, however, the DFEE-PBCL-TM NIR images showed higher intensities in the liver, lungs, and kidneys when compared to those of the DFEE-PCL-TM, while HPLC analysis showed no difference between the diclofenac concentrations from the two formulations in the liver or kidneys. The release of the encapsulated prodrug from polymeric micelles is governed by an intricate balance between drug diffusion, polymer degradation or micelle dissociation mechanisms and several factors including those relating to the composition and size distribution of the micelles have been found to influence this release. In the two traceable micellar systems in hand, the PEO-*b*-PCL based micelles appear to have a larger particle size (Table 3-1) which is expected to slow

the release of the cargo and could explain the slightly slower *in vitro* release observed for micelles based on this block copolymer (Figure 3-4). On the other hand, PEO-*b*-PBCL with a hydrophobic pendant benzyl carboxylate group attached to the PCL core block has been found to provide micellar systems with improved thermodynamic and kinetic stability and thus resist dissociation at extreme dilution conditions [16]. It is perhaps the higher extent rate of dissociation of PEO-*b*-PCL based micelles due to lower thermodynamic and kinetic stability and the subsequent clearance of the unimors that have balanced the diclofenac exposure of different organs compared to PEO-*b*-PBCL micelles while showing reduced CTF intensities in the liver and kidneys at 24 h post-dose.

The observation that DFEE formulations yielded comparable drug exposure following *iv* and *ip* injections suggests stability of the formulations through the hepatic pass. While an *iv* dose delivers the drug directly to the systemic circulation, *ip* injections need to pass the liver to reach the circulating blood. This explains the stability of the formulation, i.e., long $t_{½}$ after entry to the systemic circulation. Further, from the practical viewpoint, for animal studies involving repeated dosing, the *ip* route is more facile than *iv* ones. The blood diclofenac concentration-time profile (Figure 3-5) showed an absorptive phase with a T_{max} of 50 min post-dose and comparably high concentrations up to the 6 h of the study. The diclofenac tissue exposure, presented in Figure 3-6 (A), was similar to that achieved with *iv* dosing (at the same dose) and the slight reduction in the liver and spleen is mainly due a reduced involvement of the reticuloendothelial system in these organs at the early times.

3.5. Conclusions

Traceable DFEE loaded polymeric micelles based on PEO-*b*-PCL or on PEO-*b*-PBCL altered the expected pharmacokinetics of diclofenac, resulting in prolonged systemic circulation and reduced drug exposure of the cardiac tissues. Both micelles show strong potential for a cardiac-safe delivery of diclofenac.

References

1. Hart, F.D. and E.C. Huskisson, *Non-steroidal anti-inflammatory drugs. Current status and rational therapeutic use.* Drugs, 1984. **27**(3): p. 232-55.
2. Blower, P.R., *Non-steroidal anti-inflammatory drugs.* Br J Rheumatol, 1993. **32 Suppl 4**: p. 35-8.
3. Harirforoosh, S., W. Asghar, and F. Jamali, *Adverse effects of nonsteroidal antiinflammatory drugs: an update of gastrointestinal, cardiovascular and renal complications.* Journal of Pharmacy & Pharmaceutical Sciences, 2014. **16**(5): p. 821-847.
4. Aghazadeh-Habashi, A., W. Asghar, and F. Jamali, *Drug-Disease Interaction: Effect of Inflammation and Nonsteroidal Anti-inflammatory Drugs on Cytochrome P450 Metabolites of Arachidonic Acid.* J Pharm Sci, 2017.
5. Hwang, S.M., et al., *Non-Steroidal Anti-Inflammatory Drugs and Increased Risk of Sudden Cardiac Death*, in *Sudden Cardiac Death: Epidemiology, Genetics and Predictive/Prevention Strategies*. 2013, Nova Science Publishers, Inc.
6. Day, R.O., et al., *Pharmacokinetics of nonsteroidal anti-inflammatory drugs in synovial fluid.* Clin Pharmacokinet, 1999. **36**(3): p. 191-210.
7. Brune, K., *Persistence of NSAIDs at effect sites and rapid disappearance from side-effect compartments contributes to tolerability.* Curr Med Res Opin, 2007. **23**(12): p. 2985-95.
8. Harirforoosh, S., A. Aghazadeh-Habashi, and F. Jamali, *Extent of renal effect of cyclo-oxygenase-2-selective inhibitors is pharmacokinetic dependent.* Clin Exp Pharmacol Physiol, 2006. **33**(10): p. 917-24.
9. Harirforoosh, S. and F. Jamali, *Effect of inflammation on kidney function and pharmacokinetics of COX-2 selective nonsteroidal anti-inflammatory drugs rofecoxib and meloxicam.* J Appl Toxicol, 2008. **28**(7): p. 829-38.
10. Safra, T., et al., *Pegylated liposomal doxorubicin (doxil): reduced clinical cardiotoxicity in patients reaching or exceeding cumulative doses of 500 mg/m2.* Ann Oncol, 2000. **11**(8): p. 1029-33.
11. Zhou, Z.Y., et al., *Evaluation of the pharmacokinetics and cardiotoxicity of doxorubicin in rat receiving nilotinib.* Toxicol Appl Pharmacol, 2013. **272**(1): p. 238-44.

12. Asghar, W., A. Aghazadeh-Habashi, and F. Jamali, *Cardiovascular effect of inflammation and nonsteroidal anti-inflammatory drugs on renin-angiotensin system in experimental arthritis.* Inflammopharmacology, 2017.
13. McGettigan, P. and D. Henry, *Cardiovascular risk and inhibition of cyclooxygenase: a systematic review of the observational studies of selective and nonselective inhibitors of cyclooxygenase 2.* JAMA, 2006. **296**(13): p. 1633-44.
14. Aliabadi, H.M. and A. Lavasanifar, *Polymeric micelles for drug delivery.* Expert Opin Drug Deliv, 2006. **3**(1): p. 139-62.
15. Abu Lila, A.S., H. Kiwada, and T. Ishida, *The accelerated blood clearance (ABC) phenomenon: clinical challenge and approaches to manage.* J Control Release, 2013. **172**(1): p. 38-47.
16. Al-Lawati, H., et al., *Polymeric Micelles for the Delivery of Diclofenac and Its Ethyl Ester Derivative.* Pharmaceutical Nanotechnology, 2016. **4**(2): p. 109-119.
17. Mahmud, A., X.-B. Xiong, and A. Lavasanifar, *Novel self-associating poly (ethylene oxide)-b lock-poly (ε-caprolactone) block copolymers with functional side groups on the polyester block for drug delivery.* Macromolecules, 2006. **39**(26): p. 9419-9428.
18. Garg, S.M., et al., *Traceable PEO-poly(ester) micelles for breast cancer targeting: The effect of core structure and targeting peptide on micellar tumor accumulation.* Biomaterials, 2017. **144**: p. 17-29.
19. Sawyer, L., D.T. Grubb, and G.F. Meyers, *Polymer microscopy*. 2008: Springer Science & Business Media.
20. Shahin, M. and A. Lavasanifar, *Novel self-associating poly(ethylene oxide)-b-poly(epsilon-caprolactone) based drug conjugates and nano-containers for paclitaxel delivery.* Int J Pharm, 2010. **389**(1-2): p. 213-22.
21. Kaphalia, L., et al., *Efficient high performance liquid chromatograph/ultraviolet method for determination of diclofenac and 4'-hydroxydiclofenac in rat serum.* J Chromatogr B Analyt Technol Biomed Life Sci, 2006. **830**(2): p. 231-7.
22. Zhang, Y., et al., *DDSolver: an add-in program for modeling and comparison of drug dissolution profiles.* AAPS J, 2010. **12**(3): p. 263-71.
23. Soleymani Abyaneh, H., et al., *Rational design of block copolymer micelles to control burst drug release at a nanoscale dimension.* Acta Biomater, 2015. **24**: p. 127-39.
24. Garg, S.M., M.R. Vakili, and A. Lavasanifar, *Polymeric micelles based on poly(ethylene oxide) and alpha-carbon substituted poly(varepsilon-caprolactone): An in vitro study on the effect of core forming block on polymeric micellar stability, biocompatibility, and immunogenicity.* Colloids Surf B Biointerfaces, 2015. **132**: p. 161-70.
25. Jamali, F., et al., *Longer plasma half-life for procainamide utilizing a very sensitive high performance liquid chromatography assay.* Ther Drug Monit, 1988. **10**(1): p. 91-6.
26. Peris-Ribera, J.E., et al., *Pharmacokinetics and bioavailability of diclofenac in the rat.* J Pharmacokinet Biopharm, 1991. **19**(6): p. 647-65.
27. Xiong, M.P., et al., *Formulation of a geldanamycin prodrug in mPEG-b-PCL micelles greatly enhances tolerability and pharmacokinetics in rats.* J Control Release, 2008. **129**(1): p. 33-40.

28. Feng, R., Z. Song, and G. Zhai, *Preparation and in vivo pharmacokinetics of curcumin-loaded PCL-PEG-PCL triblock copolymeric nanoparticles.* Int J Nanomedicine, 2012. **7**: p. 4089-98.
29. Wang, Y., et al., *Pharmacokinetics and disposition of nanomedicine using biodegradable PEG/PCL polymers as drug carriers.* Curr Drug Metab, 2012. **13**(4): p. 338-53.
30. Cattani, V.B., A.R. Pohlmann, and T. Dalla Costa, *Pharmacokinetic evaluation of indomethacin ethyl ester-loaded nanoencapsules.* Int J Pharm, 2008. **363**(1-2): p. 214-6.
31. Brune, K., M. Glatt, and P. Graf, *Mechanisms of action of anti-inflammatory drugs.* Gen Pharmacol, 1976. **7**(1): p. 27-33.
32. Harirforoosh, S., W. Asghar, and F. Jamali, *Adverse effects of nonsteroidal antiinflammatory drugs: an update of gastrointestinal, cardiovascular and renal complications.* J Pharm Pharm Sci, 2013. **16**(5): p. 821-47.
33. Aliabadi, H.M., D.R. Brocks, and A. Lavasanifar, *Polymeric micelles for the solubilization and delivery of cyclosporine A: pharmacokinetics and biodistribution.* Biomaterials, 2005. **26**(35): p. 7251-9.

Chapter 4: Pharmacokinetics and pharmacodynamics of traceable polymeric micellar diclofenac in experimental arthritis rat model*

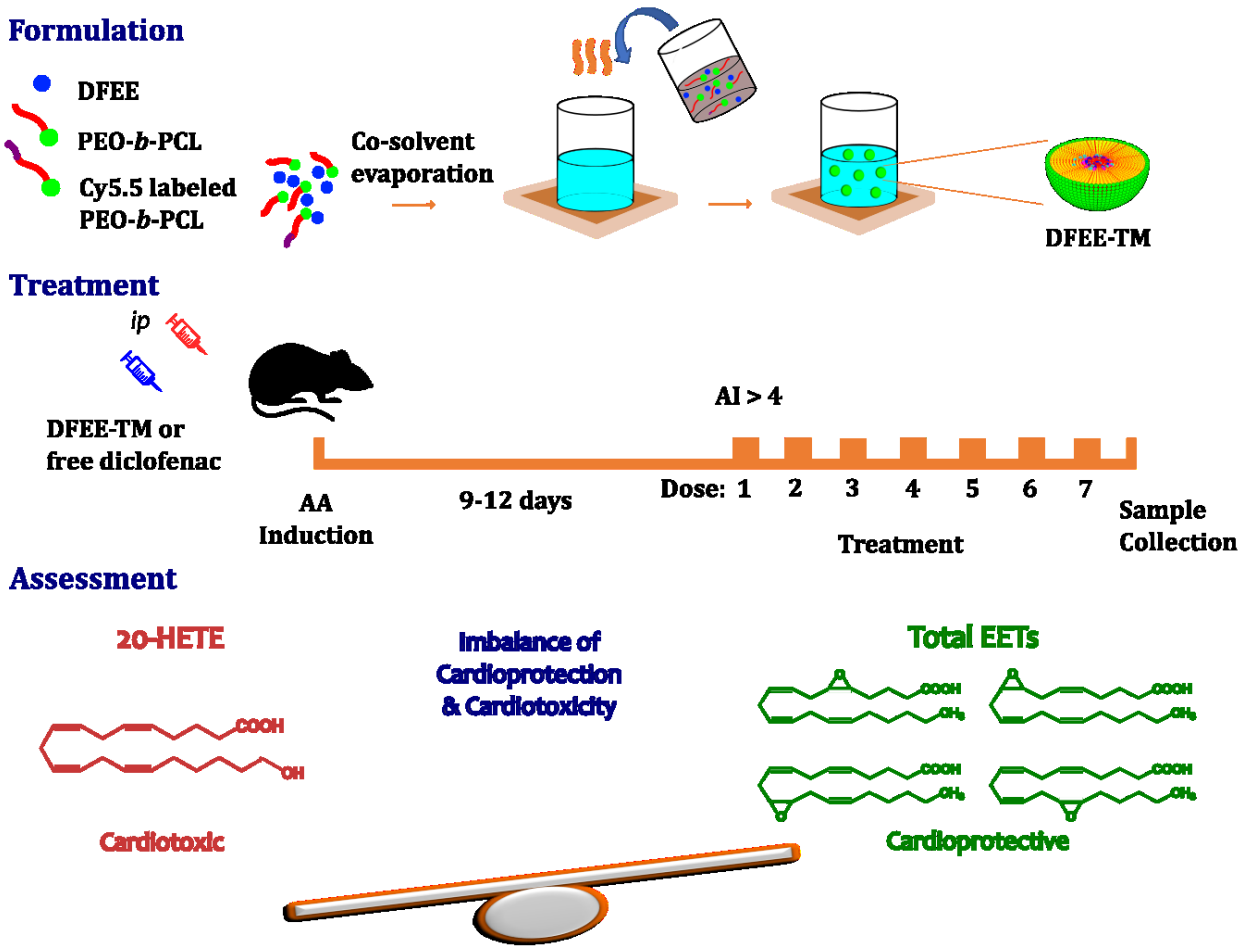

*A version of this chapter is to be submitted for publication:

Al-Lawati, H., Vakili, M.R., Lavasanifar, A., Ahmed, S., Jamali F. Pharmacokinetics and pharmacodynamics of traceable polymeric micellar diclofenac in experimental arthritis.

Abstract

Purpose: In this study we test the hypothesis that '*reduced exposure of non-steroidal anti-inflammatory drugs (NSAIDs) to the heart improves their cardiovascular safety profile'*. **Methods:** A fluorescently-tagged nanoformulation of diclofenac, a model NSAID with high cardiovascular (CV) risk profile, was prepared by encapsulating diclofenac ethyl ester (DFEE) in traceable (cyanine-5.5 labeled) polymeric micelles (DFEE-TM) based on methoxypoly(ethylene oxide)-*block*-poly(ε-caprolactone)(PEO-*b*-PCL) (MW, 5000:3500 g/mol). Diclofenac pharmacokinetics and tissue distribution as well as *ex vivo* near-infrared images of excised organs and whole bodies following administration of a single *iv* dose of DFEE-TM to adjuvant arthritic (AA) rats were compared to the same factors following *iv* administration to healthy rats. Moreover, biodistribution and anti-arthritic activity of DFEE-TM were determined and compared to those of free diclofenac following once-daily *ip* administration to AA rats (10 mg/kg/day diclofenac equivalent for 7 days, n=6/group). The concentration ratio of cytochrome P450-mediated cardiotoxic (20-hydroxyeicosatetraenoic acid (20-HETE)) over cardioprotective (epoxyeicosatrienoic acids (EETs)) metabolites of arachidonic acid (ArA) in the heart, kidneys, and plasma were also measured as markers of cardiotoxicity following administration of polymeric micellar or free diclofenac formulations and compared to that for untreated diseased animals. **Results:** The AA inflammatory disease state did not significantly alter the pharmacokinetics or biodistribution of diclofenac from labeled PEO-*b*-PCL micelles. Near-infrared images showed high accumulation of nanocarriers in inflamed joints of only AA diseased rats. In the multiple dose study, in line with the biological fate of the labeled nanocarrier, diclofenac was found in significantly lower concentrations in the heart of AA rats following DFEE-TM administration as

compared with free drug (1.5±0.60 vs 2.8±0.60 μg/g), but comparable concentrations were found in the kidneys, liver, and spleen between the two formulations. Both free diclofenac and DFEE-TM resulted in a similarly rapid reduction in the symptoms of AA. DFEE-TM yielded lower cardiotoxic metabolic profile of ArA in heart and plasma when compared to free diclofenac, i.e. significantly lower 20 HETE level (heart, 0.20±0.01 vs 0.48±0.07 μg/g; plasma, 41±6 vs 143±18 μg/L, respectively) and significantly lower ratio of 20-HETE : EETs (heart, 0.18±0.060 vs 0.45±0.030; plasma, 1.8±0.90 vs 22±9.5). **Conclusions:** Diclofenac delivery by PEO-*b*-PCL micelles encapsulating DFEE provided reduced accumulation of diclofenac in the heart of AA rats. Despite similar anti-arthritis activity, the polymeric micellar formulation showed implications of a reduced cardiotoxicity compared to the free drug as evidenced by a reduction in the ratio of cardiotoxic-over-cardioprotective eicosanoids of ArA in heart and plasma of AA rats.

Keywords

Adjuvant arthritis, arachidonic acid, biodistribution, cardiovascular risk, diclofenac, EET, inflammation, NSAIDs, polymeric micelles, 20-HETE.

4.1. Introduction

Inflammatory conditions, which include rheumatoid arthritis, psoriatic arthritis, and ankylosing spondylitis among others, have been implicated with an increased cardiovascular (CV) risk [1]. The mechanism underlying this CV risk is not fully understood, but is proposed to be through promotion of atherosclerosis and involvement of pro-inflammatory cytokines and other molecules generated in response to inflammation [2]. It is reported that the effect of inflammation is exerted, in part, through altering the homeostasis of cardiotoxic and cardioprotective components of the

renin-angiotensin system and those of the CYP mediated metabolism of arachidonic acid, towards a more cardiotoxic profile [3, 4].

Non-steroidal anti-inflammatory drugs (NSAIDs) are among the most widely prescribed medications worldwide and often considered the first line therapy for symptomatic relief in inflammatory conditions including various forms of arthritis. These agents exert their analgesic and anti-inflammatory properties by inhibiting the biosynthesis of prostaglandins (PG) achieved by blocking the activities of the cyclooxygenase (COX) enzymes, COX-1 and COX-2. However, this mechanism is also responsible for many of the well-documented adverse effects of NSAIDs including their gastrointestinal (GI), renal side effects as well as an elevated risk of CV events [5]. Research on selective inhibitors of COX-2 alarmed the increased risk of CV events associated with these agents including myocardium infarction and stroke [6]. Further examination of other NSAIDs raised similar concerns about the CV safety of non-selective COX inhibitors [7]. The exact mechanism underlying the CV risk of NSAIDs is not fully elucidated, but epidemiological data in human as well as preclinical experiments in rodents show an association between CV complications risk and NSAID dose [8, 9], duration of treatment [10], and NSAID level of accumulation in the heart and/or kidneys [4, 11].

We hypothesized that reducing the distribution of NSAIDs with proven CV complications to the heart can reduce the CV side effects. To test this hypothesis, we first developed nano-formulations of an NSAID with an established cardiovascular risk profile, namely diclofenac [8]. Diclofenac is, one of the most widely used NSAIDs worldwide with proven anti-inflammatory activity and a CV risk profile that is consistently ranked high [12]. The developed nano-formulations of diclofenac by our research group are based on micelle-forming block copolymers of poly(ethylene

oxide)-*block*-poly(ε-caprolactone) (PEO-*b*-PCL) or poly(ethylene oxide)-*block*-poly(α-benzyl carboxylate-ε-caprolactone) (PEO-*b*-PBCL) encapsulating a prodrug of diclofenac, namely diclofenac ethyl ester (DEEF). In previous studies, we have shown both of these nano-formulations to limit the distribution of diclofenac to the heart in healthy rats [13]. Herein we investigated the biodistribution, therapeutic activity as well as level of cytochrome P450-mediated arachidonic-acid metabolites as biomarkers of cardiotoxicity following the administration of traceable PEO-*b*-PCL based nano-formulations of diclofenac in adjuvant arthritic diseased rats. Comparisons of these parameters will be made after free diclofenac administration.

The nanodelivery of NSAIDs has received considerable attention in recent years as a mean of improving their activity and/or reducing their undesired toxicity. In addition to our work on polymeric micelles, diclofenac has been encapsulated in various nano-delivery systems including nanoparticles [14-16], liposomes [17-19], and lipogelsomes [20]. Several of these formulations have been shown to improve the anti-inflammatory activity and the antinociceptive effect of diclofenac in various experimental animal models, mostly by improving the biodistribution of the encapsulated drug [17, 18, 20]. Nano-delivery systems have also been developed for localized administration of diclofenac at inflamed joints so that its systemic exposure and toxicity can be limited [21, 22]. Nano-formulations of diclofenac have been shown to improve its GI or renal safety when administered systemically [15], or to reduce the muscle damage at injection sites upon parenteral administration when compared to the free drug [16, 23]. However, to the best of our knowledge, there hasn't been any reports on the alterations in the CV safety of diclofenac or any other NSAIDs when the drug distribution into the heart is influence by delivery via nanoscale advanced systems.

4.2. Materials and methods

4.2.1. Materials

Diclofenac sodium was purchased from Alfa Aesar (Tewksbury, MA), and diclofenac ethyl ester (DFEE) from TRC (Toronto, ON). Methoxy-poly(ethylene oxide) (PEO) (5000 g/mol), *N*,*N*-diiospropylethylamine, 16-hydroxydecanoic acid, indomethacin and potassium fluoride were obtained from Sigma–Aldrich (St. Louis, MO). ε-Caprolactone was purchased from Lancaster Synthesis (Lancaster, UK). α-Propargyl carboxylate-ε-caprolactone (PCC) was synthesized by Alberta Research Chemicals (Edmonton, AB). Stannous octoate was purchased from MP Biomedicals (Santa Ana, CA). Cyanine (Cy) 5.5 azide was purchased from Lumiprobe (Hallandale Beach, FL). Mycobacterium butyricum was obtained from Difco Laboratories (Detroit MI). Arachidonic acid metabolite standards 8,9-, 11,12- and 14,15-epoxyeicosatrienoic acids (EETs), 8,9-, 11,12- and 14,15-dihydroxyeicosatrienoic acids (DHETs), and 20-hydroxyeicosatetraenoic acid (HETE) were purchased from Cayman Chemicals (Ann Arbor, MI). 2-(2,3-naphthalimino) ethyl-trifluoromethanesulphonate (NE-OTf) was purchased from Molecular Probes (Eugene, OR). All other chemicals and reagents were of analytical grade and were used without any further purification.

4.2.2. Preparation of the diclofenac ethyl ester loaded traceable micelles

Block copolymer of PEO-*b*-PCL was synthesized with ring opening polymerization of ε-caprolactone (0.68 g) using methoxy PEO (5000 g/mol) (1 g) as initiator and stannous octoate as catalyst. The product (200 mg) was subsequently end-capped with α-propargyl carboxylate-ε-caprolactone (PCC) (30 mg) using stannous octoate as catalyst. This was followed by the

conjugation of the near-infrared probe Cy 5.5-azide to the terminal alkyne of PCC using the 1,3-dipolar cycloaddition (click chemistry) reaction catalyzed by copper (I) salts as previously reported [24]. DFEE was encapsulated in traceable micelles (DFEE-TM) prepared by mixing PEO-*b*-PCL and its Cy5.5 conjugated counterpart (99.2 wt. % of the unlabeled and 0.8 wt. % of the Cy 5.5 conjugated copolymers) using a co-solvent evaporation method at a drug-to-polymer ratio of 1:20 w/w and an organic-to-aqueous phase ratio of 1:6 v/v [13]. Briefly, in a typical experiment, polymers (60 mg total) and DFEE (3 mg) were dissolved in acetone (300 μL) and added dropwise to water (1.8 mL). Drug encapsulation efficiency and loading content were determined by analyzing samples of the prepared micellar formulations using high performance liquid chromatography (HPLC) as reported [13].

4.2.3. Animal studies

Animal studies were performed in compliance with the guidelines of the Canadian Council on Animal Care and following protocols approved by the Health Sciences Animal Care and Use Committee, University of Alberta. Adult male healthy Sprague-Dawley rats (230 to 250 g) were used in this study. Animals were obtained from the Health Sciences Laboratory Animal Services (HSLAS), University of Alberta, and housed in the HSLAS facility in a temperature-controlled room with a 12 h light-darkness cycle and free access to water and food. Following acclimation, the rats were anaesthetized with isoflurane in oxygen and adjuvant arthritis (AA) was induced by injection of 0.2 mL of 50 mg/mL Mycobacterium butyricum suspended in squalene in the tail base. The rats were monitored for disease progression and an arthritis index (AI) score was obtained by physical assessment of the severity of arthritis in each hind paw on a 0 to 4 scale (0: no joint involved; 1: single joint involved; 2: more than one joint involved; 3: the involvement of several

joints and moderate swelling of ankle; or 4: the involvement of several joints and severe swelling of ankle) and each fore paw on a 0 to 3 scale (0: no joint involved; 1: single joint involved; 2: more than one joint involved and/or wrist; 3: involvement of wrist and several joints with moderate-to-severe swelling) [25]. A total score of 5 or higher was considered an evidence of AA disease emergence, which normally occurred around 9-12 days following adjuvant injection.

4.2.3.1. Pharmacokinetics and biodistribution of diclofenac in adjuvant arthritic rats

Single dose pharmacokinetics and tissue distribution of the released diclofenac from the DFEE-TM were studied in rats with AA (n=3). Rats were cannulated in the right jugular vein under isoflurane/oxygen inhaled anaesthesia and were let to recover overnight. Following recovery, the rats received the DFEE-TM formulation intravenously (*iv*) through the jugular vein and were observed for 6 h. Blood samples (200 μL) were collected from the jugular vein at times at 0.03, 0.08, 0.25, 0.5, 1, 2, and 4 h post-dose and through cardiac puncture at 6 h post dose following terminal anaesthesia. Heart, kidney, liver, and spleen were removed, washed in ice-cold saline, blotted with paper towel to remove excess fluid, and frozen along with blood samples and stored at −80 °C until analyzed. The samples were assayed for diclofenac concentrations following a reported procedure [26, 27]. Moreover, *ex vivo* near-infrared fluorescence images of excised organs (heart, kidneys, liver, lungs, and spleen) and rat whole bodies after organ excision were obtained at 6 h post-dose using an IVIS Spectrum imaging station (PerkinElmer, Waltham, MA).

In addition, the diclofenac tissue distribution was also assessed in rats with AA that received multiple intraperitoneal (*ip*) doses of either free diclofenac (as diclofenac sodium in saline) or the DFEE-TM formulation as part of a multiple dose study, described in the following section.

4.2.3.2. Activity of the diclofenac ethyl ester traceable micelles in adjuvant arthritic rats

The disease progression or resolution was monitored daily by measuring the physical and visual signs and symptoms of AA according to published methods [25]. Sprague Dawley rats with AA were divided into 3 groups (6 rats/group), a free diclofenac treated group, a DFEE-TM treated group, and an inflamed untreated group. The treated rats were started on an *ip* dose equivalent to diclofenac 10 mg/Kg/day of one of the two formulations (i.e. free diclofenac or DFEE-TM) for 7 days. The paw and joint diameters were measured using a micrometer caliper (Mitutoyo Canada Inc., Toronto, ON). Rats in the inflamed untreated group were euthanized when their AI reached a score of 5 or higher to prevent/alleviate their suffering.

4.2.3.3. Measurement of cytochrome P450 (CYP)-derived eicosanoids of arachidonic acid (ArA)

The influence of diclofenac administration or its nanoformulation on the levels of cytochrome P450 (CYP)-derived eicosanoids of arachidonic acid (ArA), known for their effect on the CV system, were assessed in a multiple dose study. Treatments and dose of drugs were as described under section 4.2.3.2. The experiment was terminated 6 h following the last dose under deep-terminal inhaled anaesthesia with isoflurane/oxygen. Blood samples (1 mL) obtained through cardiac puncture were collected in tubes pre-filled with 200 µL of saline containing 0.113 mM of butylhydroxytoluene and 10 µM of indomethacin to prevent any chemical or enzymatic degradation of the eicosanoids and were subjected to centrifugation at 15,000 × g at 4 °C for 10 min. Plasma was collected, snap frozen with liquid nitrogen and then stored at -80° C until analyzed. Dissected heart and kidneys were rinsed with saline and divided into two parts, one

placed in a fixative for histopathological examination while the other stored at -80° C until analyzed.

Plasma and tissue samples were assayed for the concentration of the 8,9-, 11,12- and 14,15-EET, 8,9-, 11,12- and 14,15-DHET, and 20-HETE following a procedure previously reported in our lab with some modifications [28]. Briefly, heart or kidney samples were thawed to 4 °C and an aliquot (100 mg) was homogenized using a tissue homogenizer (Omni-TH Thomas Scientific, NJ, USA) and centrifuged for 1 min at 15,000 rpm in a glass tube containing 200 µL methanol and 0.4 µL of 96% formic acid.

Plasma samples (200 µL) and kidney or heart homogenates were spiked with 16-hydroxydecanoicacid (internal standard), and the mixture was extracted with anhydrous acetonitrile using solid phase cartridges (Oasis HLB C18 extraction cartridges, Pennsylvania laboratories, San Carlos, CA, USA). The solvent was evaporated under a stream of nitrogen. The samples were reconstituted in anhydrous acetonitrile and labeled with NE-OTf in the presence of saturated potassium fluoride solution in anhydrous acetonitrile and N,N-diiospropylethylamine as catalyst. The derivatized eicosanoids were extracted once more with anhydrous acetonitrile using solid phase cartridges. The samples were analyzed on a Shimadzu Prominence HPLC system (Mandel Scientific, Guelph ON, Canada) with a fluorescence detector set at 260 nm excitation wavelength and 396 nm emission wavelength. Chromatographic separation was performed on two reverse-phase C18 columns (100 × 4.6 mm ID, 3 µm) connected in series and guarded with a C18 guard column (4 mm × 3 mm ID) using a gradient mobile phase of water/acetonitrile containing 0.1% formic acid at 0.8 mL/min flow rate.

4.2.3.4. Histopathological examination

Segments of the dissected heart and kidney tissues of rats from the three groups as well as of healthy untreated rats were fixed in 10% neutral buffered formalin and embedded in paraffin. Thin sections were cut at 6 microns and stained with hematoxylin and eosin (H&E). The sections were analysed using a light microscope by a certified veterinary pathologist who was blinded to the treatment groups.

4.2.4. Statistical analysis

Data are expressed as mean ± standard deviation (SD). The statistical significance was calculated using the two-tailed unpaired Student's t-test to compare means of two groups or the one-way analysis of variance (ANOVA) with post-hoc Tukey HSD to compare the means of more than two groups. A value of $p<0.05$ was considered to be statistically significant.

4.3. Results

4.3.1. Preparation and characterization of the diclofenac ethyl ester loaded traceable micelles

Stannous octoate-catalyzed ring-opening polymerization of ε-caprolactone in the presence of methoxy PEO yielded PEO-*b*-PCL with a molecular weight of 3500 g/mol. This corresponds to a degree of polymerization of 30 of the core-forming PCL block. The conjugation of PCC to the terminal ends of the PCL core block of PEO-*b*-PCL (MW, 5000:3500 g/mol) was confirmed by

Table 4-1. Characteristics of block copolymers

Polymer	Polymerization degree of PEO	Polymerization degree of PCL	Mn (g/mol)*
PEO-*b*-PCL	114	30	8,500
PEO-*b*-PCL-PCC	114	23	7,850

* Number-average molecular weight measured by ^{1}H NMR.

^{1}H NMR. Details of the copolymers are given in Table 4-1. The subsequent attachment of the Cy5.5 azide resulted in a conjugation efficiency of 58% for the dye. DFEE was encapsulated in traceable micelles (DFEE-TM) based on the block copolymers of PEO-*b*-PCL (99.2 wt. %) and PEO-*b*-PCL-PCC-Cy5.5 azide (0.8 wt. %) providing a drug entrapment efficiency of 84.7±3.9% and a drug loading content of 4.2±0.2%.

4.3.2. Concentration-time profiles of diclofenac in blood of adjuvant arthritic rats

The effect of the AA disease on the pharmacokinetics and disposition of diclofenac from DFEE-TM can be realized from the 0-6 h concentration-time profile of diclofenac in the blood of AA diseased rats following a single *iv* dose shown in Figure 4-1. No significant differences are observed in the diclofenac blood concentrations of the diseased rats studied in comparison to those previously reported for healthy rats [13].

4.3.3. Biodistribution following a single dose of DFEE-TM

The accumulation of diclofenac in the heart, kidneys, liver, and spleen at 6 h following a single *iv* dose of the DFEE-TM in AA diseased rats is presented in Figure 4-2. When compared to their

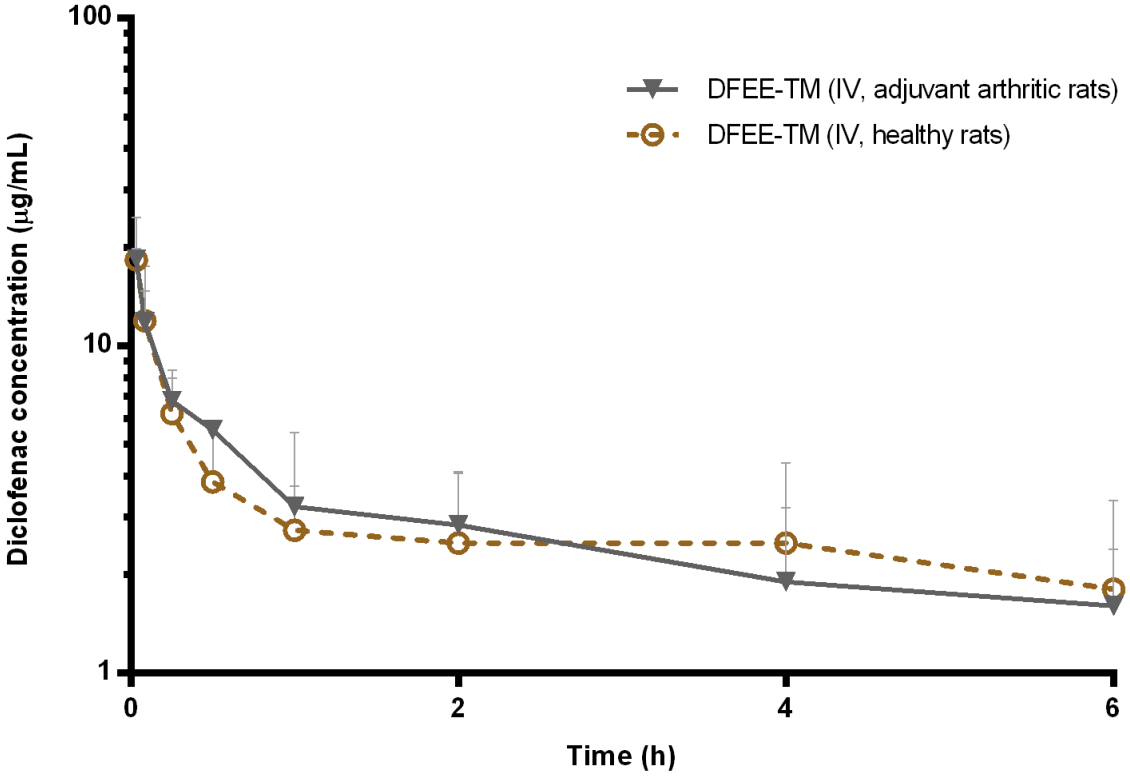

Figure 4-1. Diclofenac 0-6 h concentration-time curves in blood following the administration of a single dose equivalent to diclofenac 10 mg/kg of the DFEE-TM to adjuvant arthritic rats (n = 3) in comparison to that in healthy rats.

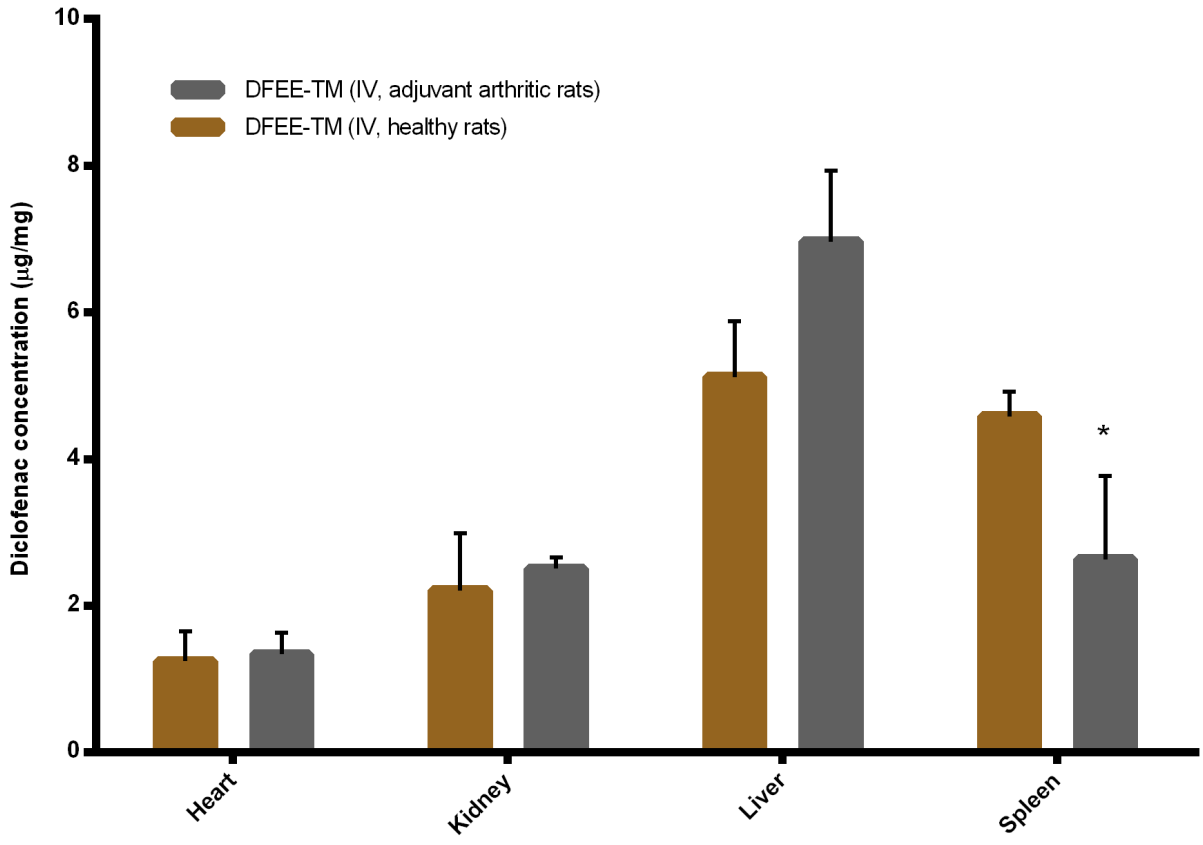

Figure 4-2. Diclofenac tissue distribution at 6 h following the administration of a single dose equivalent to diclofenac 10 mg/kg of the DFEE-TM to adjuvant arthritic or healthy rats (n=3/group). Data are presented as mean ± SD. An asterisk indicates significant difference compared to the healthy rats given DFEE-TM as an *iv* dose ($p < 0.05$, unpaired Student's t-test).

administration in healthy rats [13], DFEE-TM resulted in significantly lower accumulation of diclofenac in the spleen of AA diseased rats (2.63±1.14 μg/g vs 4.58± 0.34 μg/g) ($p<0.05$), but the concentrations in other tissues were similar and not significantly different. Near-infrared optical images of whole bodies showed higher fluorescence intensities in the inflamed joints of the hind- and fore-paws of AA diseased rats compared to the same joints in healthy rats, suggesting localization of the micelles at these joints in the inflammatory disease state (Figure 4-3). *Ex vivo* images of the major organs of AA diseased rats showed brighter fluorescence intensities, indicating higher traceable micelle accumulation, in the liver and spleen than in the heart and kidneys, where dull fluorescence intensities were observed.

4.1.1. Biodistribution following multiple dosing of DFEE-TM by *ip* route of administration

Figure 4-4 illustrates data on diclofenac tissue accumulation at 6 h following the last dose in AA diseased rats which received daily *ip* doses of DFEE-TM or free diclofenac for 7 days. Diclofenac concentrations in the heart were significantly lower in the DFEE-TM group compared to the free diclofenac group (1.48±0.51 vs. 2.84±0.55 μg/g) ($p<0.05$). The differences in other tissues were insignificant.

4.1.2. Effect of polymeric micellar delivery of diclofenac on the severity of adjuvant arthritis

The severity of the adjuvant arthritis disease following treatment with the DFEE-TM or free diclofenac at a dose equivalent to diclofenac 10 mg/kg/day was monitored daily for 7 days of treatment and factors including the AI score and the percent change in hind- and fore-paw diameters from baseline were recorded (Figure 4-5). Both treatments resulted in a decrease in the

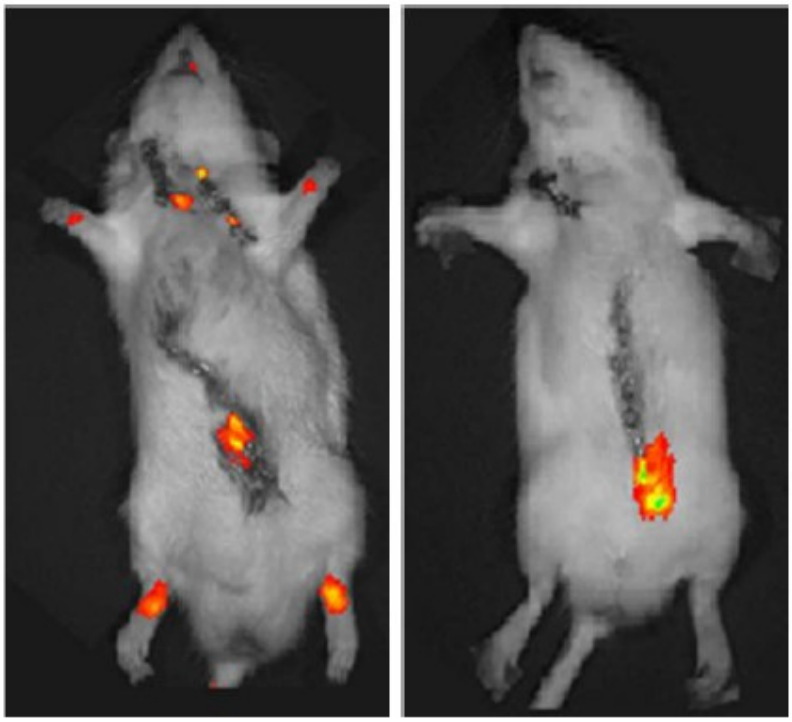

Figure 4-3. Near-infrared optical images of whole bodies following excision of major organs (heart, kidneys, lungs, spleen, and liver) of a representative rat with induced AA (left) and a healthy rat (right) at 6 h following a single *iv* dose of the DFEE-TM.

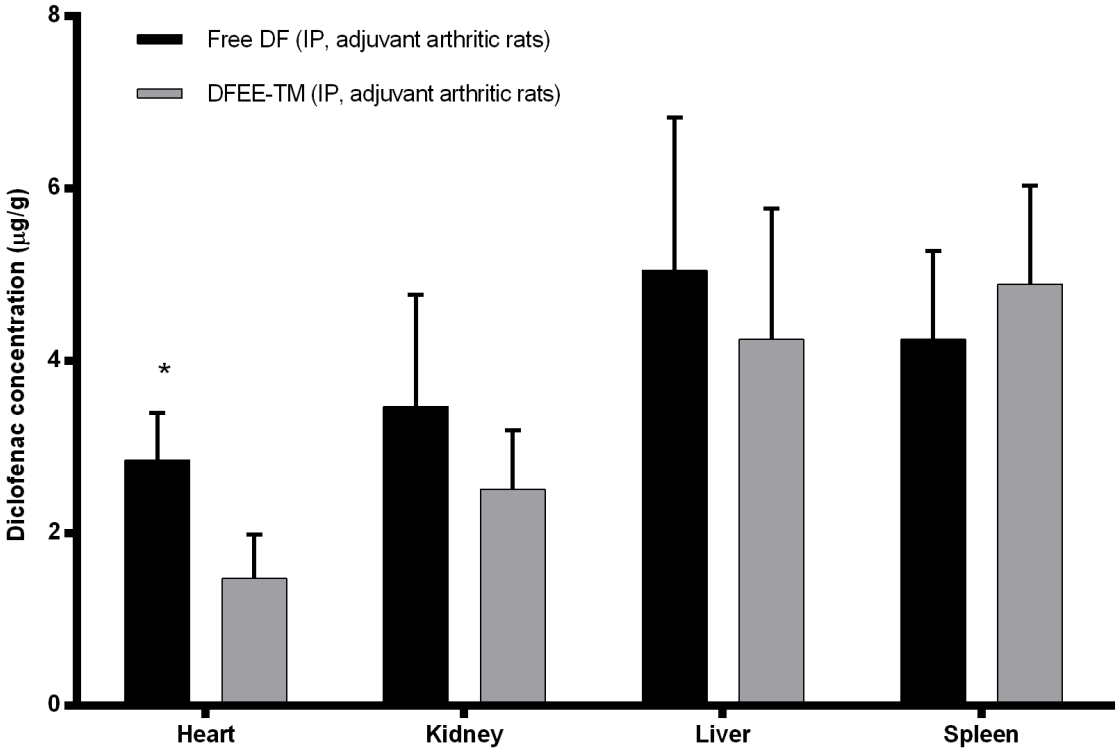

Figure 4-4. Diclofenac tissue distribution in rats which received multiple *ip* doses for 7 days (equivalent to diclofenac 10 mg/kg/day) of the DFEE-TM formulation or the free diclofenac (n = 6/group) at 6 h following the last dose. Data are presented as mean ± SD. An asterisk indicates significant difference between the two groups ($p < 0.05$, unpaired Student's t-test).

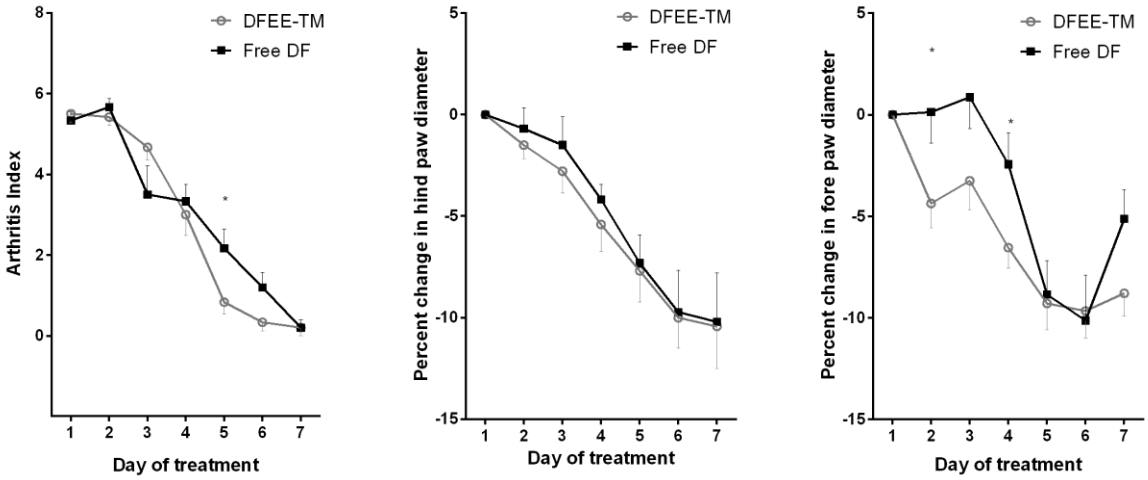

Figure 4-5. Arthritis index and percent change in hind- and fore-paw joint diameters from baseline (Mean ± SEM) as measures of severity of disease in adjuvant arthritis inflamed rats treated with free diclofenac, or with DFEE-TM (n=6/group). An asterisk indicates significant difference between the two groups ($p < 0.05$, unpaired Student's t-test).

AI score reaching an AI of 0.20±0.45 on day 7. The DFEE-TM showed a trend for a larger decrease in AI on days 3-5 and the difference was significant on day 5 (0.83±0.75 vs 2.17±1.17) compared to the free drug. No significant difference was found between the two treatments in the percent change of hind-paw diameter compared to baseline, while a significantly higher percent change in fore-paw diameter was achieved with the DFEE-TM on days 2 and 4.

4.1.3. Histopathological examination

Histopathological examination was carried out to assess the effects of diclofenac treatment as free or polymeric micellar formulation on the cardiac and kidney tissues in the multiple-dose study. Photomicrographs of heart and kidney slices of representative rats from a healthy untreated (control) group as well as from the untreated AA rats (positive control), or rats treated with either free diclofenac or with DFEE-TM are showcased in Figure 4-6. Healthy untreated rats showed normal heart architecture (Figure 4-6 A). The inflamed untreated rat heart tissue (Figure 4-6 B), on the other hand, showed multifocal to locally extensive inflammatory cell infiltration, characteristics of subacute to chronic inflammation. Rats treated with DFEE-TM or with free diclofenac presented similarly improved conditions showing either normal histology or very small localized interstitial infiltrates of small numbers of mononuclear inflammatory cells (Figure 4-6 C-D). Kidney tissues of healthy control rats showed microscopically normal organs (Figure 4-6 A). The kidney samples of AA inflamed untreated rats showed accumulation of inflammatory cell in glomerular tuft, Bowman's capsule or periglomerular connective tissue (≥10% glomeruli) (Figure 4-6 B). The DFEE-TM or free diclofenac treated rats either showed signs of normal tissues comparable to control or only showed a slight increase in glomerular cellularity (< 10% glomeruli)

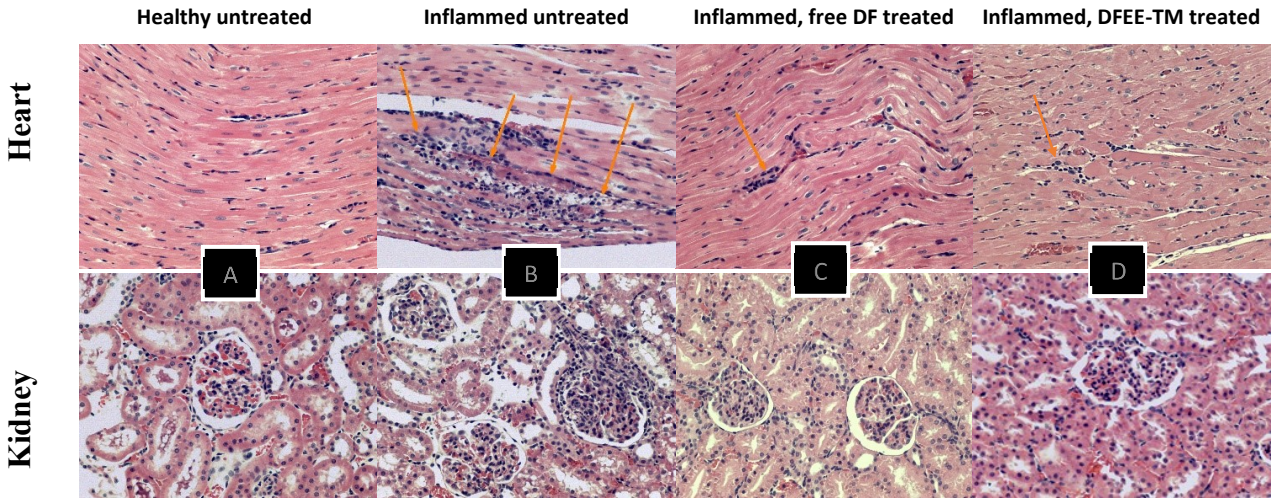

Figure 4-6. Photomicrography of heart and kidney

(H&E stained sections with a magnification of 200×) of rat from the (A) healthy untreated group, (B) inflamed untreated group (C) free diclofenac treated group and (D) DFEE-TM treated group.

(Figure 4-6 C-D). There was no difference in the histopathology of the kidney or heart between the DFEE-TM and the free diclofenac treated groups.

4.1.4. Cytochrome P450 metabolites of arachidonic acid as biomarkers of diclofenac cardiotoxicity

The CYP metabolites of ArA, known to have an effect on the CV system including 8,9-, 11,12- and 14,15-EET, 8,9-, 11,12- and 14,15-DHET, and 20-HETE were assayed in the plasma, heart, and kidney tissues of AA inflamed untreated rats, the free diclofenac treated rats, and the DFEE-TM treated rats in the multiple-dose study (n=6/group) (Figure 4-7 to Figure 4-10). In particular, levels of the cardiotoxic 20-HETE, the sum of the cardioprotective EETs (total EETs), and the ratio 20-HETE : total EETs, a measure of the balance in the cardiovascular homeostasis, are presented in Figure 4-7.

The levels of 20-HETE were significantly lower in the DFEE-TM treated group compared to the inflamed untreated and the free diclofenac treated groups in plasma (40.6±6.40 ng/mL vs 93.8±15.2 ng/mL & 144±18.3 ng/mL, respectively) and heart (0.20±0.010 ng/mg vs 0.46±0.10 ng/mg & 0.48±0.070 ng/mg, respectively) ($p<0.05$, one-way ANOVA). Free diclofenac, on the other hand, resulted in higher 20-HETE levels in the plasma when compared to the inflamed group ($p<0.05$, one-way ANOVA). In the kidneys, free diclofenac did not significantly alter the levels of 20-HETE when compared to the inflamed untreated group (0.02±0.01 ng/mg vs. 0.01±0.006 ng/mg). However, significantly higher 20-HETE levels were found in the DFEE-TM group (0.04±0.02 ng/mg) compared to the inflamed untreated group ($p<0.05$, one-way ANOVA). The

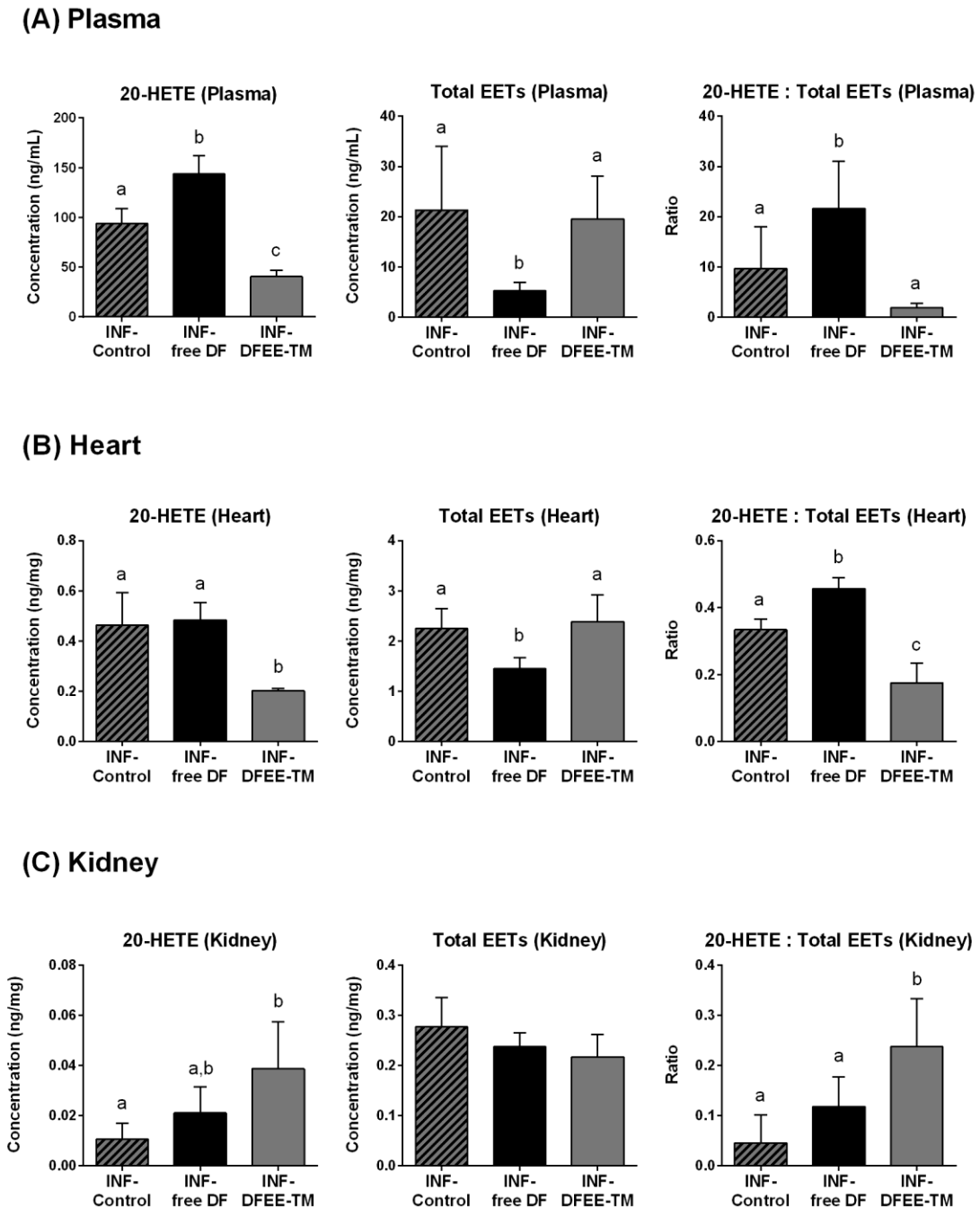

Figure 4-7. Concentrations of 20-HETE, the total EETs and the ratio 20-HETE : total EETs (mean ± SD) in (a) plasma, (b) heart, and (c) kidneys of adjuvant arthritic rats receiving no treatment (INF Control), or treated with free diclofenac (INF free DF) or with the DFEE micelles (INF DFEE-TM) (n=6/group).Bars sharing the same letter are not significantly different, based on one-way ANOVA (α=0.05) with post-hoc Tukey HSD.

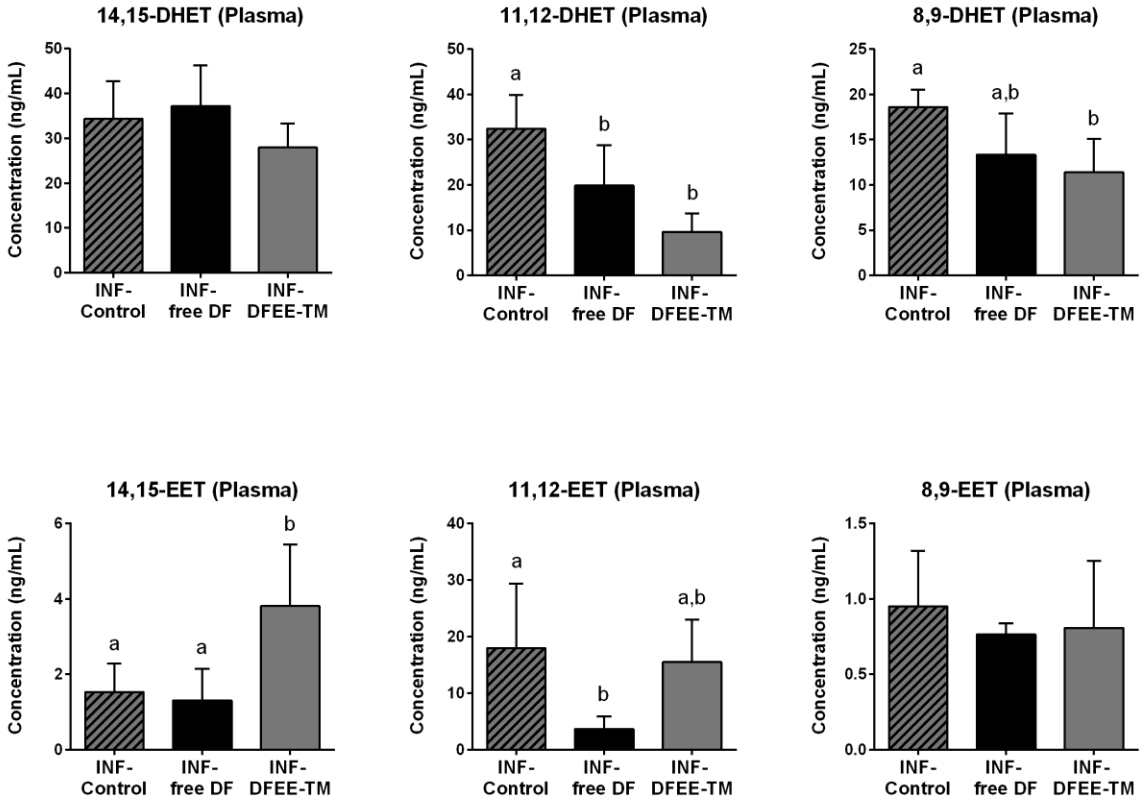

Figure 4-8. Concentrations of CYP metabolites of arachidonic acid (14,15-, 11,12- and 8,9-DHET, 14,15-, 11,12-, and 8,9-EET) in the plasma of adjuvant arthritis inflamed rats receiving no treatment (INF Control), or treated with free diclofenac (INF-free DF), or with the diclofenac ethyl ester traceable micelles (INF-DFEE-TM) (n=6/group).Bars sharing the same letter are not significantly different based on one-way ANOVA (α=0.05) with post-hoc Tukey HSD.

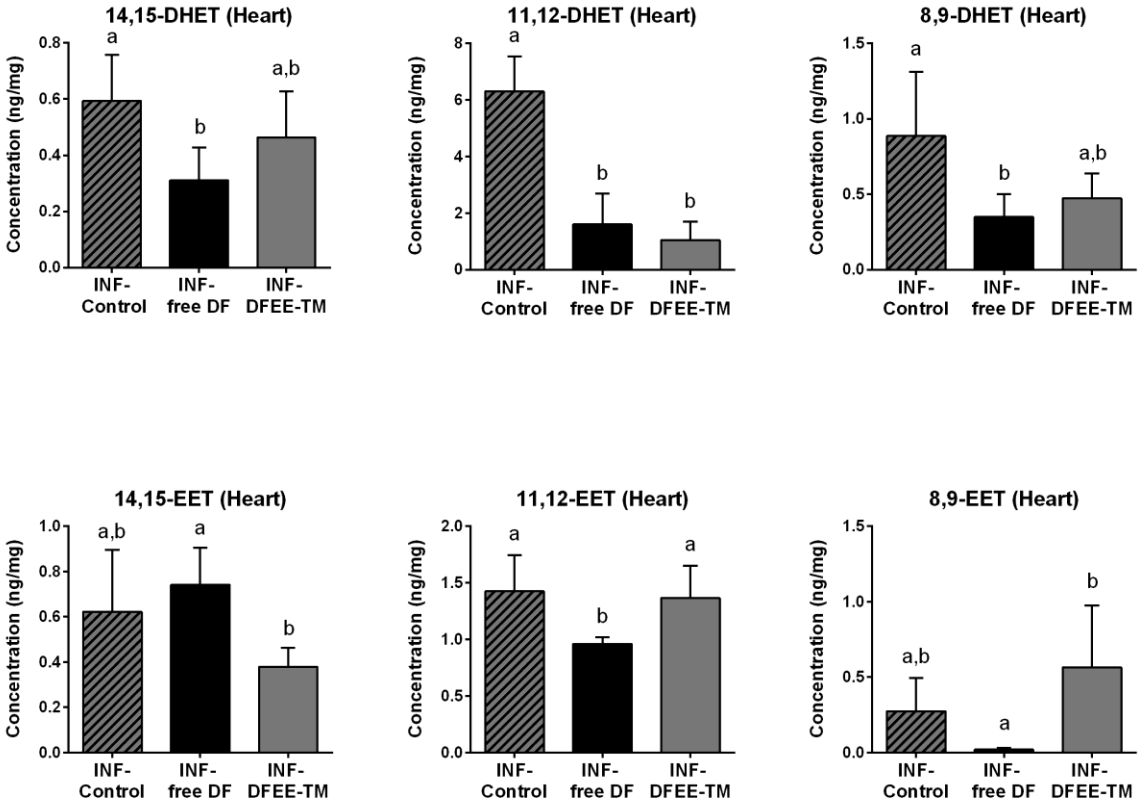

Figure 4-9. Concentrations of CYP 450 metabolites of arachidonic acid (14,15-, 11,12- and 8,9-DHET, 14,15-, 11,12-, and 8,9-EET) in the cardiac tissues of adjuvant arthritis inflamed rats receiving no treatment (INF Control) or treated with free diclofenac (INF free DF), or with the diclofenac ethyl ester traceable micelles (INF DFEE-TM) (n=6/group). Bars sharing the same letter are not significantly different based on one-way ANOVA (α=0.05) with post-hoc Tukey HSD

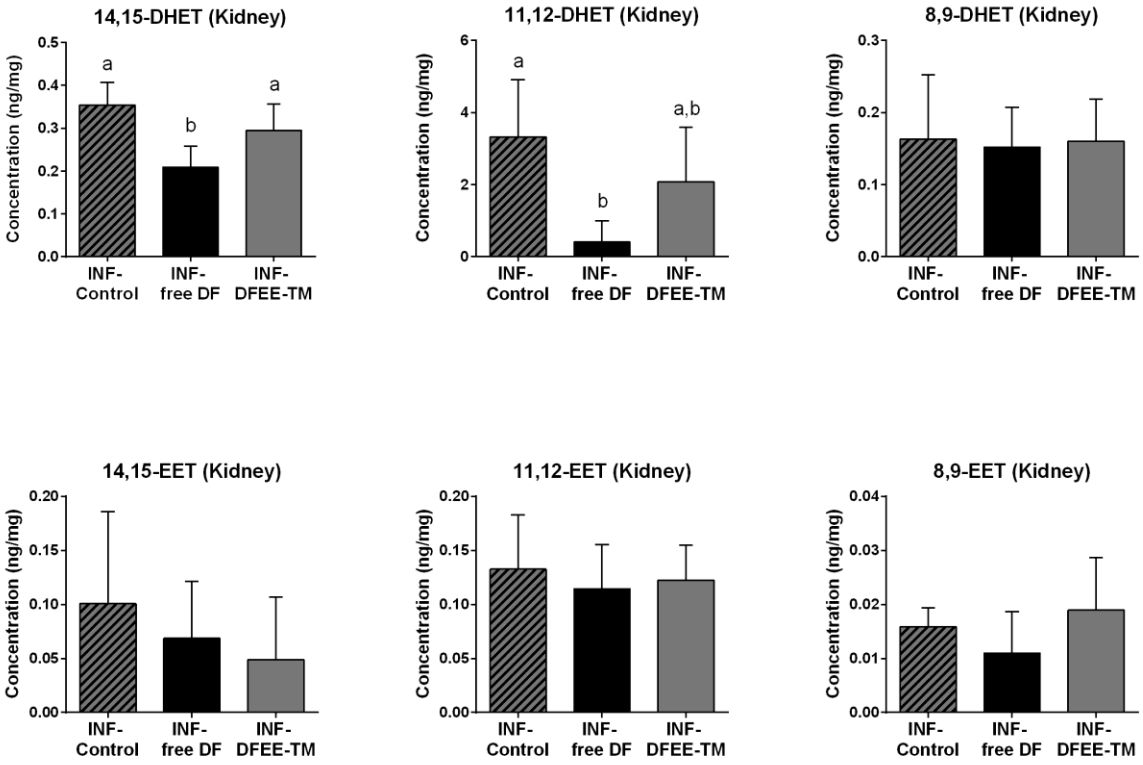

Figure 4-10. Concentrations of CYP 450 metabolites of arachidonic acid (14,15- , 11,12- and 8,9-DHET, 14,15-, 11,12-, and 8,9-EET) in the kidney tissues of adjuvant arthritis inflamed rats receiving no treatment (INF Control) or treated with free diclofenac (INF free DF), or with the diclofenac ethyl ester traceable micelles (INF DFEE-TM) (n=6/group).Bars sharing the same letter are not significantly different based on one-way ANOVA (α=0.05) with post-hoc Tukey HSD.

difference of 20-HETE levels between DFEE-TM and free diclofenac treated rats were not significant.

The total EETs were significantly lower in the plasma and heart tissue of free diclofenac treated rats when compared to the inflamed or the DFEE-TM treated groups (plasma: 5.3±1.7 ng/mL vs 21±13 ng/mL & 20±8.5 ng/mL; heart: 1.5±0.20 ng/mg vs 2.3±0.40 ng/mg & 2.4±0.50 ng/mg, respectively) ($p<0.05$, one-way ANOVA), but not in the kidneys. DFEE-TM, on the other hand, did not cause a reduction in total EETs in the plasma, heart, or kidneys when compared to the untreated inflamed rats.

The ratio of 20-HETE : total EETs was significantly lower in the heart tissues of the DFEE-TM group when compared with the inflamed and the free diclofenac groups (0.18±0.060 vs. 0.33±0.030 & 0.45±0.030, respectively). The ratio was significantly lower in the plasma compared to the free diclofenac (1.8±0.90 vs 22±9.5) ($p<0.05$, one-way ANOVA) but not the inflamed group (9.7±8.2). Free diclofenac on the other hand resulted in a significant increase in this ratio in plasma compared to the inflamed or the DFEE-TM groups ($p<0.05$, one-way ANOVA). In the kidneys, free diclofenac did not significantly alter the ratio of 20-HETE : total EETs when compared to the inflamed untreated group (0.050±0.060 vs. 0.12±0.060). DFEE-TM, on the other hand, showed a 20-HETE : total EETs ratio (0.24±0.10) that was higher compared to both the inflamed untreated and the free diclofenac treated groups ($p<0.05$, one-way ANOVA).

4.2. Discussion

The biodistribution of NSAIDs have been suggested to be an important factor contributing not only to the therapeutic activity of these agents, but also to their well-documented toxicities including gastrointestinal and renal side effects [11, 29-31]. However, to the best of our knowledge, reports which associate the extent of accumulation of NSAIDs of known cardiovascular toxicity, such as diclofenac, in the heart with the magnitude of their cardiovascular risks are lacking in the literature. In the current work we aimed to investigate if: a) the nano-delivery of diclofenac, in the form of polymeric micelles encapsulating DFEE, can improve the disposition of diclofenac in rats with AA, an experimental model of rheumatoid arthritis, redirecting the drug away from heart; b) whether such improvements, if any, will translate to enhanced cardiac safety of diclofenac, and c) if the nanoformulation of diclofenac is still equally as effective in treating inflammation as the free drug. The diclofenac dose of 10 mg/kg/day was used for the pharmacodynamics studies in AA rat model, which yields total exposure to the therapeutic dose in humans of 150 mg daily [32, 33].

Our previous work provided affirmation that DFEE-TM can favorably improve the disposition of diclofenac in healthy rats resulting in prolonged systemic circulation and reduced accumulation of diclofenac in the cardiac tissue [13]. However, as inflammation is known to potentially affect the disposition of various drugs, we investigated the 0-6 h diclofenac blood concentration-time profile following the administration of a single *iv* dose of DFEE-TM in AA diseased rats in comparison to that we previously obtained in healthy rats [13]. The profiles showed comparable diclofenac blood concentration in AA diseased and healthy rats receiving the same doses of DFEE-TM. Moreover, analytical investigation of the major organs (heart, liver, spleen, kidneys) of the same

two groups of rats (Figure 4-2), showed comparable diclofenac accumulation in the organs of the AA diseased and healthy rats, with the exception of the spleen. These results show that AA did not significantly alter the pharmacokinetics of diclofenac delivered by the nano-carrier. This result could be attributed to the low liver extraction efficiency shared by the released diclofenac (extraction ratio of ~ 0.3)[33] and the polymeric nanocarrier. The low liver extraction efficiency of the nanocarrier can be inferred from data obtained previously showing high bioavailability of diclofenac from *ip* dosed DFEE-TM relative to their *iv* dosing in healthy rats [13]. Low liver extraction efficiency was also reported for PEO-*b*-PCL micelles encapsulating other agents [34]. Low liver extraction efficiency can render the clearance to be insensitive to the inhibitory effect of inflammation on CY*P* isozyme activities [35]. The reduced diclofenac concentration in the spleen of the AA diseased rat group may be a result of the reported pathological changes in the spleen and the marked lymphoid atrophy associated with and a consequence of immunological reaction in AA [36].

Ex vivo optical images of the organs of the AA diseased rats also showed levels of fluorescence intensities in different organs that resemble those observed previously in healthy rats [13]. Interestingly, whole body images showed accumulation of traceable nano-carriers in the inflamed paws of AA diseased rats, that were not observed in paws of healthy rats. The observation may be attributed to the enhanced permeability of vasculature feeding the inflamed joints (Figure 4-3). These results are in line with previous reports for the tissue distribution of long-circulating PEO-based nano-carriers and the distribution of the encapsulated drug in the AA disease state compared to that in the healthy sate. For instance, in a study by Metselaar *et al*, whole body scintigraphic images at 4-48 h post-administration of radiolabeled PEO-liposomes encapsulating prednisolone

phosphate showed preferential accumulation of the nanocarrier at inflamed joints of AA rats at much higher levels than what was observed in the joints of healthy rats, while other organs showed comparable distribution in both healthy and AA diseased rats [37].

Following the biodistribution study in the single dose setting, we carried out tissue accumulation investigations of diclofenac released from DFEE-TM in AA diseased rats in comparison to free diclofenac using a multiple dose design with doses given *ip* over a one-week period. The analytical investigation (Figure 4-4) confirmed a reduced diclofenac accumulation in the cardiac tissues due to the DFEE-TM compared to free diclofenac without significantly affecting the concentration in other tissues, and thus corroborated the major benefit of reduced diclofenac heart exposure benefits observed in the single dose study in healthy rats [13].

Having established an altered and a potentially safer diclofenac blood and tissue distribution from the DFEE-TM, we next assessed the anti-inflammatory activity on chronic inflammation and cardiac safety of the micellar formulations of diclofenac compared to free drug using the multiple *ip* dosing study in AA rats. The DFEE-TM resulted in a rapid reduction in the signs and symptoms of AA and was at least as effective as the free diclofenac in controlling the condition, as evidenced by a reduction in AI score and in the percent change in paw diameter relative to base-line (Figure 4-5) compared to untreated control AA rats. Moreover, histopathological assessment (Figure 4-6) showed that both the DFEE-TM and the free diclofenac ameliorated the inflammatory cell infiltration that is observed in inflamed heart and kidney tissues to a comparable degree.

We next investigated the effect of multiple dose administration of DFEE-TM on the expression of CYP metabolites of ArA that are known to act predominately in an autocrine fashion and to

manifest a multitude of biological effects in the cardiovascular system related to the regulation of the vascular tone, renal function, and inflammation [38].

Free diclofenac resulted in an increase in 20-HETE levels by about 53% in plasma when compared to the inflamed untreated group (Figure 4-7 A). This is in accordance with other reports which found treatment with NSAIDs, irrespective of their COX selectivity, to cause an increase in the expression of 20-HETE in plasma of AA diseased rats [4], or in healthy mice [39]. The effect is believed to be due to decreased COX-mediated metabolism of 20-HETE to a less active product [39]. In the case of AA diseased rats, the level of 20-HETE is also affected by the altered levels of ArA due to the inflammatory state itself [4]. Increased 20-HETE levels in plasma have been shown to parallel with increased platelet aggregation and decreased blood clotting time which contribute to cardiovascular disease [39]. DFEE-TM treated rats, on the other hand, exhibited lower levels of 20-HETE in the heart and plasma (Figure 4-7 A-B) to about half of its expression in the inflamed untreated group. This reduction is likely to be a ramification of the altered biodistribution of diclofenac observed with the DFEE-TM resulting in a reduction in the net effect of synthesis and metabolism of 20-HETE. In the heart, 20-HETE has been found to enhance ischemia reperfusion injury in a canine model and its inhibition has been shown to reduce myocardial infarct size [40]. In the kidneys, where both free diclofenac and DFEE-TM showed comparable diclofenac accumulations (Figure 4-7 C), 20-HETE levels showed an increased trend by the two formulations in comparison to the inflamed untreated group, but only DFEE-TM group showed significant increase. 20-HETE in the kidneys has been shown to exert reno-protective effects and to play a regulatory role in the excretion of sodium, the retention of which is an important risk factor for some forms of hypertension [41].

The levels of 14,15-, 11,12-, and 8,9 -EET correlated with each other in plasma, heart, and kidneys, and therefore we considered the total EETs, which is the sum of the levels of the three regioisomers, as a measure of the CYP epoxygenase pathway activity. We observed that rats treated with the free diclofenac exhibited lower total EETs compared to the DFEE-TM treated group or the inflamed untreated control groups in both the plasma and the heart tissues (Figure 4-7 A-B). The DFEE-TM group maintained comparable total EET levels to those seen in the inflamed untreated controls in plasma, heart, and kidneys. EETs have been found to possess cardioprotective activities including vasodilatory, anti-inflammatory, anti-platelet and antiapoptotic effects [42]. In the heart, EETs have been shown to diminish ischemia reperfusion injury and to reduce myocardial infarct size in a canine model [43].

The two pathways of the CYP metabolism of ArA result in opposing effects on the CV system with 20-HETE showing vasoconstrictive effects while the EETs showing vasodilatory effects. As a measure of the influence of the two diclofenac formulations on the balance between these two biomarkers on the CV system, we computed the ratio of 20-HETE : Total EETs, which has been used as a biomarker of cardiotoxicity [4, 44], in plasma, heart, and kidneys. In plasma and heart, the free diclofenac resulted in a higher ratio compared to the inflamed control group indicating an imbalance leaning towards more cardiotoxicity, while the DFEE-TM showed a lower ratio which was significant for the heart tissues. This lower ratio observed in the DFEE-TM group in the heart is very promising especially considering that the actions of these eicosanoids are mainly exerted locally and that it indicates a reduced marker of cardiotoxicity than that attributed to just the inflammatory condition. In the kidney, a higher 20-HETE : Total EETs ratio was seen in the DFEE-TM compared to the other groups which is a reflection of increased 20-HETE level in that

organ rather than an alteration in the total EETs. 20-HETE regulates electrolyte excretion in the proximal tubule and thick ascending loop of Henle and results in a reduction in the risk of some forms of hypertension [41], and thus the higher ratio suggests improved electrolyte excretion in the DFEE-TM group.

4.3. Conclusions

PEO-*b*-PCL based micelles encapsulating DFEE have shown capability in altering the biodistribution of diclofenac in adjuvant arthritic rats resulting in reduced exposure to the myocardium. The micellar formulation, itself, was shown to preferentially accumulate in the inflamed joints of AA rats. The micellar formulation maintained the therapeutic efficacy of diclofenac leading to a rapid resolution of inflammation. Moreover, the micelles of diclofenac showed a reduction in biomarkers of cardiac toxicity for diclofenac. These results point to a strong potential for PEO-*b*-PCL based micelles for equally effective yet safer delivery of diclofenac.

References

1. Peters, M.J., et al., *EULAR evidence-based recommendations for cardiovascular risk management in patients with rheumatoid arthritis and other forms of inflammatory arthritis.* Ann Rheum Dis, 2010. **69**(2): p. 325-31.
2. Wilerson, J.T. and P.M. Ridker, *Willerson, James T., and Paul M. Ridker. "Inflammation as a cardiovascular risk factor.* Circulation 2004. **109**(21): p. II2-10.
3. Asghar, W., A. Aghazadeh-Habashi, and F. Jamali, *Cardiovascular effect of inflammation and nonsteroidal anti-inflammatory drugs on renin-angiotensin system in experimental arthritis.* Inflammopharmacology, 2017.
4. Aghazadeh-Habashi, A., W. Asghar, and F. Jamali, *Drug-Disease Interaction: Effect of Inflammation and Nonsteroidal Anti-inflammatory Drugs on Cytochrome P450 Metabolites of Arachidonic Acid.* J Pharm Sci, 2017.
5. Harirforoosh, S., W. Asghar, and F. Jamali, *Adverse effects of nonsteroidal antiinflammatory drugs: an update of gastrointestinal, cardiovascular and renal complications.* J Pharm Pharm Sci, 2013. **16**(5): p. 821-47.

6. Mukherjee, D., S.E. Nissen, and E.J. Topol, *Risk of cardiovascular events associated with selective COX-2 inhibitors.* JAMA, 2001. **286**(8): p. 954-9.
7. McGettigan, P. and D. Henry, *Cardiovascular risk and inhibition of cyclooxygenase: a systematic review of the observational studies of selective and nonselective inhibitors of cyclooxygenase 2.* JAMA, 2006. **296**(13): p. 1633-44.
8. McGettigan, P. and D. Henry, *Use of non-steroidal anti-inflammatory drugs that elevate cardiovascular risk: an examination of sales and essential medicines lists in low-, middle-, and high-income countries.* PLoS Med, 2013. **10**(2): p. e1001388.
9. Gislason, G.H., et al., *Increased mortality and cardiovascular morbidity associated with use of nonsteroidal anti-inflammatory drugs in chronic heart failure.* Arch Intern Med, 2009. **169**(2): p. 141-9.
10. Garcia Rodriguez, L.A., S. Tacconelli, and P. Patrignani, *Role of dose potency in the prediction of risk of myocardial infarction associated with nonsteroidal anti-inflammatory drugs in the general population.* J Am Coll Cardiol, 2008. **52**(20): p. 1628-36.
11. Harirforoosh, S., A. Aghazadeh-Habashi, and F. Jamali, *Extent of renal effect of cyclo-oxygenase-2-selective inhibitors is pharmacokinetic dependent.* Clin Exp Pharmacol Physiol, 2006. **33**(10): p. 917-24.
12. McGettigan, P. and D. Henry, *Cardiovascular risk with non-steroidal anti-inflammatory drugs: systematic review of population-based controlled observational studies.* PLoS Med, 2011. **8**(9): p. e1001098.
13. Al-Lawati, H., M. R. Vakili, A. Lavasanifar, and F. Jamali, *Delivery and biodistribution of traceable polymeric micellar diclofenac in the rat.* International Journal of Pharmaceutics. (Submitted).
14. Bouchal, R., et al., *Biocompatible Periodic Mesoporous Ionosilica Nanoparticles with Ammonium Walls: Application to Drug Delivery.* ACS Appl Mater Interfaces, 2017. **9**(37): p. 32018-32025.
15. Harirforoosh, S., et al., *Examination of the pharmacodynamics and pharmacokinetics of a diclofenac poly(lactic-co-glycolic) acid nanoparticle formulation in the rat.* Eur Rev Med Pharmacol Sci, 2016. **20**(23): p. 5021-5031.
16. Guterres, S.S., et al., *Poly(rac-lactide) nanocapsules containing diclofenac: protection against muscular damage in rats.* J Biomater Sci Polym Ed, 2000. **11**(12): p. 1347-55.
17. Goh, J.Z., et al., *Evaluation of antinociceptive activity of nanoliposome-encapsulated and free-form diclofenac in rats and mice.* Int J Nanomedicine, 2015. **10**: p. 297-303.
18. Jukanti, R., et al., *Drug targeting to inflammation: studies on antioxidant surface loaded diclofenac liposomes.* Int J Pharm, 2011. **414**(1-2): p. 179-85.
19. Elron-Gross, I., Y. Glucksam, and R. Margalit, *Liposomal dexamethasone-diclofenac combinations for local osteoarthritis treatment.* Int J Pharm, 2009. **376**(1-2): p. 84-91.
20. Turker, S., et al., *Enhanced efficacy of diclofenac sodium-loaded lipogelosome formulation in intra-articular treatment of rheumatoid arthritis.* J Drug Target, 2008. **16**(1): p. 51-7.
21. Asasutjarit, R., et al., *Development and Evaluation of Diclofenac Sodium Loaded-N-Trimethyl Chitosan Nanoparticles for Ophthalmic Use.* AAPS PharmSciTech, 2015. **16**(5): p. 1013-24.

22. Jain, S., et al., *Quality by design approach for formulation, evaluation and statistical optimization of diclofenac-loaded ethosomes via transdermal route.* Pharm Dev Technol, 2015. **20**(4): p. 473-89.
23. Lima, E.M. and A.G. Oliveira, *Tissue tolerance of diclofenac sodium encapsulated in liposomes after intramuscular administration.* Drug Dev Ind Pharm, 2002. **28**(6): p. 673-80.
24. Mahmud, A., X.-B. Xiong, and A. Lavasanifar, *Novel Self Associating Poly(ethylene oxide)-block-poly(ε-caprolactone) Block Copolymers with Functional Side Groups on the Polyester Block for Drug Delivery.* Macromolecules, 2006. **39**(26): p. 9419-9428.
25. Piquette-Miller, M. and F. Jamali, *Influence of severity of inflammation on the disposition kinetics of propranolol enantiomers in ketoprofen-treated and untreated adjuvant arthritis.* Drug Metab Dispos, 1995. **23**(2): p. 240-5.
26. Kaphalia, L., et al., *Efficient high performance liquid chromatograph/ultraviolet method for determination of diclofenac and 4'-hydroxydiclofenac in rat serum.* J Chromatogr B Analyt Technol Biomed Life Sci, 2006. **830**(2): p. 231-7.
27. Al-Lawati, H., et al., *Polymeric Micelles for the Delivery of Diclofenac and Its Ethyl Ester Derivative.* Pharmaceutical Nanotechnology, 2016. **4**(2): p. 109-119.
28. Aghazadeh-Habashi, A., W. Asghar, and F. Jamali, *Simultaneous determination of selected eicosanoids by reversed-phase HPLC method using fluorescence detection and application to rat and human plasma, and rat heart and kidney samples.* J Pharm Biomed Anal, 2015. **110**: p. 12-9.
29. Harirforoosh, S. and F. Jamali, *Effect of inflammation on kidney function and pharmacokinetics of COX-2 selective nonsteroidal anti-inflammatory drugs rofecoxib and meloxicam.* J Appl Toxicol, 2008. **28**(7): p. 829-38.
30. Brune, K., *Persistence of NSAIDs at effect sites and rapid disappearance from side-effect compartments contributes to tolerability.* Curr Med Res Opin, 2007. **23**(12): p. 2985-95.
31. Harirforoosh, S., W. Asghar, and F. Jamali, *Adverse effects of nonsteroidal antiinflammatory drugs: an update of gastrointestinal, cardiovascular and renal complications.* Journal of Pharmacy & Pharmaceutical Sciences, 2014. **16**(5): p. 821-847.
32. Willis, J.V., et al., *The pharmacokinetics of diclofenac sodium following intravenous and oral administration.* Eur J Clin Pharmacol, 1979. **16**(6): p. 405-10.
33. Peris-Ribera, J.E., et al., *Pharmacokinetics and bioavailability of diclofenac in the rat.* J Pharmacokinet Biopharm, 1991. **19**(6): p. 647-65.
34. Binkhathlan, Z., et al., *Development of a polymeric micellar formulation for valspodar and assessment of its pharmacokinetics in rat.* Eur J Pharm Biopharm, 2010. **75**(2): p. 90-5.
35. Guirguis, M.S., S. Sattari, and F. Jamali, *Pharmacokinetics of celecoxib in the presence and absence of interferon-induced acute inflammation in the rat: application of a novel HPLC assay.* J Pharm Pharm Sci, 2001. **4**(1): p. 1-6.
36. Engelhardt, G., *Pharmacology of meloxicam, a new non-steroidal anti-inflammatory drug with an improved safety profile through preferential inhibition of COX-2.* Br J Rheumatol, 1996. **35 Suppl 1**: p. 4-12.
37. Metselaar, J.M., et al., *Complete remission of experimental arthritis by joint targeting of glucocorticoids with long-circulating liposomes.* Arthritis Rheum, 2003. **48**(7): p. 2059-66.

38. Roman, R.J., *P-450 metabolites of arachidonic acid in the control of cardiovascular function.* Physiol Rev, 2002. **82**(1): p. 131-85.
39. Liu, J.Y., et al., *Metabolic profiling of murine plasma reveals an unexpected biomarker in rofecoxib-mediated cardiovascular events.* Proc Natl Acad Sci U S A, 2010. **107**(39): p. 17017-22.
40. Nithipatikom, K., et al., *Effects of selective inhibition of cytochrome P-450 omega-hydroxylases and ischemic preconditioning in myocardial protection.* Am J Physiol Heart Circ Physiol, 2006. **290**(2): p. H500-5.
41. Williams, J.M., et al., *20-hydroxyeicosatetraeonic acid: a new target for the treatment of hypertension.* J Cardiovasc Pharmacol, 2010. **56**(4): p. 336-44.
42. Imig, J.D., *Epoxides and soluble epoxide hydrolase in cardiovascular physiology.* Physiol Rev, 2012. **92**(1): p. 101-30.
43. Nithipatikom, K., et al., *Epoxyeicosatrienoic acids in cardioprotection: ischemic versus reperfusion injury.* Am J Physiol Heart Circ Physiol, 2006. **291**(2): p. H537-42.
44. Theken, K.N., et al., *Activation of the acute inflammatory response alters cytochrome P450 expression and eicosanoid metabolism.* Drug Metab Dispos, 2011. **39**(1): p. 22-9.

Chapter 5: General discussion, conclusions, and future directions

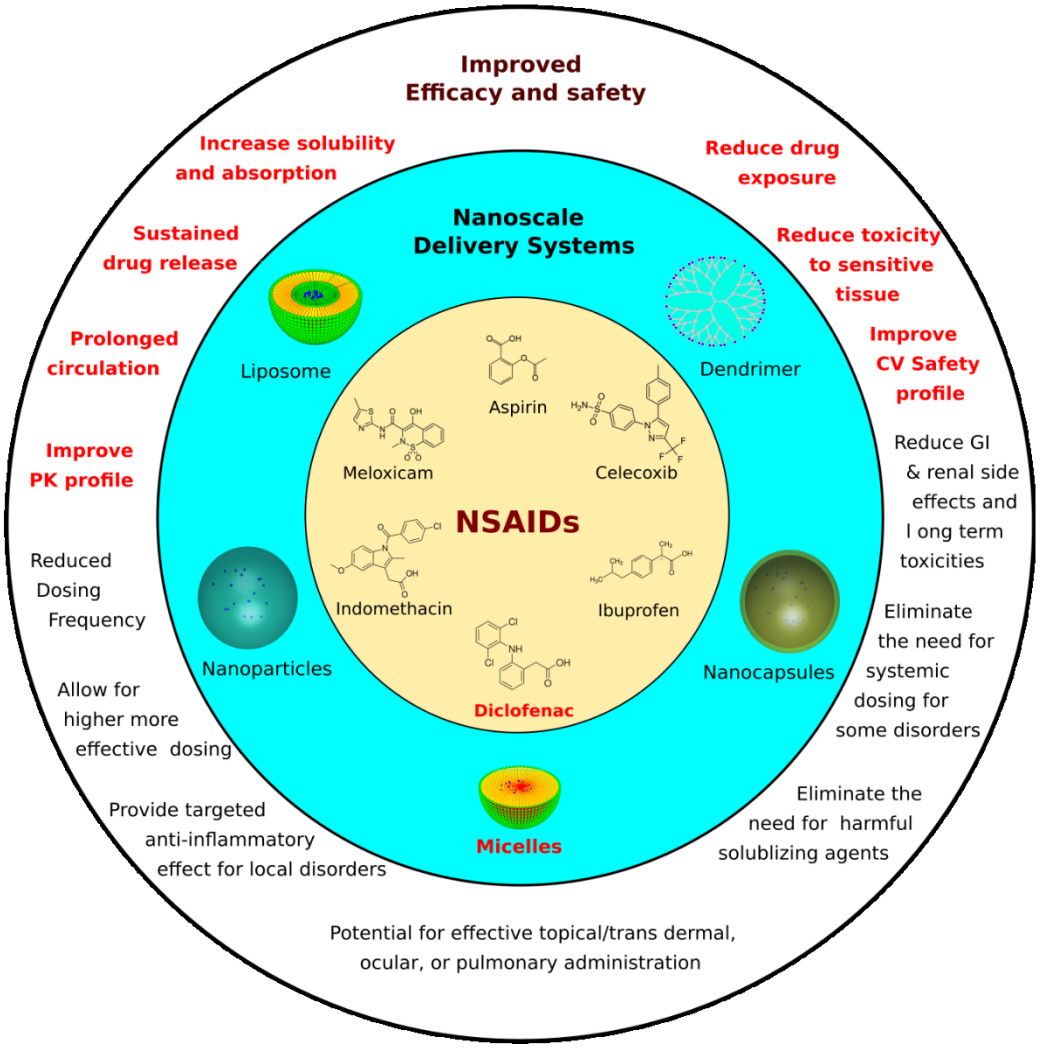

5.1. General Discussion

Conventional drug delivery methods present clinical challenges mainly because they tend to distribute the active drug molecules in the entire body and not only to the sites where the drug action is needed, thus can lead to serious side-effects [1]. This is true for most of the marketed non-steroidal anti-inflammatory drugs (NSAIDs), which are among the most widely used medications in the world [2]. The use of NSAIDs has been associated with adverse GI and renal side effects as well as an increased risk of cardiovascular (CV) events including myocardial infarction and stroke [3]. The extent of the CV risk is believed to be dose-dependent and linked to the extent of their accumulation in the heart and other tissues affecting the CV system [4, 5]. Therefore, we set to investigate the influence of the exposure of cardiac tissue to NSAIDs in causing CV effects. This was achieved by altering the distribution of a cardiotoxic NSAID in the heart tissue.

Theoretically, nanomedicine-based drug delivery systems have the potential to alter the biodistribution of drugs allowing for therapeutic concentrations at the desired sites and reducing the exposure at the sites of toxicities [6, 7]. However, following a systematic search of the scientific literature, we found no reports that investigated the use of nanodelivery system with NSAIDs for inflammatory conditions and showed evidence of reduced CV toxicity or exposure in the heart (Chapter 1). Therefore, in this project we undertook the task of designing optimal polymeric micellar formulations for diclofenac, a model NSAIDs with high CV toxicity, and used them to test the hypothesis that ‘reduced NSAID exposure to the heart improves its CV profile’.

In the initial objective of research, we developed several polymeric micellar formulations for diclofenac and its more hydrophobic derivative, diclofenac ethyl ester (DFEE), based on PEO as a shell block and various poly(ester) as core blocks. Overall, we observed that micellar formulations for the more hydrophobic DFEE illustrated more favorable properties especially the *in vitro* release characteristics. Furthermore, the stability of DFEE formulations in PEO-*b*-PCL or PEO-*b*-PDLLA 50:50 micelles investigated in fresh rat plasma showed a great potential for these formulations in changing the normal pharmacokinetics and biodistribution of the loaded DFEE and its active metabolite diclofenac (Chapter 2) [8]. The parent drug diclofenac was exclusively detected illustrating a rapid hydrolysis of the ester prodrug.

In the following objective, we designed traceable (Cyanine 5.5 labeled), DFEE loaded polymeric micelles based on PEO-*b*-PCL or on PEO-*b*-PBCL at identical degrees of polymerization in the core blocks and investigated their pharmacokinetics and biodistribution in healthy rats. We found that, in contrary to free diclofenac, the *iv* administration of both micellar formulations presented PK profiles that resemble longer systemic circulation and a sustained release of diclofenac corroborating what was observed in the *in vitro* release profiles. Moreover, the two micellar formulations similarly and comparably reduced diclofenac partition in the heart and kidneys, measured at 6 h post dose, compared to free diclofenac. When compared to each other, the PEO-*b*-PBCL further reduced the diclofenac accumulation in the heart at 24 h post-dose. Diclofenac delivery by traceable PEO-*b*-PCL micelles showed high *ip* bioavailability and improved biodistribution of diclofenac. In particular, both *ip.* and *iv* administration of the traceable micelles resulted in comparable fluorescence intensities at 6-h post-dose. Both micelles showed strong

potential for a cardiac-safe delivery of diclofenac and so it was decided to test the efficacy and safety of one of the formulations in an appropriate animal model.

Having established that DFEE encapsulating polymeric micelles based on PEO-*b*-PCL alter the biodistribution of diclofenac in healthy rats, in the following objective we tested our main hypothesis that 'reduced heart exposure to NSAIDs improves CV safety profile'. More specifically, we considered assessing their biodistribution, efficacy, and cardiac safety in the adjuvant arthritis model in rats, which is an experimental model that shares resemblance with rheumatoid arthritis in humans [9]. First, using a single *iv* dosing strategy, we could confirm that the polymeric micelles resulted in a comparable diclofenac circulation kinetics and biodistribution to that observed in healthy rats. Following that, multiple *ip* dosing studies were used over seven days of treatment. The tissue distribution assessment revealed that the diclofenac tissue accumulation was significantly lower in the heart following the administration of the polymeric micelles compared to that from the free diclofenac. In terms of efficacy, the micelles resulted in a rapid reduction in the signs and symptoms of the disease comparable to the free drug. Moreover, histopathological assessment showed that the micelles as well as the free drug ameliorated the inflammatory cell infiltration that was observed in the heart and kidney tissues of inflamed rats. As a measure of cardiotoxicity, on the other hand, the polymeric micelle formulation showed signs of decreased toxicity compared to the free drug as evidenced by a reduction in the ratio of cardiotoxic over cardioprotective eicosanoids of ArA in heart and plasma of AA rats. This remarkable result and the collective work show a strong potential for PEO-*b*-PCL based micelles in the cardiac-safe delivery of diclofenac, and possibly other NSAIDs, in inflammation.

The research project provides several contributions to the scientific literature in the related fields. The diclofenac formulation developed and optimized here (Chapter 2) combines the two approaches of using an ethyl ester derivative of the active NSAID agent together with the use of a nanodelivery system that has proven to be effective. While this combination has been considered for some other NSAIDs in the past [10], our work presents the first evidence where the combination has been found to improve the pharmacokinetics and tissue distribution of the parent NSAID in a healthy animal model. The comparative pharmacokinetics and biodistribution studies of the two traceable micellar formulations of diclofenac as well as the free drug has not been investigated in the past and provide the first effort in encapsulating an NSAID agent in PEO-*b*-PBCL based micelles. The main novelty of our work, however, stems from the fact that, to our knowledge, it is the first report to confirm that altering the biodistribution of an NSAID agent that is found clinically to be highly cardiotoxic at the therapeutic dose to reduce its accumulation in the heart can provide evidence of improved CV profile.

5.2. General conclusions

Extensive research has been carried out on the nano-delivery of NSAIDs and the therapeutic advantages that these new advanced delivery systems bring about when compared to the conventional delivery of the same agents. However, the existing published reports which review these advantages tend to focus more on the role of these NSAID loaded nano-carriers in the prevention or treatment of different types of cancer and less on other conditions such as inflammatory arthritic conditions. We undertook the task of conducting a systematic review of all relevant reports with empirical evidence on the use of nano-delivery systems of NSAIDs for the management of inflammation or arthritis. The results revealed various therapeutic benefits

achieved with the nanodelivery of these agents, including improving their efficacy and potency, improving their PK and biodistribution reducing the associated GI and renal side effects, and providing alternative routes to systemic delivery for local control of inflammation, among other benefits. However, there was a lack of investigations which link the improvements in the PK and biodistribution achieved through the nano-delivery of NSAIDs, with reduction in the CV toxicity that associates these agents. This report aims to fill in some of this gap.

In the first step, we developed and optimized micellar formulations of cardiotoxic diclofenac based on PEO-*b*-Poly(esters) where we varied the core-structure composition and varied several preparation parameters. Micelles encapsulating DFEE showed slower and more favorable *in vitro* release profiles, while those based on PCL or PBCL as a core-block proved to be optimal. PEO-*b*-PCL and PEO-*b*-PBCL based micelles were found to possess desirable characteristics including small size (≈ 40 nm) and spherical morphology which are believed to reduce their uptake by the reticuloendothelial system and promote longer systemic circulation [11]. The *in vivo* delivery of both formulations, given as single *iv* or *ip* doses to healthy rats, was very encouraging as it resulted in improved biodistribution of diclofenac revealing prolonged systemic circulation and a substantial reduction of its accumulation in the heart and kidneys, both being sites of toxicities of NSAIDs. Next, we investigated the efficacy and safety of the PEO-*b*-PCL based micelle formulation using a multiple dose study in rats with adjuvant arthritis, an experimental model of chronic arthritis that resembles RA in humans. The results showed that the micelles were effective in the management of inflammation. In terms of cardiac safety, the results revealed that while the conventional delivery of diclofenac negatively altered the balance between the metabolites of ArA in favor of a more cardiotoxic state, the micelles could reduce the levels of a cardiotoxic product

of ArA, i.e. 20-hydroxyeicosatetraenoic acid, both in plasma and heart and consequently could improve the balance in the metabolites in the two biological matrices when compared to the inflamed untreated group. These results, especially in relation to the heart, are very promising since the actions of these products are known to be exerted locally [12]. This biomarker study gave first evidence in support of the hypotheses.

5.3. Future directions

Through the various studies conducted in this report, we could provide promising evidence in support of our hypothesis that "*reduced NSAIDs exposure to the heart, improves their CV safety profile*". The evidence in support of the improved safety relied on measuring biomarkers of the CV safety/toxicity in the heart, plasma and kidneys. In future work, we hope to supplement the current evidence with a direct test of the CV effect of NSAIDs, e.g. through an echocardiographic evaluation of cardiac function in an experimental model of arthritis.

The single dose biodistribution studies as well as the multiple dose efficacy and cardiovascular safety studies were carrier out in the rat. There are differences between species in the cytochrome P450 (CYP) enzyme expression and metabolism in the different tissues, with higher degree of homology being found between humans and rats than with mice [13]. Therefore, in a future work we can consider investigation of the micellar formulation other species. Moreover, we considered diclofenac as a model study agent representing most NSAIDs, due to its high CV toxicity profile and the fact that there are no known non-class mechanisms that can affect its CV risk, such as the case with celecoxib [14]. It would be desirable to conduct the study on other NSAIDs to see if the

results translate to these agents as well and provide further evidence that nanodelivery is beneficial to the CV safety of NSAIDs therapy. Future work can address this.

The main routes of drug administration that we considered in the *in vivo* studies for the administration of the diclofenac polymeric micelles which encapsulated DFEE were the intravenous and the intraperitoneal routes. These routes have been studied more extensively than the oral route for the delivery of micellar formulation based on PEO-*b*-PCL [7, 15]. In this report, we only did a preliminary biodistribution study of the PEO-*b*-PCL based micelles that were administered by oral gavage. It is not clear if the micelles were able to pass the intestinal barrier as intact nanocarrier or not. Future work is needed to explore this and consider ways to improve micelle absorption from the GI tract.

References

1. Conte, C., et al., *Polymeric Nanoparticles for Cancer Photodynamic Therapy.* Top Curr Chem, 2016. **370**: p. 61-112.
2. Hart, F.D. and E.C. Huskisson, *Non-steroidal anti-inflammatory drugs. Current status and rational therapeutic use.* Drugs, 1984. **27**(3): p. 232-55.
3. Harirforoosh, S., W. Asghar, and F. Jamali, *Adverse effects of nonsteroidal antiinflammatory drugs: an update of gastrointestinal, cardiovascular and renal complications.* J Pharm Pharm Sci, 2013. **16**(5): p. 821-47.
4. Pepine, C.J. and P.A. Gurbel, *Cardiovascular safety of NSAIDs: Additional insights after PRECISION and point of view.* Clin Cardiol, 2017. **40**(12): p. 1352-1356.
5. Aghazadeh-Habashi, A., W. Asghar, and F. Jamali, *Drug-Disease Interaction: Effect of Inflammation and Nonsteroidal Anti-inflammatory Drugs on Cytochrome P450 Metabolites of Arachidonic Acid.* J Pharm Sci, 2017.
6. Al-Lawati, H., et al., *Nanomedicine for immunosuppressive therapy: achievements in pre-clinical and clinical research.* Expert Opin Drug Deliv, 2018: p. 1-22.
7. Aliabadi, H.M. and A. Lavasanifar, *Polymeric micelles for drug delivery.* Expert Opin Drug Deliv, 2006. **3**(1): p. 139-62.
8. Al Lawati, H., et al., *Polymeric micelles for the delivery of diclofenac and its ethyl ester derivative.* Pharmaceutical Nanotechnology, 2016. **4**(2): p. 109-119.
9. van Eden, W., J.P. Wagenaar-Hilbers, and M.H. Wauben, *Adjuvant arthritis in the rat.* Curr Protoc Immunol, 2001. Chapter 15: p. Unit 15 4.
10. Cattani, V.B., A.R. Pohlmann, and T. Dalla Costa, *Pharmacokinetic evaluation of indomethacin ethyl ester-loaded nanoencapsules.* Int J Pharm, 2008. **363**(1-2): p. 214-6.
11. Al-Lawati, H., et al., *Polymeric Micelles for the Delivery of Diclofenac and Its Ethyl Ester Derivative.* Pharmaceutical Nanotechnology, 2016. **4**(2): p. 109-119.
12. Imig, J.D., *Epoxides and soluble epoxide hydrolase in cardiovascular physiology.* Physiol Rev, 2012. **92**(1): p. 101-30.
13. Pasanen, M., *Species differences in CYP enzymes.* Monografías de la Real Academia Nacional de Farmacia, 2004.
14. Brueggemann, L.I., et al., *Novel Actions of Nonsteroidal Anti-Inflammatory Drugs on Vascular Ion Channels: Accounting for Cardiovascular Side Effects and Identifying New Therapeutic Applications.* Mol Cell Pharmacol, 2010. **2**(1): p. 15-19.
15. Binkhathlan, Z., et al., *Development of a polymeric micellar formulation for valspodar and assessment of its pharmacokinetics in rat.* Eur J Pharm Biopharm, 2010. **75**(2): p. 90-5.

Supplement 1: Preliminary investigations of the oral delivery of traceable polymeric micelles based on PEO-*b*-PCL

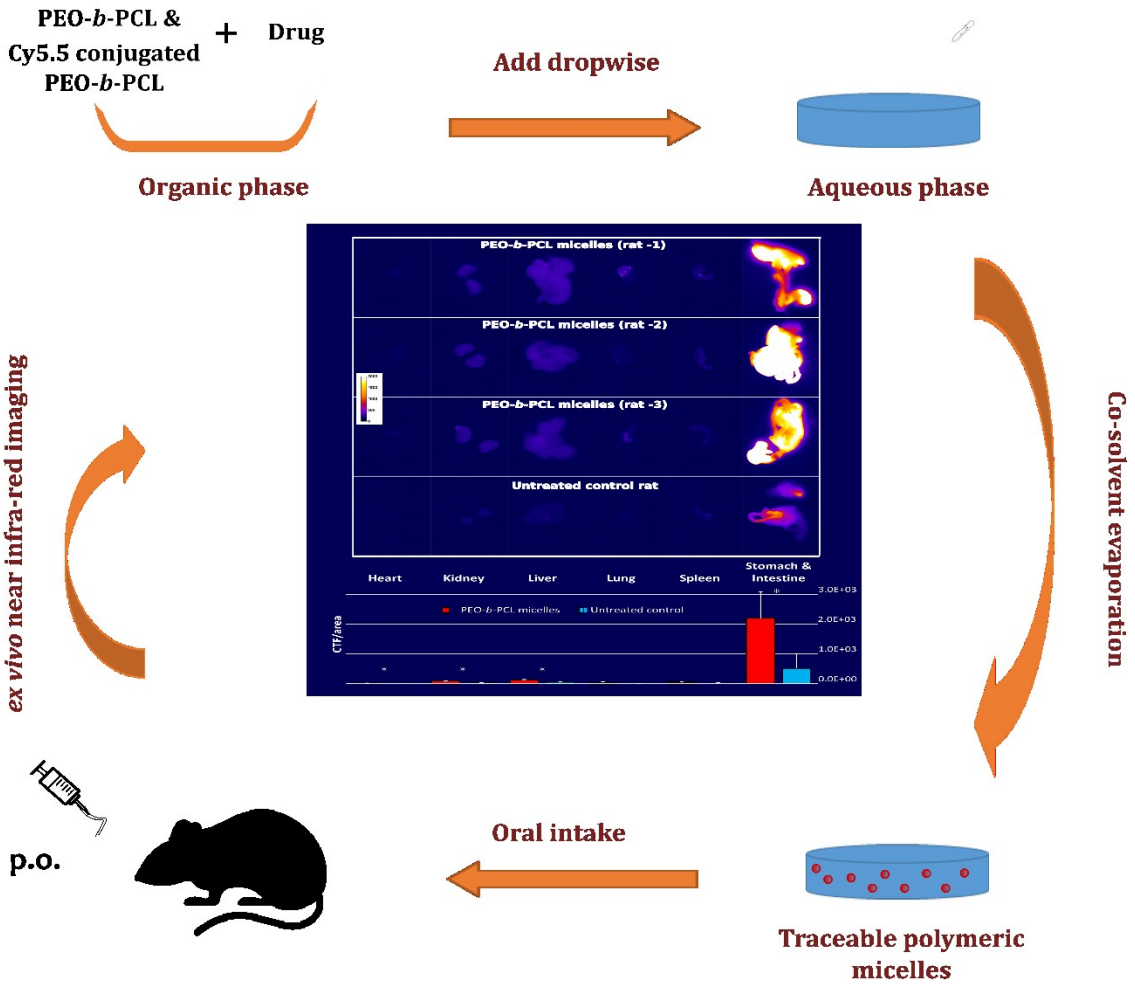

---

*A version of this supplement chapter is part of a manuscript to be submitted for publication:

Binkhathlan Z., Ali R., Qamar W., Al-Lawati H., and Lavasanifar A. Pharmacokinetic and Tissue Distribution Study of Orally administered Cyclosporine A-Loaded Poly(Ethylene Oxide)-block-Poly(ε-Caprolactone) Micelles Versus Sandimmune® in Rats (in preparation).

S1.1. Introduction

Polymeric micelles have been investigated extensively not only for their role in solubilizing poorly water-soluble drugs and bioactive agents, but also as effective nanocarriers for the targeted drug delivery [1]. However, most of the systemic polymeric micellar formulations that have been developed, including those currently in the clinical trials, are designed for intravenous administration [2, 3]. While intravenous administration may be sensible for many drugs and may carry numerous advantages, it presents substantial discomfort for delivery of NSAIDs owing to their chronic use. The administration of nano-formulations of NSAIDs through non-parenteral routes, are thus desired.

Here we investigated the potential of polymeric micellar formulations of DFEE in oral delivery of diclofenac to blood circulation as an encapsulated entity. The performance of polymeric micelles as an oral delivery system has not been evaluated, adequately. The oral administration of micelles can challenge the stability of these nano-formulations and their intact absorption through the GI tract.

S1.2. Material and methods

S1.2.1. Materials

Simulated gastric and intestinal fluids (SGF & SIF) were purchased from Biorelevant.com Ltd (London, UK) and prepared as per the provided instructions. Dialysis bags (Spectra Por S/P 2 12,000-14,000 kD - 45 mm) were purchased from Cole-Parmer Canada (Montreal, QC, Canada). The chemicals related to synthesis of the copolymers and formulation of the micelles are described

in Chapter 3. All other chemicals and reagents were of analytical grade and were used without any further purification.

S1.2.2. Synthesis and characterization of Cy5.5-conjugated PEO-*b*-PCL copolymers

Previously reported method was employed for synthesis of PEO-*b*-PCL block copolymer [4, 5]. Briefly, methoxy PEO (MW 5,000 g/mol; 5 g), ε-caprolactone (13 g) and stannous octoate (0.2% w/w) were added to a previously flamed ampoule, nitrogen purged, then sealed under vacuum. The reaction proceeded at 140 °C for 4 h. ^{1}H NMR spectrum of PEO-*b*-PCL in $CDCl_3$ at 500 MHz (Bruker Ultra shield 500.133 MHz spectrometer) was used to determine the number average molecular weight of the block copolymer. The degree of polymerization of ε-caprolactone was estimated by comparing the peak intensity of PEO (–O–CH_2–CH_2; δ =3.65 ppm) to that of PCL (–O–CH_2; δ =4.075 ppm).

Synthesized PEO-*b*-PCL (MW 5,000:12,500 g/mol) was end-capped with α-propargyl carboxylate-ε-caprolactone (PCC) using stannous octoate as catalyst as previously reported in chapter 3 and in reference [6] with slight modification. Briefly, 100 mg of PEO-*b*-PCL and 15 mg of PCC were mixed with 5 mL of dry toluene under constant stirring in a round-bottom flask. Stannous octoate (10 drops) was added as a catalyst to the flask and the contents were refluxed for 48 h. The mixture was cooled down to room temperature to terminate the reaction and then precipitated in hexane with the supernatant being discarded. This was followed by washing with ether and drying under vacuum.

The PCC attachment was confirmed by a ^{1}H-NMR spectrum that was obtained on a Bruker Avance III spectrometer (Bruker BioSpin Corporation, Billerica, MA) (600 MHz) using $CDCl_3$ as a

solvent. The number average molecular weight of PEO-*b*-PCL-PCC was determined by measuring the relative peak intensity of PCL (–O–CH2–, $\delta = 4.05$ ppm) and those of PCC (–O–CH_2; $\delta = 4.75$ ppm) to that of PEO (–CH_2–CH_2–O; $\delta = 3.65$ ppm) which is used as a reference, as the number-average molecular weight of PEO is known (5000 g/mol).

The near-infrared fluorophore Cy5.5-azide was conjugated to the terminal alkyne of PCC using a Cu(I)-catalyzed terminal azide-alkyne click chemistry reaction as reported [6]. Briefly, 10 μmol of PEO-*b*-PCL-PCC was dissolved in 2 mL of degassed DMSO with constant stirring in a round-bottom flask. Cy5.5-azide (0.7 mg) in 400 μL of DMSO was added to the mixture followed by ascorbic acid (0.1 mg) in 100 μL water with constant stirring. The solution was then degassed with argon for 30 s followed by the addition of 60 μL of Cu-TBTA Complex, 10 mM, and then degassing the mixture for 30 s using argon. The mixture was sealed and allowed to react under stirring in the dark at room temperature. After 16 h of incubation with stirring, the mixture was purified by dialysis against DMSO for 24 h followed by dialysis against water for 24 h. The conjugation efficiency of Cy5.5 to PEO-*b*-PCL-PCC was determined by fluorescence spectrophotometer using a SpectraMax M4 microplate reader (Molecular Devices, Sunnyvale, CA), measuring the excitation at 673 nm and emission at 707 nm as described by the manufacturer.

S1.2.3. *In vitro* release of Cy5.5 dye from micelles in simulated gastric and intestinal fluids

In order to predict the fate of the PEO-*b*-PCL based micellar formulation *in vivo* upon oral administration, mixed drug-free micelles based on PEO-*b*-PCL (99 wt. %) and PEO-*b*-PCL-PCC-Cy5.5 azide (1 wt %) were prepared as described in Chapter 3 and the *in vitro* release of Cy5.5 was investigated in SIF and SGF using the dialysis bag method. Briefly, a dialysis bag (MWCO:

12-14 kD) containing 1 mL of the micellar solution was incubated in 40 mL of the release medium (SGF or SIF) at 37° C under mild agitation in a Julabo SW 22 water bath (Seelbach, Germany). Samples from the recipient compartment were withdrawn at predetermined time intervals and the incubation solution was replaced by fresh release medium. The samples (100 μL) were analyzed by fluorescence spectroscopy with the intensity of light emitted at 707 nm after excitation at 673 nm being measured at 25°C using a fluorescence spectrophotometer. The cumulative profile of the detected dye at each time point was calculated. Each experiment was performed in triplicate.

S1.2.4. *Ex vivo* near infra-red (NIR) imaging

The animal study was carried out in accordance with the guidelines of the Canadian Council on Animal Care and based on protocols approved by the Health Sciences Animal Care and Use Committee, University of Alberta. Healthy male Sprague-Dawley rats (230-250 g) were obtained from the Health Sciences Laboratory Animal Services, University of Alberta, and were housed in a temperature-controlled room with a 12 h light/dark cycle and were given free access to water and food, which consisted of low chlorophyll maintenance diet (2014 S Teklad Global 14% protein rodent maintenance diet, Harlan Labs, Indianapolis, IN) to minimize fluorescence from food.

Traceable micelles based on the PEO-*b*-PCL (99 wt. %) and PEO-*b*-PCL-PCC-Cy5.5 azide (1 wt %) were prepared as described in Chapter 3. The biodistribution of the nanocarrier following a single oral dose of either of these polymeric micelles (100 mg/kg of copolymer) was investigated in healthy Sprague Dawley rats at 6 h following administration by oral gavage.

At the end of the study, the rats were euthanized using isoflurane/oxygen mixture (0.75 / 2 %) and their organs including heart, kidney, liver, and spleen were removed, washed in ice-cold saline,

and blotted with paper towel to remove excess fluid. *Ex vivo* near-infrared fluorescence images of the excised organs were obtained using a Kodak imaging station 4000M (Eastman Kodak, New Haven, CT). The fluorescence intensities in the organs were measured using the image processing software ImageJ (v 1.51n, National Institutes of Health, USA). The total corrected intensities for the organs in the images were calculated by correcting the integrated densities for background readings as follows:

Corrected total fluorescence (CTF) intensity = integrated density in selected organ –

(area of selected organ × mean background fluorescence reading).

The CTF intensities of the organs were compared to those in the corresponding organs in the control untreated group.

S1.3. Results and discussion

S1.3.1. Stability of Cy5.5-conjugated PEO-*b*-PCL micelles in SGF and SIF

The *in vitro* release of the fluorophore cy5.5, as measured by its fluorescence intensity, from the cy5.5-conjugated PEO-*b*-PCL based micelles upon dialysis in SIF and SGF is presented in Figure S1-1. This release indicates the level of dye detachment and release as a result of micelle degradation or dissociation. The profile in SIF presents an initial burst release of the dye in the first five minutes of the dialysis process amounting to the release of about 5% of the total dye in the micellar formulation. This is followed by a slow release throughout the remainder of the study showing the cumulative release of only 7.6% of the attached cy5.5 during the 6 h of analysis and indicating a good stability of the micelles in SIF.

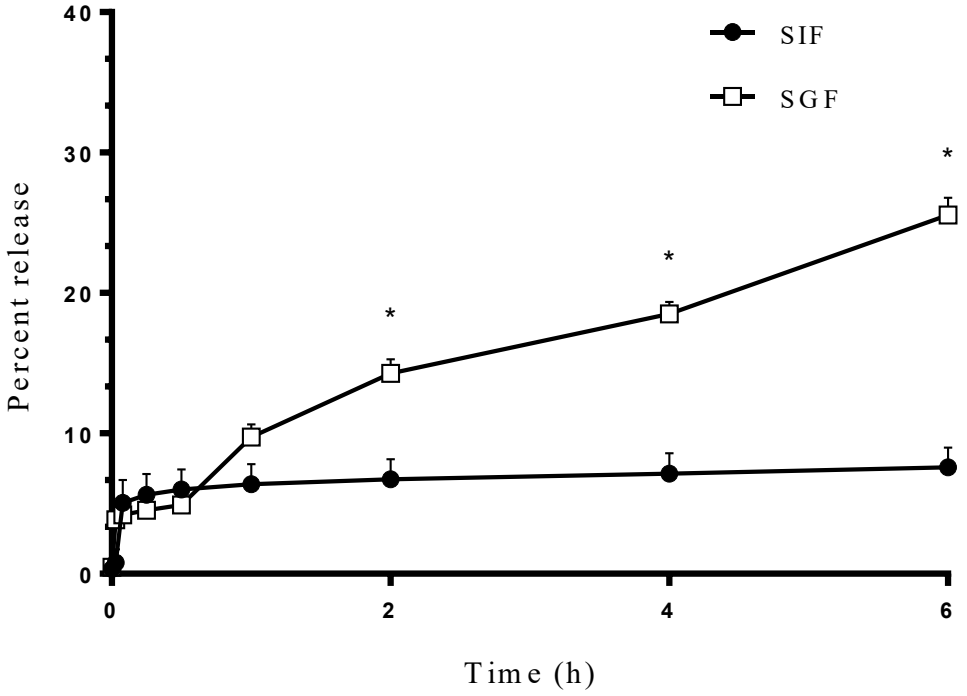

Figure S1-1 The *in vitro* percent release of Cy5.5 from the unloaded PEO-*b*-PCL based traceable micelles dialyzed in SIF and SGF as a measure of micelle dissociation and hydrolysis of the unimors. Each data point represents mean ± SD (n=3). An asterisk indicates significant difference between the two groups at the time point ($p<0.05$, Student's t-test).

In a similar manner, the corresponding dye release profile in SGF also reveals a rapid release in the first five minutes showing the release of about 4.2% of the total dye in this period. However, starting at 1 h following start of the dialysis processes, a higher rate of dye release is observed in SGF, indicating higher rate of micelle dissociation and/orunimer hydrolysis, compared to the release in SIF. The difference between the two release profiles is statistically significant at times 2, 4, and 6 h ($p<0.05$, Student's t-test). The cumulative release in SGF at 6 h totals 25.6% of the total dye.

S1.3.2. *Ex vivo* near infra-red (NIR) imaging

Near infrared optical images of rats' organs dissected at 6 h following an oral dose of the cy5.5 conjugated PEO-*b*-PCL micelles and those of a representative rat from the untreated control group are presented in Figure S1-2. The figure also contains a bar plot of the CTF intensities per unit area in the different organs in the micellar treated and untreated groups. The plots give an indication that the micelles and/or dissociated labeled unimers were absorbed across the GI tract to some extent, as significantly higher intensities were observed in the heart, kidneys, liver, and stomach and intestine of rats treated with the micellar formulation compared to the control group ($p<0.05$, Student's t-test). However, in comparison to the stomach and intestine, the intensities in the other organs are relatively dull indicating a higher proportion of the micelles remained in the GI tract.

Moreover, it appears that a smaller fraction of the micelles or unimors reach the different organs when given orally compared to their parenteral (intravenous or intraperitoneal) administration (See

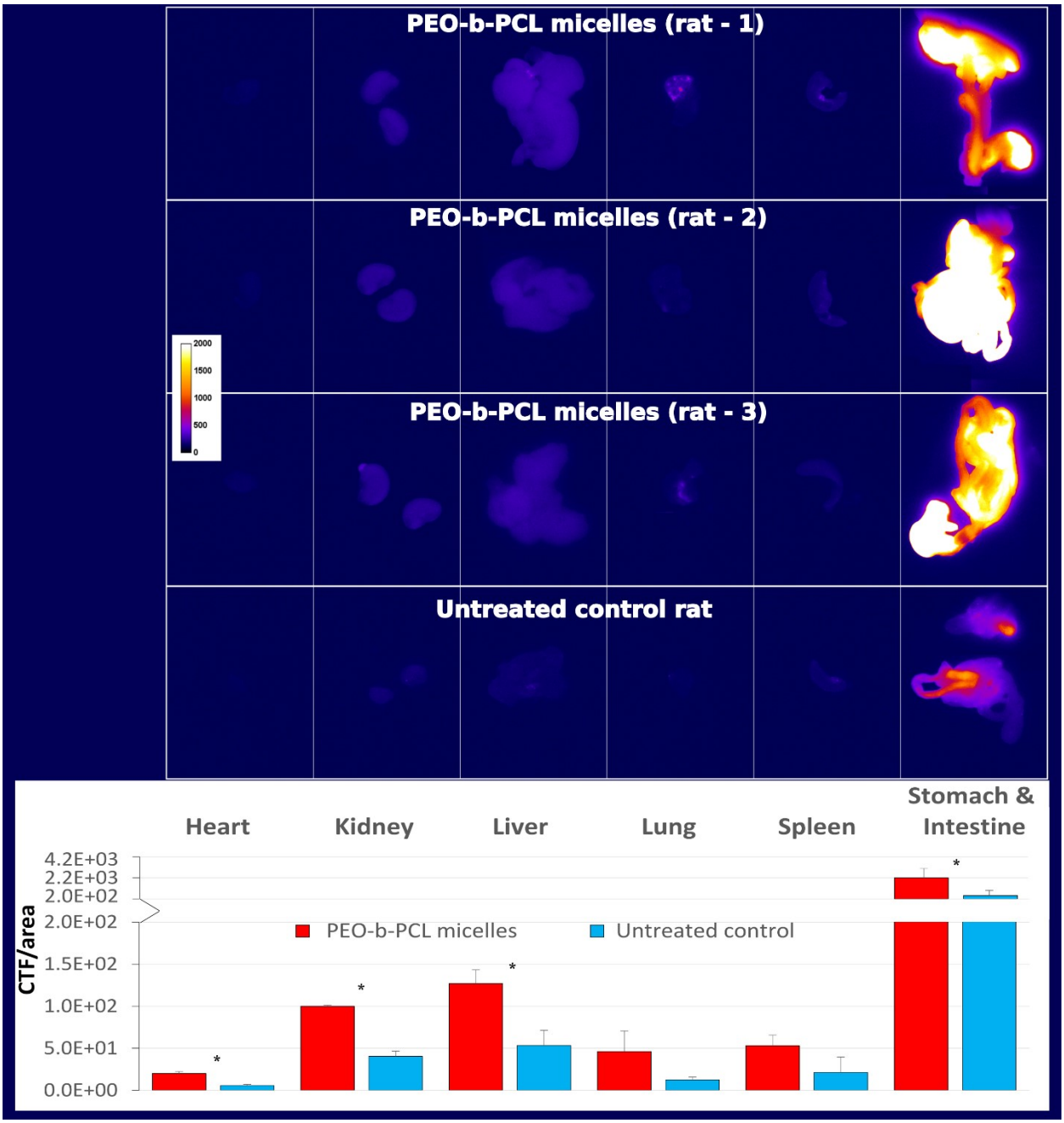

Figure S1-2. ***Ex vivo*** **Near-infrared optical images of the major organs of rats treated with the PEO-*b*-PCL based micelles (n=3) and a representative rat from the untreated control group and a bar graph of the corrected fluorescence intensities (CTF) per unit area in the organs (mean ± SD) at 6 h post-dose. An asterisk indicates significant different between the two group ($p<0.05$, unpaired Student's t-test).**

Chapter 3). These results appear to be in accordance to what was observed in a previous study which investigated the pharmacokinetics of PEO-*b*-PCL based micelles encapsulating valspodar, an experimental multidrug resistance-reversing agent in cancer therapy [7]. The study revealed that while intravenously given micellar valsdpoar showed favorable PK profile compared to the free drugs, the oral administration showed comparable PK parameters for both the micellar and the free drug formulations.

S1.4. Conclusions

The micelles showed good stability and release profiles in GI relevant conditions. Moreover, based on the *ex vivo* imaging data, it appears that the PEO-*b*-PCL micelles, when given orally, serve mainly as solubilizing vehicles for the encapsulated drug and may have a role in sustaining the release of their cargo in the GI tract. The current results warrant further investigations of the micelle possibly while considering GI-tract absorbance enhancing techniques.

References

1. Aliabadi, H.M. and A. Lavasanifar, *Polymeric micelles for drug delivery.* Expert Opin Drug Deliv, 2006. **3**(1): p. 139-62.
2. Lukyanov, A.N. and V.P. Torchilin, *Micelles from lipid derivatives of water-soluble polymers as delivery systems for poorly soluble drugs.* Adv Drug Deliv Rev, 2004. **56**(9): p. 1273-89.
3. Varela-Moreira, A., et al., *Clinical application of polymeric micelles for the treatment of cancer.* Materials Chemistry Frontiers, 2017. **1**(8): p. 1485-1501.
4. Aliabadi, H.M., D.R. Brocks, and A. Lavasanifar, *Polymeric micelles for the solubilization and delivery of cyclosporine A: pharmacokinetics and biodistribution.* Biomaterials, 2005. **26**(35): p. 7251-9.
5. Aliabadi, H.M., et al., *Micelles of methoxy poly(ethylene oxide)-b-poly(epsilon-caprolactone) as vehicles for the solubilization and controlled delivery of cyclosporine A.* J Control Release, 2005. **104**(2): p. 301-11.

6. Garg, S.M., et al., *Traceable PEO-poly(ester) micelles for breast cancer targeting: The effect of core structure and targeting peptide on micellar tumor accumulation.* Biomaterials, 2017. **144**: p. 17-29.
7. Binkhathlan, Z., et al., *Development of a polymeric micellar formulation for valspodar and assessment of its pharmacokinetics in rat.* Eur J Pharm Biopharm, 2010. **75**(2): p. 90-5.